oscilloscope techniques

Alfred Haas

OSCILLOSCOPE

TECHNIQUES

Alfred Haas

contents

introduction

A MONG the various types of indicators and measuring devices, the oscilloscope occupies a very special place. Indicators such as meters generally give only one magnitude of the variable to be investigated, be it a deflection angle or a scale division; they thus may be considered as one-dimensional devices. In an oscilloscope, the locus (called *spot*) of the impact of the electron beam on the screen depends upon two voltages. Thus we have the advantage of a two-dimensional display, and even a third dimension can be added by modulating the brightness of the spot.

Just as in a graph, the vertical deflection axis is termed Y and the horizontal one X. The variable investigated is a voltage called V_y because it is connected to the Y-posts (or vertical input terminals) of the scope, deflecting the spot vertically. (If, for example, the magnitude studied is a sound or fluid pressure or an acceleration, it has to be first translated into a voltage by use of a suitable transducer.) The two-dimensional display feature of the cathode-ray tube (or CRT) allows for representing the unknown V_y in terms of another variable, the horizontal deflection voltage V_x. The graph displayed on the screen (the oscillogram) thus represents a function $V_y = f(V_x)$.

In the most usual applications of the oscilloscope, the horizontal deflection voltage V_x is made proportionate to elapsed time by connecting a linear time base to the X input terminals. By this means the unknown is visualized as its amplitude varies with time. A "pure" ac voltage thus shows up as a perfect sinusoid. This is the function $V_y = f(t)$, the unknown in terms of time.

To investigate the frequency characteristics of a circuit, it is convenient to display its output voltage in terms of frequency to visualize the function $V_y = f(F)$, where F stands for frequency. This is

5

accomplished by making V_x proportionate to frequency F by what we will call a *frequency base*. A typical display of this type is the selectivity characteristic of an if amplifier.

V_x also may be just another voltage of different frequency or phase. This is true of Lissajous diagrams for frequency comparison or ellipses for phase-angle measurement; and also of tube characteristics.

Still another type of display uses polar instead of rectangular coordinates. The base line then becomes a circle whose diameter or brightness can be modulated; the gear-wheel pattern for frequency comparison is an example of this type of display.

These four kinds of displays outline nearly all oscilloscope applications. Understanding this fundamental classification aids in making the best use of an oscilloscope.

From the foregoing we can conclude that the oscilloscope is a device for *qualitative* evaluation, while a meter shows only a *quantity*. The magnitude of an ac voltage is rather insufficient to describe it; the waveform is a very important characteristic. The oscilloscope can also be used for quantitative evaluation, but it may be outperformed in this application by a less complicated meter type device. Its outstanding feature remains the possibility to make us "see the electric waves" and a technician or an engineer deprived of the scope feels like a blind man when investigating circuits.

There is some controversy about the terms *oscilloscope* and *oscillograph*. Etymologically, an oscilloscope is a device to display oscillations (or waveforms) while an oscillograph is a recording device. Thus it is deemed correct to give the name oscilloscope to the instrument to be dealt with, used principally for visual examination of oscillograms. Of course, if you set a camera in front of it to make photos of oscillograms, the instrument may conveniently be termed an *oscillograph*. (The word oscilloscope is often abbreviated as *scope*).

the cathode-ray tube

T HE very heart of the oscilloscope is, of course, the cathode-ray tube. To perform its work, the C-R tube has to have three fundamental parts:

1. An electron gun to emit electrons, concentrate them into a beam and focus this beam on the screen;
2. A deflection system to deflect the beam and "sweep" its impact on the screen (the spot) in accordance with the connected voltages, and
3. An evacuated glass tube with a phosphor-coated screen to make visible the impact of the (invisible) electron beam.

The electron gun

A typical electron gun is shown in Fig. 101. Electrons are emitted by a cylindrical cathode enclosing the spiraled heater. Opposing common tube practice, the oxide coating is set down, not on the envelope of the cylinder, but on its front end. This cathode is surrounded by a cylinder perforated by a small hole facing the oxide coating. This electrode or grid effectively controls the intensity of electron emission just as in a conventional electron tube. By applying more bias to the grid, the beam current is reduced and so is the brightness of the display. The bias control thus becomes a brightness control.

Leaving the cathode by the grid aperture, the diverging electron beam passes a succession of anodes composed of cylinders and perforated disks acting as diaphragms. The role of these anodes is twofold: to bunch the electron beam to focus it into a fine point on

the screen, and to impart the necessary acceleration to the electrons to enable them to reach the somewhat distant screen.

The anode system is often referred to as an electron optical system, for it acts much like an optical lens focusing a light beam. Leaving the first anode A_1, the electron beam is bunched by means of the electrostatic field as it enters the second anode cylinder A_2.
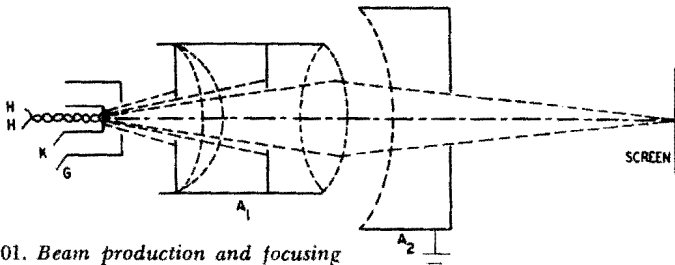
Fig. 101. *Beam production and focusing by the electron gun. (H, heater; K, cathode; G, control grid.) An optical analogue is shown below.*
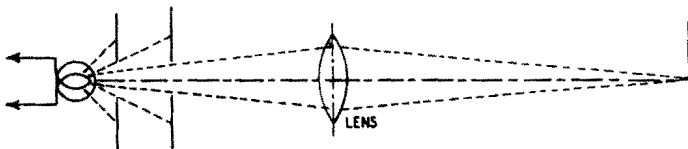
Unlike an optical lens featuring a fixed focal distance depending upon its geometrical design, the electron optical system allows focusing of the beam by purely electrical means, a very convenient property. The focal distance depends upon the relative voltages impressed upon anodes A_1 and A_2. As the potential of A_2 is generally fixed, focusing is obtained by varying that applied to A_1. Fig. 102 shows the action of a variable voltage impressed upon A_1. While the middle trace is correctly focused, the upper and lower traces are out of focus, the voltage applied to A_1 being too high or too low. With the potential of the cathode assumed to be zero, the voltage on A_1 may be about 250 and on A_2 about 1,000 (with respect to the cathode). Grid bias may be variable between 0 and —40 volts, according to the brightness desired.

The electron gun of Fig. 101 is a simple type. A third anode may or may not be internally connected to A_1. Introduction of this additional electrode avoids interaction between brightness and focus controls. Thus, the tube being correctly focused will remain so regardless of the setting of the brightness control, a very convenient feature.

Focusing may also be accomplished by a magnetic field along the

axis of the beam. This is common television-tube practice. Oscilloscope tubes, however, are always focused electrostatically.

It must be emphasized that, to close the circuit, the electrons issued by the cathode need to return to the anode after having hit the screen. From the anode the electrons travel through the high-voltage supply, finally reaching the C-R tube cathode (or starting
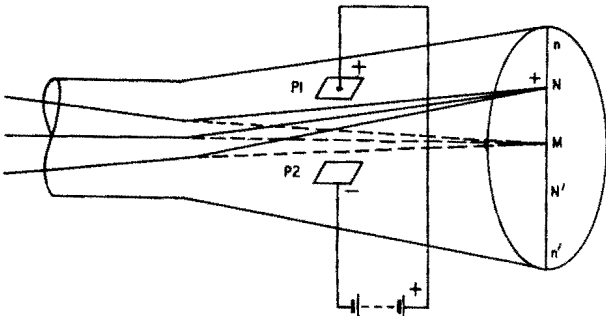
Fig. 103. *Electrostatic deflection of the electron beam.*

point) once again. If there were no return path and electrons became trapped on the screen, the screen would become negative and no pattern would be available.

The deflection system

It may be difficult to visualize the mechanism of deflecting a practically weightless and invisible cathode ray. So you may consider the beam as an extremely fine and flexible wire of negligible inertia carrying a direct current whose negative pole is situated on the cathode end. This hypothetical wire passing between two parallel plates P1 and P2 (Fig. 103) will be electrostatically attracted by the positive plate P1 and repelled by the negative plate P2. Thus, the beam initially focused at point M on the screen will hit it

9

at N, the deflection M–N being proportionate to the voltage applied between Pl and P2. Inverting the polarity of the battery would, of course, make the spot appear at point N', on the other side of M. By means of a suitable voltage connected between Pl and P2, it is possible to situate the spot anywhere on the straight vertical line nn'. These plates providing for vertical deflection are called
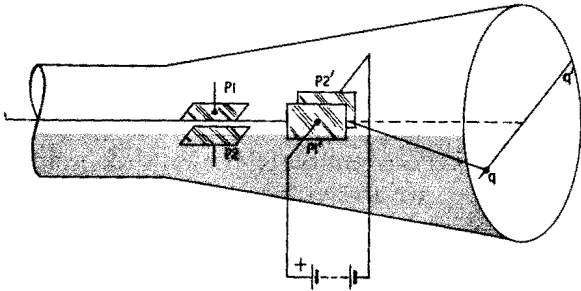
Fig. 104. *P1 and P2 represent the vertical deflection plates. P1' and P2' are the horizontal deflection plates. By means of these plates (positioned at right angles) the spot can be moved vertically and horizontally.*

Y plates. Remember, however, that their actual position is horizontal with respect to the electron beam.

If we now add a second set of plates at right angles to Pl and P2 as shown in Fig. 104, these plates Pl' and P2' will deflect the spot along the horizontal line qq', according to the voltage applied. These plates providing for horizontal deflection are called X plates but are actually positioned vertically.

By applying suitable potentials to both sets of plates, the spot may be positioned at any point on the screen, and so it is deemed unnecessary to provide pictures showing a lone spot positioned at different points on the screen.

We may also affect the position of the spot by deflecting the beam by means of a magnetic (or electromagnetic) field. A coil placed near the neck of the cathode-ray tube, with its axis perpendicular to the beam as shown in Fig. 105, will deflect the spot in the indicated direction when energized by a direct current of the polarity shown. A pair of coils placed symmetrically with regard to the electron beam is used to provide a uniform field.

While electromagnetic deflection is widely used in television practice, it is rather inconvenient for oscilloscopes. Deflection coils are usable only on a limited range of frequencies and need a heavy current to be energized. Magnetic deflection is attractive for television receivers because the tube may be made shorter for a given

screen size; the possible deflection angle being greater. Further-more, in an electrostatic tube the ease with which the electron beam can be moved (deflection sensitivity) is inversely propor-tional to the anode voltage but is inversely proportional to the square root of the anode voltage for magnetic deflection. This

Fig. 105. *Electromagnetic deflection is effected by a coil placed near the neck of the tube with its axis at right an-gles to the beam.*
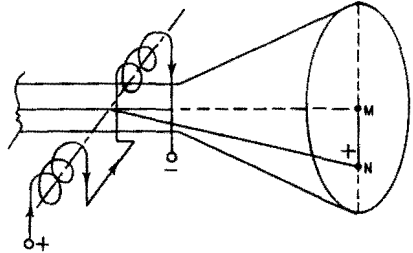
makes magnetic deflection of high-voltage tubes comparatively easy. Having no internal deflection system to align, television tubes are cheaper than comparable oscilloscope tubes and deflection coils may easily be operated at some fixed frequency.

Being concerned solely with oscilloscope applications, we will not describe magnetic deflection further. It is, however, to be empha-sized that the beam in an electrostatic tube can be deflected by a
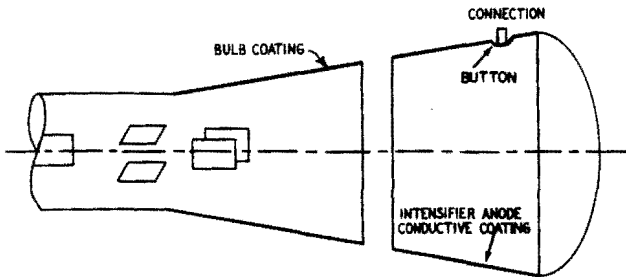
Fig. 106. *The intensifier anode is composed of a conductive coating on the wide part of the C-R tube.*

magnetic field in the same way as a television tube. Hence, stray magnetic fields are to be avoided because they may lead to misin-terpretation of oscillograms.

The screen

The faceplate of the C-R tube is coated with a thin layer of fluorescent material called phosphor. Although a screen is always more or less white, various types of phosphors are characterized by their *persistence* and *color*.

There has to be some persistence (or afterglow). If there were not, a fast-writing spot would not have enough time to impress the retina of the eye and no pattern at all would be perceived. The rapid succession of discrete points on the screen is perceived as a continuous trace, thanks to the afterglow of the excited points of the phosphor. On the other hand, an exaggerated persistence is to be avoided too, for a trace refusing to disappear may interfere with a new trace, and a slowly moving pattern may be smeared. A long afterglow is, however, necessary to visualize a rapid transient that would not be perceived otherwise. This explains why there are phosphors featuring different types of persistence.

Persistence is measured by the time it takes to decrease the initial brightness of a trace to 1% of its value. For normal oscilloscope applications, a persistence of .05 second is adequate (phosphors P1, P2, P3, P4). P6 and P11 are short-persistence phosphors (.005 second) and P7 features a long afterglow (3 seconds).

The color of the light emitted is another characteristic of a phosphor. For general oscilloscope applications, a greenish yellow is chosen because it corresponds to the greatest sensitivity of the human eye (phosphors P1, P3). Monochrome television needs pictures consisting of black and white (phosphors P4, P6), and high-speed photography of oscillograms is best accomplished with a blue-trace phosphor (P11). P7 is a special two-layer phosphor with a short-persistence blue trace followed by a long-persistence yellow trace; by use of suitable color filters, one or the other component may be filtered, thus providing two different characteristics.

The spot should never be permitted to remain stationary on the screen, for burn-in results from this practice (especially with high-intensity beams) leaving a dead spot (sometimes visible by its dark hue) at the impact spot. Even a base-line staying for extended periods on the screen with a high level of luminosity, will result in burn-in. For this reason it is good to run the C-R tube at reduced anode voltage and to decrease the brightness of the trace by increasing the control grid bias. Blue-tint phosphors are especially sensitive to burn-in, perhaps because the reduced sensitivity of the eye to this particular wavelength leads one to increase the beam current more than necessary with a greenish-yellow phosphor screen.

Deflection factor

The main characteristic of a cathode-ray tube is its deflection factor D; that is, the number of dc or peak-to-peak ac volts required on the deflection plates to obtain 1 inch of spot displacement, ex-
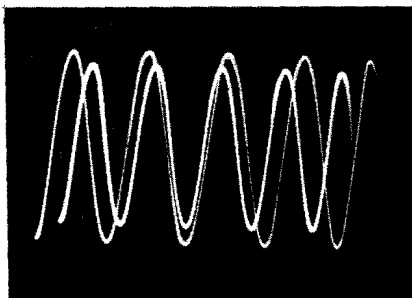
Fig. 107. *Application of intensifier voltage brightens the trace, but lowers the deflection sensitivity of the C-R tube.*
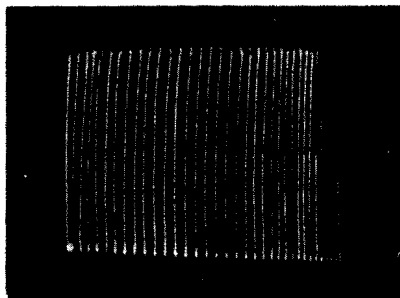
Fig. 108. *A moderate degree of trapezoidal distortion is evidenced by the lack of parallelism of the upper and lower borders.*

pressed in volts/inch. The deflection factor is, however, not a constant but depends upon the anode voltage V_a; in fact, D is inversely proportional to V_a.

A highly accelerated beam is more difficult to deflect than a slower one. For most tubes, D is approximately equal to .06 V_a (volts/inch). Thus, a tube worked with an anode voltage of 1,000 will require .06 $\times$ 1,000 = 60 dc or peak-to-peak ac volts on the deflection plates to display a 1-inch deflection. Increasing V_a to 2,000 volts will result in doubling the voltage required to obtain the same 1-inch deflection. The deflection voltage can be amplified before being applied to the deflection plates, but as good high-gain wideband amplifiers are somewhat tricky and cumbersome to realize, it is good practice to work the cathode-ray tube with the lowest anode voltage compatible with a fine and clearly visible trace. By the same token, there will be less risk of burn-in.

D = .06 V_a is, however, only a rough approximation and depends upon the particular type of tube. The set of deflecting plates near the gun is more sensitive than the pair closer to the screen side of the tube, the length of the deflected beam being greater. For short tubes, the difference of sensitivity of the two sets of plates may be as much as 2 to 1.

Intensifier anode

If a very bright trace is required (for photographic use or observation of fast transients), the C-R tube has to be worked with a high anode voltage; but the decrease of sensitivity and the voltage rating specified by the tube maker rapidly limit every effort in this direction. The difficulty can be overcome by making use of post-acceleration; that is, the beam is subjected to further acceleration

13

after having passed the deflecting system. This is accomplished by an additional electrode—the intensifier anode. As shown in Fig. 106, this electrode consists merely of a conductive coating painted on the inside of the conical part of the tube and is connected to a button sealed in the wall of that part of the tube.

This method at least partly overcomes both difficulties mentioned earlier. The decrease of sensitivity of the beam, accelerated after having been deflected, is much less, and the intensifier anode may be connected to a higher voltage (up to 25,000), the insulating problems being greatly simplified by the glass tube. The effect obtained is clearly visible in Fig. 107 which shows two traces displayed on the screen of a 5CP1 tube with and without post-acceleration. V_a was 2,000 volts and, as the anode is grounded in oscilloscopes, the cathode is at −2,000 volts. The intensifier was first grounded and then tied to the +2,000-volt terminal of the power supply; the overall acceleration voltage thus was 2,000 and 4,000, respectively. As the signal voltage and the brightness setting were the same in both cases, the gain of brightness and the decrease of sensitivity produced by post acceleration are clearly visible.

Trapezoidal distortion

To deflect the beam it is quite possible to apply the ac voltage to but one plate, say X, and ground the other plate X'. This provides more acceleration for the beam (and reduces its deflection sensitivity by the same token) on the positive-going half-waves and increases sensitivity on the negative-going ones. Thus the set of deflecting plates nearest the gun will vary the amplitude of the pattern due to the other set, and the oscillogram is no longer inscribed in a rectangle, but in a trapezoid, hence the name trapezoidal distortion. Fig. 108 shows an example of moderate trapezoidal distortion, accompanied by a certain amount of defocusing near the edges. In this scope, the plates nearest the gun were used for sweeping the tube to provide for comfortable sweep expansion; thus it is the Y signal whose amplitude varies from one side to the other.

Trapezoidal distortion may be avoided by symmetrical deflection voltages, at least for the set of plates nearest to the gun. Some tube types have one plate of one or both sets internally connected to A_2, leaving no other choice than asymmetrical deflection. These tubes do not necessarily introduce trapezoidal distortion, for it is possible to correct this shortcoming by suitable shaping and positioning of the deflecting plates.

oscilloscope circuitry

THE cathode-ray tube alone is of no use. To be operative it needs at least an adequate power supply. Furthermore, one or two amplifiers and a time base are generally required, although in certain special cases these may be omittéd. The assembly of these various devices forms the oscilloscope.

Oscilloscope circuitry could be the title of a big book; as we are, however, primarily concerned with the applications and not with the design of oscilloscopes, we will merely outline the operating principles of the fundamental circuits and describe some typical schematics.

Power supply and controls

A C-R tube requires relatively high operating voltages, from, say, 800 to 2,000 and up, depending upon individual tube types and required brightness of display. Current requirements are low. A bleeder composed of fixed resistors and various potentiometers takes about 1 ma, and this is much more than the operating currents of the electrodes. It is customary to ground A_2 (see Fig. 101 in Chapter 1) to maintain the deflection plates at or near ground potential. Thus, unlike common vacuum-tube practice, the cathode and control grid of the C-R tube are "hot." Because of the high potentials involved, caution is strongly recommended when tinkering with a working oscilloscope. Should it be necessary to service or test the energized high-voltage circuits (and sometimes it is), keep one hand in a pocket and make sure the floor is nonconducting.

A typical oscilloscope power supply is represented in Fig. 201.

Some of its parts may often be omitted and are indicated only for the sake of completeness. The power transformer is special. Besides the conventional 700-volt center-tap winding, there is an extension of, say, 450 volts, and there are some additional heater windings. V1 is a full-wave rectifier powering the amplifier(s) and the time base, and the half-wave rectifier V2 provides the operating voltages of the cathode-ray tube. As the current in this circuit is very low, the rectified voltage about equals the peak ac voltage. In the circuit described, the voltage to be rectified is 350 + 450, or 800 volts rms, and the dc voltage obtained will be approximately 800 × 1.4, or 1,120, the positive end being grounded. A third rectifier V3 similarly provides 1,120 volts to the intensifier, should the C-R tube be of the post-deflection accelerator type; if not, this circuit is omitted.

With regard to the low current, the filter is of the resistance–capacitance type (C1, C2, R1). Frequently, R1 and C2 are omitted, and there is only a buffer capacitor C1. The greater hum voltage due to this simplification does not impair the operation of the cathode-ray tube in a significant manner. Hum modulation of the grid may, however, be troublesome and can be eliminated by a simple filter R2–C4 connected between grid and cathode. Note that the working voltage of C1, C2 and C3 is 1,200 while the voltage across C4 is only 50. The intensifier supply (if any) needs no elaborate filtering; capacitor C3 is sufficient.

There are four controls: R5 controls the brightness of the trace by varying the grid bias; R6 allows for correct focusing of the spot, R7 and R8 are necessary for horizontal and vertical centering of the trace. Note resistor R3 shunting R5. If this pot were open and not paralleled by a suitable resistor, the whole high voltage would appear between grid and cathode, destroying the tube immediately.

The network R4–C5 allows for intensity modulation of the display. Capacitor C5 has to be very well insulated, for any leakage would apply a considerable positive voltage on the grid and put the tube out of commission.

The centering system shown is rather simple, acting only upon one plate of each pair of deflection plates by varying its potential between, say, −100 and +100 volts. All electrodes are ohmically connected to their tie-in points on the voltage divider to avoid erratic operation. An untraceable spot is generally due to a disconnected electrode or an open resistor.

The use of a standard power transformer instead of the special type is sometimes attractive. A conventional 700-volt center-tapped transformer will provide about 700 × 1.4, or 980 dc volts, by half-

wave rectification, the center tap being left free. This is sufficient for most tubes and applications. Should a higher voltage be required, the same transformer can provide approximately twice this value by means of a voltage doubler (Fig. 202). Two rectifier
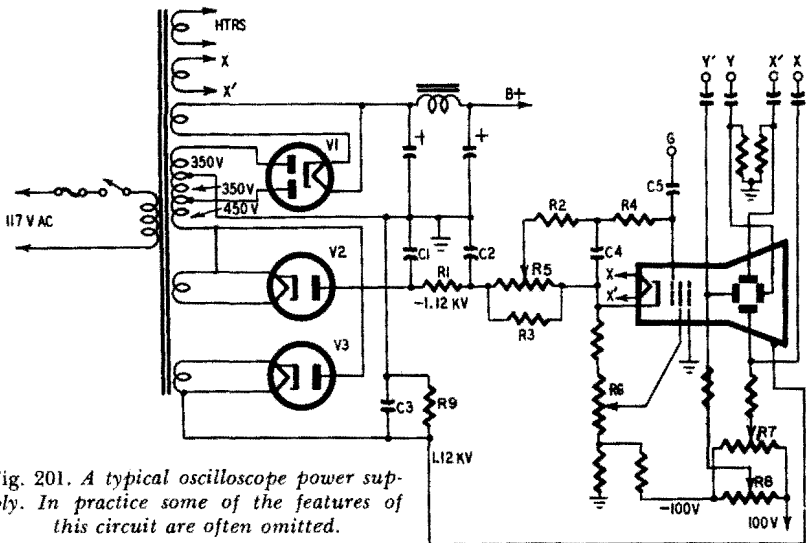

Fig. 201. *A typical oscilloscope power supply. In practice some of the features of this circuit are often omitted.*

tubes are necessary but, as the cathode of V1 is grounded, this tube may conveniently be connected to the common amplifier heater supply.

Deflection amplifiers

The average deflection factor of a normal C-R tube is about 60 volts dc per inch, though values as high as 230 volts per inch and
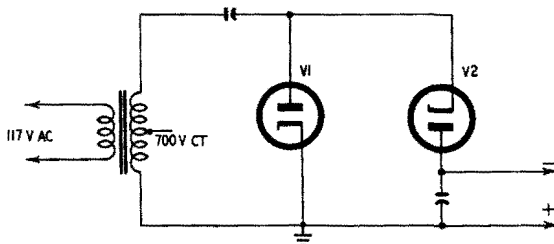

Fig. 202. *Voltage-doubler circuit using a conventional power supply transformer.*

up may occur. (Small-screen tubes, being shorter, generally have higher deflection factors than large-screen types, and thus the voltage required to sweep the screen is somewhat similar for most

types.) This means that the spot will be deflected 1 inch by a dc voltage of 60 or a peak-to-peak ac voltage of the same magnitude. The corresponding rms voltage is $60 \times 0.7/2$, or 21 volts. Considering 1 inch as the minimum height of a display to be analyzed, it is obvious that voltages of less than 20 rms must be amplified for examination.

There is no "standard" gain value; it all depends upon the application involved. While some specialized instruments need to display microvolts, high-voltage testing equipment actually requires input attenuators instead of amplifiers to reduce the deflecting voltage to a suitable value. For general radio, television and electronic applications, .02 rms volt per inch is a very good value, and .2 rms volt per inch can generally do. This means an amplifier gain of 1,000 times in the first case and 100 times in the second.

The other important characteristic of an oscilloscope amplifier is its bandwidth; that is, the range of equally amplified frequencies. It is easy to understand that a waveform can be judged only if the scope amplifier does not introduce a distortion of its own. For low-frequency work, a bandwidth extending from 20 cycles to 100 kc may be considered adequate; for displaying video frequencies, an upper frequency limit of anything between 2 and 10 mc is necessary.

To understand the problems facing the amplifier designer, consider the typical amplifier in Fig. 203. For fair reproduction of the lowest-frequency components, capacitors C1 and C2 are to be large to obtain substantial time constants with the given values of resistors R_c and R_g. This is not difficult to realize and C1 is often omitted, introducing some inverse feedback. On the high-frequency end, transmission is impaired by the undesirable capacitance C3, consisting of the output capacitance of tube V1, the input capacitance of V2 and the distributed capacitance of the wiring. Let us assume C3 is 50 μμf; it is difficult to make it much less. At 60 cycles, this represents a capacitance of $X_c = \frac{1}{2} \pi \times 60 \times 50 \times 10^{-12} = 53,000,000$ ohms, or 53 megohms. The shunting effect upon plate resistor R_L will be negligible. At 60 kc, X_c will be 53,000 ohms. If V1 is a 6SJ7 type amplifier tube with $R_L = .1$ megohm, severe shunting will occur, significantly reducing the gain at that frequency.

The remedy consists of reducing the resistance of the plate load R_L. Values of 2,000 to 5,000 ohms are common. To compensate for loss of gain, high-mutual-conductance tubes such as the 6AG7 with a mutual conductance of 11,000 μmhos—are used. A 6AG7 tube

loaded by 2,000 ohms provides a gain of about 22. This is not much, and several stages must be cascaded to obtain the necessary gain. It is difficult to design high-gain wide-band amplifiers for they tend to become cumbersome, unstable and noisy. For this reason a compromise has to be decided upon, limiting gain and bandwidth to an acceptable value.

The bandwidth can be increased by "peaking" as shown in Fig. 204. An inductance L_L tuned by its stray capacitance C_o connected
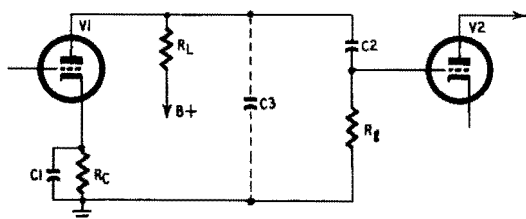

Fig. 203. *High-frequency response of a resistance-coupled amplifier is limited by the stray capacitance represented by C3.*

in series with the plate load R_L resonates at a frequency slightly above the rolloff frequency of the amplifier. If A is the character-
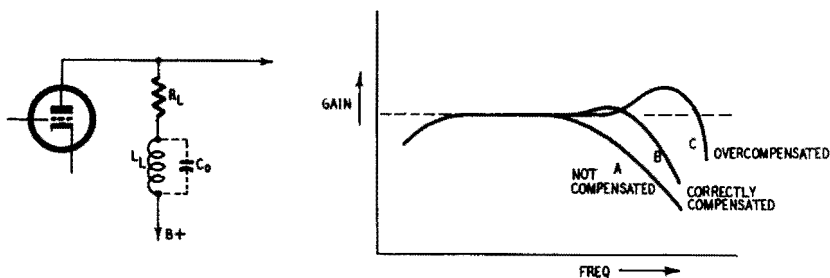

Fig. 204 (left). *Peaking coil L_L extends the high-frequency response of a resistance-coupled amplifier.* Fig. 205 (right). *Effect of peaking on the high-frequency response of a resistance-coupled amplifier.*

istic of the noncompensated amplifier (Fig. 205), an extended characteristic such as B may be obtained by correct peaking. If the inductance of L_L is not correctly designed, a rising characteristic such as C may result, introducing distortion. An uncompensated amplifier is still better than an overcompensated one.

Push-pull deflection amplifiers

Asymmetrical deflection leads to trapezium distortion, and therefore push-pull deflection is recommended. There is still another

reason for using symmetrical output amplifiers. The high output
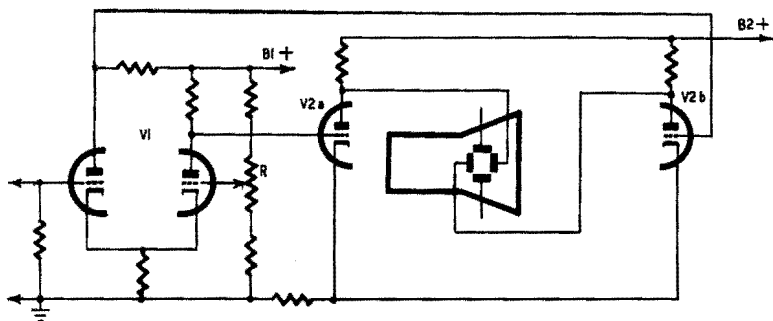voltage required to sweep low-sensitivity C-R tubes may readily

Fig. 206. *Push-pull dc amplifier featuring two long-tailed pairs.*

overload the output stage of the amplifier, introducing distortion.
When push-pull deflection is used, each output tube has to provide
only half of the total deflection voltage, and distortion is reduced.
Of course, push-pull deflection needs an additional output tube
and sometimes a phase inverter.

Dc amplifiers

It is sometimes necessary to display very-low frequency compo-
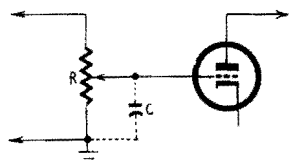nents, and even the dc component of a waveform, without phase

Fig. 207 (above). *Stray capacitance C al-
ters the frequency characteristic, the
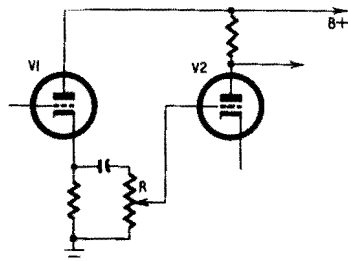change depending on the setting of R.*

Fig. 208 (right). *Cathode-follower input
attenuator stage has an extremely low out-
put impedance.*

distortion. To accomplish this, dc amplifiers are required. Such
amplifiers are liable to drift, especially if the overall gain is high.
Drift may be minimized by a symmetrically designed amplifier and
careful matching of the two halves.

A typical dc amplifier circuit is shown in Fig. 206. Tubes V1 and
V2 are so-called long-tailed pairs. By means of the common cathode
resistors, opposite voltages are generated across the plate loads, and
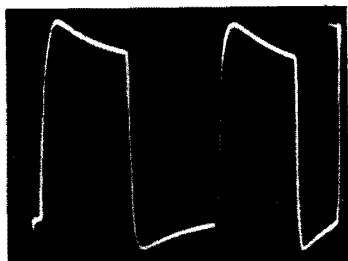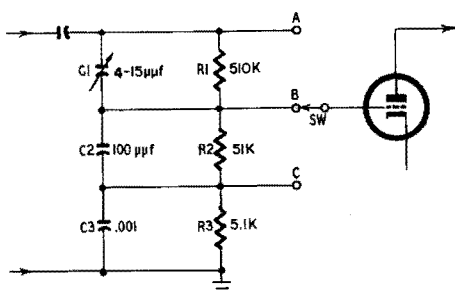a first phase inversion accomplished in V1 is followed by another

20

inversion in output stage V2. This circuit readily leads to a very effective centering control by adjusting the bias of the right-hand section of V1 by potentiometer R.

The circuit shown is good for the range extending from dc to ultrasonic frequencies. Wide-band dc amplifiers are available but their design is much more complicated.

Input attenuators

Input attenuators are necessary to adjust the deflection amplitude to a convenient level. The simple potentiometer circuit of Fig. 207 using a high-resistance unit is unsuitable for the stray capacitance C results in a frequency characteristic variable with the setting of R. The circuit may, however, be used with a low-resistance potentiometer (500 to 5,000 ohms) connected to the output of a cathode follower (Fig. 208), as cathode followers feature a very low output impedance.

As this continuously variable amplitude control allows for a variation of only say, 10 to 1, a stepped input attenuator must be provided. This is a frequency-compensated voltage divider such as in Fig. 209. The attenuation characteristic is independent of fre-
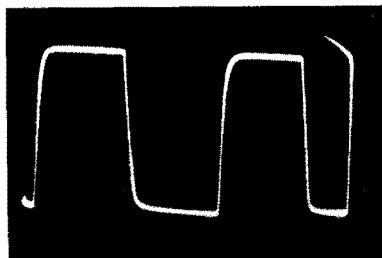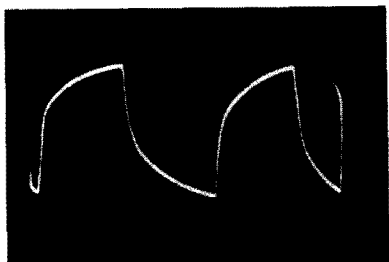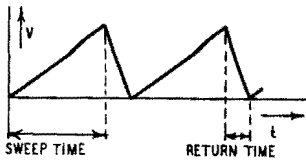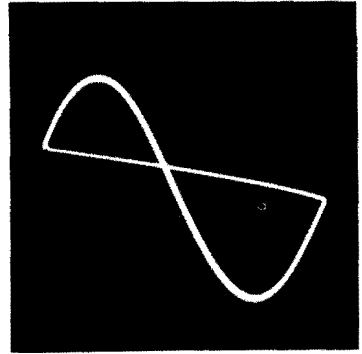
Fig. 213 (above). *Sawtooth waveform produced by a time-base generator. Return time is exaggerated for demonstration.* Fig. 214 (right). *One cycle of a sine wave displayed by a sawtooth sweep equal in frequency to the applied wave.*

quency if the time constants of all the resistors and their associated capacitors are made equal, that is R1C1 = R2C2 = R3C3. A square-wave test is used to carry out a correct equalization.

Typical values of the components are given in Fig. 209. As the capacitance of C1 is rather low and as the stray and input capacitances are not well defined, it is usual to make C1 a trimmer adjustable between, say, 4 and 15 μμf. It has no action upon the wave-
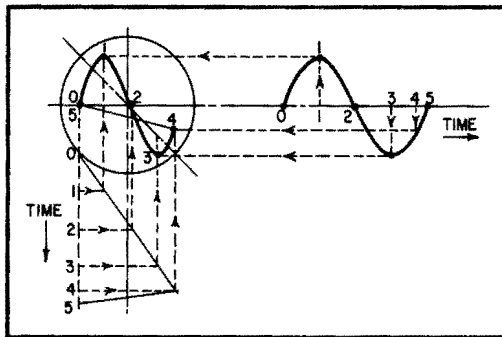
Fig. 215. *Geometrical composition of two right-angled deflection forces generating the oscillogram of Fig. 214.*

form displayed when the switch is set on position A, but its effect on position B is evidenced by the following pictures, the signal being a 50-kc square wave. Fig 210 shows a severe overshoot due to the predominant high-frequency components of the square wave, the value of C1 being excessive. Fig. 211 indicates a loss of high-frequency components by its rounded edges, C1 being set too low. With C1 correctly trimmed, the oscillogram of Fig. 212 was ob-

Fig. 216. *Display of three cycles of a sine wave. The signal frequency is three times that of the time base.*
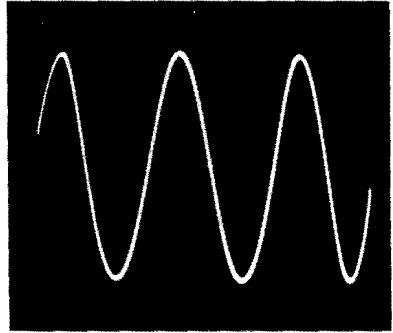
tained. A voltage divider adjusted this way is independent of frequency.

Generating a waveform display

The waveform of a signal is its amplitude variation plotted against time. To visualize it, a time-base generator is needed. This
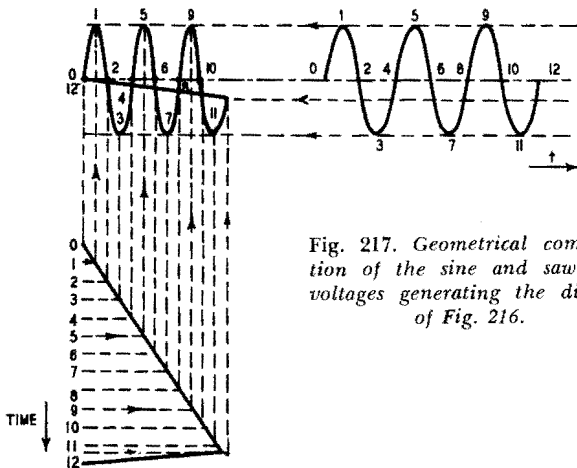

Fig. 217. *Geometrical composition of the sine and sawtooth voltages generating the display of Fig. 216.*

is a device for producing a voltage of sawtooth-like waveform (Fig. 213) composed of a linearly increasing portion called "go time" or "sweep time" and a comparatively short portion of return to the initial condition, referred to as "return time" or "flyback time." Such a voltage applied to the horizontal deflection plates makes the spot move at constant speed from one side of the screen to the other, say, left to right, and then return rather quickly to its point of departure at the left. This cycle then repeats indefinitely.

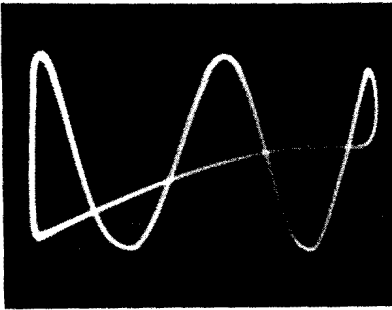If we inject now a sine wave of the same frequency as the recur-

Fig. 218. *On higher frequencies the fly-back time may no longer be negligible.*

rence frequency of the sawtooth voltage into the vertical (Y) deflection channel, we get an oscillogram such as shown in Fig. 214. The geometrical composition of these two voltages resulting in the pattern shown is indicated in Fig. 215. Each point of the display is given by reference lines corresponding to the same instant chosen on the time scale for at every instant the spot is submitted to the amplitude of the X and Y voltages at that time. If the signal frequency is made three times higher, the spot will trace three sine
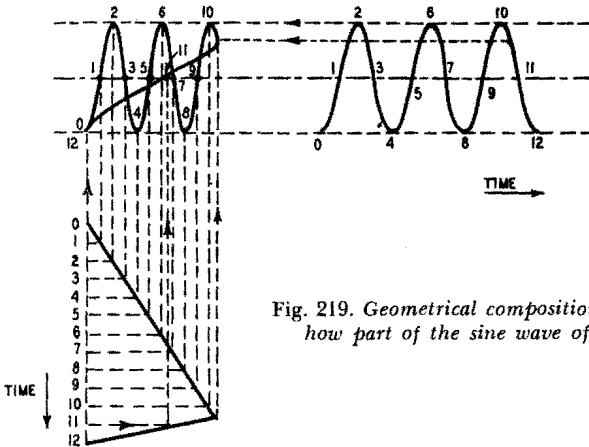
Fig. 219. *Geometrical composition of waves showing how part of the sine wave of Fig. 218 is lost.*

waves during one sweep time (Fig. 216). The corresponding geometrical plotting is indicated in Fig. 217. *It is important to understand well the mechanism of pattern generation by two right-angled deflecting forces, this being one of the fundamentals of oscilloscopy.*

The idealized sawtooth wave features a strictly linear sweep time and an extremely short flyback time. There is, however, no perfection in this world, and we will see that these conditions are not easily satisfied. Thus, it is physically impossible to reduce the fly-

24

back time to zero and, especially in the higher sweep frequencies, the flyback takes an appreciable portion of the whole cycle. This is illustrated by the oscillogram shown in Fig. 218 of a 60-kc sine wave. A portion of the last wave is lost, and the corresponding geometrical plotting of Fig. 219 shows the importance of the return time. Generally this does not matter since linearity of the return trace is often made invisible by a suitable blanking circuit.

Time-base generators

Fundamentally, a time-base generator consists of a capacitor C that charges through a resistance R, building up a voltage between
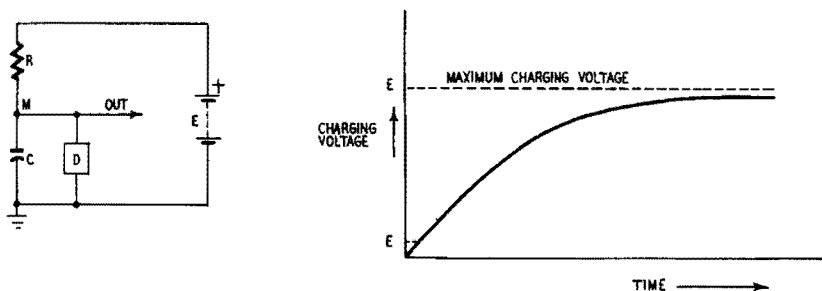

Fig. 220 (left). *Time-base generator operation. D is a triggered discharging device.* Fig. 221 (right). *Owing to the exponential nature of the charging characteristic of a capacitor, only a small portion is approximately linear, resulting in the production of a nonlinear waveform.*

point M and ground (Fig. 220). As this voltage reaches a given level a discharging device D is triggered and discharges C as quickly as possible. A voltage of sawtooth-like waveform across C will result.

Fig. 222. *Nonlinear waveform produced across C in Fig. 220.*

The voltage built up across a charging capacitor, however, is not proportional to time because of the exponential nature of the charging characteristic (Fig. 221). The charging current becomes lower and lower as the voltage across C approaches the voltage E of

25

the charging power supply, resulting in a nonlinear sawtooth waveform as in Fig. 222.

There are two fundamental methods of obtaining a linear sweep from this nonlinear device. The first consists of limiting the volt-
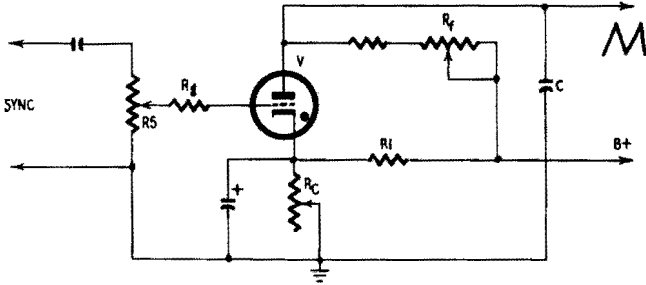

Fig. 223. *Typical gas-triode time-base generator circuit.*

age building up on C to an amplitude E′, representing only a fraction of the total voltage E—for instance, by making E′ equal to
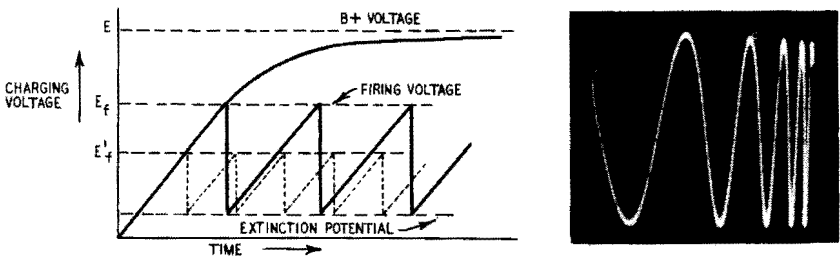

Fig. 224 (left). *The extinction potential of the gas tube in Fig. 223 determines the starting level of the sweep portion of the waveform. A potentiometer in the cathode circuit of the gas tube can be used to vary the firing voltage.* Fig. 225 (right). *Nonlinear sweep caused by the curved sawtooth wave of Fig. 222. Note severe crowding of the trace.*

E/10. The first portion of the charging characteristic being fairly linear as shown in Fig. 221 a good sawtooth wave may be obtained. Its amplitude will obviously be reduced, and a sweep amplifier following the time-base generator will be required to obtain a sufficient sweep voltage.

The other solution consists of charging C at a constant rate by a constant-current device such as a pentode tube. Time bases using this method of linearization produce an output voltage of sufficient amplitude to sweep a cathode-ray tube. However, as it is very convenient to make use of amplifiers in both Y and X channels for displays other than voltage vs. time, this may not be a distinctive advantage.

26

Gas triode time-base generators

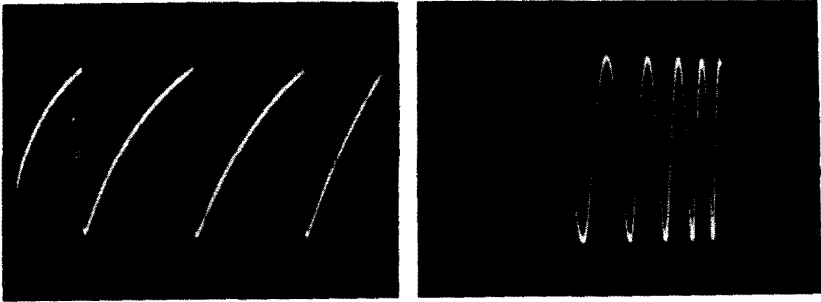The gas triode or thyratron is a very simple and efficient dis-

Fig. 226 (left). *Reducing the bias results in a less curved sawtooth wave.* Fig. 227 (right). *Sweep obtained with the sawtooth wave of* Fig. 226. *The crowding of the trace is much less marked.*

charging device (D in Fig. 220). Unlike a vacuum tube, a gas triode has only two operating states: it may be conducting or not, just as

Fig. 228. *With reduced amplitude, the sawtooth is almost linear.*
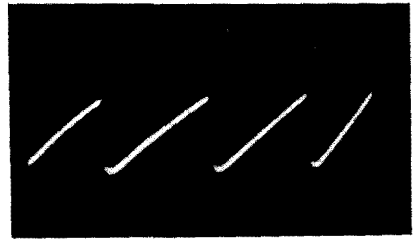
the contacts of a relay may be only open or closed. When the grid bias of an energized gas tube is sufficiently reduced, the tube "fires"

Fig. 229. *Synchronization is obtained by reducing the free running period of the time-base generator.*
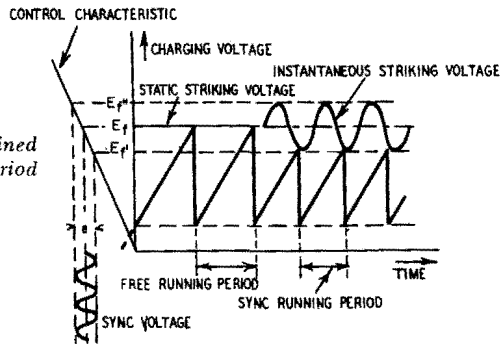
(a faint glow is generally visible) and its internal resistance becomes very low—so low that the tube may be immediately destroyed if there is no current-limiting device in its plate circuit. From now
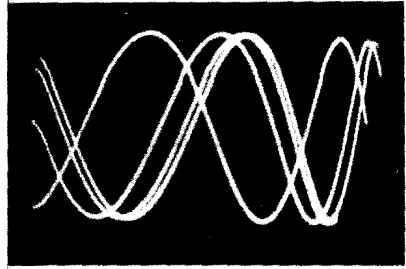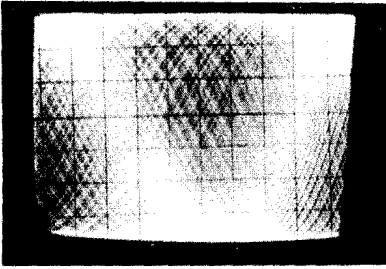
27

on, the grid is inoperative and unable to stop conduction. The tube ceases to conduct only when its plate voltage falls below a definite level, called extinction potential.

A thyratron time-base circuit is represented in Fig. 223. Capacitor C charges through the charging-current determining variable resistor R_f. Gas triode V is connected across C, but is initially nonconductive because of its grid bias (voltage divider R1, R_c making the cathode positive with regard to the grid). As the capacitor charges, the plate voltage builds up and, for a given potential depending only upon the grid bias, the tube fires and C is quickly discharged. Conduction ceases as the anode reaches the extinction potential, C charges again and a new cycle begins. The sawtooth voltage developed across C is represented in Fig. 224. Note that the starting level of the sweep is fixed by the extinction potential, a tube constant, while the firing voltage may be varied by adjusting the cathode bias resistor R_c in Fig. 223. Decreasing R_c will reduce the bias of the tube and firing will occur at a voltage level E_f' instead of E_f. Thus we obtain the dotted sawtooth pattern of reduced amplitude and of higher frequency, the charging period being shorter.

An important characteristic of a gas triode is its *control ratio*, C_r, a constant for a given tube type. The striking voltage is easily calculated by multiplying the control grid bias by C_r. For the type 884 used for demonstration, C_r is 10. This means that the tube biased at 8 volts will fire at 8 × 10, or 80 volts (provided the available charging voltage is greater than that). The total output voltage is a little less, for the extinction voltage of about 15 volts has to be deducted.

The following illustrations show the operation of the time-base generator of Fig. 223, the output being directly coupled to one of

the Y (or X) plates of the C-R tube. The markedly in-curved saw-tooth voltage of Fig. 222 was obtained for a bias voltage of 24; the corresponding striking voltage is 24 × 10, or 240, an appreciable portion of the 300-volt charging voltage. To show the effect of this curvature upon the waveform display, the time-base output was coupled to one X plate of the C-R tube, and a sine wave was injected into the Y channel. The unequal spacing of the individual periods is clearly seen in Fig. 225. Reducing the bias to 18 volts (striking voltage, 180), the sawtooth of Fig. 226 was obtained, resulting in the slightly more linear pattern of Fig. 227. The sweep approaches linearity for a bias of 10 volts (striking voltage, 100) as shown in Fig. 228. The continuous decrease of amplitude accompanying the linearization of the sawtooth is quite visible; the output voltage corresponding to Fig. 228 is insufficient to sweep the C-R tube and has to be amplified. Using an amplifier, one may, however, reduce the striking voltage still further and thus improve the linearity of the sweep.
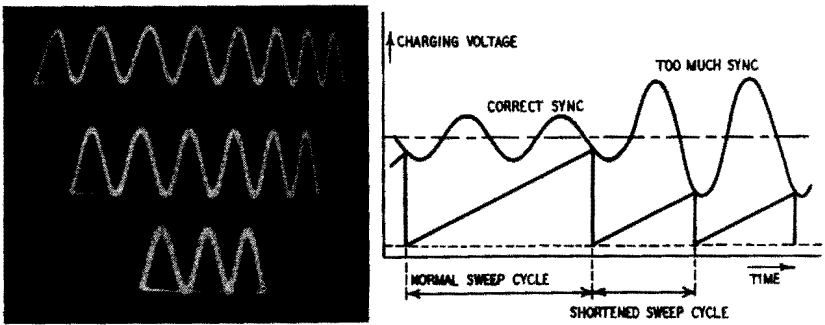

Fig. 232 (left). *Too much sync results in shortening of the base line and a loss of the cycles displayed.* Fig. 233 (right). *Excessive sync voltage results in a reduced amount of sweep.*
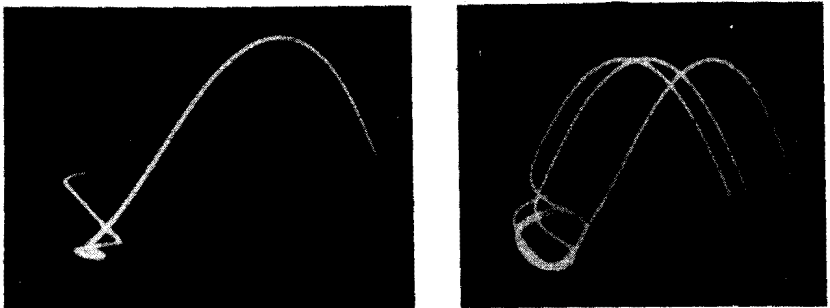

Fig. 234 (left). *Severely oversynchronized display of one cycle.* Fig. 235 (right). *Wrong frequency setting of time base combined with excessive sync. Successive sweeps of different lengths result.*

Note, too, that reducing the striking voltage increases the frequency of the sweep for the charging period is shortened and the new cycle starts earlier. This effect is used for efficient synchronization.
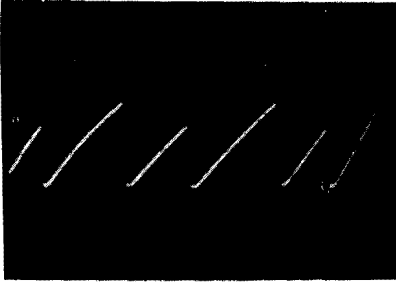
Fig. 236. *Sawtooth voltage producing sweeps of different lengths.*

Fig. 237 (left). *Display of sine wave with suppressed return trace. Reduced intensity is due to blanking.* Fig. 238 (right). *Return trace is intensified by changing the polarity of the blanking signal.*
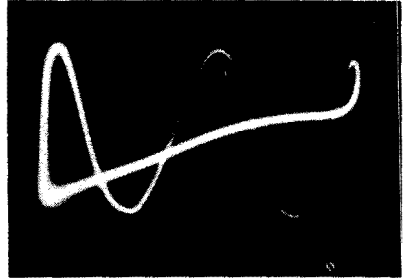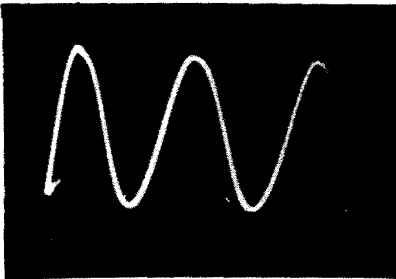
Synchronization

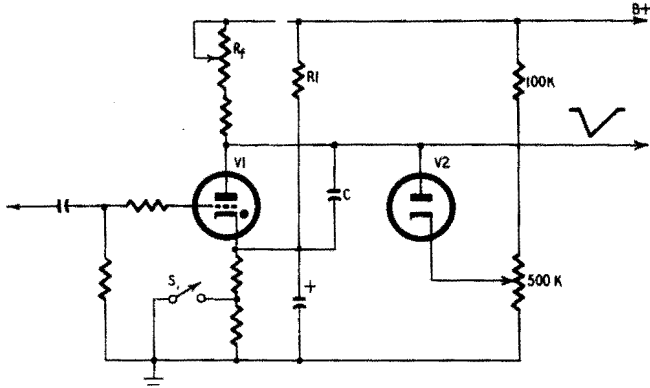To perceive a stationary pattern, it is necessary that the spot re-

Fig. 239. *Triggered time-base generator is made free running by closing switch S.*

trace indefinitely the *same* waveform at exactly the *same* place. This means that there has to be strict synchronization between the instantaneous amplitude of the waveform examined and the corresponding horizontal deflection of the spot.

Unlike tuned oscillators, time-base generators have poor frequency stability, and this turns into a distinctive advantage here because it makes for easy synchronization by the voltage to be examined. The mechanism of synchronization is explained by the diagram of Fig. 229. The sync voltage *e* injected into the control grid "modulates" the striking voltage and makes it vary between Ef' and Ef". As the tube fires at the very moment when the charging characteristic intersects with the striking voltage curve, a very efficient synchronization is accomplished by stopping the charging cycle and starting the discharge always at the same point of the striking curve and by the same token, of the waveform to be displayed. Note here that this is always done by *shortening* the charging cycle, *increasing the repetition frequency*. For effective sync, a time base has to operate at a frequency slightly higher than the ideal value.

The sync control has to be adjusted with great care if misleading patterns are to be avoided. (Some modern oscilloscopes, however, feature sync limiter circuits and thus free attention for the
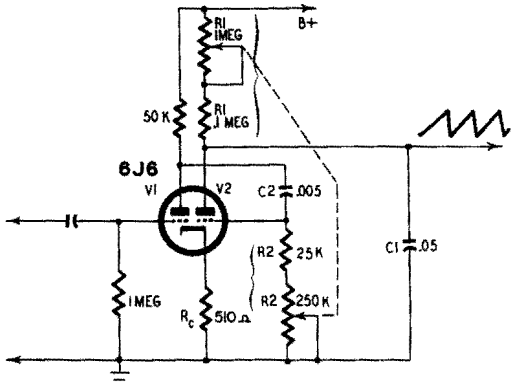
Fig. 240. *Typical multivibrator type time-base generator.*

main job.) A frankly undersynchronized sweep voltage results in a blurred and illegible pattern (Fig. 230). With a slightly higher but still insufficient sync voltage, a pattern such as Fig. 231 is obtained, showing several identical waves more or less displaced. This sort of pattern usually is highly unstable.

If the sync control is still advanced beyond the point of adequate stability of the display, a progressive shortening of the base line accompanied by the disappearance of successive cycles of the pattern is observed, as shown in Fig. 232. Three photos were taken under the same conditions except for sync control. The upper trace
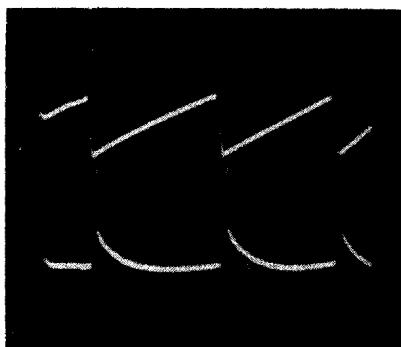

Fig. 241. *Multivibrator time-base voltage waveforms. Above: output voltage; below: plate voltage of V1 in Fig. 240.*

is correctly synchronized, the center one moderately and the lowest one strongly oversynchronized. The diagram of Fig. 233 explains why this happens. While the smaller sync voltage triggers the discharge after completion of a sweep displaying two cycles, the larger signal fires the gas tube after a sweep time corresponding to only one cycle.

If there remains but one cycle on the screen and the sync voltage is still increased, that last cycle is severely distorted as shown in Fig. 234, making it difficult to distinguish the initial sine wave. To obtain this pattern, a sync voltage of 8 rms volts was impressed on the control grid biased at 8 dc volts. Combining a wrong frequency setting with too strong sync control results in a pattern like that of Fig. 235, produced by successive sweeps of different amplitude. This corresponds to a sawtooth wave such as displayed in Fig. 236.

The question thus arises as to how a time base is to be operated for best results, without abuse of the sync facilities. The best way is to turn the sync control to zero at the beginning and to set the frequency control to obtain the desired display, and preferably at a slightly lower frequency. The obviously moving pattern is then easily stabilized by a *small* amount of sync voltage. Readjust the frequency control slightly if necessary, but don't increase the sync signal unless it is necessary.

Return-trace blanking

Although rather faint because of its greater writing speed, the return trace of the spot is normally visible (Fig. 214, for instance)

and may be confusing at higher sweep frequencies where the fly-back time is no longer negligible with regard to the sweep time—as in Fig. 218 displaying a 60-kc sine wave.

It is quite easy to blank the return trace. Probably all time-base generators feature at a definite point of their circuitry a sharp pulse

Fig. 242. *Same as* Fig. 241, *but time constant of R1C1 in* Fig. 240 *is different.*

of positive or negative polarity. A negative-going pulse may be applied directly to the control grid of the C-R tube by a small high-
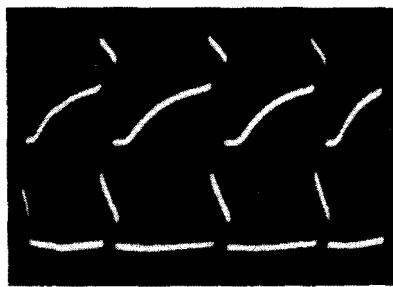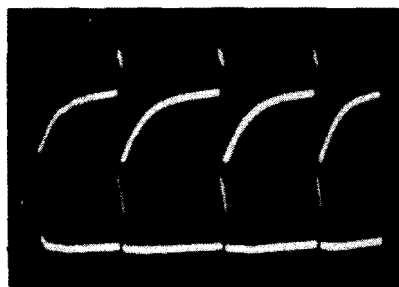

Fig. 243 (left). *Above: grid voltage of V2; below: voltage across* R_c. Fig. 244 (right). *Same as* Fig. 243, *but the time constant of R1C1 is different.*

voltage capacitor. In one multivibrator type time base, a positive-going pulse is obtained on the plate of the left-hand triode. (Refer
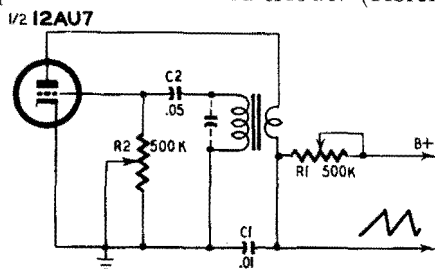

Fig. 245. *Blocking oscillator time-base generator.*

to Fig. 240 described in the section under the heading of multivibrator time-base generator.) The polarity of this pulse can be

changed using a phase-inverter tube. This complication can, however, be avoided by modulating the cathode and not the control grid of the C-R tube. Fig. 237 shows the same pattern as Fig. 218, the return stroke being suppressed, however. Applying the positive pulse on the control grid results in intensifying the return trace (Fig. 238), a feature sometimes desirable for extremely fast sweeps (though the return stroke is rarely linear).

Note that return-trace blanking will render invisible a portion of the pattern and thus may be undesirable. Optional blanking is the best solution.

Triggered sweep

The recurrent sweep generator described is adequate for examination of periodic phenomena with which we are generally concerned. It does not lead, however, to easy examination of randomly occurring phenomena, such as atmospherics, for instance, or other transients. These may take place at any moment during the sweep, possibly during the return stroke, causing poor display or even loss.

To display satisfactorily these nonperiodic events, a triggered time base is used. The recurrent sweep generator accomplishes two functions: the generation of a sawtooth voltage and the triggering of the cycle. It is easy to separate these operations, and Fig. 239 shows that a few supplementary components transform the recurrent time base of Fig. 223 into a sweep generator triggered by a suitable signal. To accomplish this, the grid bias of the gas tube is increased by opening switch S, making for a higher striking voltage. During the charging of capacitor C, the plate voltage of V1 rises to a value v_o somewhat lower than the striking voltage and determined by the adjustable cathode voltage of the diode clamp tube V2. Thus, C remains charged until a negative-going pulse of sufficient amplitude applied on the control grid reduces the striking voltage to v_o. The tube then fires, discharging C. After accomplishing a new charging cycle, the time base becomes inoperative until arrival of a new triggering pulse.

Triggered sweeps are extensively used in radar techniques, and the scopes featuring a triggered sweep are called synchroscopes. Such equipment generally provides for a delay device in the Y-channel (delay line or flip-flop) to display the beginning of the signal shortly after initiation of the sweep and so to avoid its loss.

A single sweep generator is a triggered time base made inoperative after having accomplished but one stroke. Such a device is re-

quired for detailed study of a transient where elimination of other signals may clear the pattern, which would otherwise be illegible.

High-frequency time-base generators

The gas-triode time-base generator has been treated in a somewhat detailed manner to show the mechanism of sweep voltage generation and the way to operate it. Though it is simple and efficient, and widespread in oscilloscope equipment, it has its shortcomings, the principal one being its limited operating frequency. Because of the finite time required to ionize and to de-ionize the gas in the tube, its highest operating frequency is about 40 kc, depending upon the circuit used. Moreover, this frequency limit is not clearly defined, the sweep voltage decreasing with an increasing frequency.

For high-frequency sweep generation, vacuum-tube time-base generators are used. There is quite a variety of types, but we will

Fig. 246 (left). *Above: grid voltage of blocking oscillator; below: sweep voltage across C1.* Fig. 247 (right). *Decreasing amplitude and increasing frequency result from increasing R1.*

examine only the multivibrator type extensively used in oscilloscopes, and the blocking oscillator, incorporated in every television receiver.

Until now, we expressed the sweep velocity of the *time* base in terms of *frequency*. This is very convenient for the display of periodic events characterized by their frequency. It is quite meaningless, however, if the sweep is triggered, there being no repetition frequency. Furthermore, the actual timing of an event is more complicated using a time base calibrated in terms of frequency. For this reason, many commercial oscilloscopes (especially the triggered ones) rate the sweep speeds in seconds (or microseconds) of duration. As frequency is the inverse of time, a sweep duration of, say
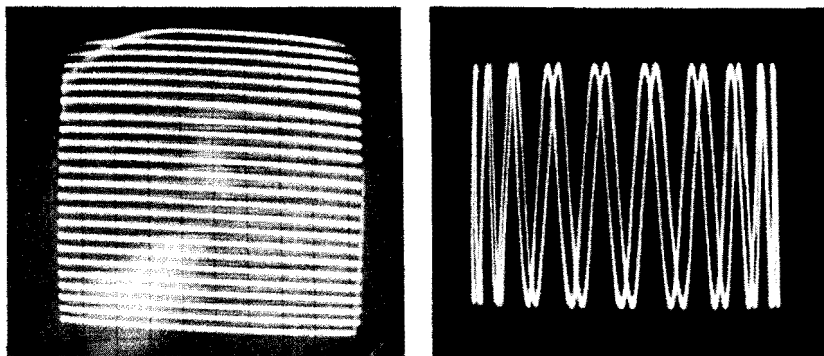
35

Fig. 248 (left). *Television type raster sweep has low frequency ratio to make individual lines clearly visible.* Fig. 249 (right). *Sine-wave sweep leads to an illegible pattern.*

10 μsec, corresponds to a frequency of 1,000,000/10 or 100,000 cycles, or 100 kc.

Multivibrator time-base generator

The multivibrator time-base generator (sometimes called Potter time base) consists of a cathode-coupled multivibrator triggering the discharge of a capacitor Cl charged through a variable resistor R1 (Fig. 240). The common cathode resistor R_c and the ac-coupling C2R2 introduce a feedback between sections V1 and V2 of the tube, making it oscillate rather violently. At the beginning, Cl charges through R1 and V2 is nonconducting. As V2 starts conduction, it raises the bias voltage across the common cathode resistor R_c, thus decreasing the plate current of V1 and increasing its plate voltage. This produces some sort of instantaneous chain reaction, for the positive pulse on the plate of V1 is transmitted by C2 to the grid of V2. The resulting heavy plate current of V2 rapidly discharges capacitor Cl, while V1 is cut off. Then the circuit returns to its initial condition and a new cycle is started. The slow charging and rapid discharging of Cl result in a sawtooth voltage across Cl.

The waveforms at different points of this generator can be studied by means of an electronic switch. The upper waveform in Fig. 241 shows the sawtooth wave developed across Cl while below it is the plate voltage of V1. The coincidence of the positive-going steep pulse and the beginning of the discharge is clearly seen.

For demonstration purposes, R2, Cl and C2 (in Fig. 240) were fixed and only R1 was varied. The pattern of Fig. 241 was obtained with R1 equal to .6 megohm, making the time constant of R1Cl

36

much larger than that of R2C2. Making R1 equal to .1 megohm resulted in the pattern of Fig. 242, presenting a wider triggering pulse and a longer flyback time.

In Figs. 243 and 244 are shown, above, the grid voltage of V2 and, below, the voltage on the common cathode, for R1 equal to .6 and .1 megohm, respectively. The grid voltage rises first slowly and then rather steeply, at the very instant of the positive-going pulse on the cathode. By comparing Figs. 243 and 244, the widening of the discharge pulse due to shortening the time constant of R1C1 is evident.

Sync voltage may be injected into the grid of V1. The pulse on the plate of V1 can be used to blank the return trace by modulating the cathode of the C-R tube. Keep the resulting stray capacitances low so as not to stretch the return time. This time base needs a dual potentiometer for fine frequency control; 1 megohm for R1 and .25 megohm for R2 are suitable values. Furthermore, C1 and C2 are to be switched simultaneously for coarse frequency control.

The Potter time base can be trigger-operated by negatively biasing the grid of V2 and limiting the charge of C1 by a diode connected as shown in Fig. 239 for a gas-triode sweep generator.

Blocking-oscillator time-base generator

This type of time-base generator differs from almost all other types: a transformer is used much like in a conventional tickler oscillator (Fig. 245). By making the time constant (i.e., the product R2C2) of the grid coupling sufficiently large, the operation of the circuit is radically changed. Because of the tight coupling of the two windings, a strong oscillation takes place as soon as the circuit is energized. This oscillation is rectified by the grid, and an important bias voltage builds up across R2 so that the tube is cut off after a few cycles. (This blocking action on the oscillation gave its name to the circuit.) The charge, of course, leaks away through R2 and the cycle starts again, but this takes a much longer time than the duration of a period of oscillation. Thus, the tube alternates a short period of heavy conduction at the starting of oscillation with a comparatively long period of nonconduction, the tube being biased beyond cutoff. Just as in the time-base generators previously described, this effect can be used to discharge capacitor C1 which is charged through resistor R1 in the plate circuit of the tube.

The upper waveform in Fig. 246 shows the grid voltage and below it the sweep voltage across capacitor C1. The superimposed oscillations during the positive stroke of the grid can be distin-

guished, and the coincidence between the period of positive grid voltage and the discharge is clearly visible. Note that the flyback period is relatively long; this is not a shortcoming inherent in this type of time base but is caused by the use of a conventional instead of a pulse type transformer.

To obtain this sawtooth voltage, R1 and R2 in Fig. 245 must be set carefully (potentiometers are used). For low values of R2, the circuit operates like a conventional sine-wave oscillator; on the other hand, if R2 is made too large, no oscillation takes place. Fig. 247 shows the result of varying R1 only. Three successive photos were taken; increasing R1 decreases the amplitude of the sawtooth wave while increasing its frequency. The high-amplitude wave is no longer linear. The same effect appeared in the other time bases for the same reason. The sawtooth of Fig. 247 is negative-going while that of Fig. 246 is rising. This is due to phase reversal because of the omission of the amplifier stage of the electronic switch. The correct polarity is that of Fig. 246.

The blocking-oscillator time base is readily synchronized by a
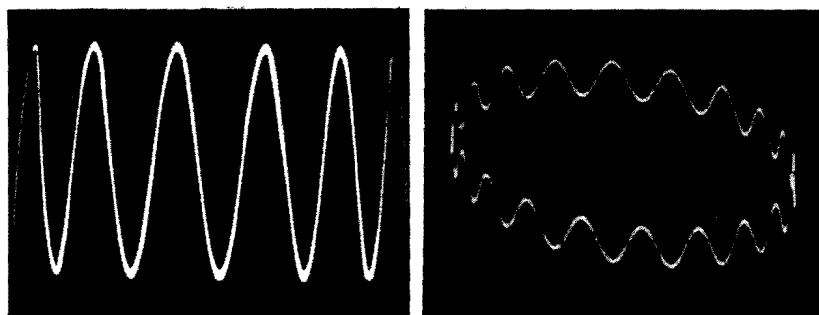
Fig. 250 (left). *Expanded sine sweep, one trace blanked.* Fig. 251 (right.) *Generation of an elliptical sweep.*

suitable pulse applied to the grid. Triggered sweep operation is possible, too. (If this circuit is rarely used in oscilloscopes, it is applied extensively to television receivers. Resistor R2 is then made partially variable and is termed the horizontal or vertical hold control, and R1 is the picture size control).

Television raster generation

A television type scan is produced by applying sawtooth waves of suitable frequency ratio to both the X and Y channels of the oscilloscope. The pattern of Fig. 248 was generated using two gastriode time-base generators. To obtain a stationary pattern, the two

generators must be synchronized. The frequency ratio has been chosen rather low to show each discrete stroke; in television practice, the lines are invisible.

Such a pattern is sometimes used to check the linearity of C-R tubes; this requires a high degree of linearity of both generators.
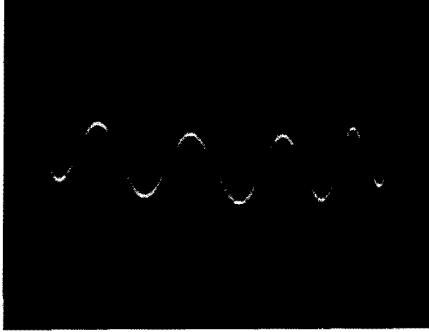

Fig. 252. *Expanding the elliptical sweep and rejecting the upper trace results in a usable pattern.*

The raster may be amplitude-modulated or, more frequently, intensity-modulated. Furthermore, if the time bases operate at suitable frequencies and if a video signal is injected into the control grid of the C-R tube, the oscilloscope becomes a television receiver.

Sine-wave sweep

The simplest way to "sweep" cathode-ray tubes consists of applying the 60-cycle line voltage to the deflection plates. The pattern thus obtained is shown in Fig. 249, which displays a 1,200-cycle sine wave. This oscillogram is illegible, for the superimposed traces left to right and right to left are similar and the linearity is poor on both sides. By increasing the applied sweep voltage so that only the central, approximately linear, portion of the trace remains on the screen, the display becomes somewhat linear. Furthermore, one of the traces can be suppressed by injecting a suitably phased 60-cycle voltage into the grid of the C-R tube. Combining these two improvements results in a pattern such as Fig. 250, much like a linear time-base display. Because of the way it is produced, this system is often referred to as a "medium-cut" time base.

A somewhat similar result can be obtained by rejecting one of the traces out of the screen instead of blanking it. This is accomplished by superimposing upon the signal a 60-cycle voltage of suit-
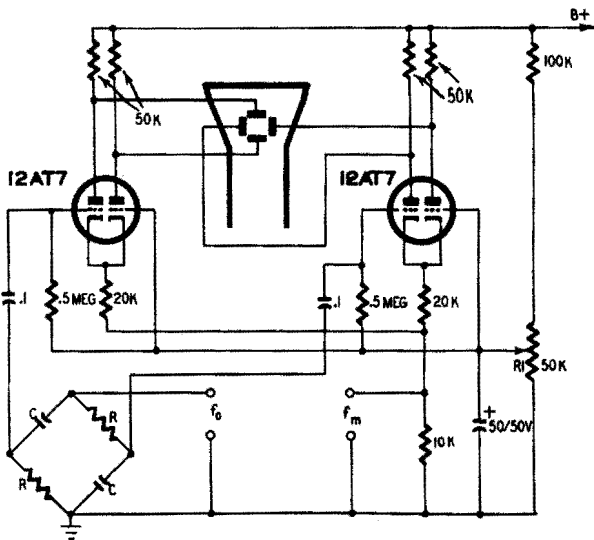
Fig. 253. *Simple circuit for the generation of a polar display.*

able amplitude, resulting in an elliptical pattern such as in Fig. 251 and explaining the name of "elliptical" time base given to this system. However, Fig. 251 is barely usable. After expanding the sweep and rejecting the upper trace, the oscillogram of Fig. 252 was obtained. Aside from the somewhat curved base line, this display is quite convenient.

The sine-wave sweep has, however, an important drawback: its frequency is fixed and cannot be synchronized. To obtain a stationary pattern, the wave to be displayed has to be an exact multiple of the 60-cycle line frequency and we actually must "synchronize" the audio oscillator manually. Furthermore, the trace is a bit faint because the high writing speed of the spot traces only the medium
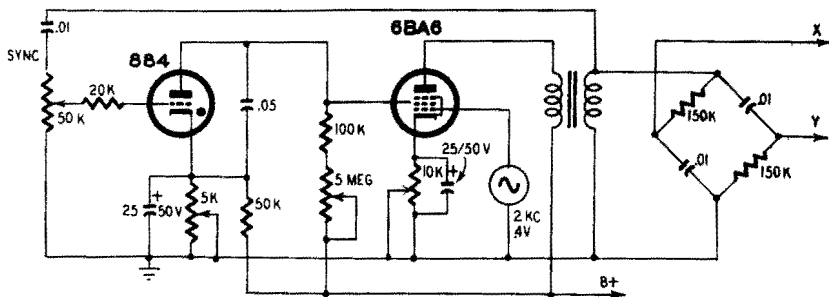
Fig. 254. *Spiral time-base generator for demonstration purposes.*

portion of the pattern. This type of sweep is, in practice, used only for tracing frequency response diagrams in inexpensive test equipment.

Circular time base

It may seem nonsensical to display a graph with rectangular coordinates on a circular screen; the introduction of oscilloscope tubes featuring a rectangular faceplate provides a more efficient use of the entire screen surface. Round tubes lead directly to polar display, the base line being a circle. Such a circular sweep avoids the return stroke and possibly the loss of a portion of the phenomenon investigated. Furthermore, the base line is lengthened. For a 5-inch C-R tube, for instance, the greatest usable base line with a linear sweep is about 4 inches. If the same tube is used with a circular sweep, the length of the base line becomes 11 inches for a circle diameter of $3\frac{1}{2}$ inches.

To produce a circular sweep, a phasing network has to apply a sine wave in phase quadrature (90°). The circular trace which results is comparatively easily intensity-modulated and is not at all difficult to carry out. The author designed the circuit represented in Fig. 253 and thus obtained the oscillograms of Figs. 453 to 457 (in
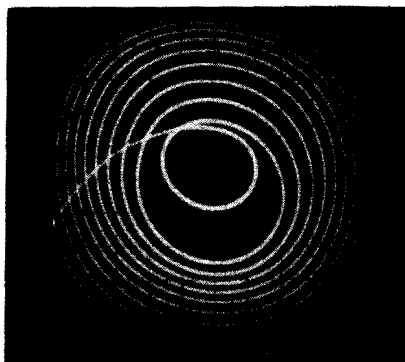
Fig. 255. *This is an example of the type of spiral sweep that can be obtained with the circuit illustrated in Fig. 254. This shows the extent to which the base line of the sweep can be lengthened.*

Chapter 4) used for frequency measurements. The circuit consists of two "long-tailed pairs" coupled to the four deflection plates, one grid of each pair being fed with the circle-generating frequency f_0 by a phasing network. The modulating frequency f_m is injected into
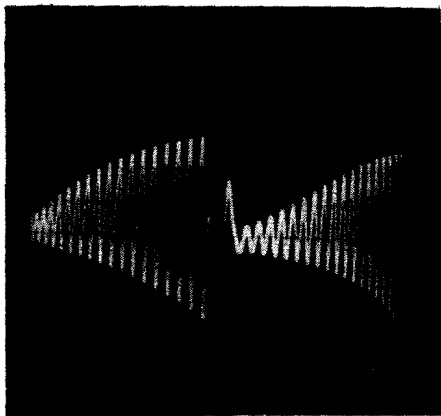
Fig. 256. *Waveform of spiral sweep voltage of Fig. 255.*

a resistor common to the four tube sections. For best results, the bias of the tubes (control R 1) and the amplitudes of f_o and f_m must be adjusted carefully.

Spiral time base

The baseline of the sweep can be lengthened further by transforming the circle into a spiral. An experimental circuit for producing such a spiral is shown in Fig. 254. A sine-wave voltage delivered by an audio oscillator is amplified by a pentode tube whose output transformer feeds a phasing network. The device described until now produces a circular trace. Adding a gas triode whose sawtooth output voltage supplies the screen makes for a (roughly) linear variation of the radius with time, and thus a spiral is traced as in Fig. 255. This display and its generating circuit are presented only for demonstration, without any claims regarding perfection. The corresponding waveform is shown in Fig. 256. To get a stable display, it is necessary to synchronize both the time base of the oscilloscope and the gas triode with the circle-generating sine wave.

oscilloscope accessories

THERE are some important devices frequently used with oscilloscopes, consisting generally of separate units. These devices will merely be considered here as tools, their actual application being shown in the following chapters.

Multiple-trace displays

It is often desirable to display two or more phenomena simultaneously to compare their characteristics. This can be done by using two oscilloscopes or equipment comprising two C-R tubes, but the actual distance between the two traces makes this a poor solution. There are multigun tubes consisting of two or more completely independent electron guns and deflection systems in a single tube. Thus each beam may be positioned, deflected, swept, modulated and blanked independently of the other, providing for the greatest possible flexibility. For multiple-display purposes, the multigun cathode-ray tube is certainly the best solution. Such tubes are rather expensive and the equipment incorporating them obviously needs two amplifier and time-base channels to operate each section (assuming the tube is of the two-beam type).

Any conventional oscilloscope can, however, be made to display simultaneously two (or more) traces by means of an accessory unit called an electronic switch. Strictly speaking the patterns are not traced simultaneously because, at any given instant, the spot can have but one impact on the screen. So the spot traces alternately one pattern (or part thereof) after the other. Fig. 301 illustrates such a way of successively writing portions of each wave. The spot
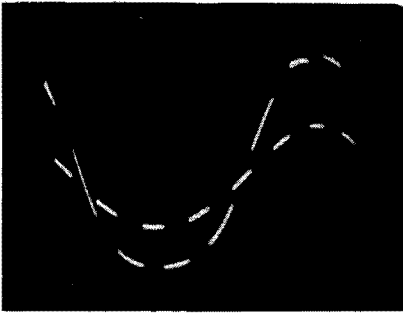
Fig. 301. *By means of an electronic switch the spot successively writes two traces or parts thereof.*

passes very quickly from one trace to the other so that its vertical sweep and return are barely visible. It is emphasized that this oscillogram was taken only to explain the operating principle of an electronic switch. For waveform examination, this makes a poor display because of the lost parts of the traces and the lack of continuity.

Electronic switch

A simple type of electronic switch is represented in Fig. 302. It consists of two gated amplifier channels (tubes V1 and V3) working with a common plate· resistance, and a multivibrator (V2) produc-
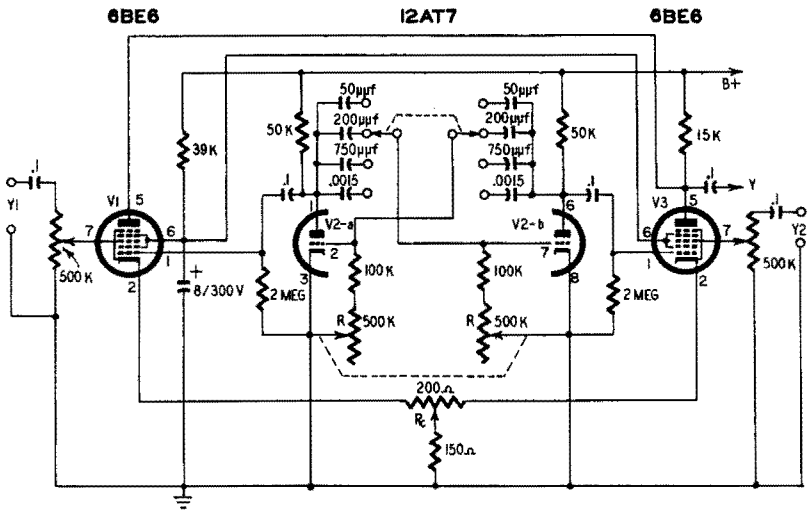
Fig. 302. *Electronic switch of the multivibrator type.*

ing a square wave to control the alternate operation of the input channels. While the two input signals Y1 tnd Y2 are applied to the modulator grids of the mixer tubes V1 and V3, the square wave is
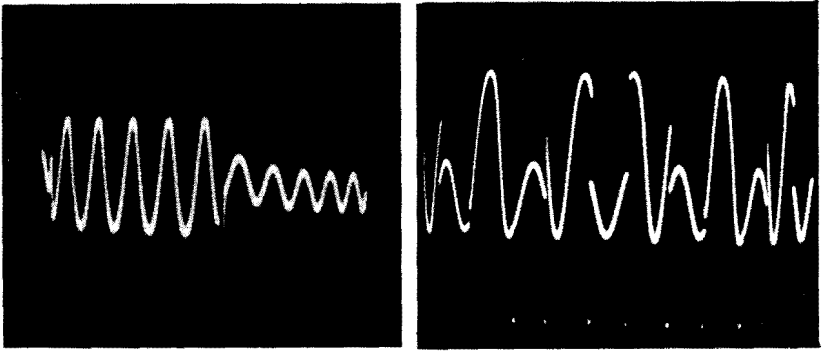
Fig. 303 (left). *Successive operation of two channels of the electronic switch. Note the presence of switching transients (descending peak at the beginning of the low amplitude trace).* Fig. 304 (right). *If the switching frequency is a multiple of the sweep frequency an illegible pattern results.*

injected with inverted phase into the oscillator grids, to key one tube while the other is inoperative. The alternate operation of the two channels is shown in Fig. 303. (This representation side by side is more interesting for demonstration purposes than for actual waveform examination.) The repetition frequency of the multivibrator is adjustable by steps by a bank of capacitors, and a dual potentiometer R allows for fine control.

To facilitate identification of similar waves, trace separation is generally provided. In the circuit described this is accomplished by potentiometer R_c by varying the bias of V1 and V3 in opposite directions. This varies the dc plate current of the tubes and the resultant dc voltage component is transmitted by the coupling capacitor. Acting upon R_c, this raises one trace and lowers the other.

Fig. 305 (left). *Same as Fig. 304: This oscillogram is of no use for interpreting waveforms.* Fig. 306 (right). *Switching frequency much higher than the sweep frequency. Note the dotted trace.*
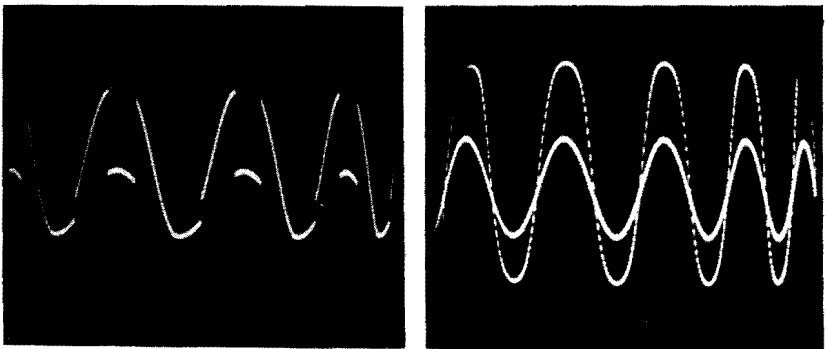
Differentiation of traces is also possible by varying the on–off ratio of the amplifiers, making one trace a bit fainter than the other. This is obtained by choosing unequal grid resistors in the multivibrator circuit.

The electronic switch described is rather simplified and some improvements are possible. The square wave generated by a multivibrator is rather imperfect and a waveform-shaping stage is often added. The input attenuators are uncompensated and suitable only for low frequencies. The output may be coupled directly to a Y deflection plate of the C-R tube. The amplifiers must not be overloaded in trying to get a pattern of suitable height. We applied the switch output to the input of the Y amplifier of the scope, enabling small-signal operation of the switch. However, the scope amplifier has to have an adequate bandwidth to transmit the switching square wave correctly.

Choice of switching frequency

The fact that the repetition frequency of the multivibrator is made variable indicates that a suitable switching frequency has to be chosen. This raises the question of the optimum frequency. First of all, the switching frequency should never be a multiple of the sweep frequency for the spot passing from one trace to the other at always the same points of the waves displayed will write the same portions of these waves again and again, omitting the others, as shown in Fig. 301. While this oscillogram is still readable, those of Figs. 304 and 305 can no longer be interpreted. Slightly resetting the fine frequency control R will continuously displace the transition path of the spot and the eye will perceive two continuous traces.

Flicker is likely to occur at low switching frequencies. On the other hand, at high switching frequencies (with regard to the frequency of the waveform displayed) the rapid back-and-forth motion of the spot makes a sort of luminous curtain appear between the two traces, and the traces show up as a succession of discrete points (see Fig. 306). The optimum switching frequency seems to be half the sweep frequency for the spot then writes one trace entirely during each go time of the sweep, and no switching transients nor back-and-forth motions appear. This condition is realized in Fig. 307, where there is no interference between the two traces. Note, however, the switching transient at the extreme right.

Correct synchronization is still another problem for three frequencies are involved. The time base has to be synchronized by the
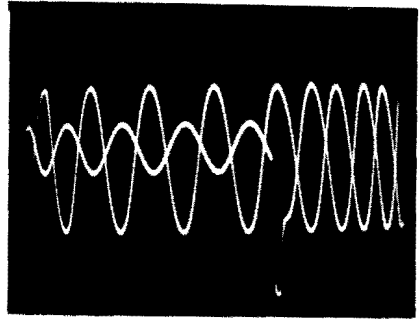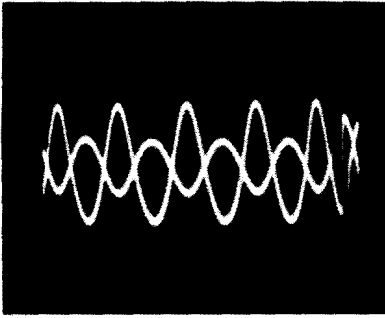
Fig. 307 (left). *If the switching frequency is half of the sweep frequency the spot writes one entire trace after the other. Note the presence of switching transients.*
Fig. 308 (right). *Faulty synchronization of electronic switch and sweep.*

signal to be displayed. If the sync selector of the scope is set on "internal sync," the time base is likely to be synchronized by the
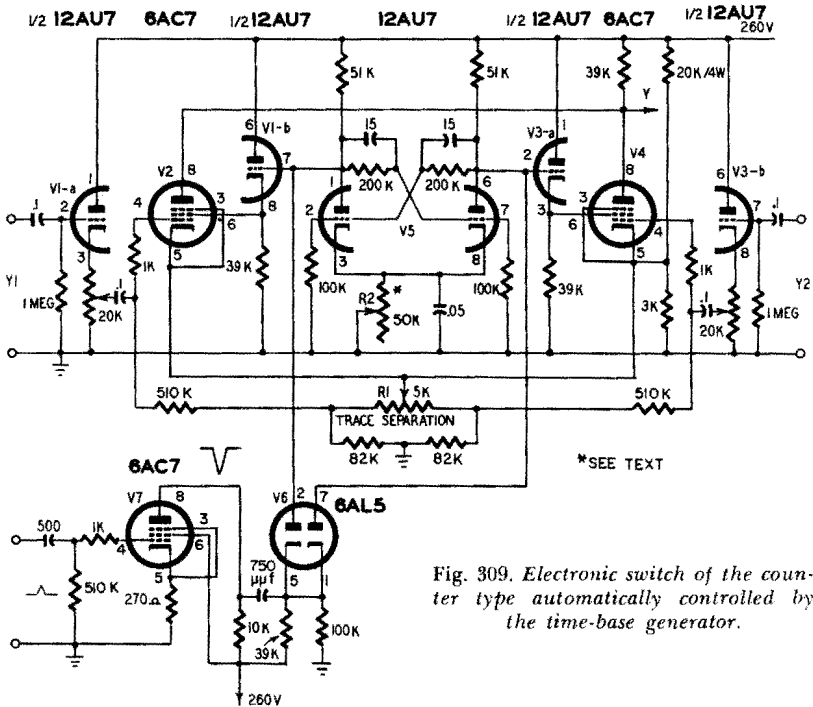

Fig. 309. *Electronic switch of the counter type automatically controlled by the time-base generator.*

switching frequency. So it is best to set the selector on "external sync" and tie the corresponding input post to the signal input.

Faulty synchronization may result in a wave pattern such as Fig. 308. Note that the apparently usable part on the left side of the os-
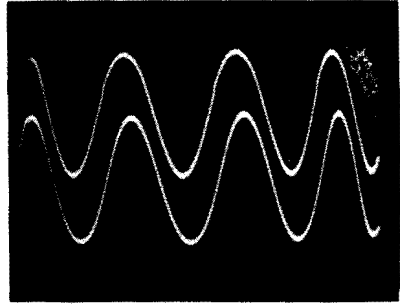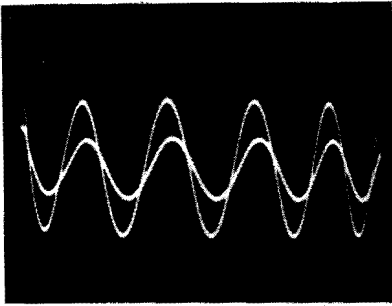
Fig. 310 (left). *Oscillogram obtained with an electronic switch of the counter type. Note the neat traces and the absence of switching transients.* Fig. 311 (right). *Same as Fig. 310; the traces are separated.*

cillogram shows a phase difference that actually did not exist, the Y1 and Y2 terminals of the switch being tied together.

Now for the multivibrator sync. If the switching frequency is very different from that of the sweep frequency, it may be left free running; but for the described half-frequency operation, sync has to be applied from the time base. The phase relation of Fig. 307 is misleading: the two voltages were actually in phase, but a faulty sync upset their display. Examination of the right-hand transient shows that the two traces are of different lengths. To conclude, half-frequency operation is very attractive, but may produce misleading phase relations if incorrectly synchronized. This danger does not exist with high-frequency switching.

Counter type electronic switch

From the preceding it is easy to guess that correct adjustment of both time-base and switching generators is somewhat tricky and tedious. However, as half-frequency operation is estimated best (if adequately performed), a switching device controlled by the time base and operating at half its frequency can easily be designed, and one can forget about switching frequency. This switching may be obtained with the Eccles-Jordan circuit called "scale of two," a multivibrator featuring two stable states. The scale of two produces a square wave very suitable for switching purposes. Its frequency is half that of the control pulses: it takes two pulses to restore the initial state in the circuit.

An electronic switch of the counter type is a little more complicated than a multivibrator. Its schematic is given in Fig. 309. Amplifier tubes V2 and V4, working with a common output resistor, receive input signals Y1 and Y2 from the cathode-follower input
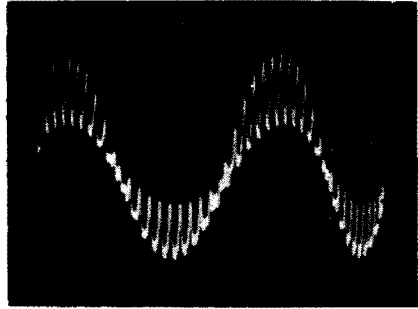
stages V1-a and V3-b. The scale-of-two V5 is triggered by pulses amplified by V7 and directed at the most favorable switching point by V6. Cathode followers V1-b and V3-a are controlled by the scale of two and thus alternately gate the amplifier tubes V2 and V4. The whole affair was designed for use with a Potter time base featuring a positive pulse. If a pulse of negative polarity and sufficient amplitude is provided (for instance, by differentiating the sweep voltage output), V7 is omitted. Trace separation is accomplished by R1, and R2 is set for best counter operation.

Figs. 310 and 311 show oscillograms obtained with this type of
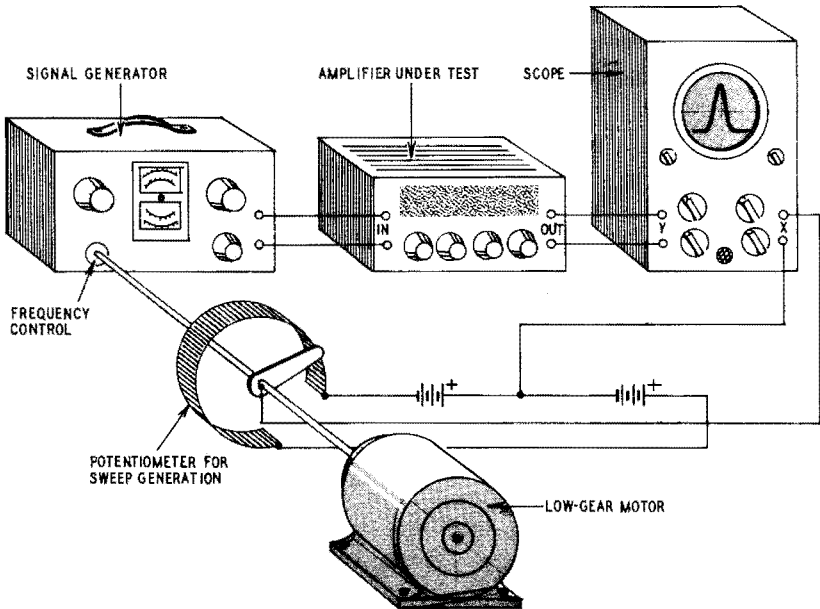
Fig. 313. *Operating principle of a motor-actuated response curve tracer. (This system is primarily of historical interest.)*

switch, the traces being first superimposed and then separated. Note the absence of switching transients, punctured traces and illuminated curtain between traces. When cathode resistor R2 is set to a very low value, the scale of two becomes a multivibrator oscillating without any external triggering, and so Fig. 312 was obtained, showing an incorrect operating mode similar to that of the multivibrator type switch.

Automatic response curve tracing

Point by point plotting of the bandpass of, say, if amplifiers, though accurate, is tedious and time consuming. By means of an accessory, the frequency sweep generator, response curves can be readily traced on the screen of a scope. This is a major application of scope techniques to radio and TV servicing.

To trace a response curve, the amplifier output voltage is plotted vertically on a graph for a certain number of frequencies, plotted
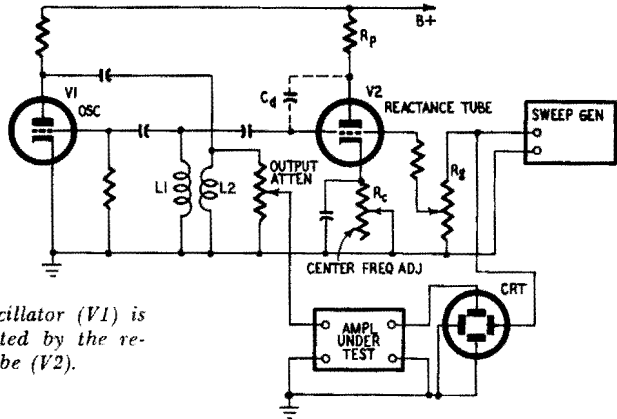
Fig. 314. *The oscillator (V1) is frequency-modulated by the reactance tube (V2).*

horizontally. Using a scope to display such curves, a graph-type two-dimensional representation can be obtained by linking the generator frequency control with the horizontal deflection device of the scope in a manner to correlate each point of the X axis on the screen to a definite frequency. This can be carried out by the motor-driven device illustrated in Fig. 313, effectively used some 20 years ago.

This electromechanical method, though quite workable, has been made obsolete by purely electronic systems, based on the operation of a vacuum tube as a variable reactance. Tube V2 of Fig. 314 is such a device. Besides the (static) interelectrode capacitances determined by the tube geometry, there is a dynamic grid-plate

50

capacitance C_d depending upon the gain of the stage. Inductance L1 of the tuned-grid oscillator driven by tube V1 is therefore paralleled by C_d in series with plate resistor R_p. Varying C_d will change the oscillator operating frequency. The gain of the tube, and C_d by the same token, can be varied by acting upon the slope at the working point of the I_p/E_g characteristic of the tube: Increasing the bias will shift the working point to a lower mutual conductance (or slope), and reduce C_d. To get the highest possible value of C_d, high
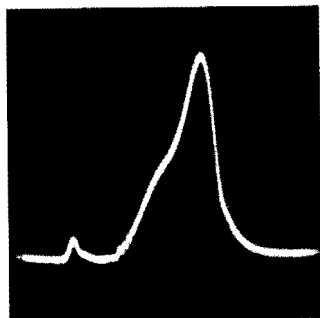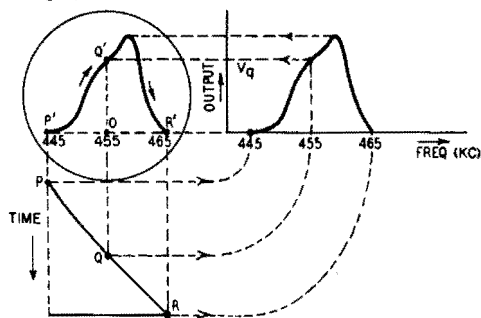
Fig. 315 (left). *Generation of a single-trace response curve pattern.* Fig. 316 (right). *Oscillogram of an assymmetric single-trace pattern.*

mutual conductance triodes or triode-connected pentodes are used. Because of the inherent low Miller effect, pentode connection is to be avoided.

Practically, the variation of C_d, and thus the frequency modulation of the oscillator is obtained by injecting a suitable ac voltage into the control grid of V2, the frequency deviation, or swing depending on the actual setting of the grid control R_g. If the same voltage (not necessarily a sawtooth wave) is used to sweep both the
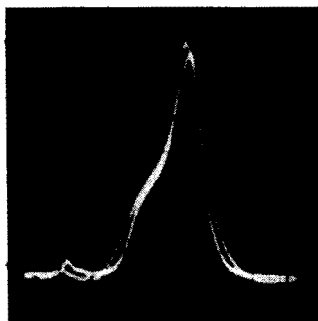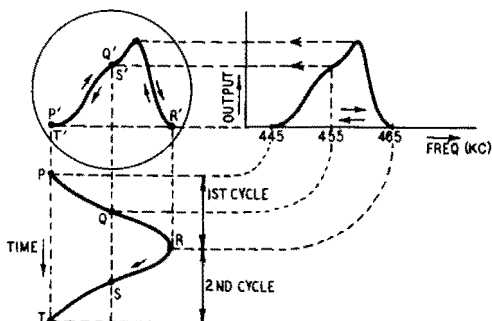
Fig. 317 (left). *Generation of a single-trace pattern using a sine-wave sweep. The spot runs the curve in both directions.* Fig 318 (right). *Single-trace pattern, sine-wave sweep.*

C-R tube and the oscillator, the horizontal spot deflections will correspond to the simultaneous oscillator frequencies, just as in the mechanically linked system described earlier.

To fully understand what is going on, let us follow the spot step by step and see how it writes the graph. Suppose the device is adjusted so that the midway point of the sawtooth wave (Q) centering
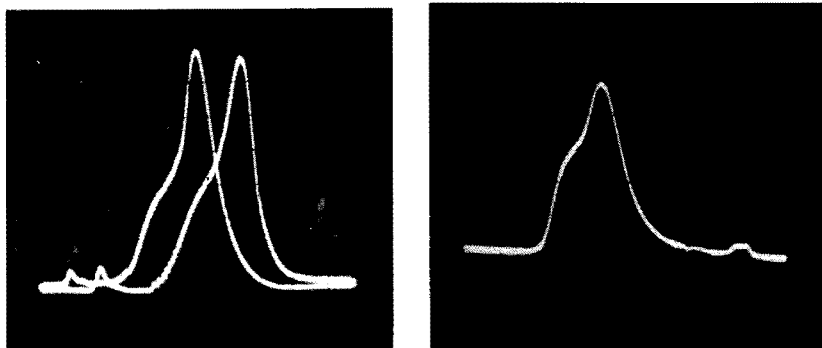
Fig. 319 (left). *Single-trace pattern incorrectly phased. The two traces can be made to coincide by the proper use of a phasing network.* Fig. 320 (right). *Single-trace pattern blanked to avoid trace superimposition problems.*

the spot on the x-axis of the screen corresponds to the center-frequency 455 kc of the oscillator (Fig. 315). As the amplifier output voltage for 455 kc is V_q, the spot will appear at point Q'. (For the purpose of demonstration, a nonsymmetrical selectivity curve is represented here.)

While the sawtooth voltage now increases up to its top (point R) sweeping the spot to its extreme position R', the oscillator frequency is simultaneously swept from 455 to 465 kc, and the spot traces the corresponding output voltage variation Q'R'. If the return time is negligible, the spot passes almost instantly to point P' on the extreme left of the screen, corresponding to an oscillator frequency of 445 kc. A new sawtooth PQR starts, sweeping the oscillator from 445 to 465 kc, and the spot traces curve P'Q'R'. As the successive traces are identical, the pattern is quite stable. An oscillogram obtained this way is shown in Fig. 316. This is called a single-trace pattern.

A similar result is obtained using a sine wave sweep as explained by Fig. 317. Owing to the reduced slope of the sine wave near its tops, the pattern is compressed on both sides, and the skirt selectivity of the circuit may appear better than it actually is. The center linearity, however, is good.

While the sweep voltage increases from **P** to **R**, the oscillator frequency varies from 445 to 465 kc as formerly, and the spot writes curve P'Q'R'. During the other half-cycle RST, the frequency varies from 465 to 445 kc, and as frequency and sweep voltage are rigidly linked, the spot now traces curve R'Q'P' exactly superimposed on P'Q'R', thus writing the same graph in both directions. An oscillogram such as Fig. 318 is obtained. There evidently is a
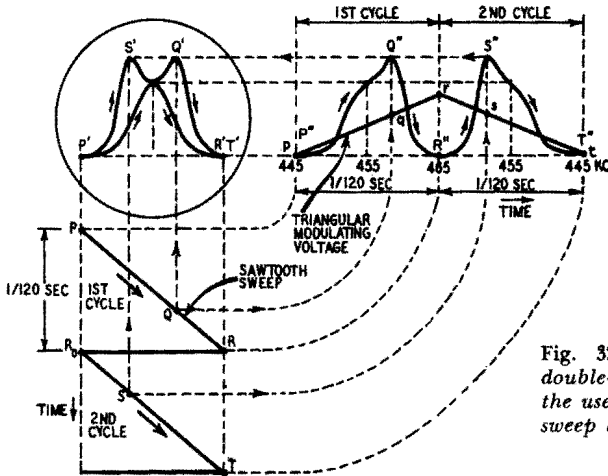
Fig. 321. *Generation of a double-trace pattern through the use of a sawtooth-shaped sweep and a triangular modulating voltage.*

gap between theory and practice, for the forward and return traces are not exactly superimposed, owing to distortion of the 60 cps sweep voltage waveform. Incorrect phasing results in patterns such as Fig. 319. Though two curves appear, note that this still is a single trace, for the two curves are identical and can be set to coincidence by means of a suitable phasing circuit.

Fig. 322 (left). *Double-trace pattern showing correct frequency and lack of skirt symmetry.* Fig. 323 (right). *Double-trace pattern showing incorrect frequency and lack of symmetry.*
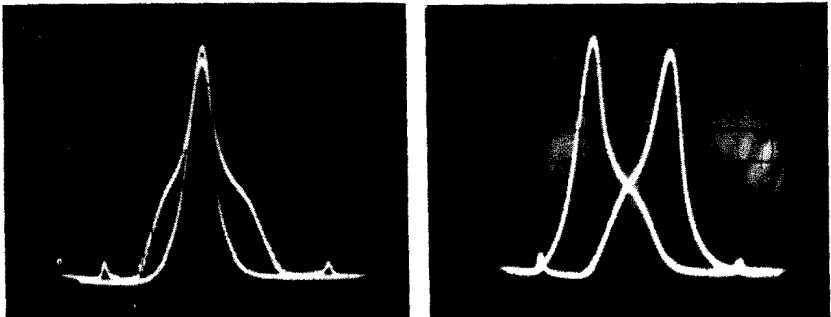
As it may be troublesome to manage an exact superposition of both traces, blanking is often preferred; that is, suppression of one of the traces by a suitably phased voltage applied to the C-R tube's control grid. Such a "blanked" single trace is shown in Fig. 320, the blanking voltage being derived from one X-deflection plate.

Double trace patterns

An interesting and useful form of display is obtained using a triangular wave (obtained, for instance, by integration of a 60 cps square wave) for oscillator control, and a 120 cps sawtooth wave to sweep the scope (Fig. 321). During the first sawtooth PQR, the triangular oscillator control voltage rises linearly (pqr), and the test
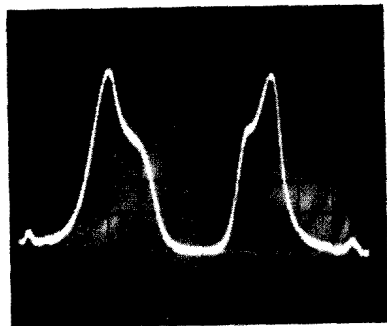
Fig. 324. *Double-trace pattern showing incorrect time-base setting. Trace is practically unusable.*
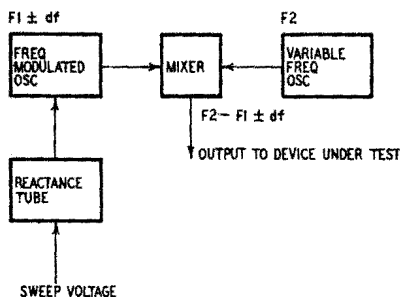
Fig. 325. *Block diagram of a multiple-range sweep generator based on the bfo principle.*

frequency varies from 445 to 465 kc. This corresponds to an output voltage curve P"Q"R", and the spot traces curve P'Q'R'. During the second sweep cycle R_0ST, the control voltage decreases (rst), varying the frequency from 465 to 445 kc. This results in an output curve R"S"T", and the spot writes curve P'S'T'. This is a true double trace pattern. Note that, while both curves are traced from left to right, one of them is reversed as in a mirror. This is very convenient for evidencing slight discrepancies by superposition.

An important lack of symmetry is seen in Fig. 322, the tuning frequency being about correct. Frequency error is indicated by spacing of the traces, as shown in Fig. 323, where lack of symmetry is also present. If the time base is operated at 60 cps, a curve such as Fig. 324 results. (Compare with P"Q"R"S"T" of Fig. 321.) Such a pattern is practically useless.

Double trace patterns allow for most accurate tracking of tuned circuits, but are more confusing than simple trace displays. Simple

trace patterns always result from oscillator and C-R tube sweep voltages of same frequency and waveform.

Variable frequency wobbulator

The simple frequency sweep generator, or wobbulator is merely an example of what can be done. The reactance tube may be worked as a variable inductance instead of a variable capacitance; but similar results are obtained.

The circuit shown in Fig. 314 is fixed-frequency device. As C_d is quite low (about 30 µµf), a tuning capacitor connected across L1 is to be avoided for it would reduce the swing. The center frequency can however be adjusted by means of cathode resistor R_c of tube V2 by shifting the operating point along the characteristic.
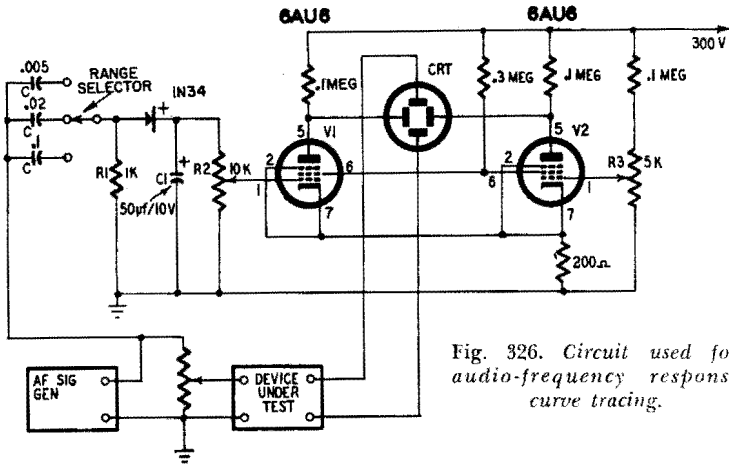
Fig. 326. *Circuit used for audio-frequency response curve tracing.*

For variable frequency operation, the bfo (beat frequency oscillator) principle is used. The output F1 ± df of the reactance tube controlled frequency modulated oscillator is mixed with the output F2 of a variable frequency oscillator in a mixer stage, and the resultant difference frequency F2 — F1 ± df is injected into the device under test, the other components being filtered as well as possible. The resultant variable frequency signal features a frequency independent swing df. See Fig. 325. Spurious frequencies (whistles) may however be troublesome, producing pips such as seen on the left side of Fig. 316.

For TV work involving much higher frequencies and greater bandwidth, the reactance tube modulator becomes somewhat complex, and electromechanical wobbulators are often used. A simple device consists in a modified speaker driving a variable tuning ca-

pacitor. The 60 cps may be used for driving the speaker and sweeping the C-R tube, and thus a single trace pattern will be obtained. Inductance variation of an iron-cored coil by means of an ac magnetizing field is also used.

Audio frequency response curve tracing

The bfo principle of Fig. 325 may be applied to response curve
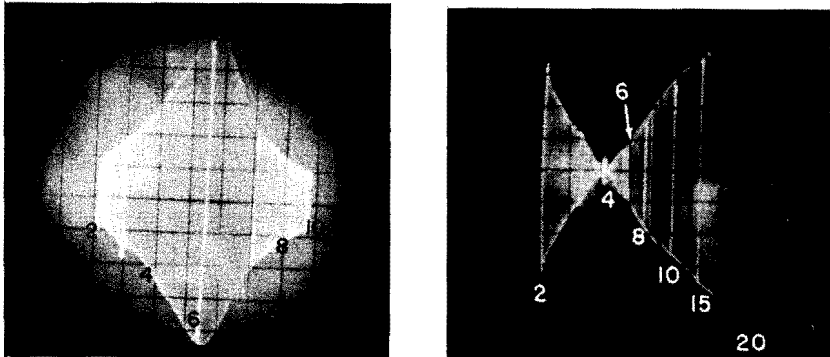
Fig. 327 (left). *Resonance curve of L-C circuit covering 200 to 1,000 cycles.* Fig. 328 (right). *Transmission curve of twin-Tee circuit between 200 and 2,000 cycles. Note the null at 400 cycles.*

tracing of amplifiers and filters operating in the af range. It is, however, necessary to use very low sweep speeds (several seconds), especially if high-Q components are involved, and a long-persistence C-R tube and dc amplifiers are required for best results. This adds to a rather complex and expensive gear if it is to work correctly. Some good af tracers are marketed, however.

A quite different method of af response curve tracing will be described using an af signal generator. The simple device of Fig. 326 is the only accessory required. Besides a push-pull dc deflection amplifier (tubes V1 and V2), it comprises a frequency-sensitive network R1-C. Provided the reactance of C is large compared with R1 at the highest frequency involved, the voltage across R1 is proportional to the frequency. This ac voltage is detected by the 1N34 diode and produces a corresponding dc voltage across the variable resistor R2, allowing for sweep amplitude control. A second control R3 is used for horizontal centering of the spot. Because of the loss introduced by the R1-C network, an input of at least 20 rms volts is required.

Prior to use, R2 and R3 are adjusted to situate the spot at the extreme left of the screen for the lowest, and at the extreme right

for the highest frequency involved, selecting a convenient input capacitor C. This rigidly links frequency and horizontal deflection and the way the sweep is varied does not matter. The af generator may be hand tuned, or motor driven. The response curve appears as a straight vertical line of varying length, wandering from one side of the screen to the other. A continuous graph is seen using a long-persistence C-R tube, or photographic recording.

By this method, the oscillograms of Fig. 327 and Fig. 328 were obtained, the former showing the resonance of an iron-cored L-C circuit, the latter the transmission curve of a twin Tee R-C filter.
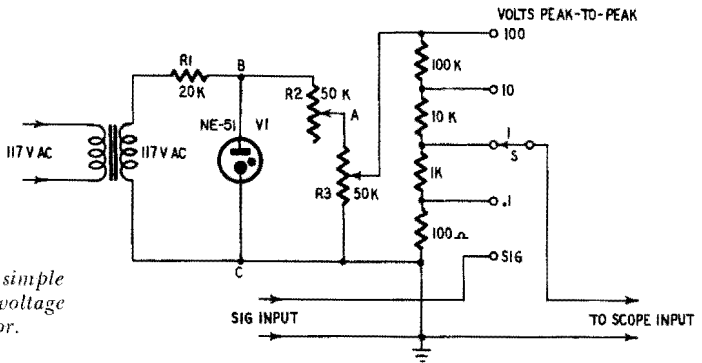
Fig. 329. *A simple neon-tube voltage calibrator.*

The frequency markings were superimposed by successive shots at fixed frequencies for reference. Because of the necessarily long-exposure, the ambient light, though reduced, produced an illuminated background. The slight irregularities in the contour of the curves are due to tuning transients of the R-C-type generator. If the output voltage is detected using a circuit of sufficiently large time constant, a single curve is obtained instead of the envelope. This however, requires a stable dc amplifier for Y-deflection.

Calibrators

Though the scope is primarily an instrument for qualitative evaluation, modern high-grade equipments often feature means for direct measurement of amplitude and time (or frequency) of the events displayed. Voltage and time measurements have been described, but these methods are comparatively slow to carry out. The calibration devices to be described are to speed-up such evaluations. They may be incorporated into existing scopes, or form easily connected adapters.

Voltage calibrators

If the gain of a deflection amplifier and the sensitivity of the
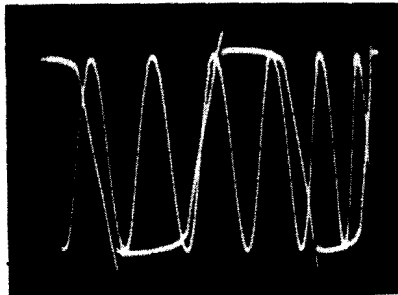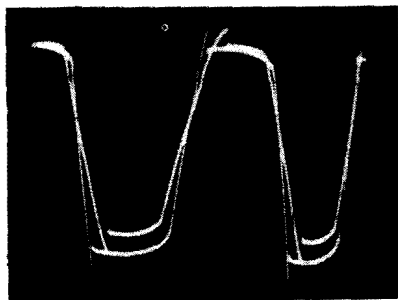
Fig. 330 (left). *The clipped-wave amplitude is fairly independent of the input voltage. Outputs are shown for 80 and 150 volt rms inputs.* Fig. 331 (right). *Method of comparing the amplitude of the clipped calibrating voltage to the size of the unknown sine wave.*

C-R tube were independent of supply voltage variations and aging effects, it would be a simple matter to calibrate the input attenuators for direct voltage reading. A good constancy of the overall deflection factor can be achieved using stabilized power supplies and inverse feedback techniques, but this implies an increase of weight and cost.
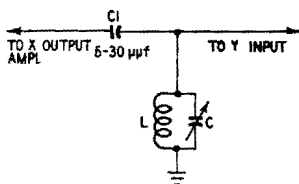
Fig. 332. *The "passive" L-C timing circuit is shock-excited into oscillation by the sweep return stroke.*

Some types of equipment use voltage-calibrated Y-shift controls. As both unknown and standard voltages act upon the deflection plates, the actual sensitivity of the C-R tube does not influence the reading accuracy, and if the calibrating voltage is injected at the amplifier input, the actual amplifier gain does not matter either. A dc amplifier is, however, required to pass the dc shift voltage.

Using an ordinary scope, the simplest method to evaluate the amplitude of a wave displayed is to substitute another wave of the same size and calibrated amplitude. Sine waves are sometimes used, but the flat top of square waves leads to easier adjustment to size and better accuracy. A constant-voltage square wave source requires, however, some involved circuitry, and the author favors the simplicity of the device to be described.

The heart of this calibrator is a small neon tube V1 connected to a 60 cps voltage by means of a series resistor R1 (Fig. 329). This

composes a very effective limiter, the positive and negative tops of the sine wave being cut as the tube ionizes. The amplitude de-limited by the flat portions is quite stable as shown in Fig. 330 where the waveforms obtained with input voltages of 80 and 150 rms volts are superimposed, the higher voltage implying, of course, a steeper slope and a more extended flat top. The pip on the lead-ing edge of the tops is due to the fact that the firing voltage is al-ways somewhat greater than the operating voltage; but this phe-nomenon does not interfere with the correct use of the device.
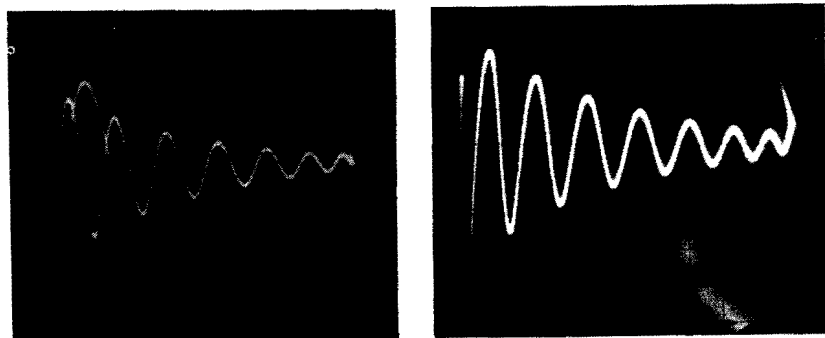
Fig. 333 (left). *Oscillogram of the damped timing oscillation which starts at the end of the linear sweep.* Fig. 334 (right). *Return-trace blanking eliminates the confusing first part of the calibrated wave. If the return trace time is short compared to sweep time, blanking is not required.*

The square wave amplitude is evaluated by substituting a 60 cps sine wave adjusted to the same size. For the neon tube used, the voltage of the sine wave was 65 rms volts; this is 91 peak volts, or 182 peak-to-peak volts, or dc volts across V1 (points B and C). If control R2 is set to leave exactly 100 peak-to-peak volts between A and C, R3 can be calibrated to read from 0 to 100, and a stepped potential divider will provide decimal attenuation of the calibrat-ing voltage. Switch S is connected to the scope input, and the signal is fed to the calibrator input terminals, and from there to the scope via S. Thus, it is a simple matter to replace the waveform displayed with the calibrating square wave by turning the switch, to set R3 for equal amplitude, and read the peak-to-peak voltage. It is even possible to evaluate the amplitude of portions of a complex wave, a feature not to be found in scopes incorporating a vtvm. The mecha-nism of comparing the calibrating square wave and an unknown sine wave (or, alternatively, a measured sine wave and the square

wave to be calibrated) is clearly shown in Fig. 331, the displays being photographically superimposed.

It is not recommended to run the device directly from the power line without interposition of an isolation transformer because of the risk of shorts and health hazards from the "live" wire. But the supply voltage is not at all critical (provided it substantially exceeds the firing voltage of the gas tube). Higher voltages, derived from any power supply transformer may be used, resistor R1 being adequately chosen.

Sweep calibration

Precision high-grade instruments generally feature a time-calibrated sweep allowing for direct measurement of the duration of an event or part thereof. This, however, requires very elaborate time bases of complex design, providing accurate timing as well as a high degree of linearity. It is much simpler to calibrate a given sweep of unknown speed and linearity characteristics by means of a suitable timing system.

Precision oscillators (possibly crystal-controlled) can be used for timing repetitive time bases only if the sweep is locked to the oscillator frequency, in order to superimpose the succeeding timing marks. This prevents setting the time base to an arbitrary repetition frequency, and limits the application of calibrating oscillators to some specific problems.

It is an easy matter to use "passive" calibrators consisting of simple L-C circuits, shock-excited by the sweep (Fig. 332). The tuned circuit, being connected to the output of the X deflection amplifier by means of a small capacitance C1, is not influenced by the (relatively slow) linear increase of the sweep voltage. The return stroke applies a pulse to L-C, and a damped oscillation starts. Its frequency depends solely on the circuit constants and thus can be considered as a good reference. Operation is fairly illustrated by Fig. 333 showing the starting of oscillation at the end of the linear sweep (at right). Because of the fairly long return time owing to the high operating frequency, several cycles are visible. Having reached the left end of the sweep, the wave is seen decreasing from left to right, and the next return stroke initiates a new damped oscillation.

As the first, right-to-left going part of the oscillation may interfere with the actual calibrating wave (from left to right), it is conveniently suppressed by blanking, as shown in Fig. 334. If the return time of the sweep is negligible compared to the forward time, the trace may be sufficiently faint to make blanking unnecessary.

Sweep calibration is carried out by removing the signal from the scope input (leaving it connected to the external sync terminal) and connecting the input of the scope to the tuned circuit L-C. To make sure that the sweep frequency remains the same (otherwise, the whole process would make no sense), it is necessary that the time base remains locked to the signal, the sync selector being set on "external sync." The sweep width control (of course, not the frequency control!) is then adjusted to make two successive positive (or negative) tops of the damped wave coincide with two vertical lines on the transparent scale placed before the screen. Assuming an oscillating frequency of 100 kc, the duration of a single cycle

Fig. 335. *Calibration of a timing wave by intensity modulation of the C-R tube grid. The modulating frequency in this case is eight times the resonant frequency of the L-C circuit.*
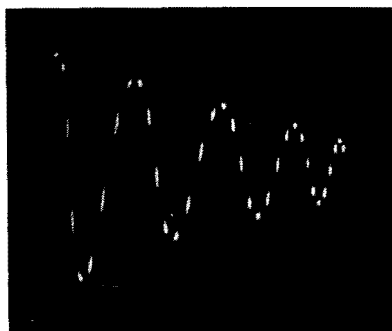
is 1/100,000 sec, or 10 μsec, and this then corresponds to the interval between the two vertical lines. Similarly, timing intervals of 1 and 100 μsec are obtained using circuits tuned to 1 mc and 10 kc respectively.

The tuned circuits can be roughly adjusted by means of a grid-dip oscillator, but a final in-circuit adjustment is necessary because of unavoidable stray capacitances. This can be carried out by modulating the grid of the C-R tube using a signal generator providing sufficient output voltage. Such an intensity modulated damped oscillation is shown in Fig. 335. The trace is seen divided into 8 dots (or spaces), and as the generator setting was 76 kc, L-C actually was resonated at 76/8 = 9.5 kc. A slight decrease of L or C would shift the frequency to 10.0 kc corresponding to an interval between two consecutive ordinates of 100 μsec.

Sweep generator markers

The calibration accuracy of wide-band sweep generators is generally poor because of the beat-frequency principle involved, implying oscillator operation at much higher frequencies. A slight

drift of oscillator frequency thus produces a notable change in the beat frequency. For this reason it is customary to rely upon independently operated marker generators for frequency calibration, and to ignore the indications of the sweep generator.

There are two basic types of marker generators: calibrated oscillators (we might call "active" calibrators), and absorption-type, or "passive" marker generators. Oscillators impress a calibrated "pip" on the trace, while absorption-type markers produce a pronounced dip at the point of the curve corresponding to the tuning frequency.

Some experience is required in using marker generators, especially of the oscillator type. Only the lowest possible signal level ought to be used if confusing patterns are to be avoided, and the injection point of the signal is to be chosen carefully. As commercial sweep generators differ widely and generally incorporate their own marker generators, this point will not be discusssed here.[1]

[1] See Sweep and Marker Generators for Television and Radio, by Robert G. Middleton. Published by Gernsback Library, Inc.

measuring electrical magnitudes

T HE oscilloscope is, above all, a device for qualitative evaluation, There are, however, some types of electrical magnitudes such as voltages, impedances, phase differences and frequency relationships that can be conveniently measured with an oscilloscope, and this may sometimes be the only practical way to evaluate them.

Measuring dc voltages

To make possible the measurement of dc voltages, the oscilloscope has to give direct access to the vertical deflection plates
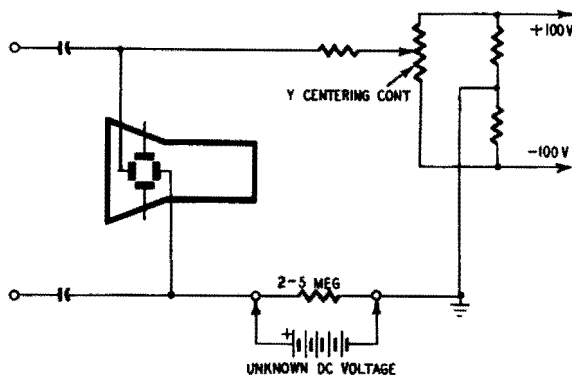
Fig. 401. *Connecting an unknown dc voltage without shorting the vertical deflection plates.*

(without interposition of any capacitor), and connection of an external circuit must not short out the vertical positioning control.
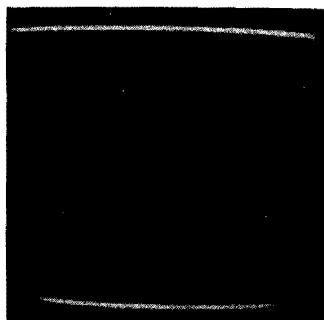
Fig. 402. *Calibration using a variable dc supply connected as in Fig. 401. The base line is shifted 3 inches.*
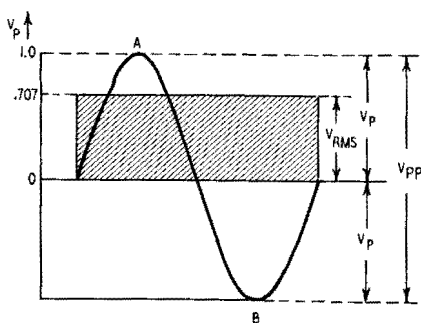
Fig. 403. *Drawing showing the relationship existing between rms, peak (maximum) and peak-to-peak alternating voltages.*

Many oscilloscopes do not feature this type of connection but can be easily modified by connecting the dc voltage to be measured across a resistor wired into one of the deflection plate leads as shown in Fig. 401. One side of this resistor should be grounded.

First of all, the instrument has to be calibrated. The time base is left running to avoid a motionless spot liable to cause screen burn. Then, the base line, positioned at the top or bottom of the screen according to the polarity of the voltage to be applied, is shifted exactly 3 inches (for a 5-inch cathode-ray tube), using a variable-voltage dc power supply, and the (external) deflection voltage is measured. The successive positions of the base line are shown in Fig. 402. On the author's type 5CP1 tube, operated with an overall acceleration voltage of 4,000, the dc deflection voltage measured was 225. Thus, the deflection factor is 225/3 = 75 dc volts per inch. (Because of manufacturing tolerances and differences of supply voltages, somewhat different values may be obtained with the same tube type.)

It is now easy to measure unknown dc voltages, the deflection being always proportionate to the applied emf. Avoid using the curved ends of the screen. Also, too small deflections are liable to introduce significant determination errors. The measurable voltage range is thus limited to, say, 10 to 300. Higher values can be measured using calibrated attenuators; lower voltages require stable dc amplifiers that may not be available.

A good practice for spotting the initial position of the trace to be shifted is to mark it with a tiny inkspot made with a fountain pen. This mark may be easily deleted later.

The accuracy of this device is poor, however. Neglecting errors

in measuring the displacement of the trace, it has to be recalled that the deflection of a C-R tube is inversely proportional to its supply voltage, itself generally proportional to the line voltage. Thus, a 10% variation of the line voltage will produce a 10% error in voltage measurement.

Measuring ac voltages

Nearly all oscilloscopes provide means for connecting ac voltages to the deflection plates. Furthermore, while the measurement of dc voltages is a somewhat dubious facility, the possibility of measuring peak-to-peak ac voltages it quite attractive.

While things are rather simple in dc, there being but one kind of voltage, there are several ways to characterize an ac voltage, and

Fig. 404. *Calibrating the C-R tube by using a variable ac voltage to produce a 3-inch deflection. The time base is turned off.*

it is very important to make them clear. Consider the sine wave of Fig. 403. Applied to the deflection plates of a C-R tube, this wave will make the spot go upward to peak A and then downward to peak B; the deflection thus is proportional to the peak-to-peak voltage V_{pp}.
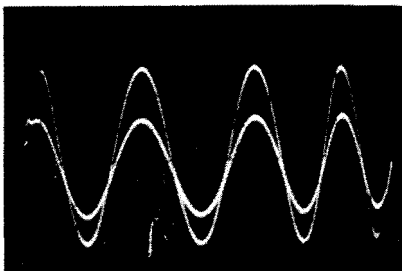
Fig. 405. *Two sine waves of equal frequency which are in phase.* $\phi = 0$. *($\phi = $ phase angle.)*
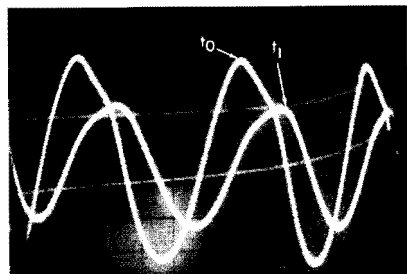
Fig. 406. *Phase difference is less than 90°. The larger wave is leading.*

Conventional vacuum-tube voltmeters offering half-wave diode detection give an indication proportional to the peak voltage V_p,

(or half the peak-to-peak voltage V_{pp}) provided the wave is symmetrical with regard to the base line. This relationship is upset by the presence of even harmonics.

The rms voltage V_{rms} is the ac voltage dissipating in a resistor the same amount of heat as a dc voltage of same magnitude. This dc voltage of the same "thermal efficiency" is represented in Fig. 403 by the cross-hatched rectangle of ordinate $V_{rms} = 0.707\ V_p$. *This holds true only for a pure sine wave.* It is easy to understand
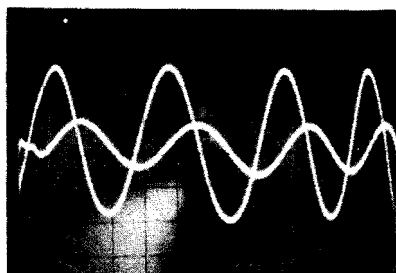
Fig. 407. *Two sine waves in quadrature.* $\phi = 0$. *The peak of one wave occurs simultaneously with the zero base point of the other.*
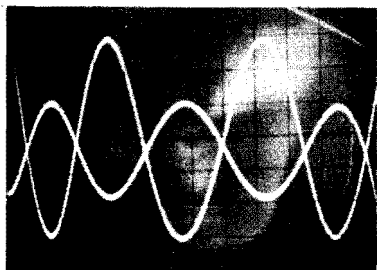
Fig. 408. *Two sine waves of opposite phase. The zero axes coincide but the peaks of the waves are opposite to the valleys.*

that for a square wave, $V_{rms} = V_p$ and, on the other hand, if the wave considered is composed of narrow pulses, V_p can be very high, V_{rms} nevertheless remaining small. This explains why there are two ways of evaluating voltages. If one is interested in dissipated power, the rms voltage is to be measured; on the other hand, the breakdown of dielectrics depends upon the peak (or peak-to-peak) voltage.

To calibrate the C-R tube, a variable ac voltage is applied to the Y deflection plates to obtain a 3-inch line as shown in Fig. 404. (There is no need for running the time base here.) The voltage (which can be conveniently adjusted by means of a Variac) was measured with an rms voltmeter that read 80 rms volts. Thus, the deflection factor is $80/3 = 27$ rms volts per inch, *provided we are concerned with a pure sine wave.* Transforming into peak-to-peak volts: $80/0.707 = 112.5$ peak volts, or $112.5 \times 2 = 225$ peak-to-peak volts. The deflection factor then is: $225/3 = 75\ V_{pp}/$inch. Note that the deflection factor in dc and in V_{pp} per inch is expressed by the same number. Thus, it is necessary to carry out only one of the two calibration operations. This being done, ac voltages can be measured as described for dc voltages. If evaluation is made in terms of peak-to-peak volts, the result is independent of the wave-
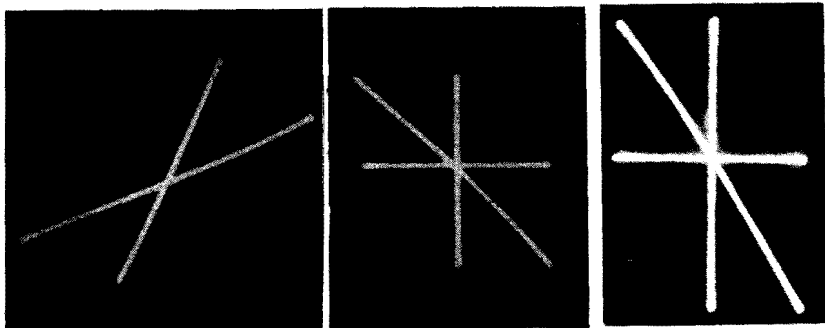
Fig. 409 (left) . *X and Y voltages are phased. The slopes of the straight lines depend upon their relative amplitudes.* Fig. 410 (center). *Phase opposition. The voltages are of equal amplitude. This display was obtained by triple exposure.* Fig. 411 (right) . *Phase opposition. Dissimilar amplitudes are evidenced by the slope of the reference line.*

form. That's why the use of the cathode-ray tube to measure amplitude of pulses and complex waveforms is very attractive. Of course, the limitations indicated concerning the accuracy to be expected still hold.

Evaluating phase relations

Before describing the measurement of the phase difference of two sine waves of same frequency, let us show the physical representation of these waves. The waves of Fig. 405 are in phase—the phase angle is $0°$. Fig. 406 shows a phase difference of less than $90°$. The voltages of Fig. 407 are in quadrature, that is, the phase angle is $90°$. Note that the top of one wave occurs simultaneously with the base-line crossing of the other. The waves displayed in Fig. 408 are $180°$ out of phase; a positive top of one wave is simultaneous with a negative top of the other.

To know which wave is leading, refer to Fig. 406. At a given instant t_0, the large-amplitude wave attains its apex. The same happens to the smaller wave at a time t_1 a little later (because the sweep goes from left to right). Thus, the leading wave is the larger one, although at first glance, one might think the contrary.

If their amplitudes are sufficient, the deflection voltages can be applied directly to the Y and X plates of the C-R tube. It is, however, more convenient to use the regular amplifiers. But remember that amplifiers introduce a phase distortion of their own toward the ends of their frequency transmission range, causing errors at these frequencies. (Some oscilloscopes feature identical Y and X amplifiers, cancelling the phase distortion in the resulting pattern.)
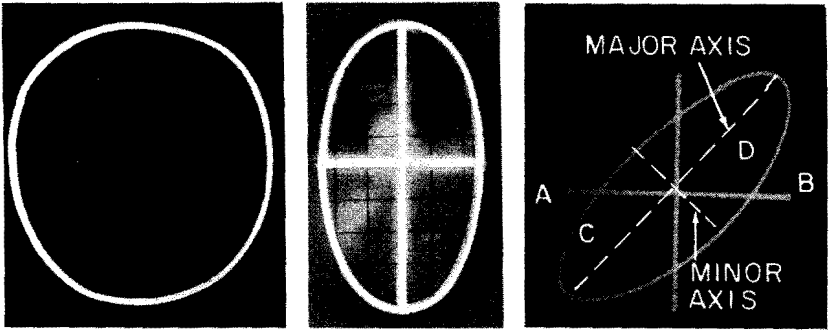
Fig. 412 (left). *Quadrature voltages* ($\phi = 90°$ *or* $270°$). *The applied voltages are of equal amplitude.* Fig. 413 (center). *Quadrature voltages of unequal amplitudes. The principal axis of the ellipse can be either vertical or horizontal.* Fig. 414 (right). *Tilted ellipse showing intermediate phase angle* ($\phi = 42°$).

First of all, the zero phase reference has to be determined by tying together the Y and X inputs and applying a sine-wave voltage to both. This will result in a straight line extending from the lower left to the upper right, such as one of those displayed in Fig. 409. It is quite possible for the line to go from the lower right to the upper left as shown in Fig. 410 and 411. This depends upon the way the deflection plates are connected and the number of amplifier stages involved. But it is important to make sure which position actually corresponds to a zero phase angle. On our scope, phase was $0°$ for Fig. 409 and $180°$ for Fig. 410 and 411. Should the opposite occur in your scope, just add $180°$ to the computed phase angles. Of course, $180° + 180° = 360° = 0°$. The slope of the line indicates only the relative amplitudes of the two voltages, the phase

Fig. 415. *Tilted ellipse indicating a phase angle somewhere between 90° and 180°.*
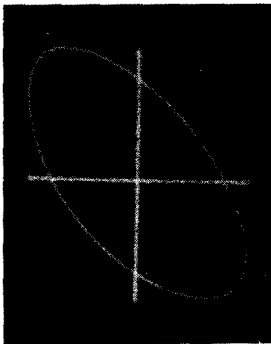
Fig. 416. *Measuring impedances with a calibrated resistor.* (Y, *vertical deflection*; X, *horizontal deflection*).
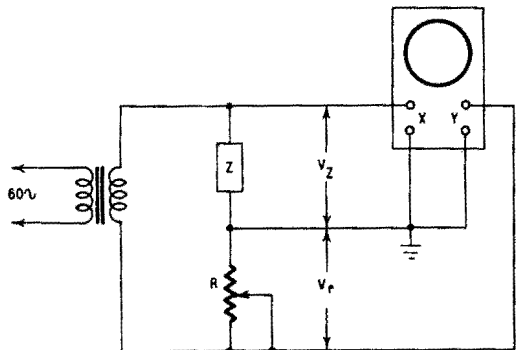
relationships being the same. Figs. 410 and 411 were obtained by a triple exposure displaying the two component voltages separately and together. Equal amplitudes result in a line having a slope of 45° (Fig. 410). Two such lines corresponding to different voltage ratios are shown in Fig. 409.

If the two voltages are in quadrature (90° or 270°), the pattern becomes a circle (Fig. 412) or an ellipse, the great axis of which is either horizontal or vertical (Fig. 413). Besides these special cases, there are the intermediate phase angles indicated by tilted ellipse patterns. Fig. 414 indicates a phase angle between 0° and 90° (or 180° and 270°) and Fig. 415 one between 90° and 180° (or 270° and 360°).

The actual phase angle can be calculated in the following manner: The distances AB and CD are measured on the screen or,
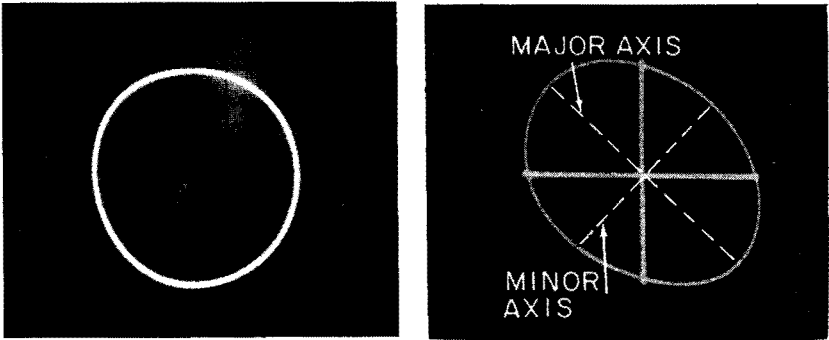
Fig. 417 (left). *When a capacitor of negligible loss at the line frequency is substituted for Z in Fig. 416, a circle is obtained.* Fig. 418 (right). *Oscillogram used for measuring the inductance and resistance of a filter choke.*

if possible, on a print. Thus for Fig. 414 AB = 15/16 or 0.937 inch, and CD = 5/8 or 0.625 inch. Now we have:

$$\sin \phi = CD/AB = 0.625/0.937 = 0.667$$

The phase angle ϕ can be obtained from a sine function table or a slide rule. Thus we found $\phi = 42°$ (or $42 + 180 = 222°$).

There is still another method of phase-angle evaluation that can be carried out more easily on the screen. Provided the horizontal and vertical axes traced in Fig. 414 are equal, let us call D the major axis of the ellipse and d the minor axis. Then $\tan \phi/2 = d/D$. Evaluating the two lengths on the print, we find d = 15/32 or 0.47 inch, and D = 1-1/4 or 1.25 inches. Thus $\tan \phi/2 = 0.47/1.25 = 0.37$. From this we get: $\phi/2 = 21°$, and $\phi = 42°$ as above.

Measuring impedances

The impedance Z to be measured is series-connected with a calibrated decade resistor R (Fig. 416). A transformer is used to supply a balancing voltage of 60 cycles. Another frequency may be used, provided it is of known value and reasonably free of distortion. The voltages V_z and V_r across Z and R are applied to the X and Y input terminals, respectively. It is necessary first to equalize the deflection sensitivities in both directions.

We now connect a capacitor of 0.1 µf in place of Z. As the loss factor of such a capacitor is negligible at line frequency, an ellipse oriented horizontally or vertically will be displayed on the screen.

Fig. 419 (left). *Lissajous figure where $f_y/f_x = 2$.* Fig. 420 (center) . $f_y/f_x = 2$. *The two loops are superimposed, but are nevertheless counted.* Fig. 421 (right). $f_y/f_x = 3$.

This ellipse will become a circle if the capacitance equals the resistance, or $1/2\pi fC = R$ (provided the amplifiers are correctly equalized). This will occur when R is 26,400 ohms, and Fig. 417 shows the circle obtained. It lacks perfect roundness because of the presence of a slight distortion in the line frequency.

Now connect a filter choke in place of Z. The resulting ellipse is somewhat tilted, indicating that the choke is not a "pure" reactance
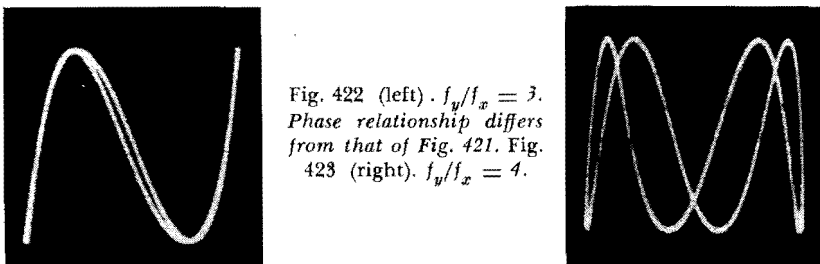
Fig. 422 (left) . $f_y/f_x = 3$. *Phase relationship differs from that of Fig. 421.* Fig. 423 (right). $f_y/f_x = 4$.

and that its losses are not negligible. Adjusting R for equal length results in the oscillogram of Fig. 418. Now the reactance equals the resistance, or $2\pi fL = R$. As R = 2,400 ohms, L = R/2\pi f = 2,400/2\pi 60 = 6.35 henries.
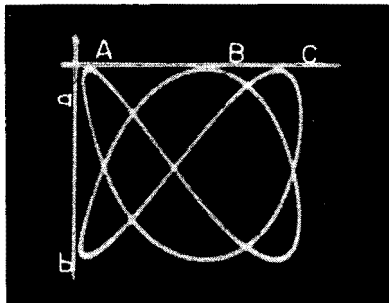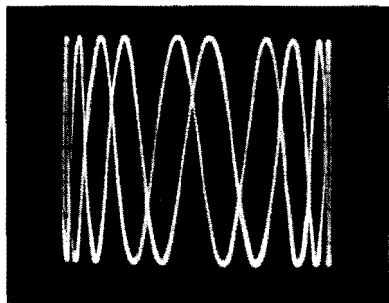
Fig. 424 (left) . $f_y/f_x = 10$. Fig. 425 (right). $f_y/f_x = 3/2$. *There are three tangent loops horizontally and two vertically.*

Measuring on Fig. 418 the length of the axes of the ellipse, we find D = 1-1/16 or 1.06 inches, and d = 13/16 or 0.81 inch. It follows that tan $\phi/2$ = d/D = 0.76, $\phi/2$ = 37.5° and ϕ = 75°. To find the ohmic resistance r of the choke, we have tan ϕ = X_L/r = R/r. As tan ϕ = 3.73, we have r = 2,400/3.73 = 643 ohms. This method obviously does not have great accuracy and there is no point in looking for the fifth decimal.

Lissajous patterns for frequency comparison

Jules-Antoine Lissajous found out that the composition of two sine waves results in a peculiar, closed-line pattern. Curiously enough, his discovery was not made with the oscilloscope in mind, for he died in 1880.

Lissajous figures are easy to obtain. The time-base generator being inoperative, the standard frequency f_x is applied to the input terminals of the X amplifier and the unknown frequency f_y to the Y input. (Direct connection to the deflection plates may be used if sufficiently large voltages are provided.) A moving pattern inscribed in a rectangle or square results; it becomes stationary if f_y/f_x is a whole or fractional number. If one of the frequencies drifts slightly, the pattern turns around its horizontal or vertical axis and seems to be traced on a rotating transparent cylinder.

The calibration of variable-frequency oscillators is an important application of Lissajous figures for frequency comparison, and we will show how to interpret these patterns when calibrating the 200–2000-cycle range of an audio oscillator. A 500-cycle tuning-fork frequency standard was used. The 60-cycle line frequency might have been used as a standard but its use leads to more complicated calculations.

Starting with $f_y = f_x = 500$ cycles, an ellipse is obtained, widen-

ing to become a circle (if the deflections in both directions are equal) and narrowing in a straight line, according to the phase relationships. Let us now increase the frequency of the audio oscillator. For $f_y = 1,000$ cycles $(f_y/f_x = 2)$, we obtain a pattern such as Fig. 419, showing two loops on the top (or on the bottom) of the pattern. This oscillogram seems to be written on a transparent cylinder turning around a *vertical* axis, *as is always the case if f_y is greater than f_x*. Thus, for a different angular position of the virtual cylinder, the forward and return traces may be superimposed as shown in Fig. 420. There are still two loops to be counted, for a Lissajous figure is always endless, like a snake that bites its tail.
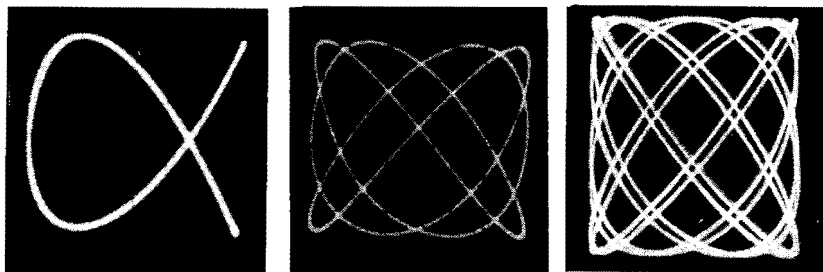
Fig. 426 (left). *Another aspect of* $f_y/f_x = 3/2$. Fig. 427 (center). $f_y/f_x = 4/3$. Fig. 428 (right). $f_y/f_x = 8/7$.

For $f_y = 1,500$ cycles $(f_y/f_x = 3)$, the oscillograms of Figs. 421 and 422 were obtained, showing different phase relations. The four loops on the top of Fig. 423 indicate a frequency ratio of 4, or
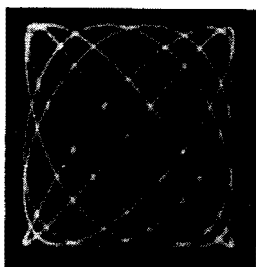
Fig. 429 (left). $f_y/f_x = 6/5$.
Fig. 430 (right). $f_y/f_x = 5/4$.
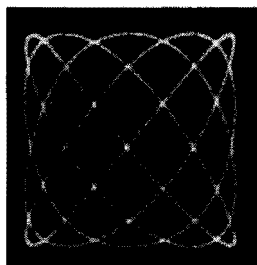
$f_y = 2,000$ cycles. This ends the range but, for the sake of completeness, the oscillogram corresponding to $f_y = 5,000$ cycles $(f_y/f_x = 10)$ is shown in Fig. 424.

These easily identified significant calibration points will now be completed by some intermediate points. Figs. 425 and 426 show two aspects of the ratio $f_y/f_x = 3/2$, corresponding to $f_y = 750$
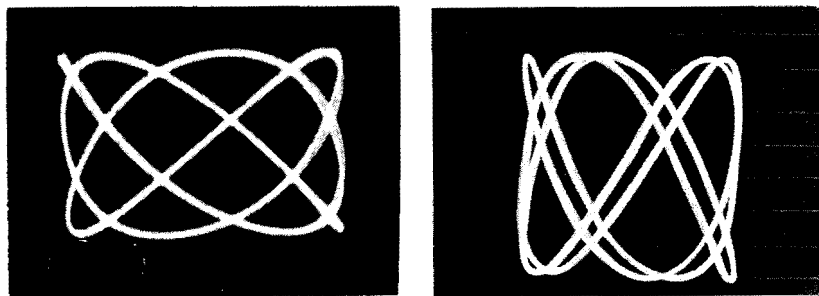
Fig. 431 (left). $f_y/f_x = 7/5$, *not 4/3. The superimposed traces create an illusion.*
Fig. 432 (right). $f_y/f_x = 5/3$.

cycles. To understand the method of determination of the frequency ratio, refer to Fig. 425 where two straight lines tangent to the top and a side of the oscillogram are traced. We have the ratio

$$f_y/f_x = \frac{\text{number of loops tangent to the horizontal line}}{\text{number of loops tangent to the vertical line}}$$

Having three loops (A, B, C) tangent to the horizontal line and two loops (a, b) tangent to the vertical line, we have $f_y/f_x = 3/2$. Fig. 427 shows four loops tangent to an (imaginary) horizontal line, and three loops on each side; thus, $f_y/f_x = 4/3$ and $f_y = 666\text{-}2/3$ cycles. Figs. 428 to 436 show a certain number (by no ways exhaustive) of such frequency ratios, and it is easy to learn to interpret them.

We now tune the audio oscillator to frequencies lower than the standard frequency. *These patterns seem to turn around a horizontal axis.* For $f_y/f_x = 1/2$ ($f_y = 250$ cycles), the oscillogram of Fig. 437 was obtained. This is *exactly the same pattern* as displayed in Fig. 419 *but rotated 90°.* You may compare, too, Fig. 438 showing a frequency ratio of 2/5 ($f_y = 200$ cycles) with Fig. 435 ($f_y/f_x = 5/2$) and Fig. 439 (ratio 2/3, $f_y = 333\text{-}1/3$ cycles) with Fig. 425 for a ratio of 3/2. Thus, it is deemed unnecessary to present a large number of oscillograms for $f_y/f_x < 1$.

Lissajous patterns with distorted waves

The diagrams shown thus far are generated by two sine waves. If one or both waves are distorted, more or less confusing patterns may result.

Figs. 440, 441 and 442 showing frequency ratios f_y/f_x of 2, 4 and 2/3, respectively, were obtained with Y input voltages of triangular waveform derived from the filter input capacitor of a conventional power supply. Note the resulting sharp edges. Applying a 60-cycle
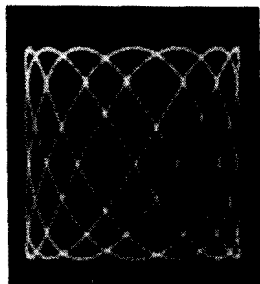
Fig. 433 (left). $f_y/f_x = 7/4$.
Fig. 434 (right). $f_y/f_x = 9/5$
(a bit difficult to count).
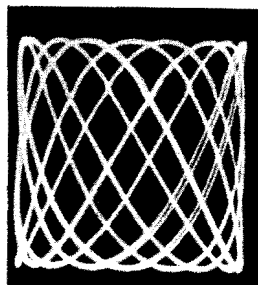
square wave to the Y input and a 60-cycle sine wave to the X terminals resulted in Figs. 443 and 444, corresponding to the circle and the straight line of the 1/1 ratio figure. Because of the rapid rise of the square wave, the vertical lines of the diagram are not visible; if they were, Fig. 443 would show a square and Fig. 444 a Z-like figure. Fig. 445, corresponding to a frequency ratio of 3/1 (to be compared with Fig. 421), is still more difficult to interpret, and so we will not proceed further this way.

The two diagonally positioned points of Fig. 446 result from applying square waves of same frequency and phase to both inputs. This is in fact a sloped straight line, but, because of the very short rise and fall times of the square wave, the spot passes almost instantly from one extreme position to the other, and stays there for a relatively long time because of the flat top and bottom of the wave, generating no displacement. With a phase difference of 90° between two square waves of the same frequency, four points representing the corners of a square (or rectangle) will be obtained, corresponding to a quadrature circle or to the half-written square of Fig. 443. The number of such distorted Lissajous figures being infinite, their interpretation has to be left to the ingenuity of the technician or engineer. If the frequency of such waves is to be determined, transformation into a sine wave (by filtering, for instance) should be considered.

Amplitude-modulated circle

The methods to be described now make use of a quadrature circle generated by the standard frequency f_s and modulated by the unknown frequency f_u. There are different ways to determine the ratio f_u/f_s. A phasing bridge is always required to generate the circle, but there are various methods of modulating it.

Connecting f_u between the "cold" terminal of the phasing bridge and the "ground" terminal of the scope (Fig. 447) results in patterns somewhat similar to crown wheels such as Fig. 448, showing a
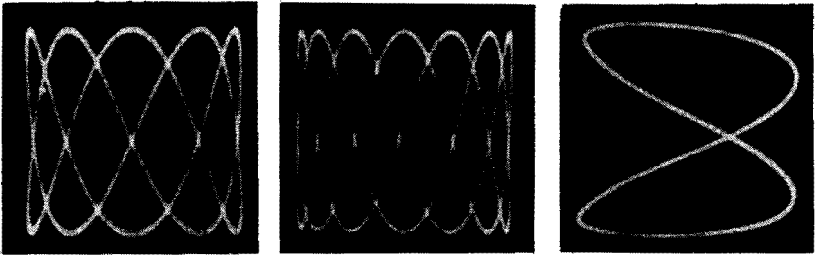
Fig. 435 (left). $f_y/f_x = 5/2$. Fig. 436 (center). $f_y/f_x = 7/2$. Fig. 437 (right). $f_y/f_x = 1/2$. Compare this photo with that shown in Fig. 419.
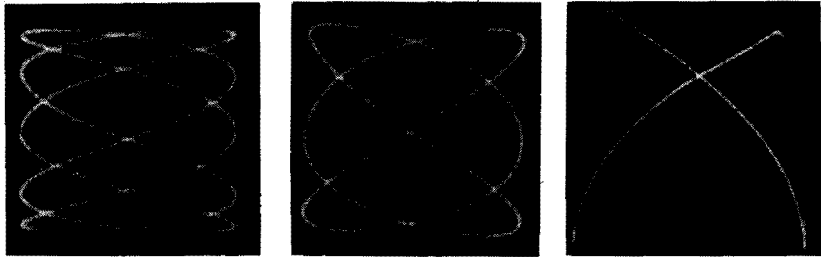
Fig. 438 (left). $f_y/f_x = 2/5$. Compare this with the photo shown in Fig. 435. Fig. 439 (center). $f_y/f_x = 2/3$. Compare with Fig. 425. Fig. 440 (right). $f_y/f_x = 2$. The waveform of f_y is triangular.
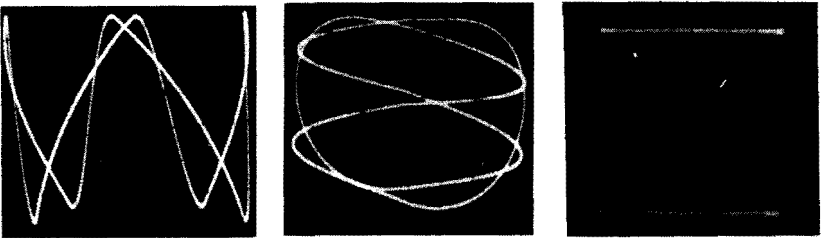
Fig. 441 (left). $f_y/f_x = 4$. The Y voltage is triangular. Fig. 442 (center). $f_y/f_x = 2/3$. The Y voltage is triangular. Fig. 443 (right). Equal frequencies. The Y voltage is a square wave.
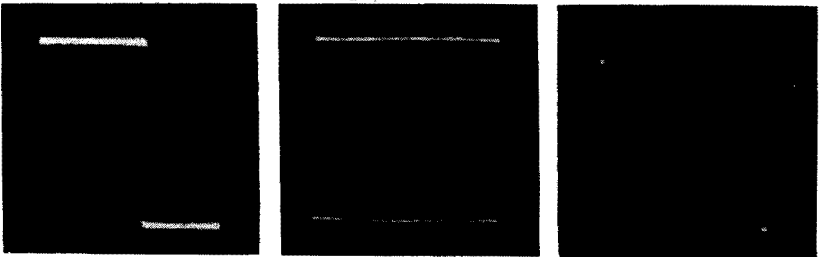
Fig. 444 (left). Same as Fig. 443, but phased differently. Fig. 445 (center). $f_y/f_x = 3$. The Y voltage is a square wave. Fig. 446 (right). Square waves of the same frequency and phase result in two diagonally positioned points.
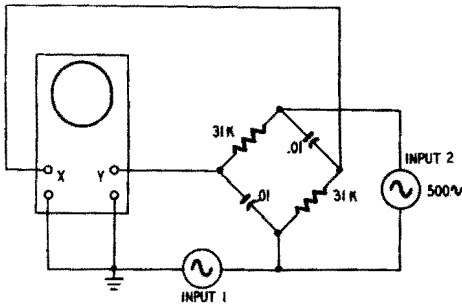
75
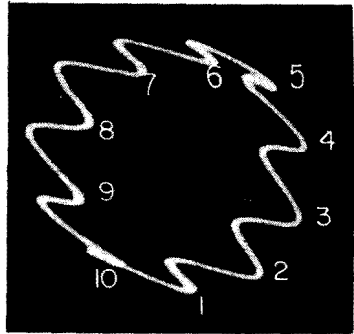
frequency ratio $f_u/f_s = 10$. To know this ratio, one has to count the *number of teeth on the same side of the crown wheel;* for convenience they have been numbered from 1 to 10. Some of them such as tooth No. 10 may not be very distinct, and it is important not to omit any one of them. Of course, counting the teeth on the opposite side of the crown will lead to the same result. A slowly rotating wheel makes counting obviously difficult if not impossible, but the teeth appear more distinctive than in the photo.

Fig. 449 represents the easily interpreted ratio $f_u/f_s = 5$. There are three teeth in Fig. 450, thus $f_u/f_s = 3$. Fig. 451 is more difficult to interpret; there is one tooth for two revolutions, or half a tooth for one, and $f_u/f_s = 1/2$. This indicates that the present method (and all other systems using circle modulation) is best suited for a value of f_u greater than f_s. The oscillogram of Fig. 452 shows a

Fig. 449 (left). $f_u/f_s = 5$. Fig. 450 (right). $f_u/f_s = 3$.
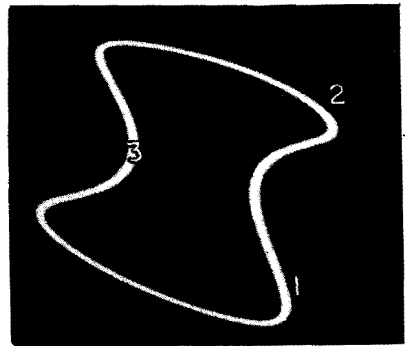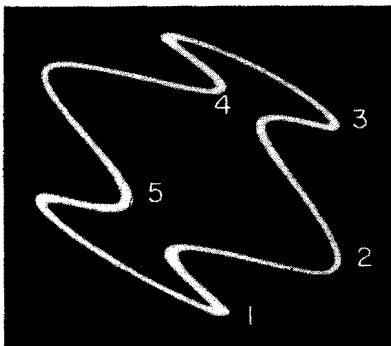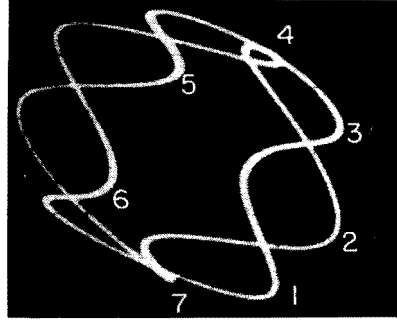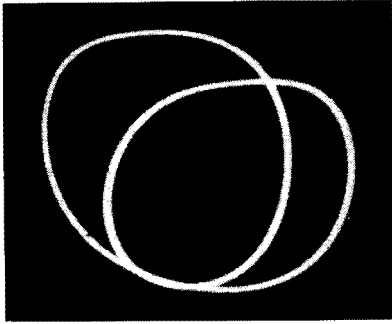
double-trace wheel supporting seven teeth. Dividing the number of teeth by the number of traces, we obtain $f_u/f_s = 7/2$.

Note that this type of pattern does not always allow for easy counting, especially' on the sides of the crown. By means of the circuit of Fig. 253 (described in Chapter 2) a gear-wheel pattern such as Fig. 453 is obtained, showing clearly six teeth. Thus, $f_u/f_s = 6$. This type of display permits determination of somewhat intricate ratios (at least on the print!). If you are patient enough, you will count 20 teeth in Fig. 454; thus, $f_u/f_s = 20$. Fig. 455 displays one tooth for two revolutions: $f_u/f_s = 1/2$ (compare with Fig. 451). Fig. 456 features 13 teeth and a double trace, and so we have $f_u/f_s = 13/2$. In the oscillogram of Fig. 457 we count 11 teeth and 3 traces, obtaining $f_u/f_s = 11/3$. These odd ratios are presented to prove the merits of this method; simpler ratios are of course easier to determine.

Intensity-modulated circle

This method is very easy to carry out. The quadrature circle

77
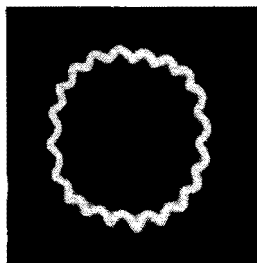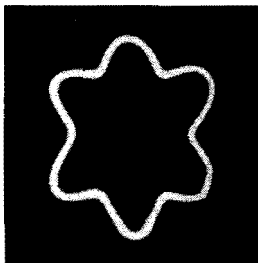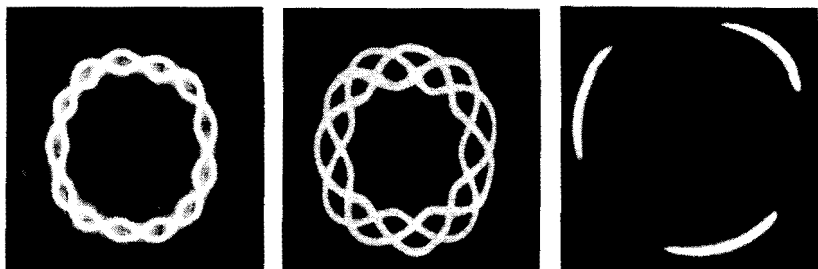
Fig. 456 (left). $f_u/f_s = 13/2$. *Thirteen teeth, two traces.* Fig. 457 (center). $f_u/f_s = 11/3$. *Eleven teeth, three traces.* Fig. 458 (right). *Intensity-modulated circle.* $f_u/f_s = 3$.

being generated by f_s as above, f_u is applied to the control grid of the C-R tube to modulate the beam intensity. For $f_u/f_s = 3$, for instance, the circle will be interrupted 3 times as shown in Fig. 458, and the 10 marks or spaces of Fig. 459 indicate a ratio of 10. For $f_u = f_s$, a half-circle is obtained (Fig. 460), and the 40 dots of Fig. 461 indicate a ratio of 40. To count 40 dots on the screen of a C-R tube, an absolutely motionless pattern is necessary and it will be useful to mark with a fountain pen the beginning of the count.

Very neat dots or spaces can be obtained using a square wave or pulses instead of the sine wave to modulate the circle. It is easy to understand that no fractional ratios can be displayed this way, and misleading diagrams may be obtained for a value of f_u less than f_s for, at a given point, the circle will be interrupted once for several revolutions.

Use of markers for frequency or time measurement

Instead of intensity-modulating a quadrature circle, we can modulate the waveform displayed by means of a time base, enabling

Fig. 459 (left). $f_u/f_s = 10$. Fig. 460 (right). $f_u = f_s$.
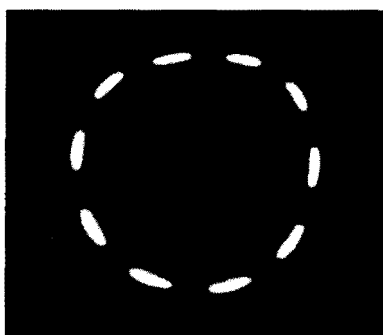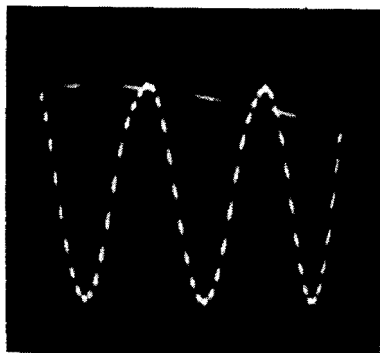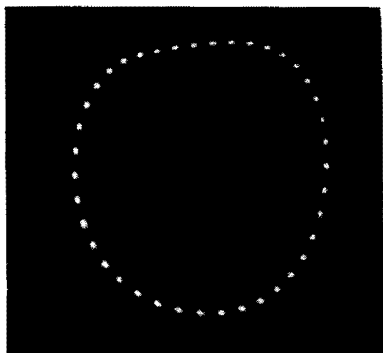
Fig. 461 (left) . $f_u/f_s = 40$. Fig. 462 (right) . *Intensity modulation of a 500-cycle sine wave with a 10-kc voltage.*

us to study simultaneously the waveform and the frequency of the voltage examined. Fig. 462 shows a 500-cycle sine wave intensity-modulated by a 10-kc voltage. Counting the number of dots from one apex to the next, we find a ratio of 20.

This method presents, however, a different and more interesting aspect. The modulation provides a fair means for timing the wave or event. The duration of a period of a 10-kc wave is 1/10,000 second, or 100 µsec. This equals the distance between two consecutive dot or space centers and allows for easy determination of the duration of some portion of the wave. The simple sine wave of Fig. 462 does not yield many indications but we can see that the duration of the flyback is 500 µsec (five spaces) and that the spot slows down considerably when writing the tops of the wave, for the spaces become quite narrow.

Fig. 463 (left) . *Comparing frequencies by means of an electronic switch. The frequency ratio is 2 to 1*. Fig. 464 (right) . *Superimposed traces, 2-to-1 ratio.*
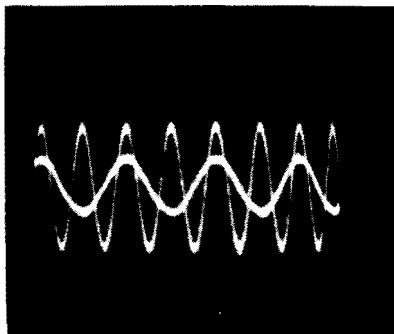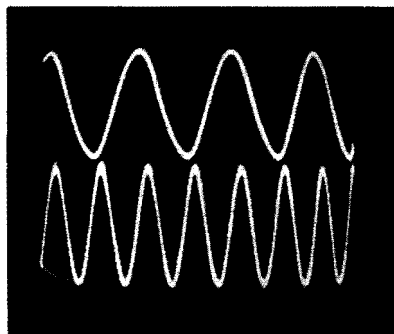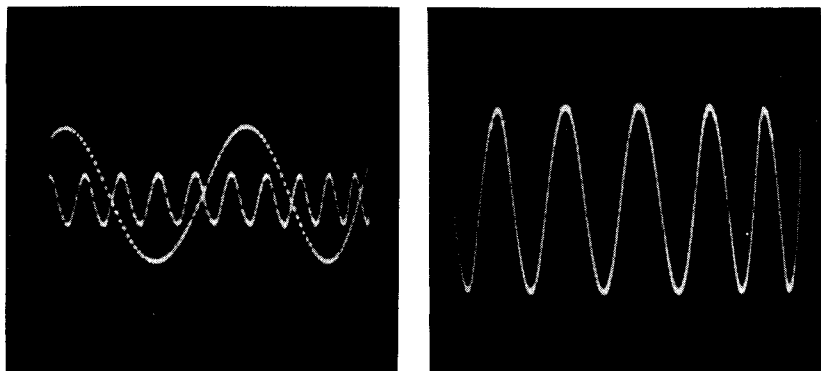
Fig. 465 (left). *Frequency ratio of 10 to 2 or 5 to 1.* Fig. 466 (right). *Time base running at 1/6 of signal frequency.* $f_y/f_x = 6$.

Just as the quadrature circle can be amplitude- or intensity-modulated, some sort of amplitude modulation of the waveform can be accomplished for timing or frequency measurement by introducing marker "pips." This method is widely used for the calibration of wide-range frequency sweep generators. It is, however, not recommended for general use for the pips are liable to modify the waveform displayed and their generation and super-position are more complicated than those of intensity markers.

Comparing frequencies with an electronic switch

An electronic switch can also be used to determine frequency relations, and this method is especially useful when odd-shaped waveforms are involved. To avoid errors in frequency determination, an electronic switch of the type shown in Fig. 302 in Chapter 3 is preferred, and the switching frequency is chosen higher than the sweep frequency. The optimum operating condition (half-frequency operation) is not recommended here because the duration of the successive sweeps may be different, thus omitting one or more cycles or parts thereof. The return trace should not be blanked in order not to hide cycles occurring during the return time.

Figs. 463 and 464 display two sine waves of 500 and 1,000 cycles, respectively. The frequency ratio of 2 to 1 is easy to note, for there are 4 cycles of one wave for 8 cycles of the other. Superimposition of the traces (Fig. 464) may lead to easier evaluation. A frequency ratio of 10 to 2, or 5, is shown in Fig. 465.

To display these patterns, the time base is synchronized with
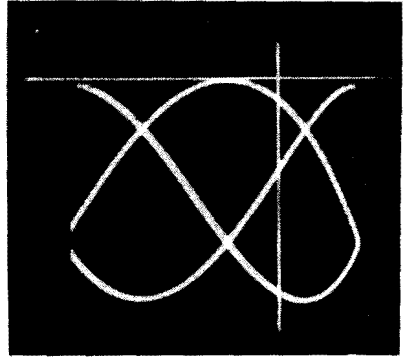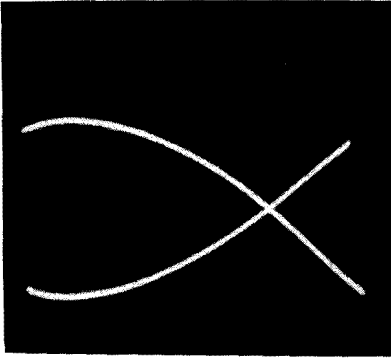
Fig. 467 (left). *Time base running at twice the signal frequency.* $f_y/f_x = 1/2$. Fig. 468 (right). $f_y/f_x = 2/3$. *There are two complete loops tangent to the horizontal line and three traces crossing the vertical line.*

one of the signals, locking its trace. The other one will come to a standstill only if its frequency is an exact multiple or submultiple of the first. The switching multivibrator may be left running free.

Evaluating running frequency of time base

The time-base generator cannot be used for determination of the frequency of a signal for its repetition frequency is generally known only approximately and is readily altered by a slight amount of sync. It is, however, necessary to be able to evaluate it.

The time base is normally operated to display between 1 and, say, 10 cycles of the wave under study; for best study of the waveform 3 or 4 cycles should be traced. In Fig. 466, almost 6 cycles are visible. There are 6 peaks at the bottom and at the top of the oscillogram, taking into account the flattened peak traced on the

Fig. 469 (left). $f_y/f_x = 3/2$. Fig. 470 (right). $f_y/f_x = 3/4$.
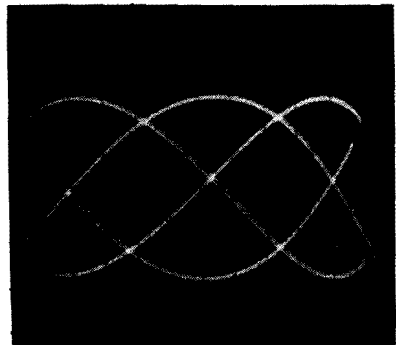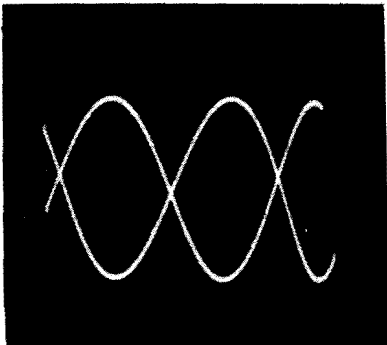
return stroke. To display 6 cycles, the time base has to run at 1/6 of the signal frequency. Calling f_y the signal frequency and f_x the sweep frequency, we have here $f_y/f_x = 6$.

Things are slightly more complicated if there are several traces. Fig. 467 shows only one *complete* loop at the top or at the bottom but there are two traces. This means $f_y/f_x = 1/2$. To state a general rule, consider Fig. 468 where two auxiliary lines have been drawn, a horizontal one tangent to the loops and a vertical one crossing all the traces present. Here is the formula:

$$f_y/f_x = \frac{\text{number of complete loops on the topside}}{\text{number of traces crossed}}$$

As there are 2 complete loops and 3 traces crossed, we obtain $f_y/f_x = 2/3$. Compare this pattern with Fig. 469 where we have 3 loops and 2 traces, resulting in $f_y/f_x = 3/2$. A frequency ratio of 3/4 is found for Fig. 470, and Fig. 471 yields the ratio 7/5

There is generally no point in accurate determination of the running frequency of the time base. Knowing how to interpret
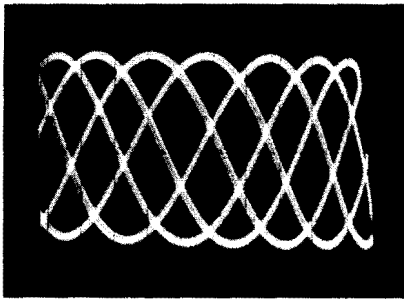
Fig. 471. $f_y/f_x = 7/5$.

these oscillograms may, however, avoid hesitation about the direction the frequency controls are to be varied to obtain the desired form of display. Generally speaking, if there is too great a crowding of the waveform, the frequency is set too low; if more or less horizontal lines appear, the operating frequency is too high.

networks and waveforms

I N the techniques of television, radar and electronic computers, the generation and use of special waveforms are of the utmost importance. The oscilloscope is the only practical device to visualize them. Some fundamental networks are used to shape and to transform these waveforms.

Harmonic content of sine wave

Among all possible waveforms, the "pure" sine wave is unique in that it is composed of but one frequency. It can be shown mathematically (and even experimentally, using a device called a waveform synthesizer) that any waveform can be generated by adding to a sine wave (called the fundamental) a number of components of suitable amplitude and phase whose frequency is a multiple of the fundamental. These components are called harmonics and their order indicates their relationships to the fundamental frequency. Thus, the second harmonic of a 60-cycle sine wave is twice that frequency, or 120-cycles, and the third harmonic is a 180-cycle component. In a distorted wave, the lower harmonics are generally of greatest importance (up to the fifth), but the correct reproduction of a square wave may need as many as 20 correctly phased and sized harmonics.

A sine wave is said to be distorted if it contains harmonics. Harmonics are generated by nonlinear devices such as detectors and incorrectly operated amplifiers. The photo of an oscillogram can give an idea of the type and amount of harmonics present, and so we will show some waves of known harmonic content. Comparison
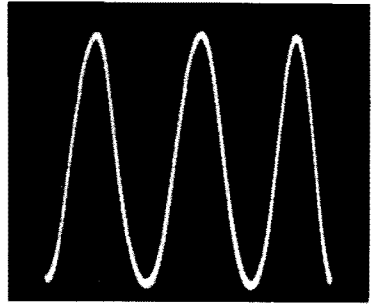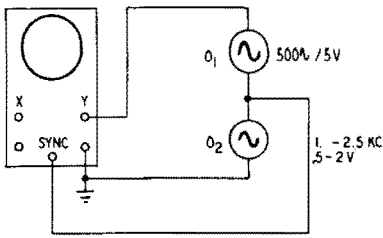
Fig. 501 (left). *Circuit used for synthesizing waves containing predetermined amounts of harmonic distortion.* Fig. 502 (right). *10% second harmonic is hardly discernible. Note the slight spreading of the trace.*

between these waveforms and those actually displayed on the screen of a C-R tube will allow for a rough approximation of the type and amount of harmonic content.

All possible varieties of waveforms can be produced at will by means of a waveform synthesizer, an apparatus generating a fundamental and a number of harmonic oscillations and providing means for mixing component waves of adjustable amplitude and phase. A simple (but rather imperfect) substitute for such an elaborate gear is the circuit shown in Fig. 501, which we used to produce the waveforms. There is a fixed-frequency 500-cycle tuning-fork oscillator O_1 and a variable frequency oscillator O_2. They are series-connected to the Y input of the scope. (We did not use the line frequency as a fixed-frequency scource because of its harmonic content.) With this type of connection, the output impedance of O_2 has to be rather low if hum voltage is not to be superimposed upon the output of O_1. The time base has to be synchronized externally

Fig. 503 (left). *20% second harmonic. The tops are flattened on one side only.* Fig. 504 (right). *30% second harmonic. Note the double-humped nature of the peaks. This phenomenon becomes pronounced as the percentage of distortion increases.*
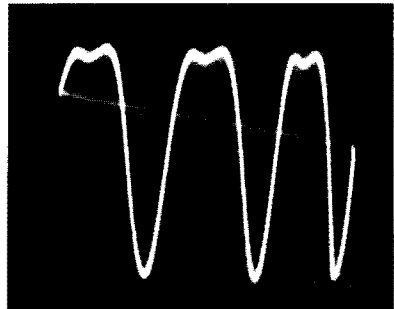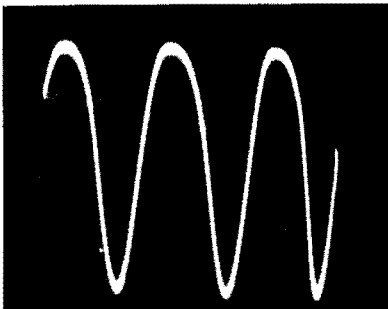
by O_2, and not internally by the composite voltage if sync jitter is to be avoided. Needless to say, some patience is required to set the variable oscillator to an exact multiple of the fixed frequency for a time long enough to make a photograph.

The operating princple is rather simple. To generate harmonics 2, 3, 4 and 5, O_2 is set on 1,000, 1,500, 2,000 and 2,500 cycles, respec-

Fig. 505 (left). *40% second harmonic. The photo shows flattening at the bottom but flattening can also occur on the top of the wave.* Fig. 506 (right). *30% second harmonic as in Fig. 504, but the phasing is different. The wave seems much less distorted.*
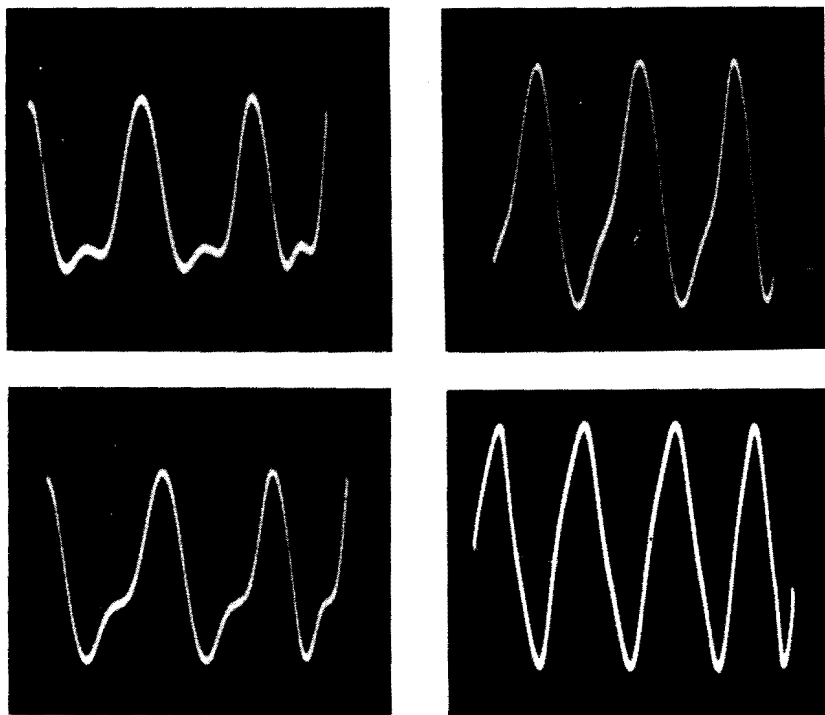
Fig. 507 (left). *40% second harmonic as in Fig. 505, but phased differently.* Fig. 508 (right). *10% third harmonic. Note the symmetry of odd-harmonic distortion.*

tively. As the output of O_1 happened to be 5 volts rms, harmonic contents of 10, 20, 30 and 40% were produced by setting the output of O_2 to 0.5, 1.0, 1.5 and 2.0 volts rms, respectively.

Let us first consider the effect of the second harmonic upon the waveform. It will be seen that 10% second harmonic is hardly discernible in Fig. 502, while 20% of the second harmonic significantly flattens the tops on *one* side of the wave of Fig. 503. For an

even greater harmonic content, the tops become double-peaked as shown in Fig. 504 (30% second harmonic) and Fig. 505 (40% second harmonic).

Note that the aspect of the oscillogram changes notably with the phasing of the component waves. Thus, Fig. 506 obtained with
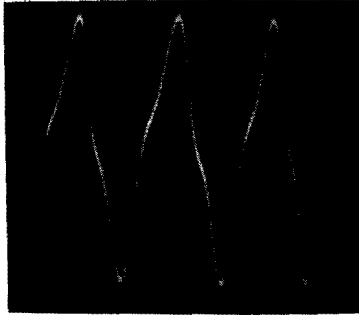
Fig. 509. *20% third harmonic.*

30% second harmonic seems relatively little distorted and Fig. 507 (40% second harmonic) appears less distorted than Fig. 505, differing only in its phasing. *All these waveforms show an asym-*
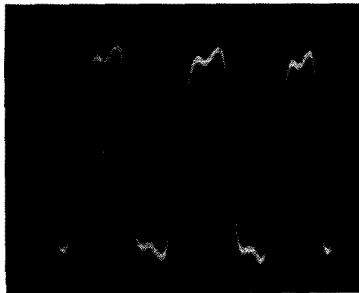
Fig. 510. *20% third harmonic. Due to different phasing, the distortion seems more severe. Note the definite symmetry of the flattened tops.*

metric distortion relative to the base line, as is always the case for even-order harmonics—an important fact to remember.

Adding now some third harmonic to the fundamental, we obtain Fig. 508 for 10% third harmonic. The distortion is more apparent than it is for the same amount of second harmonic. Distortion due to 20% third harmonic is visible in Figs. 509 and 510, the phasing being different. For 30% third harmonic, Figs. 511 and 512 were obtained, and Figs. 513 and 514 show 40% third harmonic. *Note*
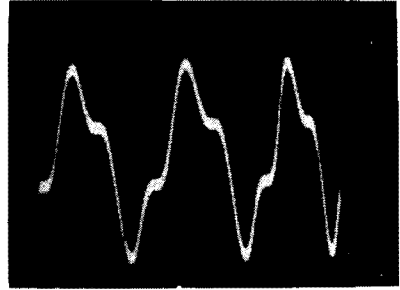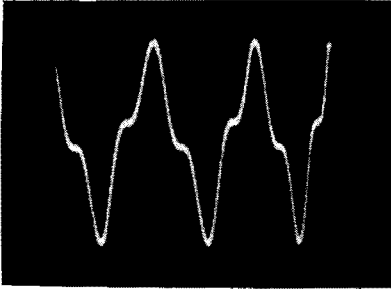
Fig. 511 (left). *30% third harmonic.* Fig. 512 (right). *Another photo of 30% third harmonic.*

the symmetry of these distortions regarding the base line, indicating the presence of odd harmonics.

The effect of only 10% of fourth harmonic is shown in Fig. 515, and Fig. 516 was obtained with 30% fourth harmonic. Only 10% fifth harmonic was responsible for the marked distortion evidenced in Fig. 517.
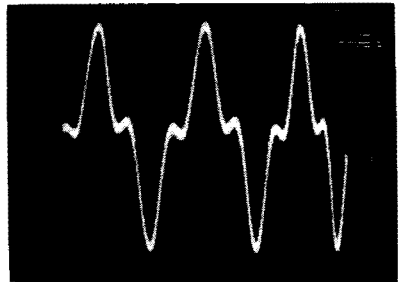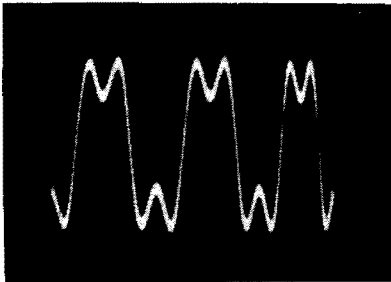
Fig. 513 (left). *40% third harmonic.* Fig. 514 (right). *Another photo of 40% third harmonic.*
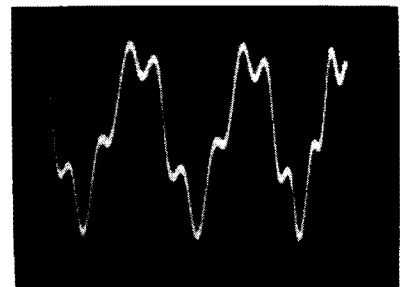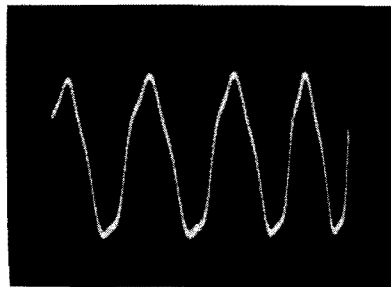
Fig. 515 (left). *10% fourth harmonic creates a clearly visible amount of distortion. This is typical of low levels of the higher-order harmonics.* Fig. 516 (right). *30% fourth harmonic. Note the lack of symmetry due to the even-harmonic distortion.*

87

In brief, the following conclusions are to be remembered:

Even harmonics produce asymmetric and odd harmonics symmetric distortion with reference to'the base line.

The presence of higher-order harmonics introduces more visible distortion than equal amounts of low-order harmonics.

An harmonic content of less than 10% is not readily visible on
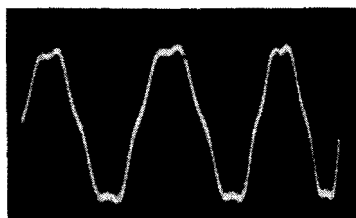
Fig. 517. *Only 10% fifth harmonic is responsible for the marked distortion of this sine wave. Note the symmetry.*

the oscilloscope, especially for the second and third harmonics. This is of particular importance for checking audio systems. An amplifier presenting from 5 to 10% harmonic distortion obviously does not qualify for a high-fidelity label. The oscillogram of its output may, however, appear quite perfect. To show the actual distortion, other methods must be employed. If the output wave-
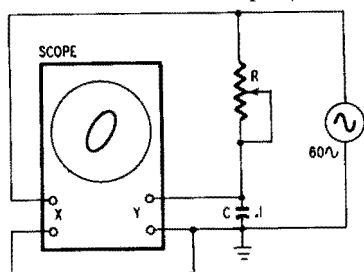
Fig. 518. *Simple resistance–capacitance phasing circuit.*

form corresponding to a sine-wave input shows a visible deformation, the actual distortion is liable to be more than 10%.

Phasing circuits

Phasing a voltage is accomplished by shifting its wave along the time axis, making it lead or lag with regard to a time reference. This may imply a reduction of its amplitude but should not alter its waveform.

As phasing circuits are networks comprising resistance and reactance, they are frequency-sensitive. Thus, the components of the different frequencies of a complex wave are likely to be unequally
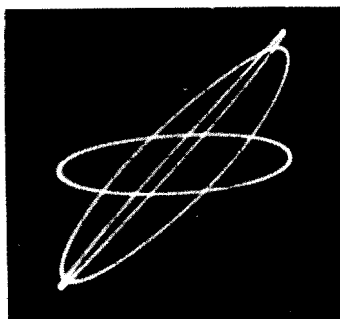
Fig. 519. *Phasing ellipses obtained with R = 1,000, 10,-000 and 100,000 ohms (in the circuit of Fig. 518).*

transmitted, and waveform distortion will result. The only one-frequency wave is the "pure" sine wave, and only this wave can be phased without distortion. If a complex wave such as a square wave
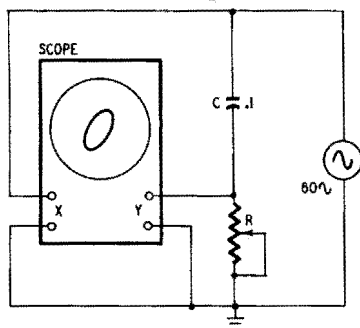
Fig. 520. *Resistance-capacitance phasing circuit.*

is to be phased, one has to act upon the original sine wave, prior to squaring.

The simplest phasing circuit, consisting of only a resistor and a capacitor, is shown in Fig. 518. Connected to the scope as shown, a variable resistor R is used to show the action of the circuit: Fig. 519 displays three typical phasing ellipses obtained. For R = 0, a sloped straight line (not shown) is obtained, indicating an in-phase condition. Increasing R opens the line into an ellipse whose major

axis tilts to become horizontal. The 90° limit value of phase angle is obtained theoretically, but it postulates an infinitely large value of R. As R is series-connected, it follows that the phased voltage decreases its amplitude with an increasing phase angle. When R is infinite, the output voltage is zero. The ellipses shown were ob-
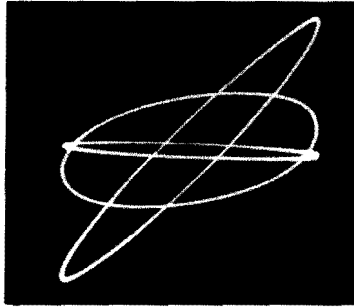
Fig. 521. *Phasing ellipses obtained with the same values of R as in Fig. 518.*

tained with R = 1,000, 10,000 and 100,000 ohms and the loss of amplitude is clearly seen for the ellipse with a horizontal axis (R = 100,000 ohms).

Phasing can also be accomplished by the network of Fig. 520, using a series capacitor and a parallel resistor. Three typical phasing ellipses are shown in Fig. 521, corresponding to the same R
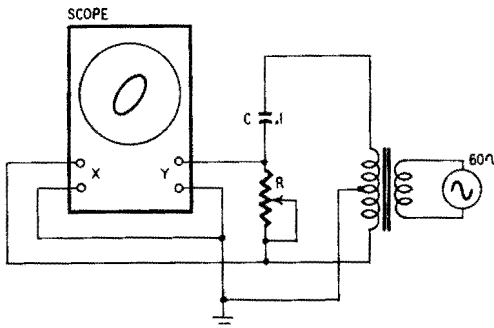
Fig. 522. *Constant-amplitude phasing circuit using a tapped transformer.*

values mentioned in the previous paragraph. However, the increase of the phase angle accompanied by a loss of amplitude is obtained here with a decreasing value of R. The most flattened ellipse with a horizontal axis was obtained with R = 1,000 ohms.
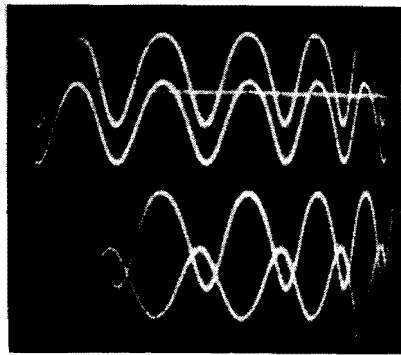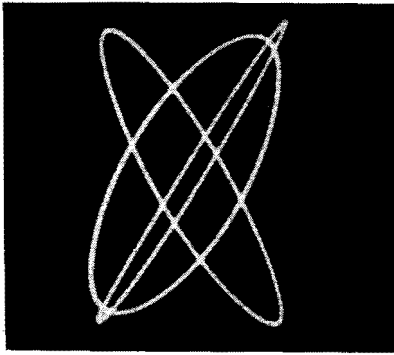
Fig. 523 (left). *Phasing ellipses obtained with the constant-amplitude phasing circuit of Fig. 522. R and C as in Fig. 518.* Fig. 524 (right). *Phasing conditions for two different values of R. Simultaneous viewing is obtained by using an electronic switch. Upper waveform: R = 1,000 ohms; lower waveform: R = 100,000 ohms.*

The most serious drawback of both these circuits is the great loss of amplitude of the phased output voltage for phase angles of, say more than 50°. Using the same R-C network and the same values, this can be overcome by feeding the network by a center-tapped secondary transformer (Fig. 522). The phasing ellipses corresponding to the same values of R specified earlier are shown
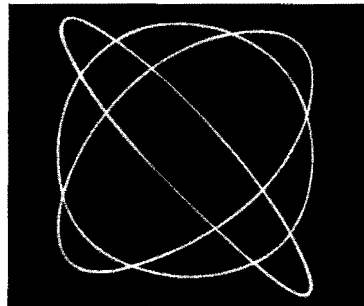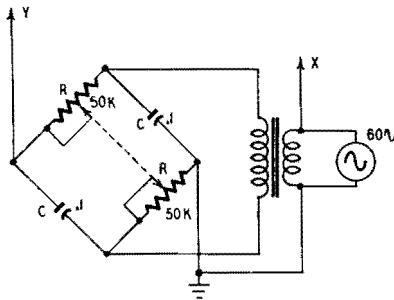
Fig. 525 (left). *Phasing bridge using a dual control.* Fig. 526 (right). *Phasing ellipses obtained with the bridge of Fig. 525.*

in Fig. 523; the most flattened one occurs when R equals 1,000 ohms. Using an electronic switch, the waveforms of Fig. 524 were obtained, showing (upper waveform) the nearly phased condition for R=1,000 ohms, and (lower waveform) a phase angle approaching 180° for R = 100,000 ohms. Figs. 523 and 524 show two significant advantages of this circuit: a phase-angle variation nearly 180°, and a practically constant output voltage.

Combining two similiar R-C networks results in the phasing

bridge of Fig. 525, using a dual control. The three ellipses of Fig. 526 obtained with both an extreme and intermediate setting of the dual control indicate a constant output voltage and a possible phase-angle variation similar to that of the circuit of Fig. 522. Feeding the phasing bridge by a center-tapped secondary transformer results in the circuit of Fig. 527 where two output voltages (Y1 and Y2) are phased with regard to the input voltage X. This result would not justify the use of the relatively complicated com-
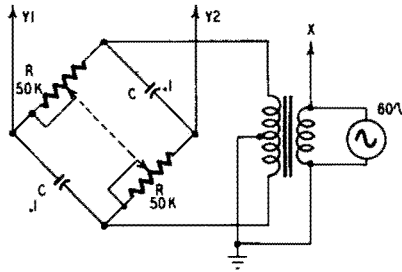
Fig. 527. *This phasing bridge maintains a constant out-of-phase condition between Y1 and Y2.*

ponents, were it not for another reason. While Y1 and Y2 are phased regarding X, their mutual phase relationship is maintained equal to 180°, a condition to be fulfilled for phasing push-pull amplifiers. This rigid phase relationship is displayed in Fig. 528 for both extreme settings of the dual control; the slight phase error in the upper waveform is due to an improper balance of the phasing bridge.

Fig. 528 (left). *The constant out-of-phase condition of Y1 and Y2 is shown for the two extreme settings of the dual control (R in Fig. 527). Fig. 529 (right). Phase-shifting network using cascaded C and R sections*
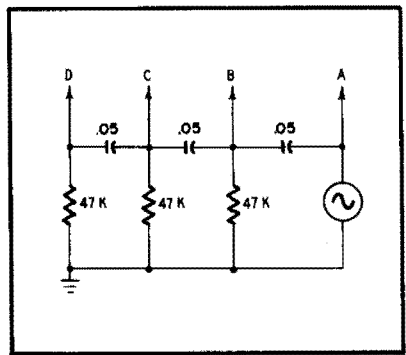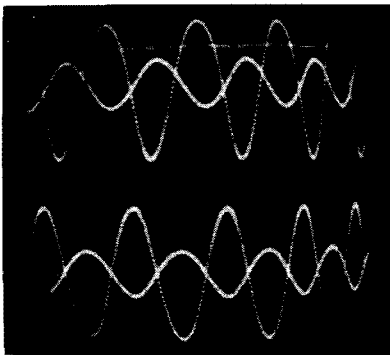
As the usable phasing introduced by a simple R-C section is often insufficient, cascaded sections such as shown in Fig. 529 are sometimes used, for instance, in phase-shift oscillators. The input voltage A is compared with the voltage at B, C and D by an electronic switch (upper, center and lower traces respectively, Fig. 530). The larger amplitude identifies the input voltage. Though the overall phasing introduced is about 120° the loss of ampli-
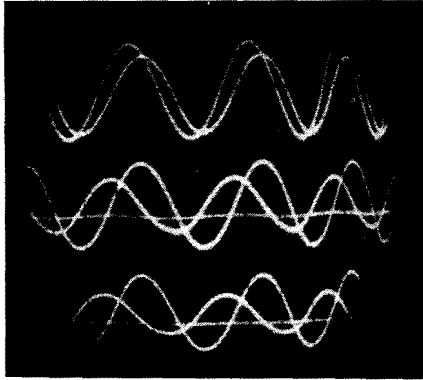
Fig. 530. *Comparison of phasing conditions between points A and B (top), C (center) and D (bottom) of Fig. 529.*

tude is not prohibitive. In a conventional phase-shift oscillator, such a network will permit oscillation for the frequency introduc-
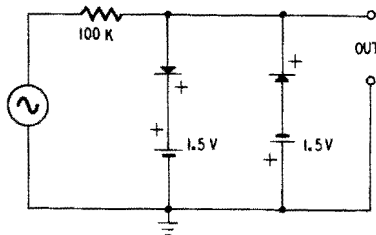
Fig. 531. *Simple clipping circuit using two germanium diodes.*

ing a phase-shift of 180° between points A and D (taking into account the input impedance of the tube).

Producing square waves

Square waves are used extensively for testing and as a "raw material" for production of pulses and other waveforms. Square waves may be generated by multivibrators. In the present section we will

consider only squaring devices, that is waveform transformers, fed by an external oscillator supplying a sine input voltage.

There are two types of squaring devices: limiters or clippers, and the Schmitt trigger. There are quite a variety of limiters, for any overdriven amplifier delivers a (more or less) square wave. We will examine here only the very simple and reliable clipping circuit of Fig. 531 using two crystal diodes. These diodes are biased to conduct only for voltages exceeding the bias voltage, clipping the part of wave exceeding that amplitude. The square wave obtained
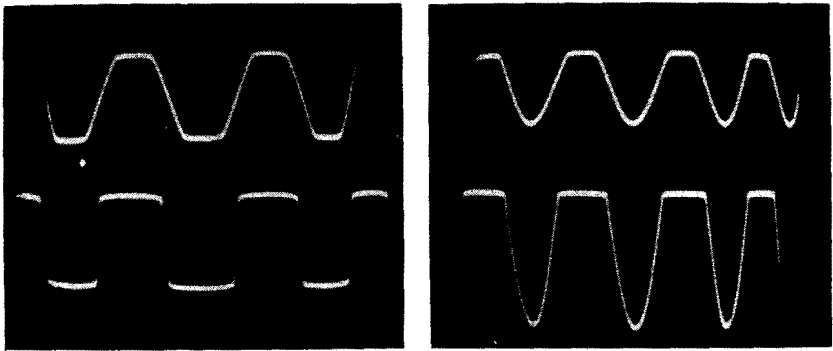
Fig. 532 (left). *Square wave obtained with the diode clipper. The input voltages were 2 volts rms (above) and 10 (below). Fig. 533 (right). Clipped waveforms produced by using one diode only.*

is shown in Fig. 532. Insufficient input voltage (2 volts rms) results in a trapezoidal wave (upper waveform) by clipping the wave tops only, while adequate clipping is accomplished by an input of 10 volts rms (lower waveform). Using a single diode, the waveforms of Fig. 533 were obtained for the same input voltages.

This very simple squaring device exhibits somewhat low rise and fall times, making it unsuitable for higher-frequency use. Moreover, its output impedance is high. Much better performance is
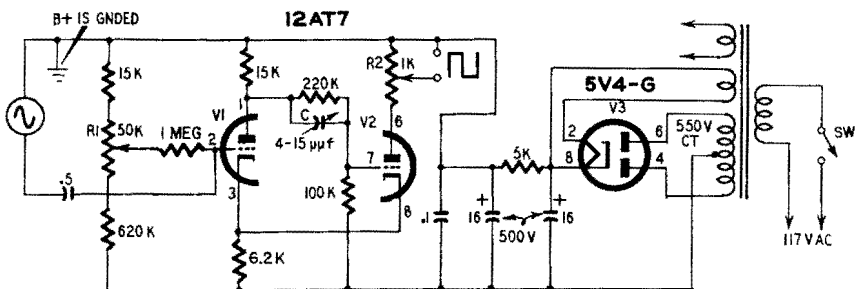
Fig. 534. *Schmitt trigger circuit used to produce clean square waves.*

94

featured by the Schmitt trigger used as a square-wave generator. The circuit of Fig. 534 consists of a duo-triode whose two sections are coupled in a multivibrator-like manner by two dc couplings. For a sufficiently biased section V1, the bias of V2 is decreased. This section passes heavy current, increasing the bias of V1 by means of the common cathode resistor. If a positive voltage is now impressed upon the grid of V1, nothing happens until this voltage exceeds a given level. V1 then passes a heavy current, suddenly in-
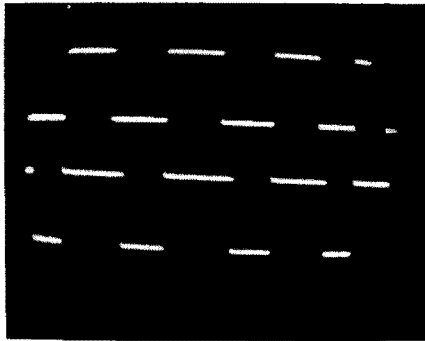
Fig. 535. *Square wave obtained with the Schmitt trigger circuit of Fig. 534. Different mark–space ratios are shown.*

creasing V2's grid voltage making it less conductive. Simultaneously, V1's plate current also adds bias to V2 by means of the common cathode resistor. Owing to this sort of "chain reaction," the plate current of V2 (and thus the potential of its plate) has only
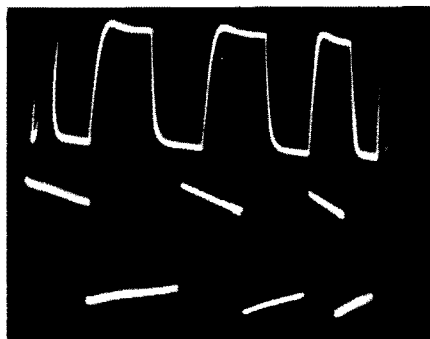
Fig. 536. *100-kc square wave passed by a scope amplifier of insufficient bandwidth (above) and 20-cycle square wave (below) passed by a coupling circuit having too low a time constant.*

95

two possible states, making it very suitable for square-wave production. The resulting square wave is shown in Fig. 535. The mark–space ratio of this wave is adjusted to about unity by setting control R1. The oscillogram below displays a mark–space ratio greater than 1, for a different setting of R1. Furthermore, some overshoot is noted. This is due to an incorrect setting of adjustable
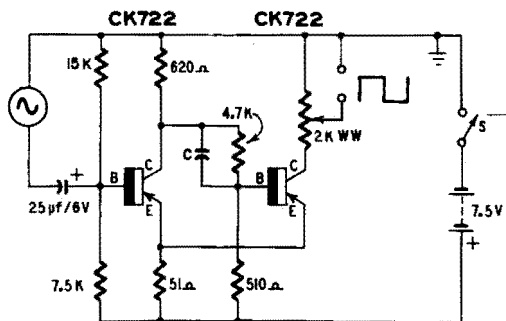
Fig. 537. *Transistor version of the Schmitt trigger circuit.*

capacitor C, introduced to assure a steep transition from one state to the other.

A "fine" square wave can be badly distorted by an inadequate
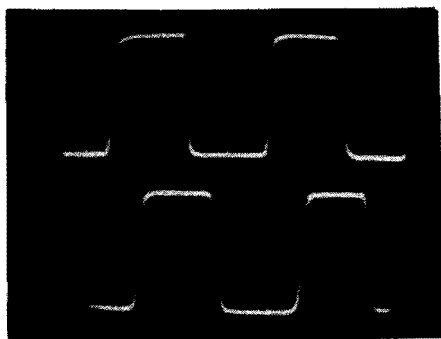
Fig. 538. *A 20-kc square wave (upper trace) produced by the circuit of Fig. 537. Omission of capacitor C in Fig. 537 results in a lower rise time (bottom trace).*

or incorrectly used scope amplifier. The upper oscillogram of Fig. 536 shows a 100-kc square wave handled by a scope amplifier of insufficient bandwidth. Note the rounded corners. The lower waveform represents a 20-cycle square wave passed on by a dc ampli-

fier using a 0.1-μf input capacitor. Eliminating this capacitor makes the droop disappear, the tops becoming perfectly flat. Always remember that the best amplifier used beyond its bandwidth is liable to introduce distortion of its own.

Transistorizing the Schmitt trigger circuit of Fig. 534 results in a very handy and economic squaring device, (Fig. 537). Although transistors are shown replacing the vacuum tubes, the circuit remains about the same. An input signal of about 1 volt rms is adequate, and the output is about 4.5 peak-to-peak volts. The current taken from the 7.5-volt battery is 7 ma.

The shape of the square wave produced is quite good. A 20-kc square wave is shown in Fig. 538 (upper waveform); omission of C
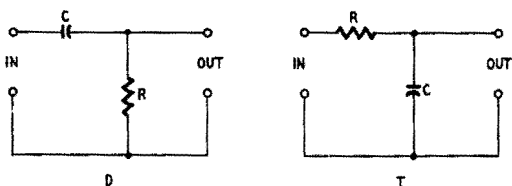
Fig. 539. *Differentiating (D) and integrating (I) circuits.*

resulted in the lower oscillogram, showing smaller rising and fall times. As the duration of a cycle of a 20 kc wave is 50 microseconds, the rise time of the upper wave can readily be estimated to be at about 2 μsec.

Differentiation and integration of waveforms

Examining the phasing circuits of Figs. 518 and 520, we saw that

Fig. 540 (left). *Differentiating a square wave with RC = T (above) and RC = 0.1 T (below).* Fig. 541 (right). *Differentiating a square wave with RC = .01 T (above) and .001 T (below).*
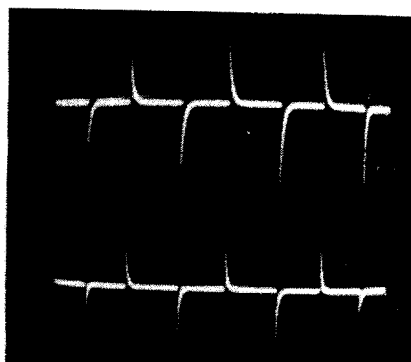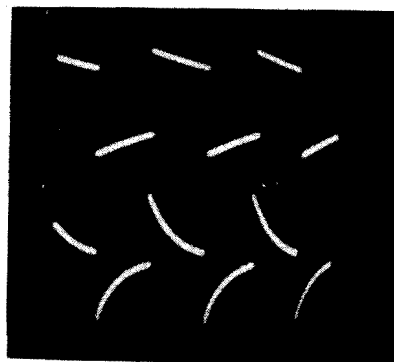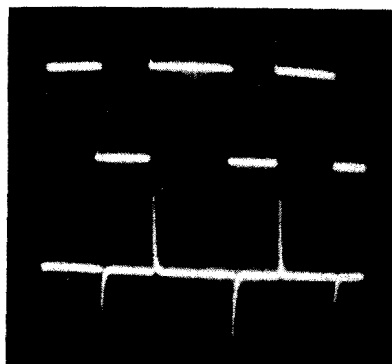
Fig. 542. *A square wave of nonunity mark–space ratio produces unequally spaced pulses.*

they are to be used with sine waves to accomplish phasing, and that complex waves are more or less distorted. We can now determine the kind of "distortion" introduced.
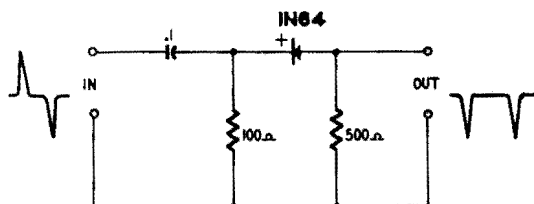
Fig. 543. *Circuit used for clipping pulses, on one side of the base line.*

Let us redraw these important circuits (Fig. 539). Circuit D (for differentiating) at the left looks like conventional grid coupling. Used as such, the capacitance of C, or reactance $\frac{1}{2\pi fC}$, has to be large in relation to R to avoid attenuation of the lower-frequency

Fig. 544 (left). *Unipolar pulses obtained with the circuit of Fig. 543.* Fig. 545 (right). *Integrating a square wave with RC = .01 T (above) and 0.1 T (below).*
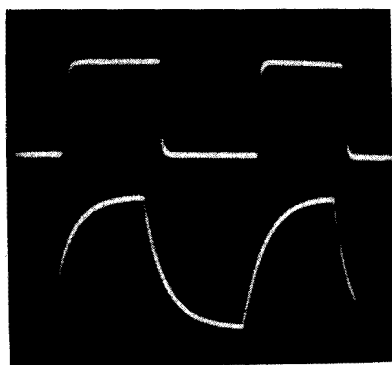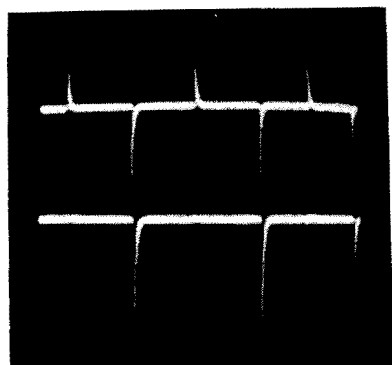
Fig. 546. *Integrating a square wave with RC = T (above) and RC = 10 T (below).*
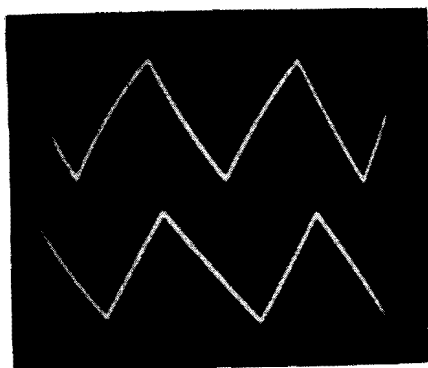
components. Decreasing R or C (that is, reducing the time constant RC) results in suppression of the lower-frequency components, thus emphasizing the "rapid" components. Mathematically speaking, this corresponds to a differentiation of the function represented by the waveform.

Circuit I (for integrating) at the right is not unknown either: this is a conventional filter, extensively used to smooth the residual ac components in a dc power supply. Here, too, however, the difference is merely the result of the time constant RC. In a filter, RC is made sufficiently large to filter the ac component. Here, on the contrary, we are interested in that residual component, and we will make RC a little lower. Nevertheless, this circuit will smooth the rapid transitions of the waveform and accentuate the slow ones. Mathematically speaking, this means integrating the function of the waveform.

Some characteristic waveform transformations accomplished by differentiation and integration are given below:

Original wave	Differentiated wave	Integrated wave
sine	cosine	cosine
square	pulses alternatively above and below the base line	triangular
sawtooth	pulses of same polarity	parabolic
triangular	rectangular	pairs of parabolic half-cycles

The differentiating or integrating action of a given circuit depends upon both its time constant RC and the operating frequency. For example, as we worked with 1,000 cycles, the duration of a cycle is $T = 1$ millisecond, and RC may conveniently be expressed in terms of T. The time constant RC (in seconds) is obtained by multiplying R (in megohms) by C (in microfarads).

99

Fig. 547. *Staircase wave obtained by adding saw-tooth waves.*
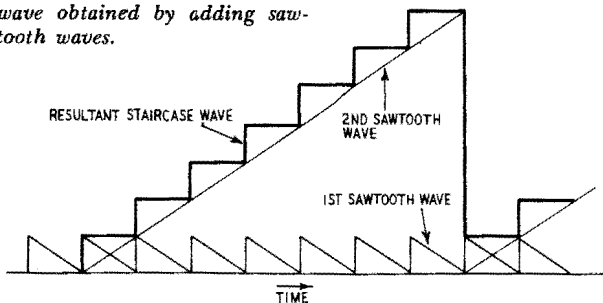
Generation of pulses

Pulses may be obtained by differentiating a square wave. Circuit D of Fig. 539 was used with C = 0.1 µf, R being variable. With R = 10,000 ohms (RC = 1 millisecond), the upper oscillogram of Fig. 540 was obtained, showing merely a bad transmission of the low-frequency components. With R = 1,000 ohms (RC = 0.1 millisecond), we obtained the lower oscillogram. More pulselike wave-forms resulted for R = 100 ohms (RC = .01 millisecond, Fig. 541, upper waveform), and R = 10 ohms (RC = .001 millisecond,
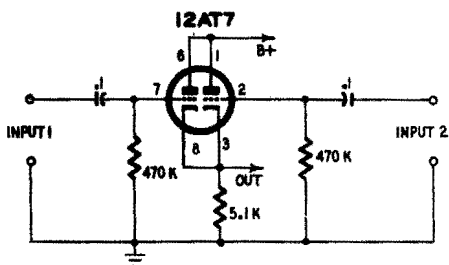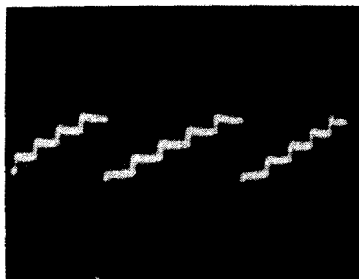
Fig. 548 (left). *Staircase wave produced by two sawtooth waves.* Fig. 549 (right). *Simple mixer for the production of complex waveforms*

lower waveform). Comparing these waveforms, we can state that *adequate differentiation is obtained with RC smaller than T/100.*

If the original square wave features a nonunity mark–space ratio, pulses unequally spaced regarding the base line are obtained as shown in Fig. 542 where RC = T/100. Thus, pulses can be phased by varying the duty ratio of the square wave.

Pulses most frequently required are of but one polarity. This can be easily obtained by using a germanium diode as shown in Fig. 543. Pulses of only one polarity are passed as shown in Fig. 544. The positive pulses of the oscillogram above are properly clipped (lower waveform). Of course, the gain of the scope ampli-
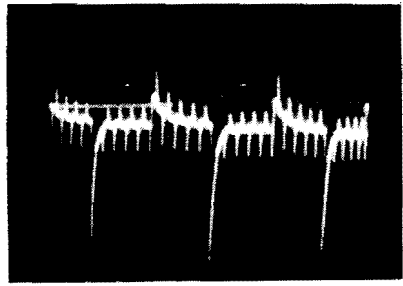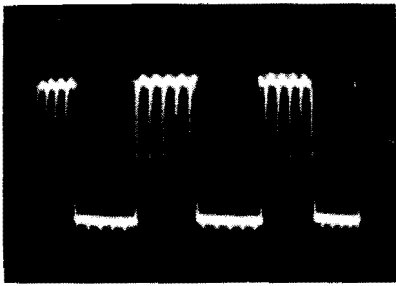
Fig. 550 (left). *Waveform produced by mixing a 500-cycle square wave and 5,000-cycle pulses.* Fig 551 (right). *Waveform produced by mixing pulses of 500 and 5,000 cycles.*

fier is somewhat larger for the second display. Needless to say, positive pulses are obtained by merely connecting the diode the other way round.

As indicated above, unipolar pulses may be obtained directly by differentiating a sawtooth wave.

Generation of triangular waves

Let us now integrate the square wave (T = 1 millisecond) by means of circuit 1 of Fig. 539 where C = 0.1 μf, R being made variable. With R = 100 ohms (RC = .01 millisecond), only a slight rounding of the corners and some deterioration of the rise time occur, as shown in Fig. 545. For R = 1,000 ohms (RC = .1 millisecond), the wave is composed of parabolic portions (Fig. 545, lower waveform). A fairly triangular wave is obtained with R = 10,000 ohms (RC = 1 millisecond) as displayed by the upper oscillogram of Fig. 546, while the lower one, obtained with R = 100,-000 ohms and RC = 10 milliseconds, features rather perfectly linear portions. Comparing these oscillograms we conclude that *good integration is obtained with RC greater than T.*

If the mark–space ratio of the original square wave differs from unity, the triangular wave becomes a sawtooth wave as shown in the lower part of Fig. 546. It is, however, difficult to obtain by this method a sweep voltage featuring a negligible return time.

Generation of complex waves

Applications such as the generation of a complex video signal involve rather complicated waveforms. Voltages of this type cannot be produced directly (at least by purely electronic means), but are obtained by adding and mixing more elementary waveforms, principally pulses and square waves. Of course, the generators produc-

101

ing these components must be interlocked by suitable synchronization if they are not driven by a common generator.

As an example of a complex waveform, let us study the staircase wave, useful for frequency division and for tracing a family of characteristics. As shown in Fig. 547, such a waveform may be obtained by adding two sawtooth waves of suitable frequency and amplitude. Such a staircase wave pattern, produced for demonstration purposes only, is shown in Fig. 548. It was obtained using two gas triode sweep oscillators with a frequency ratio of 5 to 1 (there are five steps), the whole affair being properly synchronized. These voltages are added in the C-R tube, for the sawtooth waves are directly injected into the Y1 and Y2 deflection plates. This overcomes a minor difficulty. Instead of adding two waves of opposite polarity the C-R tube actually substracts waves of the same polarity. If the gas triodes are used for frequency division, this pattern gives a good visual check of the dividing ratio.

To study the operation of a signal mixer, the simple circuit of Fig. 549 was used. A 500-cycle square wave and pulses with a repetition frequency of 5,000 cycles were applied on both grids. The resulting waveform is shown in Fig. 550 where the gating effect of the square wave upon the pulses is evident. Applying pulses of 500 and 5,000 cycles on both grids resulted in Fig. 551; the frequency ratio of 10 to 1 is easily verified.

chapter

6

display of characteristics

P OINT-BY-POINT plotting of characteristics of vacuum tubes, semi-
conductor devices and other nonlinear components is very
tedious and time-consuming. Because of its two-dimensional type
of display, the cathode-ray tube is suited for this kind of work, and
readily lends itself to automatic tracing. The rapid exploration of
the working characteristic even allows for plotting of portions situ-
ated beyond the rated power dissipation, without damaging the
tube, a significant advantage over the point-to-point method. On
the other hand the displays, obtained rather easily, *do not provide
for numerical evaluation.* Systems featuring graduated coordinates

Fig. 601. *Operating principle of the automatic curve tracer.*
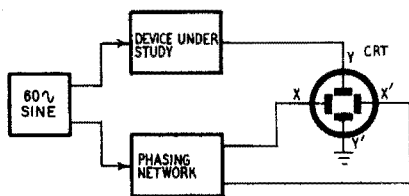
have been developed, but they are very complicated, and their use
is practically restricted to specialized laboratories and tube fac-
tories.

Mechanism of automatic plotting

To trace its characteristic, a signal is injected into the input of
the device under study, and the resulting output is measured. A
graph is obtained by plotting the measured output along the Y
axis and the corresponding input signal along the X axis, adequate
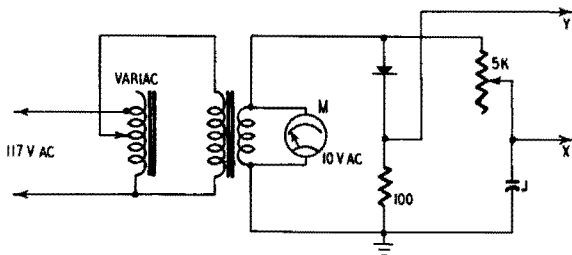
Fig. 602. *Circuit used for tracing diode characteristics.*

scales being chosen for both of them. The intersection of both co-ordinates situates the point of the characteristic.

The absence of inertia of the writing spot of the C-R tube permits replacing the point-by-point exploration by a continuous sweeping of the characteristic; this can be done conveniently by a 60-cycle sine-wave voltage of suitable amplitude. A plot is obtained by deflecting the spot horizontally by a voltage of the *same frequency and phase* and of adequate amplitude.

The operating principle of the automatic tracer is illustrated in Fig. 601. Amplifiers can be provided in one or both deflection channels, depending upon the required amplitudes. The phasing network compensates for phase errors between the signal and the sweep voltage.

Confusing characteristics may result from a wrong connection of the C-R tube, but this condition generally is easily corrected. If the display appears upside down, the connections to the Y-plates are to be reversed; if the trace slopes to the wrong side (as if seen in a mirror), the connections to the X-plates should be reversed.

If the output of the device under study has a dc component, there will be a self-centering action of capacitance-coupled amplifiers.

Fig. 603 (left). *Characteristic of a selenium rectifier.* Fig. 604 (right). *Characteristic of a point-contact silicon diode.*
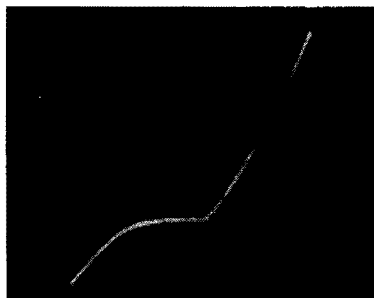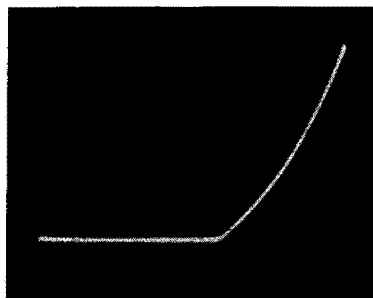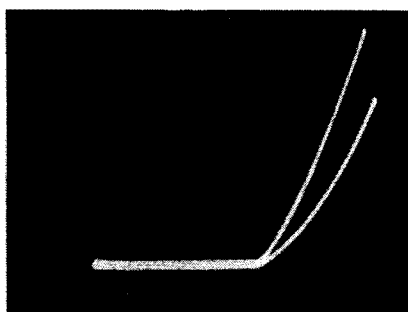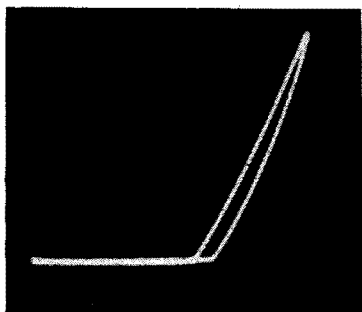
Fig. 605 (left). *Phase shift produces a looped characteristic.* Fig. 606 (right). *Spread of characteristics of diodes from the same production run.*

Unless the sweep is sufficiently rapid with regard to the time constant of the channel, the dc component will be lost. For this reason, dc amplifiers are to be preferred, at least for the Y deflection channel.

Rectifier characteristics

To display the characteristic of all kinds of rectifiers (vacuum tubes and semiconducting devices), the circuit of Fig. 602 was used. The Variac allows for convenient voltage control, but it is not an absolute requirement. The rectified current passing through the 100-ohm resistor develops the Y deflection voltage; because of the low amplitude, amplification is necessary. The phasing device of Fig. 601 is composed of the 5,000-ohm control and the .1-μf capacitor.

A typical rectifier characteristic (selenium) is shown in Fig. 603. The straight horizontal portion on the left side corresponds to the negative half-cycle of the 60-cycle voltage; the rectifier passes no current. The slightly curved, sloped portion on the right side indicates the current passed by the rectifier in terms of the applied voltage. With but one exception, the impressed emf uniformly was 7

Fig. 607. *Testing a selenium photocell as a rectifier. As the illumination increases, the forward current also increases.*

Fig. 608 (left). *Characteristic of a 5V4-G rectifier tube.* Fig. 609 (right). *Characteristic of one section of a 6AL5 duo-diode. Note that there is no reverse current in vacuum tube diodes.*

volts rms, or about 10 volts peak, assuming a reasonable sine wave. Thus, the characteristic is swept between —10 and +10 volts. Most rectifiers examined did not present a visible backcurrent at so low

Fig. 610. *Circuit used for tracing the I_p/E_g characteristic of a vacuum tube.*

an inverse voltage. This backcurrent is, however, clearly visible in Fig. 604, which represents the characteristic of a 1N23A point-contact silicon diode designed for early radar applications. At the left is a small straight portion corresponding to the so-called Zener voltage, the diode becoming conductive again. The applied emf was reduced here to 5 volts rms, or 7 volts peak. Thus, the diode is nonconductive only for potentials between 0 and about —4 volts.

Comparing these characteristics with curves published by manufacturers, one may be surprised by the different appearance of the left side of the characteristic. Remember that this results from the use of different scales for the positive and negative sides of the coordinates, to give the most useful information in a limited space.

106

As we use a signal of equal positive and negative amplitudes, impressing a voltage sufficient to show the back current would imply excessive forward current on the positive peaks.

Elimination of the phasing network resulted in the looped characteristic shown in Fig. 605. The phase error responsible for the phasing loop is often difficult to correct, and compensation may be easier to carry out.

While this simple automatic tracer does not provide numerical results, it may be used nevertheless for comparison purposes. Test-
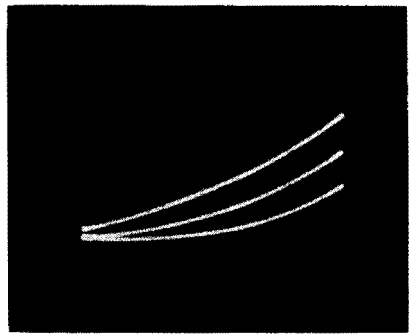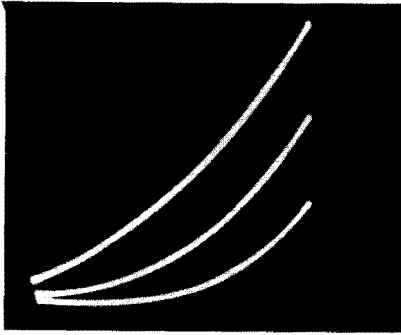
Fig. 611 (left), I_p/E_g curves of a 12AX7. Plate voltages used were 300, 250 and 200.
Fig. 612 (right). Characteristic curves of the 12AX7 with a plate load of .05 megohm.

Fig. 613 (left). Effects of various load resistances on 12AX7 characteristics. The top curve is for a zero load. Fig. 614 (right). I_p/E_g curves for different bias voltages.
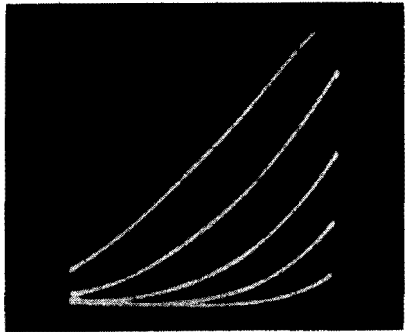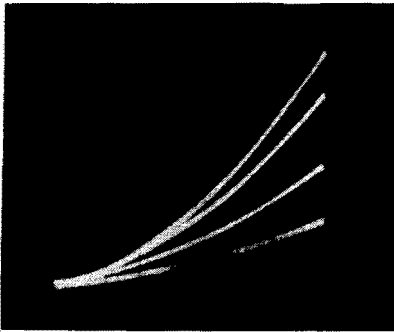
ing two 1N89 germanium diodes of the same batch resulted in the clearly spread characteristics shown in Fig. 606; the higher-sloped curve indicates the more efficient unit. Testing these diodes for forward current, the vom gave readings of 45 and 200 ohms, respectively, on a low-resistance scale (readings of forward resistance on high-resistance scales are meaningless).
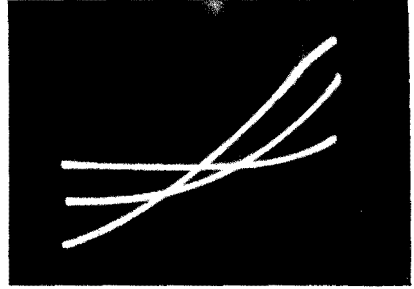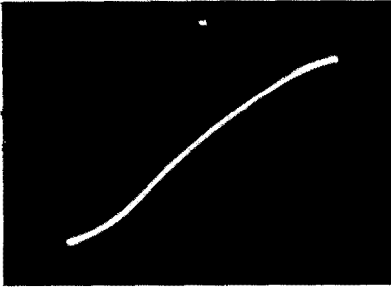
Fig. 615 (left). *Photo shows the effect of running the tube into the grid current region.* Fig. 616 (right). *Same as Fig. 614. The use of a capacitance-coupled scope amplifier is responsible for the loss of the zero reference level.*

As a selenium photocell is structurally similar to a selenium rectifier, it seemed interesting to test it as a diode, and so we obtained the display of Fig. 607 (IRC sun battery B2M). Note that this component makes a poor rectifier, the reverse voltage being quite low but then it has never been designed for rectifier use. It is also worth noting that the two superimposed characteristics were obtained for dark and light conditions, and that incident light increases the forward current, a common feature of semiconductor rectifiers.

Characteristics of vacuum type diodes and rectifiers are traced in exactly the same way; Fig. 608 depicts the operation of a 5V4-G rectifier tube and Fig. 609 is that of a 6AL5. The last oscillogram shows a higher slope, resulting from the lower internal resistance due to the close spacing of the electrodes of the detector tube. Of course, there is no reverse current in vacuum diodes.

(Photographs were made of several other solid-state devices and vacuum tubes, but the prints looked so similar that nothing was to be gained in presenting them here.)

Characteristics of vacuum tubes

The static characteristics of an amplifier tube are shown by two sets of curves: the transfer (or mutual) characteristics, and the plate characteristics. These curves present the same information, but in two different forms. They permit graphical determination of the optimum working conditions of the tube. However, the curves traced will lack numerical values if the display device is to remain simple, and no accurate evaluation will be possible. On the other hand, the oscilloscope permits study of the amplifier tube in its actual dynamic working condition, with neither plotting nor calculus, and this method is to be preferred for rapid results.

The transfer characteristic is the curve relating the plate current
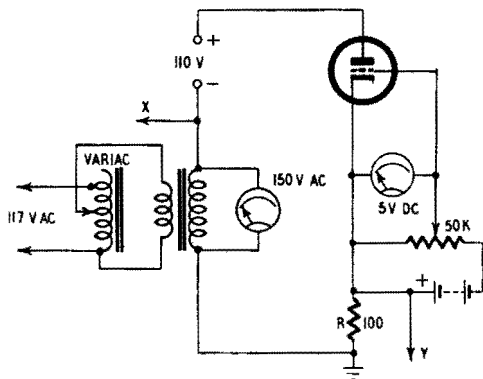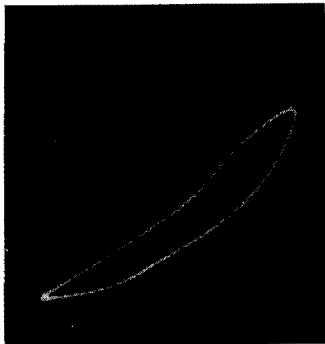
Fig. 617 (left). *Looped characteristic due to phase shift*. Fig. 618 (right). *Circuit used for producing the I_p/E_g characteristics of triodes.*

I_p to the grid voltage E_g. A family of curves is obtained by tracing this curve for different values of plate voltage E_p. For automatic tracing of these characteristics, the circuit of Fig. 610 was used. The actual grid voltage is made up of an ac voltage (controlling simultaneously the horizontal deflection of the beam) and a dc bias, both of them being adjustable for convenience. The plate current I_p develops across R (100 ohms). Note that the use of an oscilloscope implies particular grounding conditions, so that both terminals of the plate and bias supplies are above ground. The use of batteries is recommended, but high-voltage batteries are expensive and a "floating" regulated B-supply is adequate.

A family of transfer characteristics of one section of a high-mu twin-triode 12AX7 is shown in Fig. 611, for plate voltages (from top to bottom) of 300, 250 and 200, respectively. The actual emf on the grid was made up of a dc bias of —2 volts and an ac potential of 0.7 volt rms, or 1 volt peak. Thus, the grid is swept between —3 and —1 volts. Introducing a load resistance of $R_p = .05$ megohm resulted in the family of curves of Fig. 612. The flattening and the reduced slope of the curves are evident; these are dynamic characteristics. Another set of such curves is shown in Fig. 613 for $R_p = 0, .01, .04$ and 0.1 megohm, respectively (from top to bottom), the grid being swept from —2.5 to —0.5 volts for B-plus = 200 volts.

Varying the dc bias results in different static characteristics as shown in Fig. 614 where the bias was 1 volt (top), 1.5, 2, 2.5 and 3 volts (bottom). As the ac "signal" was 0.7 volt rms, the actual grid swings were from —2 to 0 volts in the first case, and from — 4 to —2 volts in the last. The top of the upper curve shows the begin-
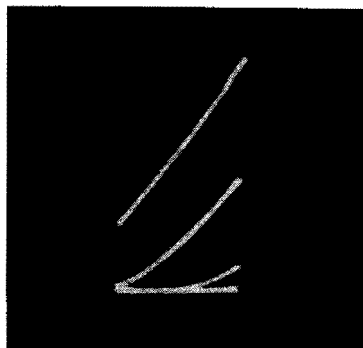
Fig. 619 (left). I_p/E_g characteristics of a 12AX7 for bias voltages from 0 (top) to —3 volts (bottom). Fig. 620 (right). Reducing the sweep voltage results in incomplete curves.

ning of grid current, and the lower curve illustrates the cutoff condition, I_p being zero during the major part of the sweep cycle because of excessive bias. Running the tube into grid current resulted in Fig. 615 where the flattening of the top portion is clearly visible; the actual grid swing was from —2.4 to +0.4 volts, with B-plus = 200 volts.

The self-centering action of an ac amplifier has been mentioned earlier. Displaying the set of curves of Fig. 614 by a capacitance-
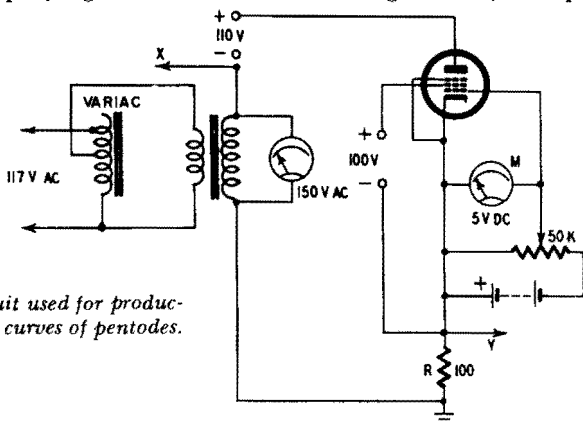
Fig. 621. Circuit used for producing the I_p/E_p curves of pentodes.

coupled amplifier resulted in Fig. 616 (for a dc bias of —1, —2 and —3 volts only). The curves are exactly the same, but the zero plate current reference is lost and no comparison of the actual plate currents is possible. The ellipse of Fig. 617 was obtained by omitting the phasing circuit; such an oscillogram has poor information value.
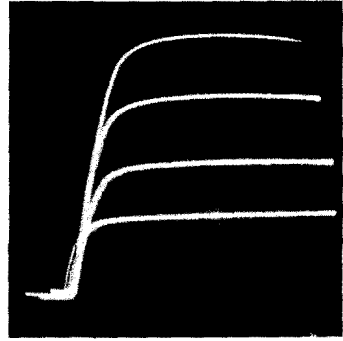
The plate characteristic relates plate current I_p to plate voltage E_p for different bias voltages V_g. It can be traced automatically by the circuit of Fig. 618 where a large-amplitude ac voltage is introduced in series with the B-plus supply. Note that this B-plus supply operates well above ground and has to be adequately insulated
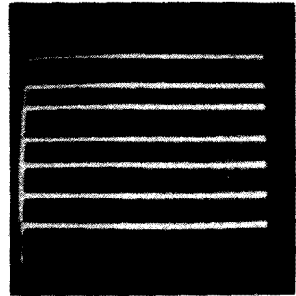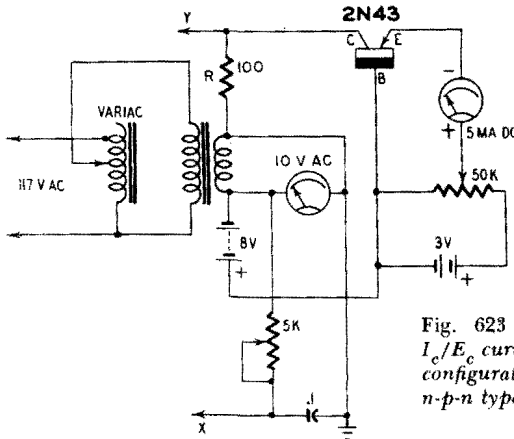
Fig. 623 (left). *Circuit for producing I_c/E_c curves of transistors in common-base configuration. (Reverse the batteries for n-p-n types).* Fig. 624 (right). *I_c/E_c curves of a 2N43 transistor.*

or breakdown may be experienced. The amplitude of the "signal" is sufficient for direct deflection of the C-R tube, and no phasing device is necessary.

Plate characteristics of the 12AX7 obtained with this circuit are shown in Fig. 619 for a bias of 0 (top), —1, —2 and —3 volts (bottom). A knowledge of the actual variation of V_p is important. V_p consists of 110 volts dc supplied by B-plus, and 78 volts rms, or 110 volts peak. Thus, V_p varies between 0 and 220 volts, an adequate scale. Reducing the ac to 39 volts rms (or 55 volts peak) resulted in Fig. 620, showing only portions of the curves. The obvious reason is the restricted variation of V_p from 55 to 165 volts only.

111

The same methods are used for tracing characteristics of multi-grid amplifier tubes. An additional floating power supply is, however, necessary to supply the screen voltage and, unless a battery is
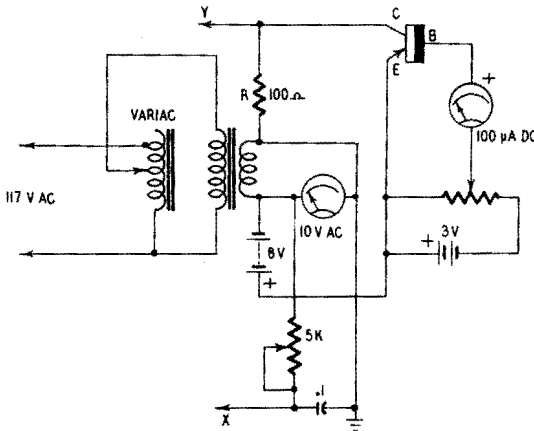
Fig. 625. *Circuit for tracing the* I_c/E_c *characteristics of p-n-p transistors, common-emitter configuration. For n-p-n units reverse the batteries.*

used, this may introduce additional complications. Screen voltage, of course, will constitute another parameter.

Using the circuit of Fig. 621, the family of plate characteristics of a 6SJ7 pentode amplifier tube (see Fig. 622) were obtained, evidencing typical pentode curves. Grid bias was 0 (top), -1, -2 and -3 volts (bottom). With B-plus $= 110$ volts dc and a sweep of 106 volts rms, or 150 volts peak, V_p varies between -40 and $+260$. Thus, the small horizontal portion on the lower left corresponds to a negative plate voltage and may be used as a reference for $I_p = 0$. Screen voltage was maintained at 100 and had to be readjusted for each bias value because a nonregulated power supply was used.

Characteristics of transistors

Tracing transistor characteristics is very similar to displaying curves of vacuum tubes. For accurate results, constant-current power supplies should be used instead of the familiar constant-voltage supplies. For demonstration purposes, small dry batteries can be used, however, and this, together with the absence of a hum-generating heater supply, makes for a very simple and foolproof experimental setup.

Because of the low input impedance and the frequency characteristic peculiar to transistors, more types of characteristics are to be

considered than for vacuum tubes. Since an exhaustive study is beyond the scope of the present book, only the two most important sets of curves will be considered. These are the collector current vs.
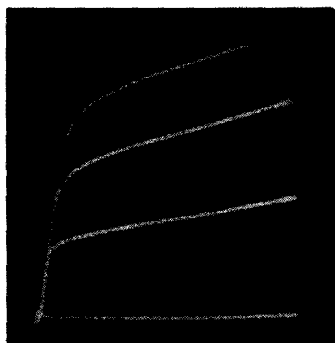
Fig. 626. I_c/E_c curves of a 2N34 junction transistor, common-emitter configuration.

collector voltage (I_c/E_c) characteristics for the common-base and common-emitter configurations.

The circuit of Fig. 623 was used to trace the I_c/E_c characteristics of a 2N43 junction transistor, common-base configuration. The set

PROPORTIONAL TO
FIELD H

PROPORTIONAL TO
INDUCTION B
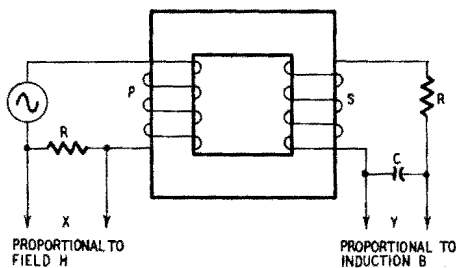
Fig. 627. Operating principle of B/H curve tracing of magnetic cores.

of curves obtained is shown in Fig. 624 for various values of constant base current I_b (from top to bottom: $I_b = 3$, 2.5, 2, 1.5, 1, 0.5 and 0 ma). The collector potential is composed of 8 volts dc and 5.6 volts rms, or about 8 volts peak. Thus, E_c is swept from 0 to 16 volts. Note the perfect linearity of the characteristics, and compare with the pentode curves of Fig. 622.

Minor modifications of this circuit (Fig. 625) permit tracing the I_c/E_c characteristics for the common-emitter configuration. The set of curves of Fig. 626 was obtained for constant base-current

values of $I_b = 60$ (top), 40, 20 and 0 μa (bottom), the E_c sweep being about the same. These curves are not as evenly spaced and as flat as the previous ones and show less linear operation for the common-emitter configuration.

Readings of I_c with a dc meter while tracing one of the curves are meaningless, for the meter will indicate only a mean value during the cycle, and not the peak current encountered. Thus, do not exceed rated values.
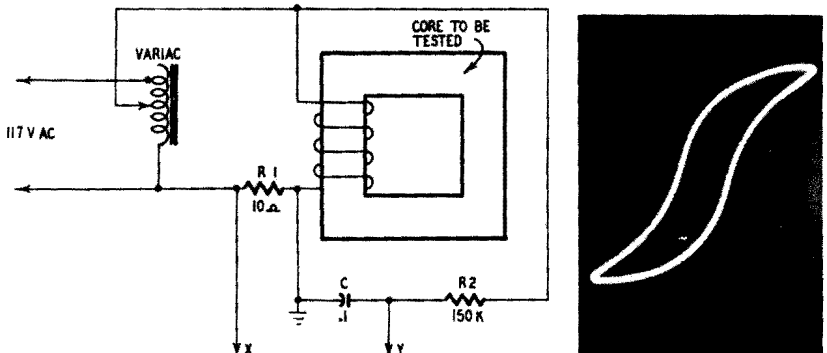
Fig. 628 (left). *Practical circuit for tracing B/H curves.* Fig. 629 (right). *Typical B/H curve for silicon iron.*

Hysteresis loop of magnetic cores

The main characteristic of a ferromagnetic material is its hysteresis loop, relating the magnetic induction B to the magnetizing field H. Because of magnetic saturation, this curve is approximately linear for small values of H only; furthermore, the phenomenon of magnetic remanence (or hysteresis) is responsible for the fact that different values of B are obtained for the same values of H,

Fig. 630. (left). *B/H curve of ordinary transformer laminations. The inner curve was run at a reduced level of magnetizing current.* Fig. 631 (right). *B/H curve of Mumetal laminations.*

depending upon the direction (increasing or decreasing) of the variation of H. That explains the loop-shaped aspect of the B/H characteristic.

To understand the mechanism of B/H curve tracing, consider Fig. 627. It represents a magnetic core with primary P and secondary S windings. As P is energized by an ac voltage, an emf pro-
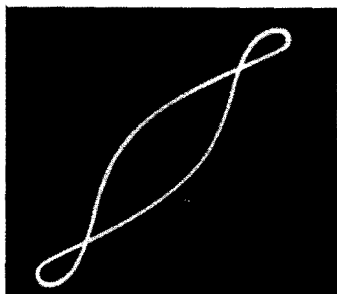
Fig. 632. *Faulty loop display due to time constant of integrating circuit being too low.*

portional to the magnetizing current or field H develops across series resistor R, of small ohmic value. By means of the magnetic core, an ac voltage proportional to the variation of the flux is in-
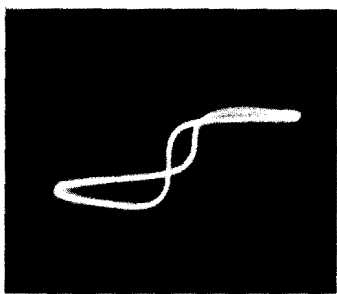
Fig. 633. *B/H loop of Mumetal core. Note the phase shift.*

duced in the secondary. To obtain a voltage proportional to induction B, this voltage has to be integrated by an RC integrating circuit. Assuming very tight coupling of P and S, a single winding may do as well, and the circuit simplifies to that represented in Fig. 628 which we actually used; it worked as well as the first one.

A typical B/H curve for silicon iron is shown in Fig. 629, indicating a rather progressive saturation. The inner area of the loop is proportional to the iron losses due to hysteresis and measures the

energy necessary for reversing the elementary magnets in the material to follow the opposite magnetizing polarities. Ordinary transformer laminations display a B/H curve such as shown in Fig. 630;
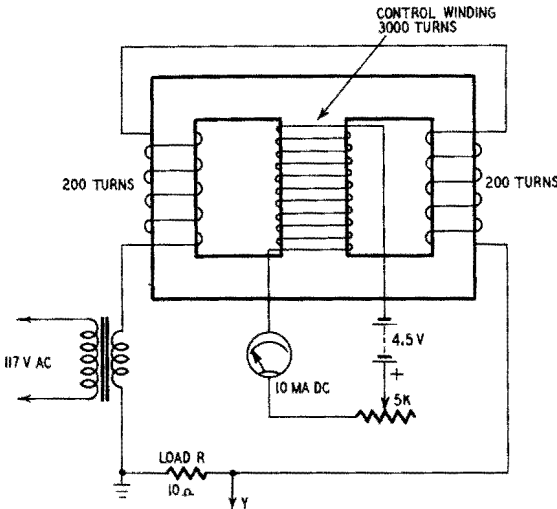
Fig. 634. *Saturable reactor used to control a resistive load.*

the large area in the loop points to relatively heavy iron losses. (The inner curve was run at reduced amplitude of the magnetizing current; saturation is not evidenced so well.) A B/H curve of a Mu-
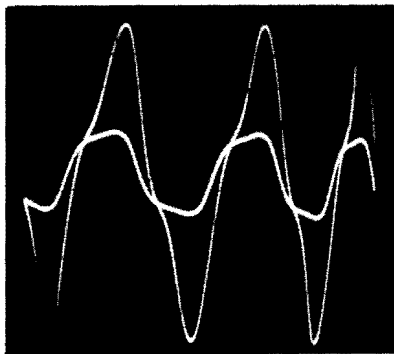
Fig. 635. *Increase of load current due to dc control.*

metal core is shown in Fig. 631; it approximates a rectangular characteristic. After a steep rise, there is a rather short curved portion, and nearly complete saturation follows. This shape is important for applications such as magnetic memories and transducers. The reduced inner area of the loop indicates low iron losses.

116

Phasing errors and unsuitable integration may cause important picture distortions. Reducing R2 from 0.15 megohms to 5,000 ohms is responsible for altering the shape of Fig. 630 to that of Fig.
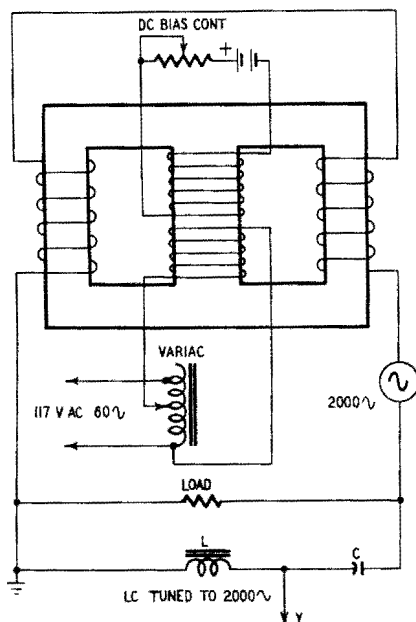
Fig. 636. *Magnetic modulator for modulating a 2,000-cycle voltage by 60 cycles.*

632. To test a core made of Mumetal and bearing only a few turns of wire, a transistorized preamplifier was hooked up; it introduced a phase shift, well noticeable in Fig. 633.

Experiments with saturable reactors

Saturable reactors, the major component of magnetic amplifiers, are an important application of the properties of B/H loops. Strictly speaking, for the sake of consistency, this section should not be placed into the present chapter but there is no place in the book that suits better.

A saturable reactor is a sort of transformer having at least two windings: an ac winding in series with the load, and a dc control winding. A direct current of suitable amplitude passing in the control winding saturates the iron core and significantly lowers the reactance of the series winding, thus increasing the load current.

If a conventional transformer were used, an ac voltage would be

induced into the control winding. As this is inconvenient, the ac windings are arranged on the core so that their ac fluxes compensate in the control winding, inducing no ac voltage. An experimental reactor and its connection to control a load are shown in Fig. 634. Correctly matched, the saturable reactor will yield a very
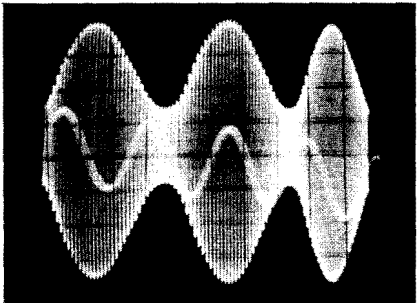
Fig. 637. *The pattern of the modulated voltage obtained.*

good efficiency; the experimental model, made by laboriously adding turns on the side-limbs of an existing Mumetal core, could not be matched correctly, and results are to be considered only qualitatively.
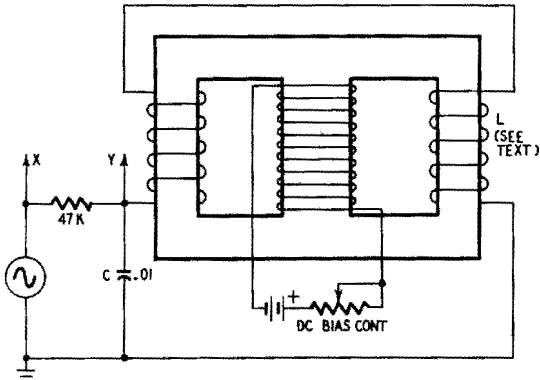
Fig. 638. *Determination of the inductance variation of a saturable reactor.*

Connecting the scope across the load resistor (10 ohms) resulted in Fig. 635, representing two successive photos. The low-amplitude wave was obtained with no dc passing in the control winding; with a control current of 10 dc ma, the larger-amplitude wave was obtained. It is easy to see that the peak current passed by R is about

four times higher; because of the distorted waveform, the rms current rise cannot easily be calculated. This experiment demonstrates the possibility of controlling the load current by a relatively small amount of direct current.

A saturable reactor may be controlled by an ac voltage, provided

Fig. 639. *Phasing ellipses obtained with the circuit of Fig. 638.*

its frequency is much lower than the supply frequency. Energizing the reactor by an audio generator operating at about 2,000 cycles and using a variable 60-cycle voltage to control the load current (Fig. 636), a modulator was obtained. Carefully adjusting the
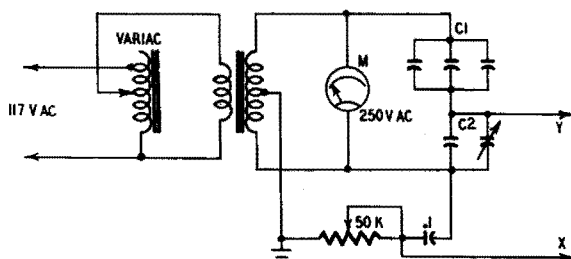
Fig. 640. *Circuit for tracing the hysteresis loop of the nonlinear dielectric capacitor C1.*

working point by a dc bias current passing in a third winding resulted in the correctly modulated wave shown in Fig. 637.

The saturable reactor can also be operated as a dc-controlled variable inductor. To demonstrate this possibility, the circuit of Fig. 638 was hooked up. Reactor L is tuned by a .01-μf capacitor and fed by an audio oscillator through a series resistor. At resonance, the impedance of L–C is purely resistive; it becomes inductive or capacitive at frequencies near resonance, and the resulting

phase difference is easily observed by a Lissajous pattern. Adjusting the oscillator frequency to obtain an ellipse approaching a line for the noncontrolled condition, a somewhat broader ellipse appeared when dc control was applied (Fig. 639). To restore the ini-
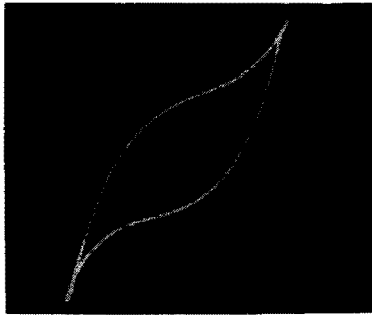
Fig. 641. *Hysteresis loop of barium titanate capacitor.*

tial pattern, the oscillator frequency had to be shifted from 4,250 to 5,000 cycles. It is easy to calculate that this implies a variation of L from 0.14 to 0.1 henry, or a decrease of 29%.

Hysteresis loop of dielectrics

Some dielectric materials such as barium titanate exhibit some rather peculiar properties. First, they feature dielectric constants

Fig. 642. *Characteristic of a non-linear thyrite resistor (varistor).*

of about 2,000 to 6,000; that is a thousand times more than those of conventional insulating materials. For this reason, a 470-$\mu\mu$f capacitor is just as large as a matchhead. The "constancy" of this constant is not great: for a Glenco type rated K = 3,300, a dc bias of 300 volts results in K = 2,000. This means that the capacitance of a 330-$\mu\mu$f capacitor using this dielectric material will be reduced to

200 μμf if a dc bias of 300 volts is applied, a very noteworthy variation.

But this is not all. Just like a ferromagnetic material, this type of
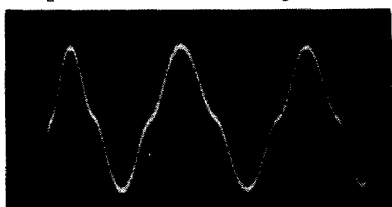
Fig. 643. *Waveform of the load current of the varistor shows some third-harmonic content.*

dielectric exhibits hysteresis, and for this reason it is often referred to as a ferroelectric. But don't believe that it actually contains iron; it only behaves as though it does. As there is a hysteresis loop, there
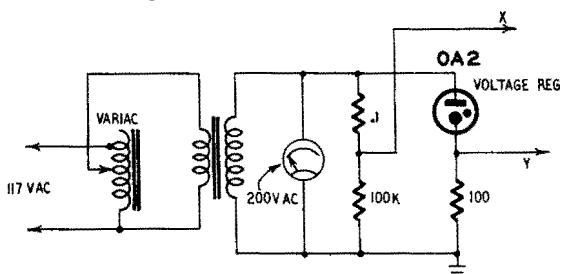
Fig. 644. *Circuit for obtaining curves of VR tubes.*

are losses too, and these losses are temperature-dependent. Just a lot of exciting (or confusing) properties, interesting to investigate!

The circuit of Fig. 640 was set up to study the behavior of a ferroelectric capacitor of 2,260 μμf made up by paralleling smaller units to avoid working with high impedances. This is a bridge circuit. Assuming the bridge balanced, C1 and C2 being conventional ("linear") capacitors, a straight horizontal line will appear on the screen of the C-R tube if the phasing is correct. A sloped line indicates unbalance of the bridge. Increasing the applied voltage will lengthen the baseline, but nothing else will happen.

If you are confused by the strange aspect of an oscillogram obtained with some nonlinear material, try replacing it by a similar one of known linear behavior whose operation you can predict. This may help detect some error or faulty component in the setup.

121

Connecting the barium titanate capacitor into the bridge and balancing it with a low voltage applied, the emf was increased to 200 volts rms, or 280 volts peak. (As the capacitors are series-con-
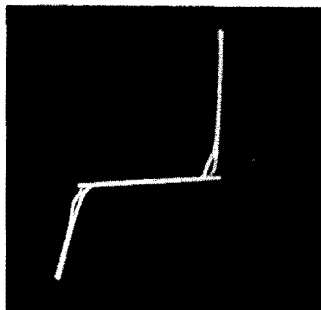
Fig. 645. *Characteristic curves of an OA2 voltage-regulator tube.*

nected, only half this voltage should be applied upon each unit, but because of the variable losses of the ferroelectric, this does not hold.) The oscillogram of Fig. 641 thus obtained is noteworthy for two reasons: The loop formed by the trace as the applied voltage increases and decreases indicates a dielectric hysteresis, and the loop area is a measure of the losses. Second, the curvature shows an unbalance of the bridge, increasing with the applied voltage; C1 is very voltage-dependent.

Of course, very different aspects of the same phenomenon can be displayed for different phasing conditions and an unbalanced bridge. And how accurately can one balance a bridge containing a variable component to be checked!

Other nonlinear components

Just like inductors and capacitors, resistors can be nonlinear. Certain silicon carbide compounds (for instance, thyrite, manufactured by General Electric Co.) are voltage-sensitive; that is, the resistance of such a resistor decreases rapidly as the applied voltage is increased. This property is used for control purposes and for protection against surge voltages. Unlike semiconductors, these nonlinear resistors, or varistors, have no polarity, and there are no forward and reverse currents.

Just like a diode, the varistor was connected into the circuit of Fig. 602, and the characteristic of Fig. 642 was obtained. On both sides of an inflection point in the middle of the curve the current increases more rapidly than the applied voltage (the component tested presented a resistance of 300 ohms at 6 volts, and only 92

122

ohms at 12 volts). The same curve could be obtained with two-back-to-back connected diodes, a more expensive solution, however.

Applications in voltage regulators are evident, and a less well-known property will be demonstrated. Replacing the sine sweep of the scope by a linear time base, the waveform shown in Fig. 643 appeared on the screen, denoting some third-harmonic content (compare with Fig. 511 in Chapter 5.). It should be easy to filter the

Fig. 646. *The load current of the voltage-regulator tube shows clipping of the middle portion of the waveform.*

fundamental and retain the harmonic alone, thus realizing a very simple frequency tripler. The writer, however, is unable to specify the highest operating frequency of this device.

Thermistors belong to another class of nonlinear resistors. These temperature-sensitive components feature a high negative temperature coefficient (the resistance decreases rapidly with increasing temperature). By self-heating, the resistance obviously decreases too if a current is passed, be it ac or dc.

The circuit of Fig. 602 should permit tracing the characteristic of a thermistor too. However, owing to the large thermic time constant of the device, the sweep frequency ought to be lowered considerably. A sweep duration of at least 10 seconds is necessary for small bead type thermistors, and minutes are required for the other models. For this reason, oscilloscopic curve tracing is definitely unsuitable for thermistors.

Voltage–regulator tubes

VR tubes and all other types of gas diodes are just another class of nonlinear devices. The circuit of Fig. 644 is self-explanatory. The curve of Fig. 645 was obtained with a regulator tube, showing the typical behavior of gas tubes. The applied emf was 150 volts

rms. That means the tube was "swept" from −210 to +210 volts. During the major part of the cycle there is no Y-deflection, or no current flowing, and the current, once it sets in, rises very abruptly, evidencing a steeply falling internal resistance. (The tube is easily destroyed if insufficient external resistance is provided.) Note that the baseline exceeds somewhat the knee of the curve; this is due to
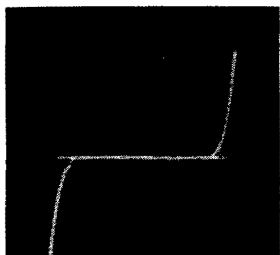
Fig. 647. *Characteristic of a small neon pilot tube. Note the symmetry of the curve.*

the sudden striking (conduction) of the tube, decreasing the transformer voltage. At low currents the rising and falling traces are not superimposed, indicating erratic low-level operation (it is not recommended by the manufacturer). This type of VR tube is designed for operation with a specified polarity, and its electrodes are dissimilar. That is why the right-hand slope is steeper than the left-hand one. The true operating point is to be situated on the right-hand slope.

Sweeping the C-R tube by a time base resulted in the display of Fig. 646, showing a somewhat peculiar clipping action. Instead of clipping the tops of the wave, this circuit has suppressed the middle portion. If one is interested in visualizing the tops of an oscillogram only, this circuit may prove valuable.

The characteristic of a small neon pilot tube is shown in Fig. 647. The sweep had to be reduced to 75 volts rms, or about 100 volts peak, and the rated current, of course, is lower. As identical electrodes are used, the curve is quite symmetrical.

fundamental electronic circuits

A TUBE or transistor can perform only four fundamental types of operation (or a mixture thereof). Understanding their basic principles and spending the time necessary to see how they work always leads to understanding the operation of the whole. The four fundamental functions of electronic circuits are: amplification, oscillation, modulation and detection.

Optimum working point of an amplifier

An amplifier is a device for reproducing a signal (fed to its input terminals) with increased amplitude (at its output terminals). Thus, the principal feature of an amplifier is its gain. Voltage gain is not the only thing to be considered; there actually may be a voltage loss, but a current (or power) amplification. You must understand what magnitude has to be amplified.

But the available gain is not the unique characteristic to be specified. The waveform of the input signal has to be reproduced with the best possible fidelity, and this means that the amplifier has to introduce the lowest possible amount of distortion. High gain and low distortion are somewhat conflicting conditions, and a compromise is generally worked out to optimize operation as a whole.

To study the operation of a typical voltage amplifier, the circuit of Fig. 701 was set up. Although it is never used in modern radios and TV receivers, the method of obtaining variable grid bias by means of a battery and a potentiometer is best for demonstration purposes. The input signal is delivered by an audio oscillator. The 60-cycle line voltage may be used instead if its waveform is good;
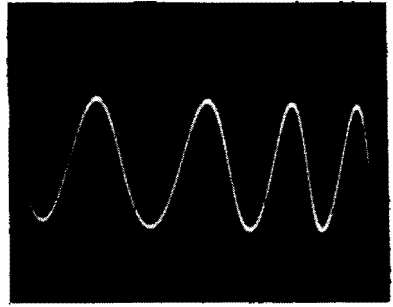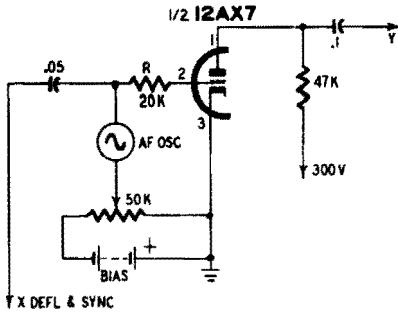
Fig. 701 (left). *Audio amplifier circuit with arrangement for using different amounts of fixed bias.* Fig. 702 (right). *Sine-wave output from the circuit of Fig. 701.*

if noticeable distortion is present, it is impossible to evaluate the amount of distortion originating in the amplifier.

As there is sufficient gain, the output of the 12AX7 was connected to one Y-plate of the cathode-ray tube. Thus, the height of the oscillogram is proportional to the output voltage.

Setting the bias control at —2 volts and injecting an af signal of 1 volt rms or 1.4 volts peak, the approximately "pure" sine wave of Fig. 702 was obtained. (The lack of linearity of the sweep should not be attributed to the amplifier under test.) Switching the scope to the X-amplifier, the diagonal line of Fig. 703 was displayed. Though reasonably straight, it is not accurate, for even the "straight" portions of a characteristic are never exactly linear and there is room for compromise. Of course, the curvature being slight, a very small portion of the characteristic can be considered as being linear, but the resulting small output voltage may be insufficient.

Increasing the input to 2 volts, rms (the bias remaining unchanged) results in the waveform shown in Fig. 704. The amplitude

Fig. 703 (left). *Fairly straight characteristic obtained by feeding the output of the audio amplifier (Fig. 701) to the X-amplifier of the scope.* Fig. 704 (center). *With increased signal input, bias remaining unchanged, tops of the waveforms begin to flatten.* Fig. 705 (right). *Ends of the characteristic bend horizontally, indicating excessive signal voltage.*

126
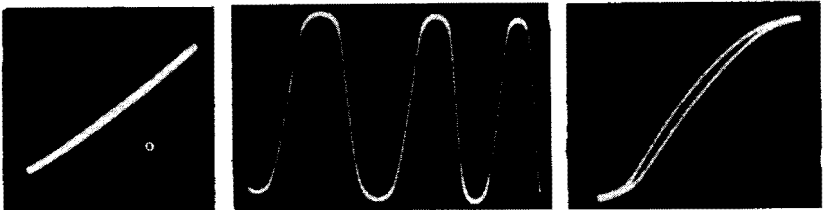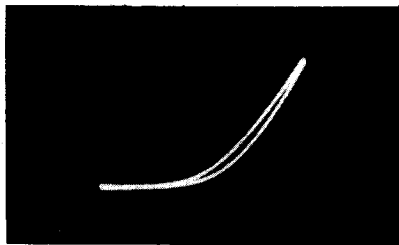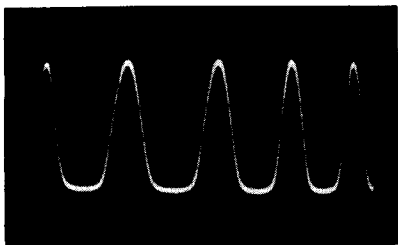
Fig. 706 (left). *Flattening of the negative peaks indicates excessive bias voltage.* Fig. 707 (right). *Characteristic shows condition of plate-current cutoff due to high bias.*

is increased, but the tops of the wave are flattened on both sides, indicating nonlinear operation. This condition is more clearly shown in Fig. 705 where both ends of the sloped line bend horizontally. The lower bend is due to an exaggerated negative grid-voltage swing (−4.8 volts peak); for a 12AX7, this corresponds to the cutoff condition. The upper bend indicates that the tube is running into grid current, the positive grid swing being 0.8 volt peak. Note that this bend would not appear were the grid directly connected to the low impedance of the generator. Of course, grid current still would be present, but no bias-changing voltage would develop. To simulate operation with a medium-impedance driver stage, the series grid resistor R (Fig. 701) was introduced, and the voltage
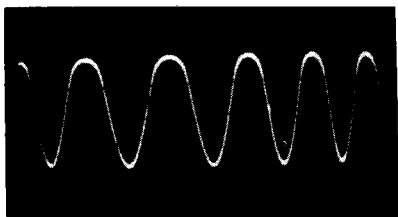
Fig. 708 (left). *Insufficient bias rounds the tops of the waveform.* Fig. 709 (right). *Characteristic corresponding to the condition shown in Fig. 708.*

Fig. 710 (left). *Audio amplifier with provision for varying the cathode bias.* Fig. 711 (right). *Characteristic shows a small amount of overloading.*
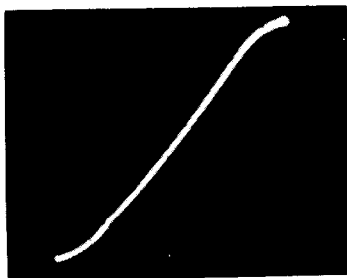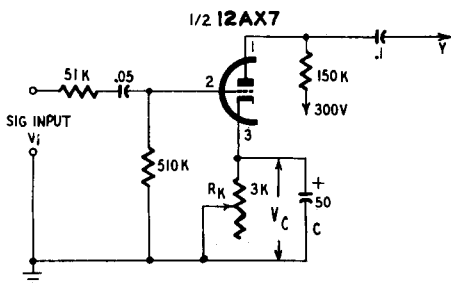
across this resistor passing grid current is responsible for the upper bend.

This working condition is typical for overload, the working point being correct. With an exaggerated bias (−4 volts) and a signal of 2 volts rms, the waveform of Fig. 706 was obtained, showing badly flattened negative tops. This cutoff condition is evident in Fig. 707. Insufficient bias (−1 volt; signal, 1 volt rms), on the contrary, results in flattened or rounded upper tops of the sine wave, as shown in Fig. 708. The corresponding characteristic (Fig. 709) shows this condition.

Though two methods were used to demonstrate the amount of distortion introduced by the amplifier and simultaneously to eval-
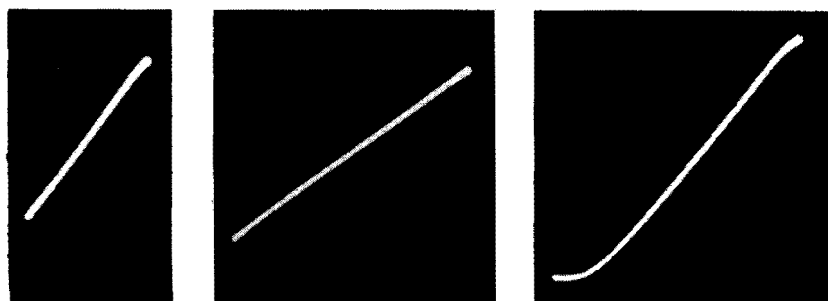
Fig. 712 (left). *Reducing the signal voltage results in fairly linear operation.* Fig. 713 (center). *More linear operation is obtained by removing the cathode bypass capacitor.* Fig. 714 (right). *With an unbypassed cathode resistor, severe overdrive results in moderately nonlinear operation.*

uate its output voltage, the characteristic seems best suited for adjusting for optimum working conditions, for the linearity departure of a straight line is easily appreciated while small amounts of low-order harmonic distortion may not be noticed. Furthermore, the 60-cycle line voltage or any other source presenting some distortion may be used as a signal without falsifying the display; the same waveform acting upon both pairs of deflection plates (assuming a distortion-free amplifier). .

Using one method or the other, first make sure that the deflection directions are correct, to know whether a bent or a flattened top corresponds to grid current or to cutoff. If necessary, the connections to the Y- or X-plates or both must be reversed to get the familiar display.

Operating the tube with conventional cathode bias and a higher plate resistor (Fig. 710) results in similar oscillograms. With a
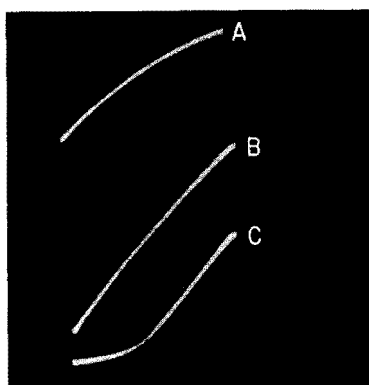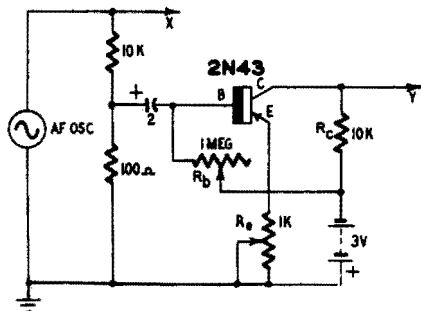
Fig. 715 (left). *An experimental transistor amplifier.* Fig. 716 (right). *Common-emitter transistor amplifier output characteristics. The curves are for different values of base resistor.*

cathode resistor $R_k = 1,500$ ohms (cathode voltage $V_c = 1.1$ volts) and an input signal of $V_i = 2$ volts rms, the characteristic of Fig. 711 was obtained, showing some overload but a correct working point. Reducing V_i to 1 volt rms resulted in Fig. 712, indicating linear operation.

Removal of the cathode bypass capacitor (C) introduces some inverse feedback, reducing the gain of the tube and straightening its characteristic. Thus, Fig. 713 shows a rather straight characteristic obtained with $R_k = 2,000$ ohms ($V_c = 1.6$ volts) and $V_i = 2$ volts rms. There is no sign of grid current. Severe overdriving ($R_k = 3,000$ ohms, $V_c = 1.8$ volts, $V_i = 5$ volts rms) is responsible for the characteristic of Fig. 714 where only the ends are bent. This
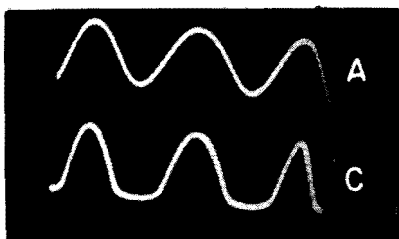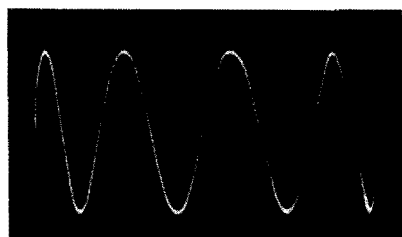
Fig. 717 (left). *Sine wave obtained with a value of 0.55 megohm for the base resistor in Fig. 715.* Fig. 718 (right). *Output waveforms corresponding to characteristics A and C in Fig. 716.*

explains why omission of the cathode bypass capacitor is a good trick to reduce amplifier overdrive, provided the resultant loss of gain can be tolerated.

Working point of a transistor amplifier

Adjusting a transistor amplifier for optimum operation is somewhat similar to adjusting vacuum-tube units. Use caution to avoid

severe overloading, for a transistor is easily damaged. Use correct polarities and voltages well below the maximum ratings.

A simple common-emitter transistor amplifier is represented in Fig. 715. After choosing the collector load, only the base resistor R_b is to be adjusted. An input voltage divider with a 100 to 1 ratio delivers a small signal to the transistor while providing sufficient input for the X-amplifier.

For different values of R_b, the three curves of Fig. 716 were obtained, using a dc amplifier for Y-deflection to show the dc component. Connection of the plates was such that a negative voltage
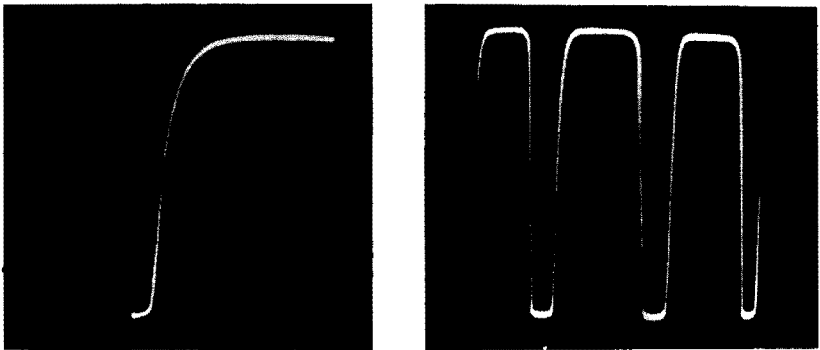
Fig. 719 (left). *Overloaded transistor amplifier characteristics.* Fig. 720 (right). *Squared sine wave produced by an overloaded transistor amplifier.*

produced an upward deflection. The signal amplitude was 5 mv rms. Curve B is approximately straight, and the height of vertical deflection indicates that its output is highest among the three curves displayed. An ac millivoltmeter connected to the output read 270 mv; thus, the gain was 270/5 = 54. The correctly amplified sine wave is reproduced in Fig. 717. R_b was 0.55 megohm.

Curve A of Fig. 716 was obtained with $R_b = 0.8$ megohm. Some curvature and low output are apparent. Displayed against time (Fig. 718, top), the rounded tops and the reduced amplitude are clearly visible (compare Fig. 717; the setting of the scope amplifier was the same). Measured gain was 42. With too low a base resistance ($R_b = 0.4$ megohm), curve C was obtained, showing a pronounced knee and low gain. The corresponding waveform is shown in Fig. 718, bottom; the lower peaks are just as clipped. Measured gain was 40.

Because of the temperature dependence of transistors, this simple arrangement offers poor stability, and more evolved circuitry is
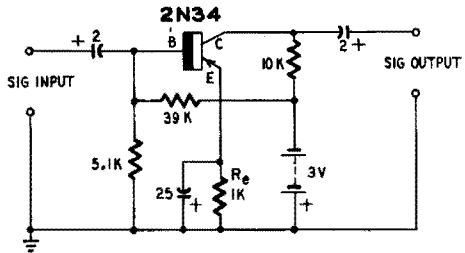
Fig. 721 (left). *Effect of presence (A) and absence (B) of emitter bypass capacitor.*
Fig. 722 (right). *Transistor amplifier circuit is stabilized when base bias voltage is obtained from a voltage divider.*

often required. If this circuit is used, it is best to make R_b slightly higher rather than lower than the optimum value, for the resulting distortion will be less pronounced. On the other hand, increasing

Fig. 723. *Circuit arrangement which can be used for measuring the gain of an amplifier.*
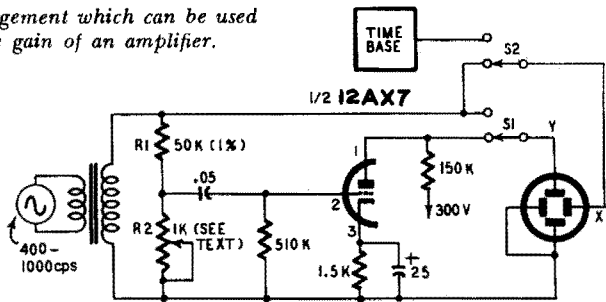
R_b will lower the collector current, and, by the same token, the power supplied by the battery.

Of course, a transistor amplifier can be overdriven, and Fig. 719 shows the input–output characteristic for a signal voltage of 100 mv rms; R_b was 0.55 megohm. The corresponding waveform is given in Fig. 720. By carefully adjusting the operating point, a unity mark–space ratio could be obtained.

Temperature dependence of the transistor amplifier can be reduced by introducing a resistor R_e in series with the emitter. The inverse feedback thus obtained can be restricted to dc only by decoupling R_e by means of sufficient capacitance. Omitting this capacitor results in improvement of linearity and loss of gain, just as in the case of the cathode resistor of a vacuum tube. This effect is demonstrated in Fig. 721 where curve A was obtained with a 25-μf capacitor shunting an emitter resistor R_e of 1,000 ohms. For an input signal of 18 mv rms, the measured gain was 39, but the linear-

ity is poor. Omitting this capacitor reduced the gain to 7.8, but considerably improved the linearity (curve B). Further stabilization against thermic effects is obtained by supplying the base bias voltage from a voltage divider. The stabilized circuit of Fig. 722, experimentally adjusted for optimum operating conditions, yielded a gain of 43.

Measuring amplifier gain

A straightforward method of measuring amplifier gain consists in connecting suitable vtvm's to the input and output terminals of the amplifier to be tested. Dividing the output V_o by input V_i yields a gain $G = V_o/V_i$. To avoid the need for two accurately calibrated instruments, a single vtvm can be switched from input to
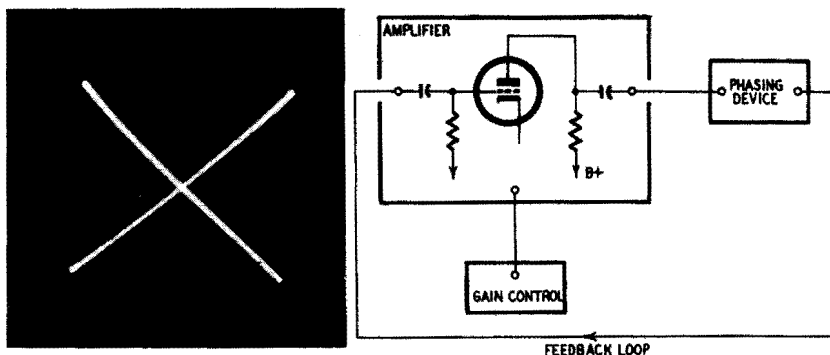
Fig. 724 (left). *Input and output characteristics of an amplifier. The two-shot oscillogram allows gain measurement and linearity checks. Crossing of lines indicates phase shift.* Fig. 725 (right). *With the addition of a suitable phasing circuit, the amplifier becomes an oscillator.*

output. But the range has to be switched simultaneously, and use of different ranges introduces an error. This can be overcome using a calibrated attenuator set to give equal readings for V_o and V_i. Used this way, the vtvm introduces no possible error, and does not even need calibration.

This principle can be applied for measuring amplifier gain, with the scope replacing the vtvm as a device to compare input and output voltages, simultaneously allowing for linearity checking. In the circuit of Fig. 723, S1 can be thrown to connect the Y-deflection plate to the top of voltage divider R1–R2 or to the tube output. Equal deflections will be obtained if the tube gain equals the attenuation introduced by the voltage divider, or:

$$G = \frac{(R1 + R2)}{R2}$$
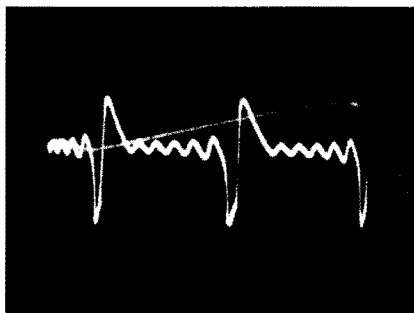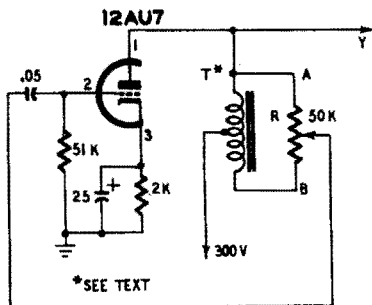
Fig. 726 (left). *With this circuit arrangement, a variable in-phase or out-of-phase signal can be returned from the output to the input.* Fig. 727 (right). *Waveform obtained through the use of the circuit in Fig. 726. The amount of feedback was small.*

R1 was a 50,000-ohm 1% tolerance unit and R2 a decade resistance box. Instead of the decade, a variable resistor can be used. Once set for equal deflections, its actual resistance is then measured on a Wheatstone bridge.

As direct connections to the deflection plates were made, the signal amplitude had to be increased to about 100 volts by a stepup transformer. As low-frequency rolloff may be present at 60 cycles,
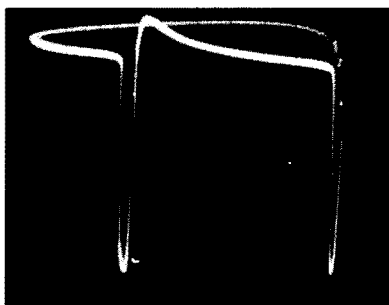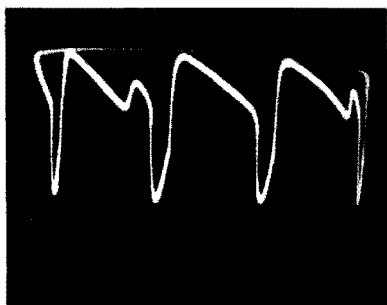
Fig. 728 (left). *Increasing the amount of positive feedback reinforces the pulses.* Fig. 729 (right). *A large amount of feedback produces typical blocking oscillator operation.*

a medium frequency such as 400 or 1,000 is preferable. S2 permits displaying the characteristic or the waveform of the output voltage.

With this circuit, the two-shot oscillogram of Fig. 724 was obtained, showing crossed lines of equal height. The line sloping from the lower left to the upper right is the output characteristic; the other line represents the total input voltage applied to both deflection plates. Crossing of these lines indicates the phase reversal or 180° phase shift introduced by the tube. Equal deflections were

133

obtained for $R1 = 50,000$ ohms and $R2 = 900$ ohms, yielding a gain of $G = 50,900/900 = 57$ times. This is the mid-frequency gain.

The same method can be used to investigate the rolloff characteristic of the amplifier operating at different frequencies. Identical techniques are used for gain measurements of transistor amplifiers.

Oscillation

As shown in Fig. 724, a one-tube amplifier introduces a phase reversal. A positive pulse injected into the grid will result in a negative pulse on the plate, and feeding back some energy from output to input will oppose the original signal and decrease its amplitude. This is inverse feedback, and its effects are studied in the next section.

Suppose, however, that the feedback loop contains some phasing device (to be specified later) introducing a 180° phase shift (Fig.
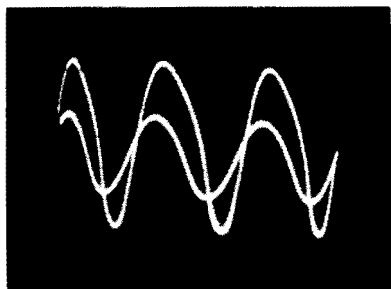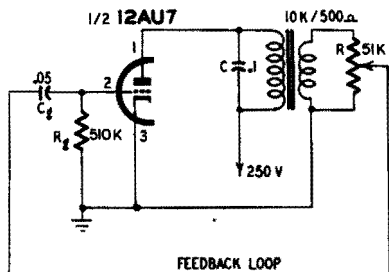
Fig. 730 (left). *Experimental oscillator circuit providing good waveform and easy adjustment.* Fig. 731 (right). *Waveforms obtained with two different settings of feedback control R in Fig. 730.*

725). The signal fed back from the output to the input is now in phase with the original signal and will tend to reinforce it. The signal amplitude will grow steadily and would increase indefinitely were there nothing to stop its rise. But, actually, there is something that limits the amplitude of the wave, and that is the nonlinearity of the working characteristic. The more or less straight characteristic of an amplifier is limited on both sides by horizontal portions where no further increase of amplitude can occur. Sweeping this portion of the curve implies severe distortion, and a gain control has to be provided to restrict the operation to the linear part of the characteristic if a "pure" wave is to be obtained.

This is a simplified theory of the physical phenomenon; let us now see how it works. To accomplish the necessary phase reversal, we used the center-tap winding of a transformer (T) connected as

the plate load of a triode amplifier (Fig. 726). A potentiometer (R) is connected across the whole winding. At its electrical mid-point there is no feedback at all. If the slider is set near point A, we have
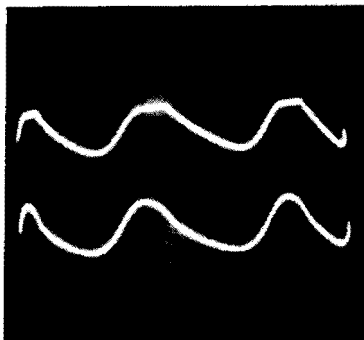
Fig. 732. *Waveform clipping (upper trace) is present on the grid in the circuit of Fig. 730, but is absent on the transformer secondary (lower trace).*

inverse feedback for the output voltage opposes the signal and no oscillation occurs. On the contrary, if the slider is moved toward point B, the electrical mid-point being passed, an increasing voltage of opposite phase is injected into the grid, reinforcing any varia-
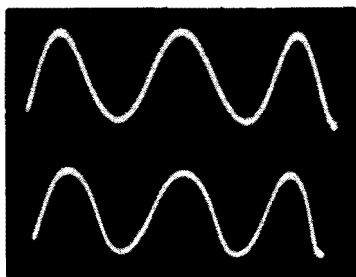
Fig. 733. *The shape of the sine wave (above) is improved by the introduction of negative feedback (below).*

tion of initial conditions, for the total phase shift now is 180 + 180 = 360°, or 0°.

The setting of R determines the amount of energy fed back and thus modifies to a considerable extent the waveform of the resulting oscillation. First, a small-amplitude sine wave was obtained, but adjustment was somewhat tricky and lacked stability. Then pulses

of much greater amplitude than the sine wave appeared (Fig. 727). When the feedback was increased, the sine wave tended to disappear (Fig. 728), and then the pulses remained alone (Fig. 729). This condition identifies a blocking oscillator, usable as a triggering device.

The difficulty of obtaining a stable sine wave stems from the exaggerated amount of disposable feedback voltage. Taking into
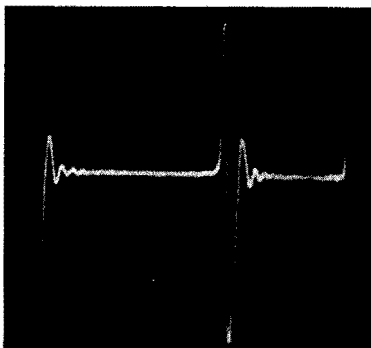
Fig. 734. *Increasing the value of the grid-return resistor shown in Fig. 730 produced this waveform.*

account the tube gain, it is easy to understand that only a small amount of the total output should be fed back if the tube is not to be strongly overdriven. To obtain a low, easily controlled feedback voltage, a stepdown transformer was used (Fig. 730) and its primary was tuned by capacitor C. (Were there no tuning capacitor, the winding would be tuned by its distributed capacitance and

Fig. 735. E_p/E_g *characteristic of a blocking oscillator.*

would resonate at a much higher frequency.) Thus, the waveforms shown in Fig. 731 were obtained for two different settings of the control. The larger-amplitude wave shows distortion; reducing the

136

amount of feedback resulted in the smaller-amplitude, but reasonably pure waveform.

Note that the circuit of Fig. 730 contains no cathode bias resistor,
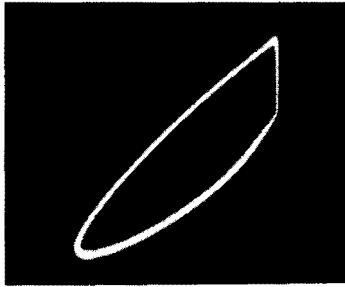
Fig. 736. E_p/E_g characteristic of a sine-wave oscillator showing the effect of grid clipping.

and yet the tube operates in a biased condition. As oscillation starts, the grid is at cathode potential, and its mutual conductance is highest, making for easy starting. As the first oscillations appear on the
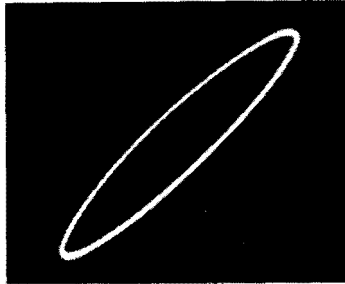
Fig. 737. Grid clipping is eliminated by using cathode bias. Sustained oscillation having a good waveform is obtained.

grid, the positive half-waves are detected (or rectified), and the resultant grid current biases the grid through grid leak R_g. As the mutual conductance of the biased tube is somewhat lower, the tube gain is decreased, limiting the buildup of oscillations. Thus, the grid coupling introduces true amplitude regulation, suitable circuit constants being provided. The actual waveform on the grid (Fig. 732, top) shows the clipping due to grid current. This effect was not present at the transformer secondary (Fig. 732, bottom). Though these waves are distorted, the tuned primary features a pure sine wave.

Introducing inverse feedback by an unbypassed cathode resistor improves the waveform (Fig. 733) where the lower oscillogram corresponds to the introduction of a 1,000-ohm cathode resistor. Higher values result in decreased output.

Grid coupling time constant

Since an oscillator is a sort of amplifier, it is understandable that the time constant of the grid leak, i.e., the product R_gC_g, has to be
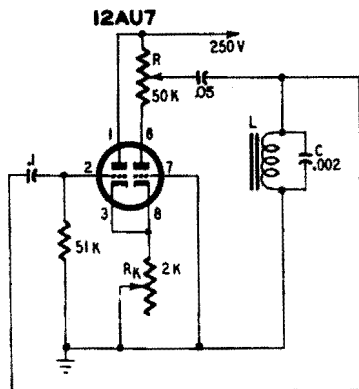
Fig. 738. *Cathode-coupled duo-tri-ode oscillator.*

large enough to transmit a sufficient amount of energy to allow for sustained oscillations. On the other hand, if R_gC_g is made too large, the detection of one or several cycles may build up an important
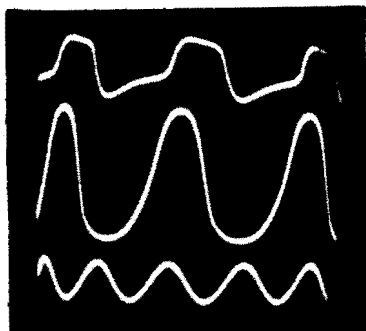
Fig. 739. *Waveforms obtained for three different settings of the variable feedback resistor R of Fig. 738.*

bias voltage which leaks away very slowly. Meanwhile, the tube is in a cutoff condition, and oscillations cease until the bias is reduced to a value sufficiently low to make the tube operative again. This

starts a new short oscillation cycle. This blocking effect upon oscillation gave its name to the blocking oscillator, a triggering device used extensively in TV time bases.

To study the effect of the time constant on oscillation, R_g was replaced by a 5-megohm control resistor. Setting R_g at 2 to 5 meg-
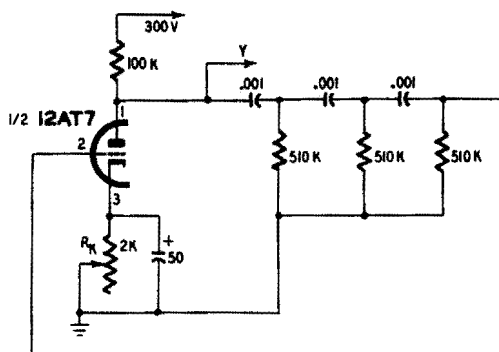
Fig. 740. *Simple phase-shift oscillator using re-sistance—capacitance-coupled sections.*

ohms, oscillations of the type displayed in Fig. 734 were obtained—one cycle of large-amplitude oscillation followed by some other
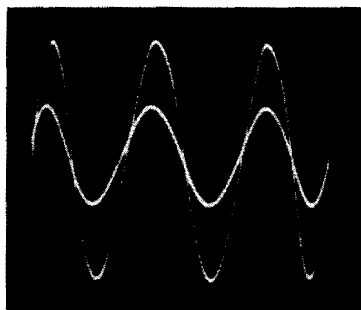
Fig. 741. *Waveforms obtained with and without the use of the cathode bypass capacitor in Fig. 740.*

cycles of rapidly decreasing amplitude, and then oscillation ceases. After a while, a new rapid buildup is initiated.

Like an amplifier characteristic, an oscillator characteristic can be displayed by connecting the Y-deflection to the plate and the X-deflection to the grid of the tube. For the blocking oscillator waveform of Fig. 734, the characteristic of Fig. 735 was obtained.

The bright spot on the lower right is a moving, flattened spiral corresponding to the fading of oscillations. The photo was deliberately overexposed to show the outer contour corresponding to the single large-amplitude cycle. The straight portion on the right side is due to clipping of the positive top grid current.

TUNED PLATE
a

TUNED GRID
b

ECO
c

HARTLEY
d

✳ SEE TEXT
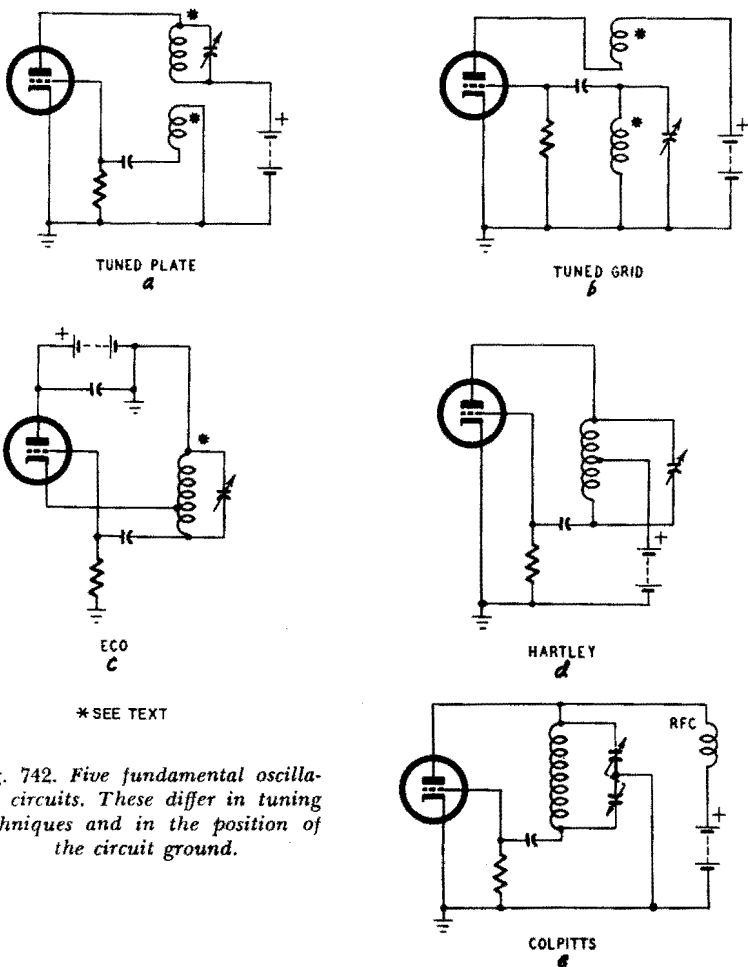
Fig. 742. *Five fundamental oscillator circuits. These differ in tuning techniques and in the position of the circuit ground.*

COLPITTS
e

Reducing R_g to about 0.1 megohm resulted in sustained oscillations. The flat spiral disappeared, but not the straight portion on the right side, for grid current continues to flow (Fig. 736). However, introducing a 1,000-ohm cathode resistor provides enough bias to avoid detection, at least at low oscillation amplitudes, as shown by the ellipse of Fig. 737.

Two-tube oscillators

The in-phase condition necessary for generation of oscillations can also be realized by using a two-stage amplifier, each stage introducing a phase reversal. A cathode-coupled amplifier is shown in Fig. 738. A portion of its output voltage, variable by means of control R, is applied to the tuned circuit L-C, in turn connected to the

Fig. 743. *Distorted high-frequency voltage. The individual cycles cannot be seen. The scope sweep frequency may be too low or sync may be inadequate.*

grid, closing the feedback loop. As L-C introduces no phase shift at its resonant frequency, oscillation will take place, provided there is no phase shift in the amplifier circuit at that frequency.

It is commonplace to state that the frequency of an oscillator is—mainly—determined by the resonant frequency of the tuned circuit.
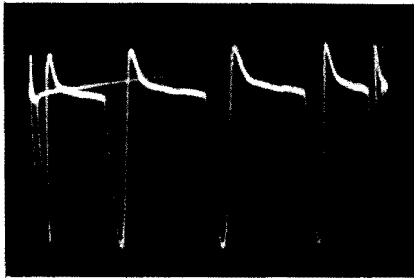
Fig. 744. *Waveform of Fig. 743 when proper synchronization is used.*

While this is true, it is preferable to say that the oscillating frequency is determined by the in-phase condition of the entire loop, consisting of the frequency selective network as well as the amplifier. This approach helps in understanding the operation of resistance–capacitance oscillators. This type of circuit presents a rather

broad resonance curve, with a phase angle varying rapidly in the vicinity of the resonant frequency.

By changing the amount of feedback with control R, the oscillograms of Fig. 739 were obtained. The distorted waveform on the top of the display corresponds to maximum feedback, the slider being set on the plate side. Moving the slider towards B-plus, a point
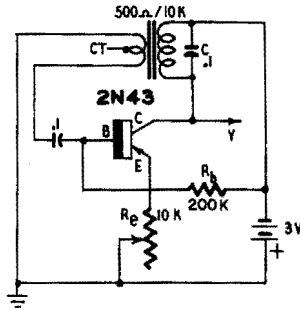
Fig. 745. *Transistor oscillator circuit.*

of maximum amplitude was found (middle oscillogram), but presenting some second-harmonic distortion. Moving the slider still farther decreases the output voltage, but improves the waveform as
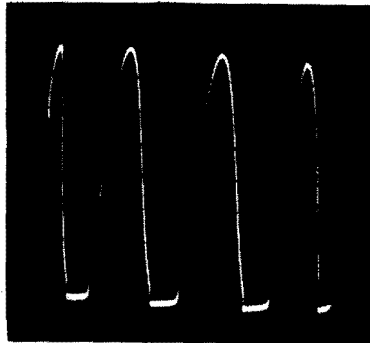
Fig. 746. *Oscillation waveforms produced by the circuit of Fig. 745.*

shown by the lower oscillogram. A very pure sine wave can be generated by this circuit and, as only a simple two-terminal inductor is needed, nearly all types of coils can be used—a very convenient feature for experimental purposes and quick hookup. In a practical circuit, L-C may be placed directly in the plate circuit, and amplitude and waveform can be controlled by a variable resistor (R_k) in the common cathode path.

R-C phase-shift oscillators

Examining Fig. 725 again, it is clear that oscillations can be produced with a one-tube amplifier using an R-C network as a phasing
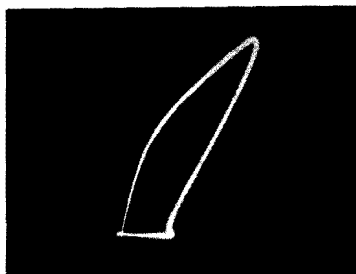
Fig. 747. E_o/E_b *characteristic of the transistor oscillator.*

device. Oscillations will occur at that frequency which introduces an overall phase shift of 360°, or zero, assuming the amplifier gain to be at least equal to the loss introduced by the phase-shift net-
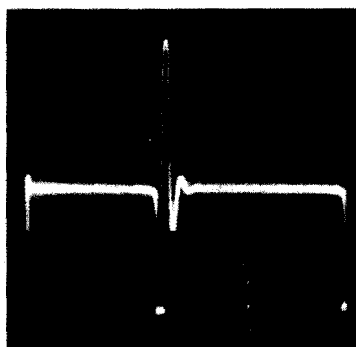
Fig. 748. *When the tuning capacitor C in Fig. 745 is omitted, the circuit becomes a blocking oscillator, as shown by this waveform.*

work. As R-C networks are always lossy, this condition is less easily satisfied in this type of oscillator.

A simple phase-shift oscillator is represented in Fig. 740. The output is fed back to the grid by means of three R-C sections. The only variable is cathode resistor R_k. Fig. 741 shows the waveforms obtained with $R_k = 1,600$ ohms shunted by a 50-µf capacitor (large amplitude waveform), and $R_k = 800$ ohms, the capacitor being omitted to introduce some inverse feedback (low amplitude waveform). The oscillating frequency was 100 cycles. This high-pass

type of network is best suited for low-frequency generation; for high-frequency oscillators, the low-pass, R-series, C-parallel network is preferable. Because of the high output impedance, a buffer
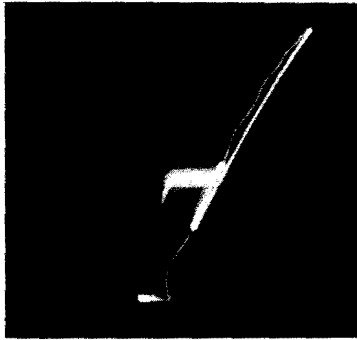
Fig. 749. E_o/E_b *characteristic of the blocking oscillator.*

amplifier is necessary to secure stability of amplitude and frequency. Output voltage is, however, liable to vary with the fluctua-
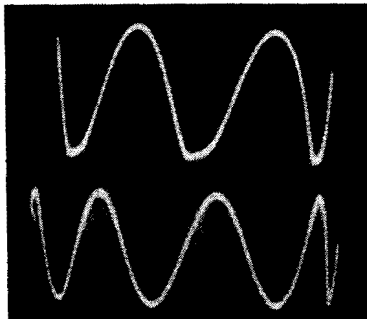
Fig. 750. *Sine waves obtained by reducing coupling and introducing emitter resistance.*

tions of the power supply, especially if the cathode resistor is decoupled by a capacitor, because there is no agc circuit.

High-frequency oscillators

Until now, we have investigated only low-frequency oscillators because of the simplicity of display. Of course, up to the vhf region the same principles apply, but because of the low time constants required, R-C oscillators are not practical for frequencies higher than, say, 200 kc. On the other hand, variable capacitors used in L-C circuits for high-frequency tuning are common.

144

The five fundamental types of high-frequency oscillators (usable also at low frequencies) are represented in Fig. 742 in a way to emphasize their basic resemblance. The principal difference is in tuning the entire coil or only a part thereof, and in the choice of

Fig. 751 (left). E_c/E_b characteristic corresponding to the upper trace of Fig. 750.
Fig. 752 (right). E_c/E_b characteristic corresponding to the lower trace of Fig. 750.

the grounding point. If a fractional coil is used, the plate circuit (A) may be tuned or the grid circuit (B). In the electron-coupled oscillator (C), the plate is grounded for ac, the grid and the cathode
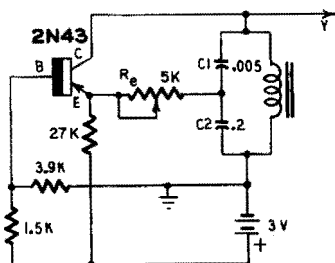
Fig. 753. *Transistor oscillator using a two-terminal inductor.*

being "hot." The Hartley oscillator (D) bears a strong resemblance to the eco (C), the only difference being the choice of the grounding point. The Colpitts oscillator (E) is derived from the Hartley (D), a two-gang variable capacitor being used instead of the center-tapped coil to get a grounding point.

The problem of generating a "pure" wave is somewhat less acute in high-frequency work. If you consider an af wave of, say, 1,000 cycles, its harmonics up to the 5th (or 10th or even 15th) are still in the audio band, and thus are liable to falsify the initial audio signal. In high-frequency work, because of the small bandwidth of

145

the operating frequency, harmonics are too far away to be included in the bandpass; they may however create interference in other channels, or "birdies" in superheterodyne circuits. Thus, the possible effects of harmonics should be investigated in each case to decide whether they can be tolerated. Signal generators, for instance,
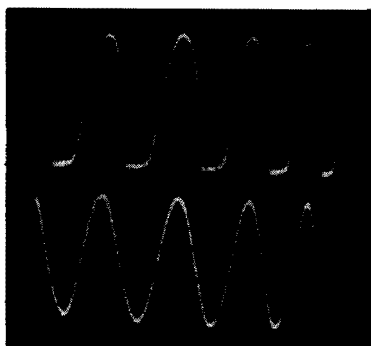
Fig. 754. *Waveform (upper trace) obtained when emitter resistor R_e in Fig. 753 is set to 0 ohms. The lower waveform is obtained when the resistor is set to 2,500 ohms.*

often use harmonics to provide signals in the upper bands, to avoid complication of their vhf circuitry.

It is sometimes difficult to view the individual cycles of a high-
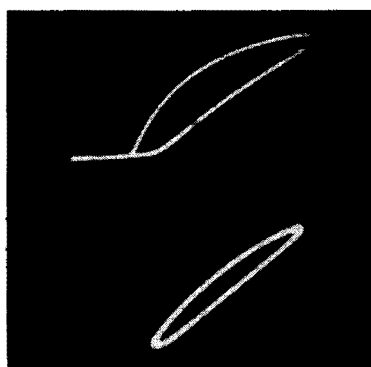
Fig. 755. E_c/E_e *characteristics corresponding to the two traces shown in Fig. 754.*

frequency wave on a scope because of insufficient sweep speed or inadequate operation of the sync circuit at high frequencies. A pattern such as Fig. 743 may be obtained, and indicates distortion.

146

The more brilliant horizontal stripes are caused by more or less horizontal portions of the wave, making the spot stay much longer in these regions. A waveform of the same voltage, properly synchro-
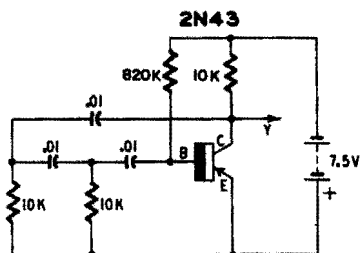
Fig. 756. *Transistor phase-shift os-cillator.*

nized, is shown in Fig. 744. This actually is the output of a 100-kc crystal frequency standard, and harmonics are desirable here.

Transistor tickler oscillators

Although there are some similarities between transistor and vacuum-tube circuits, there are some important differences in their physical behavior. For instance, the input impedance of a common-emitter transistor may jump from about 600 ohms to 0.5 megohm if
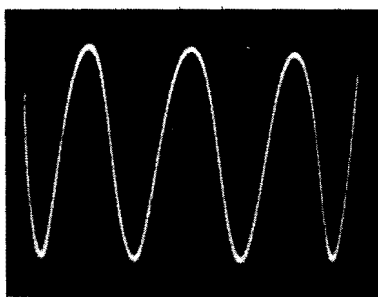
Fig. 757. *Waveform produced by the transistor phase-shift oscillator.*

the base is driven through cutoff. And if the oscillation produced is strong enough to realize this condition, the different damping of positive and negative half-cycles will result in a waveform unilaterally clipped. A suitable means of limiting the amplitude of oscillation is needed to insure sinusoidal operation.

On the other hand, the internal phase shift of a transistor is not exactly zero for common-base or common-collector configurations or 180° for the common-emitter circuit, but depends upon current

gain and operating frequency. Such a variable phase shift may change the oscillating frequency and jeopardize stability.

The transistor oscillator circuit of Fig. 745 is very similar to the familiar tickler oscillator (A in Fig. 742). The waveform of the
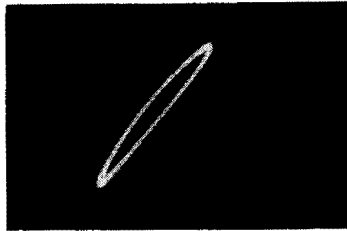
Fig. 758. E_c/E_b characteristic of the transistor phase-shift oscillator.

oscillations produced is shown in Fig. 746, where the clipping of the negative peaks due to cutoff driving of the base is clearly visible. Connecting the base to the X-deflection amplifier, the characteristic
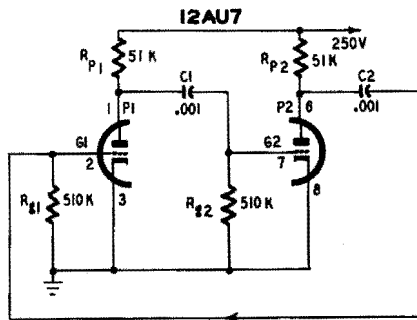
Fig. 759. Multivibrator is a closed-loop two-stage amplifier.

of Fig. 747 is obtained, demonstrating this effect during a part of the cycle. Omitting tuning capacitor C of Fig. 745 resulted in typical blocking-oscillator operation (Figs. 748 and 749). The time constant of the base coupling (R_b was increased to 0.3 megohm) was too long in relation to the oscillating frequency of the distributed-capacitance tuned inductor, and excessive feedback caused too strong oscillations.

Trying now to generate sine waves, the coupling was reduced by connecting the base to the center tap of its winding and by introducing a series resistor R_e into the emitter circuit. The resultant waveforms are shown in Fig. 750 for $R_e = 5,100$ ohms (top) and 8,200 ohms (bottom). While the former displayed some distortion,

the latter is a reasonably pure sine wave. The corresponding E_c/E_b characteristics are shown in Figs. 751 and 752, evidencing the presence and absence, respectively, of the flattened portion. Better than
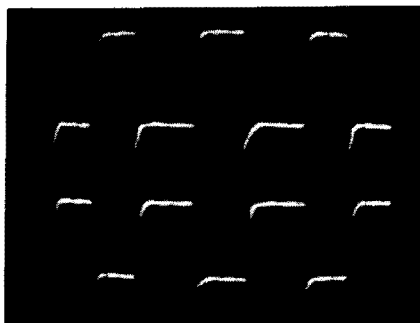
Fig. 760. *Multivibrator waveforms. Double trace was obtained by using an electronic switch.*

Fig. 750, Fig. 752 indicates absence of distortion. Oscillations ceased when R_e was greater than 10,000 ohms.

Transistor oscillator using a two-terminal inductor

Oscillators using simple two-terminal inductors are attractive; the circuit of Fig. 753 is an example of what can be done. This is a common-base configuration, introducing no phase shift, so that the feedback voltage can be derived from the tuned circuit, the capacitive voltage divider C1-C2 determining the amount of feedback.
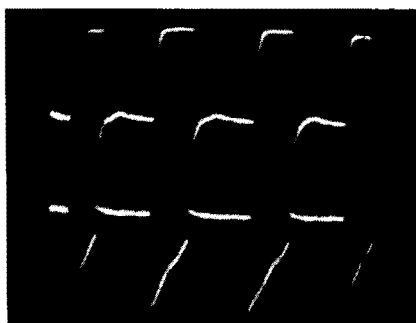
Fig. 761. *Upper trace shows waveform at P1 (in Fig. 759). Lower trace shows waveform at G1.*

Amplitude and waveform are controlled by the variable resistor R_e, adjusting the current fed back to the emitter.

The waveforms of Fig. 754 were obtained with $R_e = 0$ (top) and

2,500 ohms (bottom), showing the effect of R_e upon the waveform. The corresponding E_c/E_e characteristics are represented in Fig. 755.

With a high-impedance inductor and the components indicated, the oscillating frequency was 800 cycles. Battery current was 0.55 ma. Though a single winding is shown in Fig. 753, a stepdown transformer can be used for low-impedance output. The output

Fig. 762. *P1/P2 characteristic of the multivibrator.*

between collector and ground was 2.2 volts rms for $R_e = 0$, and 1.7 volts for sine-wave output.

Transistor R-C phase-shift oscillator

The R-C phase-shift oscillator of Fig. 740 has its transistor counterpart, Fig. 756. Application of this principle is, however, more

Fig. 763. *P1/G1 characteristic of the multivibrator.*

difficult with transistors, for the high collector impedance and the low base impedance require some matching of the phasing network. Moreover, the voltage gain has to be superior to the losses of the circuit, and low-gain transistors will not work.

This circuit yielded the waveform of Fig. 757 and the E_c/E_b characteristic is shown in Fig. 758. The oscillating frequency was 500 cycles, with a battery current of 0.45 ma. As the series capaci-
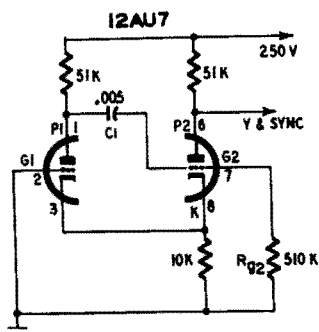
Fig. 764. *Cathode-coupled multivibrator.*

tors of the network were increased to .05 μf, no oscillation occurred until the battery emf was raised to 15 volts, increasing amplifier gain. Output was 1 volt rms.
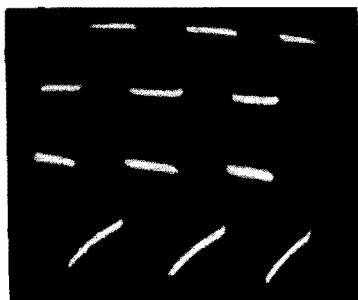
Fig. 765. *Waveforms at P1 (above) and P2 (below) of the cathode-coupled multivibrator.*

Relaxation oscillators

While the oscillators examined until now rely upon a frequency-selective device, such as a tuned circuit or a phasing network to generate sine waves, relaxation oscillators are based upon the charging and discharging of a capacitor through a suitable resistance. The generated wave is not sinusoidal, but approximates square or triangular waves, or pulses. Its repetition frequency depends partly upon the time constants of the couplings, but may vary widely according to the initiating and triggering conditions of the

charge or discharge. The inherent stability of these oscillators is poor, but this apparent inconvenience turns into a distinct advantage because it makes for easy synchronization.

Speaking of time bases, we just examined some types of relaxa-

Fig. 766. *Waveforms at P1 (above) and G2 (below) of the cathode-coupled multivibrator.*

tion oscillators, and the blocking oscillator operation mentioned in this same section is also based on a relaxation phenomenon. So the present investigation will deal only with multivibrators.

The multivibrator

This important circuit is nothing more than a conventional R-C-coupled two-stage amplifier whose output is fed back to its input.

Fig. 767. *Waveforms at P1 (above) and K (below) of the multivibrator circuit of Fig. 764.*

As the total phase shift is $2 \times 180 = 360°$ or $0°$, oscillation is to be expected, and the combined gain of two tubes makes the oscillation very strong. There are, however, no resonant components, and the operating frequency is mainly determined by the time constants of the couplings. For the circuit of Fig. 759, the operating frequency is approximately equal to $f = 1/(R_{p1} \times C2 + R_{p2} \times C1)$.

An electronic switch is used to study the operation of the multi-vibrator. Connecting its inputs to P1 and P2 resulted in Fig. 760, representing two approximate square waves of opposite phase.
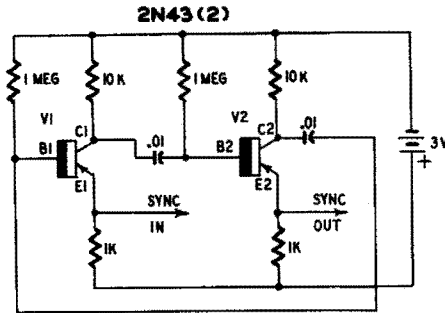
Fig. 768. *Transistor multivibrator.*

This means that one plate carries current while the other is at or near cutoff. The voltage at P1 is again shown in Fig. 761 (top), to be compared with the grid voltage (G1) of the same tube section (bottom). There is a flat portion where the grid is at about 0 volt, corresponding to a relatively heavy plate current and low plate voltage for the same tube section. Then the relaxation phenomenon takes place; the potential of P2 decreases, driving G1 deeply
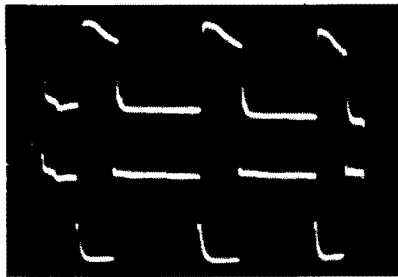
Fig. 769. *Waveforms at C1 (above) and C2 (below) of the transistor multivibrator in Fig. 768.*

into the negative voltage region by means of C2. P1 immediately rises to B-plus potential. The negative charge built up on C2 leaks away through R_{g1} (rising portion of the lower trace) and, for a given bias, G1 again controls the plate current, initiating a new reversal. As indicated by the very steep rises and falls, the transition is extremely rapid.

Just as for sine-wave oscillators, the E_p/E_g characteristic of the oscillating tube can be traced. Of course, no simple straight line or

153

ellipse is to be expected. Fig. 762 shows the P1/P2 characteristic, and Fig. 763 the P1/G1 characteristic of the multivibrator. These
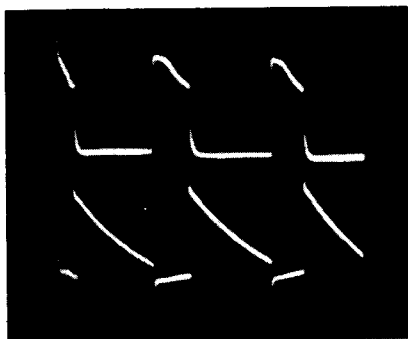
Fig. 770. *Waveforms at C1 (above) and B1 (below). Refer to Fig. 768.*

curves are looped but, because of the very rapid transitions, portions of it are invisible on the oscillograms.

Cathode-coupled multivibrator

Replacing one of the plate-grid couplings by cathode coupling results in the cathode-coupled multivibrator of Fig. 764. This circuit is very convenient because the only frequency determining
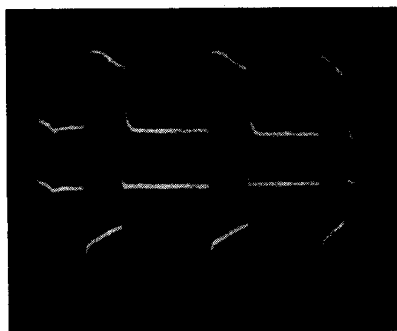
Fig. 771. *Waveforms at C1 (above) and E1 (below). See the transistor multivibrator in Fig. 768.*

components are C1 and R_{g2}. Therefore, it is used extensively in time-base generators. Grid G1, left free, can be used for sync purposes without disturbing normal operation.

Using the voltage on P1 as a reference (upper traces), Figs. 765, 766 and 767 show the waveforms on P2, G2 and K, respectively (lower traces). Operation can be explained as formerly. Note that a fair square wave is obtained at P1.

154

Transistor multivibrator

The transistor counterpart of the multivibrator of Fig. 759 is shown in Fig. 768. This is a back-coupled, two-stage, common-
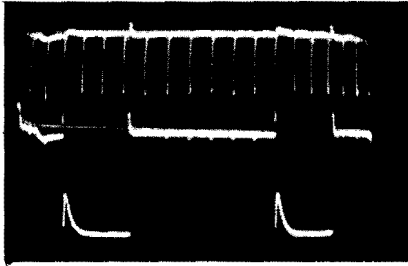
Fig. 772. *Multivibrator frequency division. Sync pulses are shown above and collector voltage below.*

emitter transistor amplifier. The emitter resistors are conveniently used for sync purposes.

Using the waveform on collector C1 as a reference (upper trace), Figs. 769, 770 and 771 display the voltages on C2, B1 and E1, respectively. Just as with vacuum-tube multivibrators, this circuit
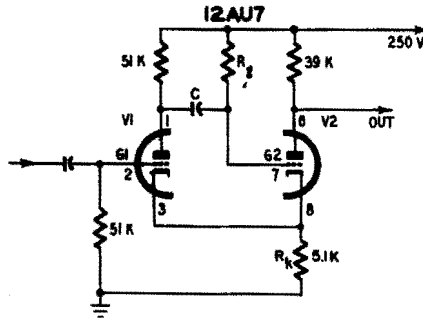
Fig. 773. *One-shot multivibrator or flip-flop circuit (also known as a univibrator).*

yields approximate square waves of opposite phase at the collectors of the transistors. To obtain perfect square waves, further squaring is necessary.

Multivibrator frequency dividers

The poor frequency stability of relaxation oscillators implies ease of frequency control by a suitable sync voltage, an important feature for frequency division circuits. Stable dividing ratios up to 10 to 1 and more are possible, provided an adequate sync signal is

injected at a suitable point. For accurate triggering of the multi-vibrator, pulses are preferable.

Frequency division by the multivibrator of Fig. 768 is illustrated by Fig. 772, which shows the collector voltage (below) and the sync pulses (above). As there are 10 pulses for 1 operating cycle, the
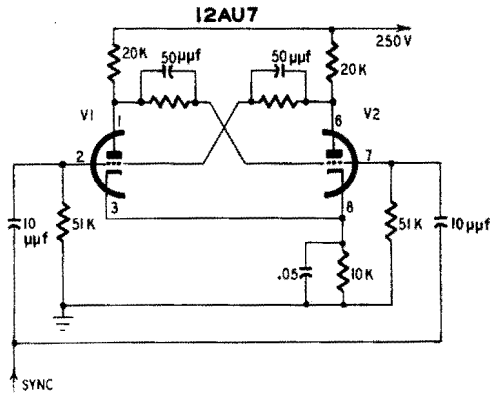
Fig. 774. *Multivibrator-derived scale-of-two circuit.*

dividing ratio is 10 to 1. The pulse-repetition frequency was 1,650 cycles, and the resulting operating frequency of the multivibrator thus is 165 cycles. This is about twice its "natural" frequency. For best stability, the "forced" frequency has to be slightly higher than
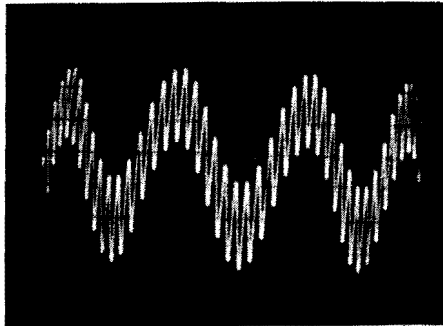
Fig. 775. *Linearly superimposed voltages, no modulation.*

the "natural" frequency to allow for easy triggering. The same condition applies to time-base sync, a very similar case.

Flip-flop and scale-of-two circuits

The multivibrator is a device featuring two unstable states; that

is why it oscillates all the time. Minor modifications lead to very important non-oscillating circuits.

The cathode-coupled multivibrator of Fig. 773 is derived from Fig. 764 by returning grid resistor R_g to B-plus instead of ground. The higher plate current flowing through cathode resistor R_k cuts
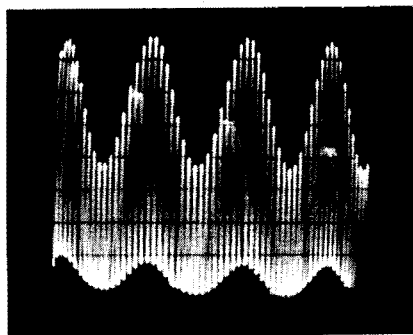
Fig. 776. *Waveform showing carrier modulated by a signal voltage.*

off V1, and no oscillation takes place. A stable state is thus obtained. If a signal of positive polarity reaches G1, the plate current of V1 is restored, and the circuit "flips over." After a time, depending mainly upon the time constant of $C \times R_g$, the circuit "flops back"

$$M = \frac{100\ (a-b)}{a+b}$$
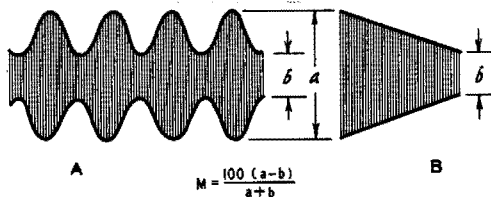
Fig. 777. *Determination of depth of modulation, using modulated waveform (A) and modulation characteristic (B).*

to the stable condition, hence the name of flip-flop or univibrator. Flip-flops are used extensively as delay triggering devices.

While univibrators feature one dc coupling, the other multivibrator-derived scale-of-two circuit of Fig. 774 has two dc couplings, making for two stable states. If suitable signals are injected into the grids, V1 and V2 become alternately conducting. As it takes two pulses to return to the initial state, this circuit is a 2-to-1 frequency divider. Digital calculators use large quantities of such counters. Another use of this circuit in an electronic switch has been de scribed previously.

The mechanism of amplitude modulation

Modulation consists in varying the amplitude, phase or frequency of a carrier wave (frequency, f_c) in accordance with a modulat-
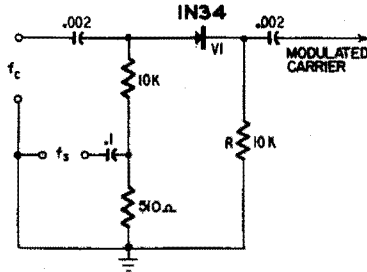
Fig. 778. *Germanium diode modulator.*

ing signal (frequency, f_s). By impressing a low-frequency on a high-frequency wave, it can be transmitted by a radio link. At the receiving end of the link, the wanted information is extracted from the carrier by a process called demodulation or detection.

The wave represented in Fig. 775 is *not* modulated; this is merely a superimposition of two voltages of different frequency. An un-
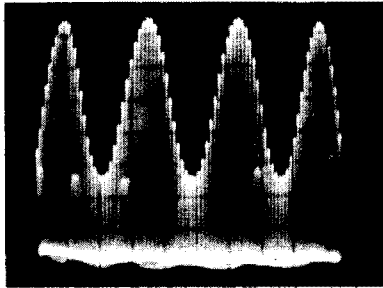
Fig. 779. *Modulated waveform obtained by using the germanium diode of Fig. 778.*

modulated carrier is obtained by filtering the low-frequency component by a high-pass filter.

The wave represented in Fig. 776 is modulated for there is some amplitude variation during the modulating cycle. The visibly superimposed f_s component can be filtered by a circuit tuned to f_c, leaving a modulated carrier.

To accomplish modulation, two voltages are mixed in a non-linear circuit. As diodes, vacuum tubes and transistors never have strictly linear characteristics, it is difficult to avoid modulation (or

158

detection) completely. However, good high-level modulation is not obtained easily.

Modulation percentage

The more strongly the signal is impressed upon the carrier, the higher will be the detected signal voltage for a given carrier strength. Modulation depth depends upon the maximum and mini-
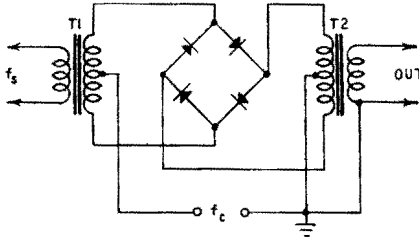
Fig. 780. *Bridge modulator circuit.*

mum instantaneous amplitudes of the modulated carrier and is given by $M = 100 \, (a - b)/(a + b)$, the magnitudes a and b being those of Fig. 777-a. The highest possible correct modulation is
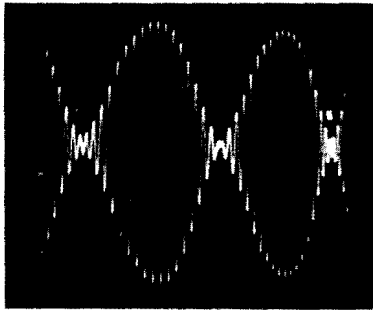
Fig. 781. *Modulation pattern produced by bridge modulator. The percentage of modulation is 90%.*

achieved with b = 0, making $M =$ 100%. Practically, the highest modulation depth accomplished with a low distortion level is somewhat lower. Overmodulation (M exceeding 100%) always introduces severe distortion and should be avoided.

If the horizontal deflection of the scope is accomplished by f_s instead of the time-base voltage, a trapezoid (Fig. 777-b) results. This second aspect of the same phenomenon that might conveniently be termed "modulation characteristic," gives a better insight

into modulation performance, for the display is independent of the modulating waveform. If the signal is distorted, the waveform display will yield no information on modulator performance. If, however, the display of the modulated wave is good, it can be stated that both signal and modulator are satisfactory.

Simple diode modulator

A very simple modulator using a germanium diode and a few resistors and capacitors is represented in Fig. 778. The modulated
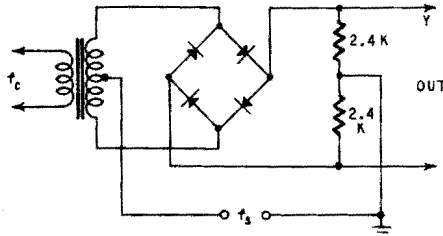
Fig. 782. *Ring modulator circuit.*

waveform (Fig. 779) shows the similarity between modulation and detection, because the negative half-cycles are clipped. This, nevertheless, is true modulation because the amplitude of the carrier varies with the signal. Passing this wave through a subsequent L-C circuit tuned to f_c will restore the missing half-cycles.

To explain the operation of this circuit, remember that the forward resistance of a diode (for small-signal condition) depends upon the current passed. As diode V1 and resistor R form a voltage divider, the output will vary with the series resistance offered by V1. According to the sum of the instantaneous amplitudes of f_c and f_s, the diode characteristic is swept and its slope is varied. Of course, nothing happens if this sum is negative.

Bridge and ring modulators

These are evolved modulators for carrier-current applications

Fig. 783 (left). *Signal-controlled half-cycle modulation obtained with the ring modulator circuit of* Fig. 782. Fig. 784 (right). *Modulation characteristic (trapezoidal waveform) produced by the ring modulator.*
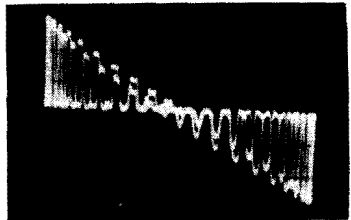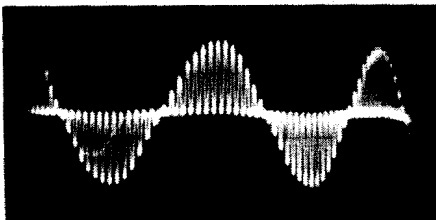
using four ring-connected semiconductor diodes. A bridge modulator is shown in Fig. 780. Modulation is accomplished by varying the resistances of the diodes in accordance with f_s, thus upsetting the balance of the bridge. The waveform for a modulation depth of $M = 90\%$ (Fig. 781) is quite good.

In the ring modulator circuit (Fig. 782), the diodes act as signal-controlled switches transmitting carrier half-cycles of amplitude
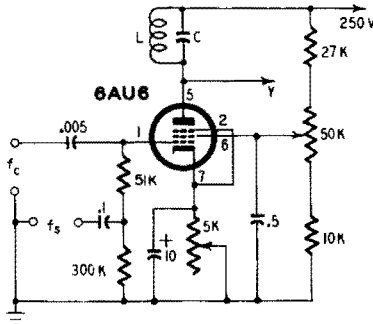
Fig. 785. *Pentode modulator with signal and carrier voltages injected into the control grid.*

and polarity corresponding to the signal, as shown in Fig. 783. This feature is useful in carrier-current bridges. After amplification,
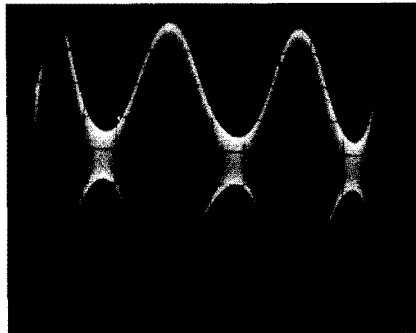
Fig. 786. *Modulation pattern using the pentode modulator of Fig. 785.*

such a voltage is demodulated in a phase detector by means of a reference voltage (f_c) and yields a dc output whose polarity indicates the direction of unbalance of the bridge, just as in a dc Wheatstone bridge. The corresponding modulation trapezoid is shown in Fig. 784.

Bridge modulators transmit in either direction and can be used equally well as demodulators.

Grid modulators

Modulation can be accomplished by injecting voltages (f_c and f_s) into the same grid of an amplifier tube operating in the curved portion of its I_p/E_g characteristic. The circuit of Fig. 785 was used, and
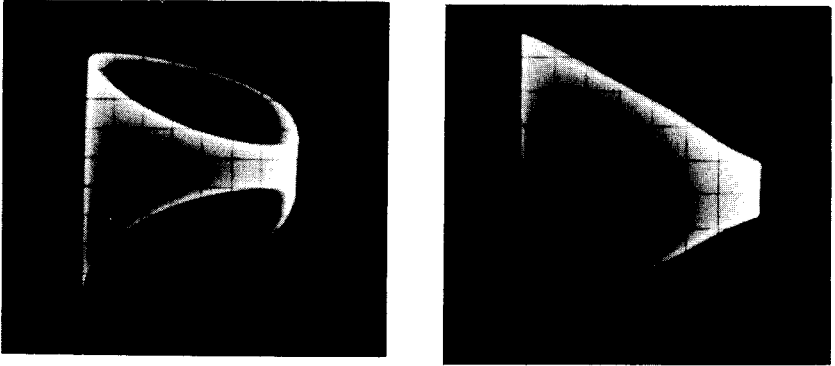
Fig. 787 (left). *Modulation trapezoid exhibiting phase shift.* Fig. 788 (right). *Correctly phased trapezoid. The percentage of modulation is 72%.*

both the screen voltage and cathode resistor were adjusted for optimum performance. Plate circuit L-C, tuned to f_c, filters the superimposed f_s component, resulting in the waveform of Fig. 786.
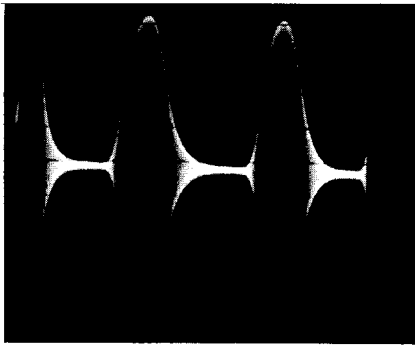
Fig. 789. *Overmodulated carrier. This is an indication that the modulating voltage is excessive.*

Switching the X-deflection plates from the time base to the signal, the trapezoid of Fig. 787 was obtained, indicating a phase shift. As in other cases of tracing characteristics presenting some phase shift, a variable phasing network was introduced, leading to the correctly phased trapezoid of Fig. 788.

To evaluate the modulation depth of this wave, lengths a and b

162

are measured on one of these oscillograms. We find a = 18/16″ and b = 3/16″. Using our formula:

$$M = 100 \, (a - b)/(a + b)$$

we find that the modulation equals 72%.

Increasing the modulating voltage results in overmodulation, as

Fig. 790. *Overmodulation as shown on the modulation characteristic (trapezoidal waveform).*

displayed by Figs. 789 and 790. While the carrier amplitude can still be increased, there is no way to decrease below zero and, for a good portion of the cycle, no carrier is present.

Instead of using the same grid, f_c and f_s can be injected into two

Fig. 791. *Modulated high-frequency oscillator using a pentagrid tube.*

different grids of the same tube. In the 6AU6 pentode, for instance, the suppressor grid can be used for modulating purposes. However, as the mutual conductance of the suppressor is low, a large modulating voltage is required, and this implies sufficient bias to avoid

Fig. 792 (left). *Nonlinear modulation characteristic (trapezoidal waveform) due to incorrect adjustment of tube voltages.* Fig. 793 (right). *The modulation waveform (corresponding to the trapezoid shown at the left) illustrates the flattening of the positive and negative modulation peaks.*

Fig. 794 (left). *Correct modulation trapezoid results when the circuit of* Fig. 791 *is adjusted for a percentage of modulation (M) of 52%.* Fig. 795 (right). *Modulated waveform which corresponds to the modulation characteristic shown at the left.*
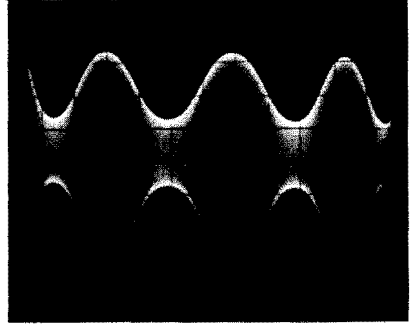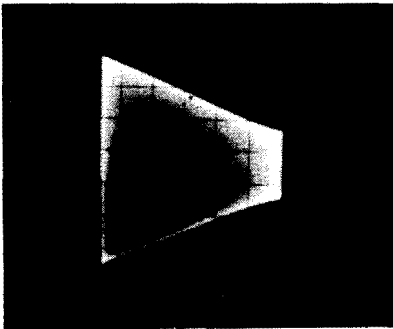
Fig. 796 (left). *Overmodulation results if the bias and screen voltages in the circuit of* Fig. 791 *are incorrect. Compare this with the waveform shown in* Fig. 792 *at the top of the page.* Fig. 797 (right). *Waveform corresponding to the trapezoid shown at the left.*
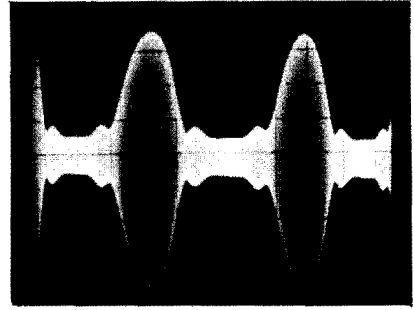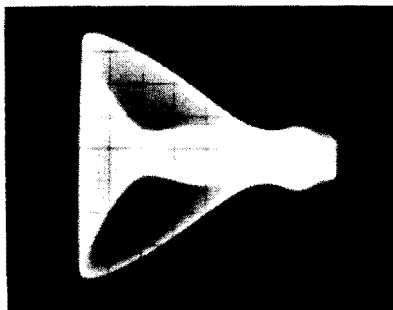
suppressor grid current. Mixer tubes such as the 6BE6 featuring two control grids are preferable.

Grid-modulated oscillator

As a converter tube used as a two control grid modulator will only provide information of the same type as just described, we will
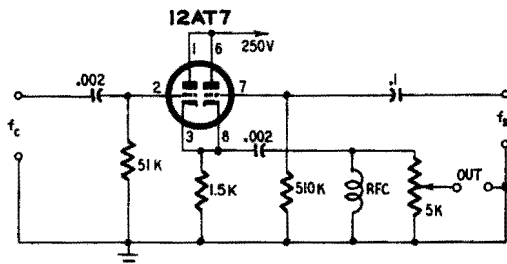
Fig. 798. *Cathode-coupled modulator devised by by the author.*

use it as a modulated high-frequency oscillator (Fig. 791) such as is found in signal generators. The oscillator is electron-coupled, a cathode tap being provided at one third to one tenth of the total
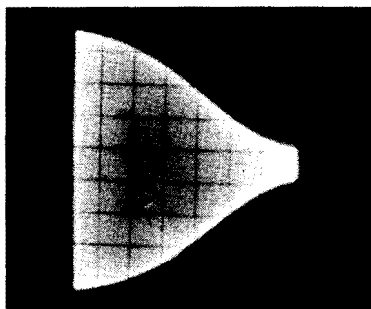
Fig. 799. *Modulation characteristic (trapezoid) obtained with the circuit of* Fig. 798. *The percentage of modulation is 78%.*

number of turns from ground, depending on frequency. A radio-frequency choke, rfc, in the plate circuit filters the f_s component. The signal is injected into grid G3 (pin 7).

As the bias of grid G1 (pin 1) increases with oscillation, the modulation depth varies too and, if a stable oscillation amplitude all over the band is not achieved, modulation depth will not be constant either. The screen voltage must be adjusted carefully, and the signal too. A very nonlinear modulation characteristic is shown in

165

Figs. 792 and 793 where flattening due to saturation is evident for positive as well as negative modulation peaks. Correct modulation
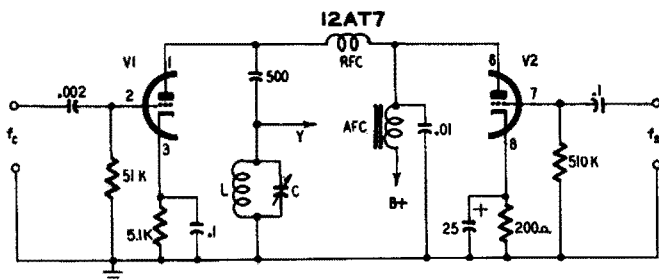
Fig. 7100. *Technique for obtaining plate modulation. The audio choke is common to the plate circuits of both tubes.*

could, however, be achieved by careful adjustment for a modulation depth not greater than 52% (Figs. 794 and 795). Using the 6BE6 as an overdriven modulator, the displays of Figs. 796 and 797 were obtained, showing generation of new (and thus unwanted) modulation components in the region of the negative modulation peaks. Improper screen and bias voltages are responsible for such distortion.

Simple cathode-coupled modulator

Some years ago, the author devised the very simple and foolproof modulator of Fig. 798, using a twin-triode whose cathode-follower-
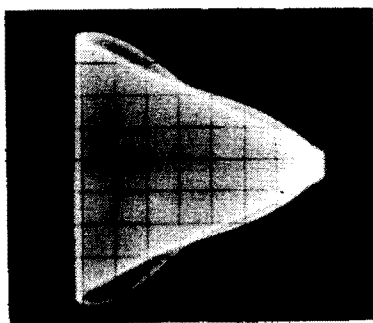
Fig. 7101. *Modulation characteristic (trapezoid) produced by using the plate modulation circuit in* Fig. 7100.

connected sections are cathode-coupled. This circuit has the desirable feature of high-impedance input and low-impedance output, and there is nothing to be adjusted except for the common cathode

resistor. The trapezoid obtained for a modulation depth of 78% (Fig. 799) is still usable for most service signal generators and insures a fine characteristic at lower levels. The choke, rfc, is necessary to filter the superimposed low-frequency component.

Plate modulator

Plate modulation frequently used in transmitters is accomplished by using an audio-frequency choke (afc) in the circuit supplying power to rf and af amplifier tubes (Fig. 7100). The instantaneous
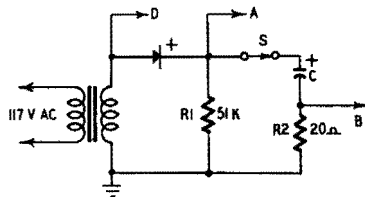
Fig. 7102. *Half-wave copper-oxide rectifier circuit.*

af plate voltage of modulator V2 adds to the plate supply voltage of rf tube V1, and modulation takes place in its plate circuit. As the plate current of V2 cannot be reduced to zero without introducing
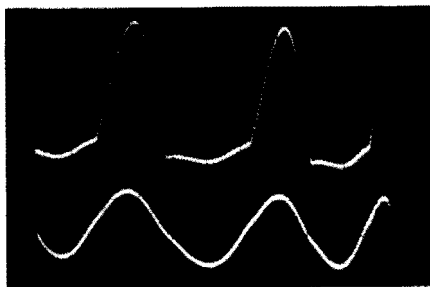
Fig. 7103. *The upper trace (with the input filter capacitor omitted) shows the output of the half-wave rectifier of Fig. 7102. The lower waveform is a 60-cycle reference voltage.*

audio distortion, V2 has to be operated at a higher plate current than V1. In our circuit, this was obtained by using widely different cathode resistors. The trapezoid for a modulation depth of 81% (Fig. 7101) is slightly nonlinear, but modulation is quite good at lower levels. Remember that in actual transmitters, V1 is class-C operated, and, instead of V2, a class-B-operated push-pull stage is

often used to prevent saturation of the transformer core by the dc plate current component.

Demodulation

Demodulation or detection is the process of extracting the desired information or signal from a modulated carrier by a device termed a demodulator, detector or discriminator. It is generally followed by a suitable network for filtering the residual carrier voltage, which is of no further use.

Logically, demodulator circuits should be studied here; however,

Fig. 7104. *Upper trace shows the effect of connecting a capacitor across the load resistor in Fig. 7102. The lower waveform is the 60-cycle reference.*

as they form part of the if amplifier stages of radio and TV sets, they will be more conveniently investigated in the next chapter.

Half-wave rectifiers

Power rectifiers are a special class of detectors used for ac–dc conversion in power supplies. There are many types of rectifying
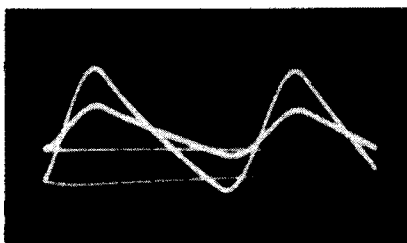
Fig. 7105. *As the amount of filter capacitance in the circuit of Fig. 7102 is increased, the hum voltage decreases.*

devices, their only common characteristic being to pass a high forward and a negligible back current.

To study the behavior of a simple half-wave copper-oxide recti-

fier, the circuit of Fig. 7102 was used. As the back resistance of such a rectifier is not infinite, a load resistor R1 had to be provided. Its resistance needed to be small in relation to the back resistance of the rectifier and large in reference to its forward resistance, for efficient operation. Using an electronic switch with inputs connected to points A and D, Fig. 7103 was obtained. The wave displayed above the 60-cycle reference shows how the rectifier passes current only during the positive half-cycles of the ac input voltage. Note
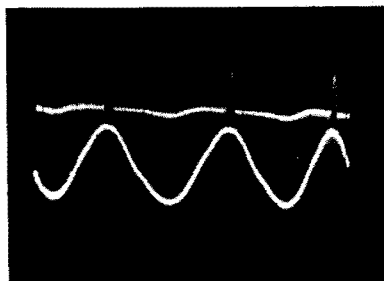
Fig. 7106. *The charging current flows only during a small part of each cycle. The lower waveform is the reference voltage.*

that there is a small downward-directed peak in the baseline, indicating some reverse current near the negative voltage peak. This effect is minimized by using a lower load resistance and will not be found at all with vacuum-tube rectifiers.
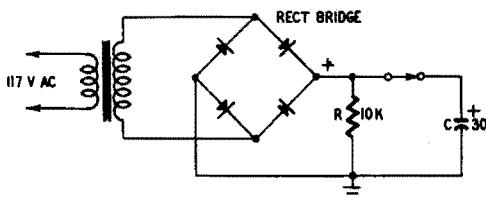
Fig. 7107. *Semiconductor bridge rectifier produces full-wave rectification.*

The indicated waveform actually is dc, for the current does not change its direction, but the voltage is pulsating and not steady. Connecting capacitor C across the load more or less smooths the variations of instantaneous amplitude, for C charges when the applied voltage is higher than its own and discharges into R1 when it is lower. This results in the sawtooth wave of Fig. 7104 displayed above the 60-cycle reference. (The unsmoothed and smoothed

169

waves are not in scale, of course!) The capacitor charges during a small fraction of the cycle and discharges more slowly.

High capacitance improves the smoothing effect as shown in Fig. 7105; two successive photos were made with C equal to 8 µf and 24
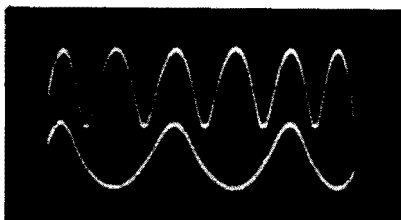
Fig. 7108. *Full-wave rectifier output obtained with the circuit of Fig. 7107. The filter capacitor was omitted. The lower waveform is the 60-cycle reference voltage.*

µf respectively. As the same scope gain was used, the lower "hum" voltage due to higher capacitance is evident. However, note the charging portion of the smaller wave is somewhat shorter and slopes more. As the energy dissipated in the load is about the same (not exactly, because the voltage depends upon C), a higher current has to be passed by the rectifier during a shorter time. This may put a tremendous load on the rectifier, and that is why the manufactur-
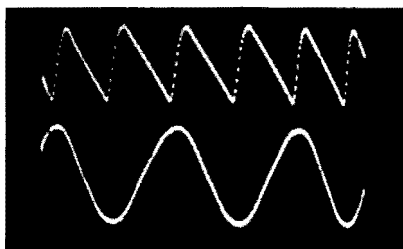
Fig. 7109. *When a capacitor (C) is connected across the load resistor (R) of the circuit of Fig. 7107, the waveform becomes a sawtooth (upper trace). The lower waveform is the 60-cycle reference voltage.*

ers' rating sheets always specify the maximum capacitance of C for a given set of conditions. The very short charging cycle of C is clearly seen in Fig. 7106, one of the inputs of the electronic switch being connected to point B to display the voltage across series resistor R2 (20 ohms).

170

Full-wave rectifiers

Two or more rectifier elements may be associated to rectify both half-waves. The selenium bridge rectifier of Fig. 7107 uses four elements. Disconnecting capacitor C, Fig. 7108 was obtained, showing successive positive half-cycles above the 60-cycle reference. This oscillogram clearly explains the term rectification, for the device acts in a way to set the negative half-cycles upright, just as if they were folded over. Connecting C across R resulted in the sawtooth wave of Fig. 7109. As the capacitor charges twice as frequently with full-wave rectification, the hum voltage on C is much smaller. Furthermore, the repetition frequency of the sawtooth wave (or the pitch of the hum) is now 120 cycles, instead of 60, and the filter is twice as efficient.

Similar results are obtained with a conventional full-wave vacuum-tube rectifier (Fig. 7110). Correct operation is shown in Fig.
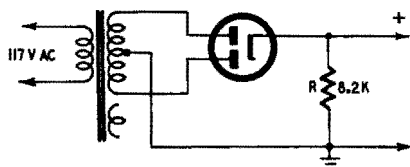
Fig. 7110. *Vacuum-tube full-wave rectifier.*

7111, while the unequal amplitudes of the consecutive half-cycles (Fig. 7112) denote a lack of balance between tube sections or an off-center transformer center tap.
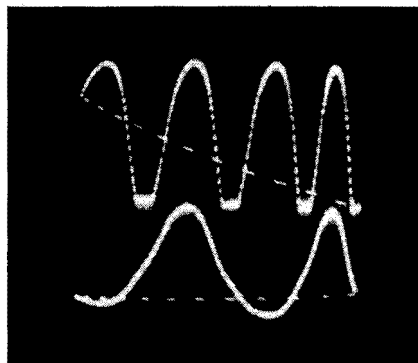
Fig. 7111. *Upper waveform shows the output of the full-wave rectifier circuit of Fig. 7110. No filter capacitor was used (60-cycle reference below).*

171

Grid-controlled rectifiers

Grid controlled gas tubes make very efficient rectifiers, and the ease of electronic lossless voltage control makes them suitable for applications such as power supplies for dc variable-speed or load drives. Of course, high-powered industrial applications require ig-
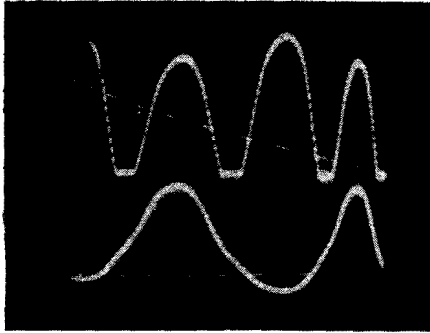
Fig. 7112. *Upper waveform shows full-wave rectifier output (no filter capacitor) indicating an unbalanced tube or transformer (60-cycle reference below).*

nitrons; but for currents up to 200 ma, gas tetrodes such as the 2D21 or 2050 are almost ideal.
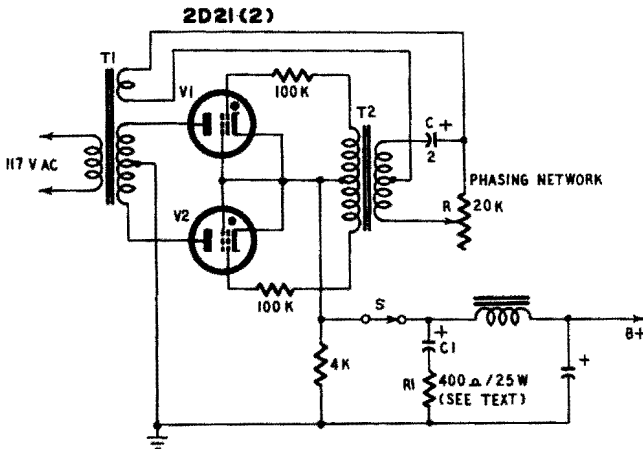
Fig. 7113. *Grid-controlled rectifier using gas tubes. The phasing network controls the rectified output voltage by varying the firing point of the tubes.*

A typical grid-controlled power supply is shown in Fig. 7113. Tubes V1 and V2 have no (steady) bias. Instead, a suitably phased
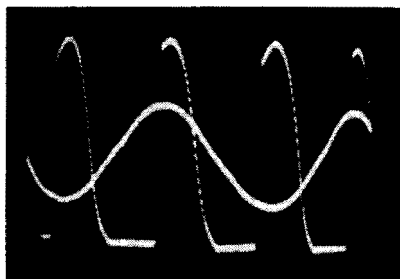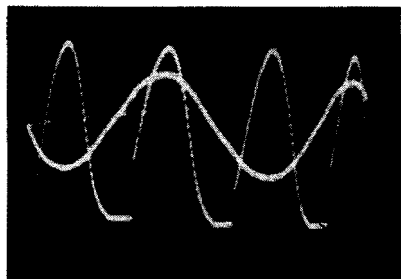
Figs. 7114 to 7117 incl. *Working cycle of the gas tubes of Fig. 7113 for different settings of phasing control R (no input filter capacitor). A 60-cycle reference voltage is displayed simultaneously. The double waveforms were obtained by using an electronic switch. Fig. 7114 (upper left). 220-volt output. Fig. 7115 (upper right). 160-volt output. Fig. 7116 (lower left). 100-volt output. Fig. 7117 (lower right). 22-volt output.*
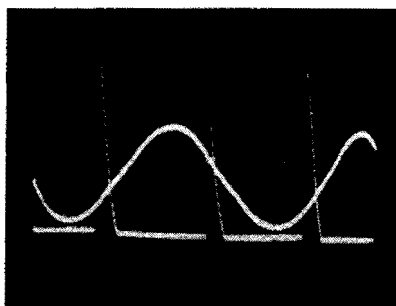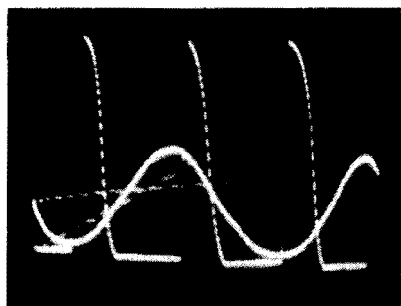
ac voltage of the supply frequency is fed to both grids by transformer T2. Phasing circuit C-R allows for shifting the firing point of the

Fig. 7118. *Waveform showing the operation of a half-wave grid-controlled rectifier. The timing reference is 60 cycles.*
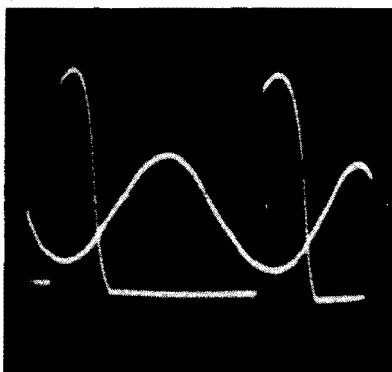
gas tubes between the starting and the end of each half-cycle. The tube, once fired, automatically extinguishes as its plate voltage nears zero, and nothing happens during the negative half-cycle, when the other tube becomes operative.

173

The following oscillograms (Figs. 7114 through 7117) were taken with an electronic switch to display simultaneously the 60-cycle reference wave. The load resistor was 4,000 ohms, no filter capacitor being used. The firing-point variation during the half-cycle is well determined. The output voltages were 220, 160, 100 and 22, respectively, a fairly extended operating range. It may seem surprising that such a large voltage variation corresponds to an approximately constant amplitude of the wave displayed; but remember that the rectified energy is proportional to the area between the curve and the baseline and, if firing occurs toward the end of the half-cycle, this energy will be quite low.

A slight unbalance between the firing points of the tubes is noted, especially in Figs. 7114 and 7117 where the slopes of the control voltage are greatest. This is probably due to a slight spread of the working characteristics, but transformer dissymmetry can be suspected too.

If a single gas tube is used as a half-wave grid-controlled rectifier, a waveform such as Fig. 7118 is obtained. The rectifier passes current only during part of the positive half-cycles. (The 60-cycle reference voltage shown is out of phase.)

A word of caution regarding the filter input capacitor. During the charging cycle, Cl in Fig. 7113 presents a negligible impedance and, as the internal resistance of a gas tube is very low, the tube may quickly become inoperative. To avoid this, a resistor R1 is series-connected with Cl to limit the surge current to its rated value. As the rated short-time peak current of these tubes is 1 ampere, R will be about 400 ohms 25 watts, depending upon the transformer voltage.

checking receiver circuits

Engineers and service technicians are generally concerned with complete assemblies such as those found in radio receivers, rather than with isolated circuits. As electronic gear of all kind is composed of basic circuits, the foregoing chapters dealing with fundamentals are necessary to understand the operation of the whole assembly. Special techniques are, however, used to check complete circuits.

Investigating audio amplifiers

An audio amplifier is expected to deliver the required output (power) with the best possible fidelity. This means that all types of distortion must be minimized. In the preceding chapter, we studied the effects of distortion due to overload and incorrect choice of the operating point. We will now be concerned with frequency, phase, intermodulation and transient distortions, overloading being deliberately avoided.

The following tests apply to a typical audio amplifier represented in Fig. 801. It is customary to replace the speaker voice coil with an equivalent resistor (4 to 10 ohms). Besides the fact that this provides a quiet working condition, oscillograms are easier to explain, for the operating moving coil reflects rather surprising effects of motional (acoustic) impedance. On the other hand, tests made on an output resistor allow for evaluation of the amplifier, but not of the whole audio system. Strictly speaking, such a test would require a "sound dead" room, a standard mike, laboratory amplifiers and analyzers.

Our experimental amplifier features an overall inverse feedback loop (from output resistor to cathode of tube V1). To evaluate the effect of feedback on overall performance, this feedback can be eliminated by opening switch S.

Square-wave testing

Square waves are extensively used for testing audio amplifiers. They are composed of a number of components bearing a definite mutual amplitude and phase relationship, so that any frequency or
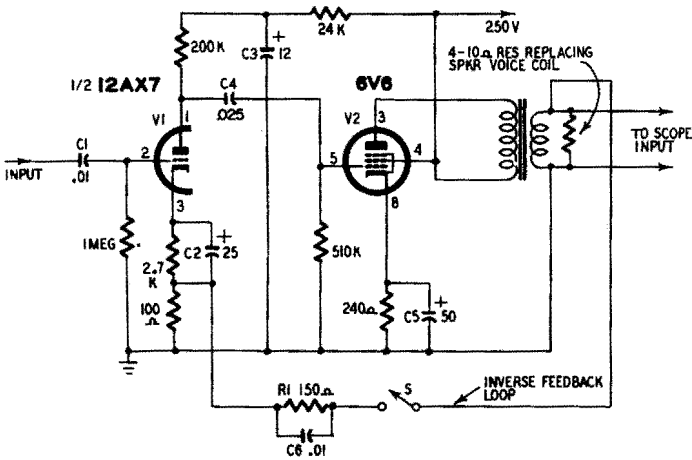
Fig. 801. *Representative audio amplifier. Negative feedback is applied when the switch (S) is closed.*

phase distortion results in departure from the original square wave-form. As actual music or speech consists of a number of simultaneous components of different amplitude, frequency and phase, such tests are more realistic than sine-wave tests. However, if a correctly reproduced square wave means a perfect amplifier, even actual reproduction can be more or less far from linear. The reasons for departure must be analyzed to find out how to improve the overall performance.

In the following, the upper oscillogram is for operating the amplifier with inverse feedback (switch S closed), while there is no feedback for the lower one (S open). Input was set to yield approximately the same output; the feedback being degenerative, input obviously had to be increased on closing S.

A 50-cycle square wave resulted in Fig. 802, which shows poor low-frequency response. The downward tilt following the (correctly reproduced) leading edge is indicative of attenuation and
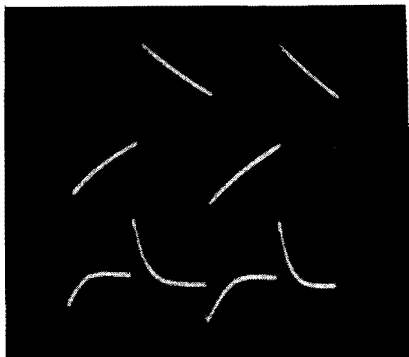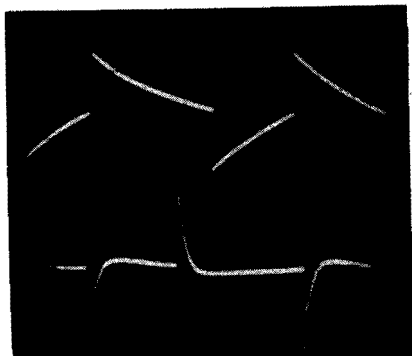
Fig 802 (upper left). *Audio-frequency amplifier test waveforms are shown in all of the photos on this page. Upper traces are with inverse feedback operative; lower traces with no inverse feedback. Fig. 802 is the response to a 50-cycle square wave. Fig. 803 (upper right). 100-cycle square wave. Fig. 804 (lower left). 100-cycle square wave when the input capacitor is increased from .01 to 0.1 μf. Fig. 805 (lower right). 1,000-cycle square wave.*
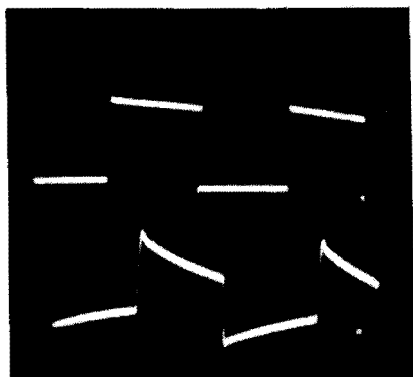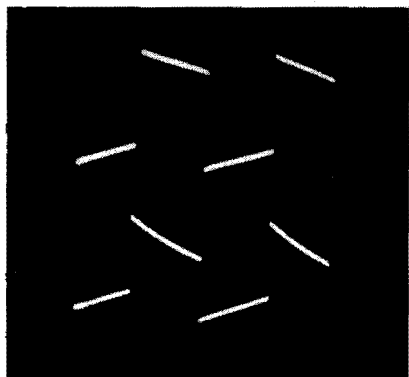
Fig. 806 (left). *10,000-cycle square wave. Fig. 807 (right). 20,000-cycle square wave. (These are the illustrations at the bottom of the page.)*
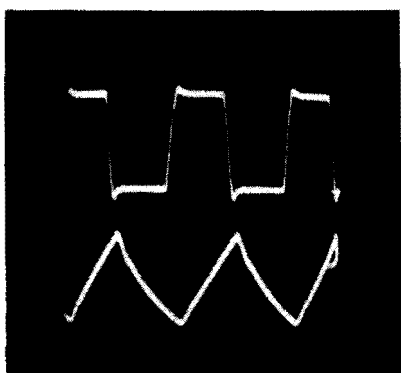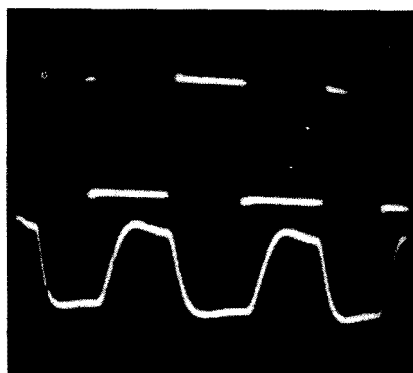
phase shift of low-frequency components. A distinct improvement is obtained by inverse feedback, for some low-frequency components, while attenuated, are still present. They disappeared entirely when eliminating the feedback loop. A very slight improvement is noted at 100 cycles (Fig. 803).

Poor low-frequency performance is due to two major factors: insufficient capacitances of coupling and bypass capacitors, and inadequate output transformer primary inductance. To yield a good low-frequency response, a transformer has to use a core of large

Fig. 808 (left). *Rounded tops indicate low-frequency boost. The test frequency was 180-cycles.* Fig. 809 (right). *Overshoot (upper trace) caused by shunting the transformer primary with a capacitor; ringing (lower trace) produced by shorting the feedback resistor.*

cross-section composed of high-grade laminations and a lot of wire. This adds up to an expensive unit. The transformer used was of a cheap radio type.

Increasing the values of the different capacitors in Fig. 801 did not result in significant improvements, except for input capacitor C1, because this component is not in the feedback loop. This is seen in Fig. 804 where C1 was made 0.1 μf (upper waveform) instead of .01 μf (lower waveform). The frequency was 100 cycles. At 1,000 cycles, the square-wave reproduction is rather good with inverse feedback (Fig. 805), while poor low-frequency response is still visible as the feedback loop is opened. At 10,000 cycles, the upper oscillogram (Fig. 806) is good, while the sloped rising and falling portions of the lower one indicate a loss of high-frequency components. At 20,000 cycles, the square-wave reproduction of the degenerated amplifier is still good (Fig. 807), though some overshoot and lowered rise and fall times can be discerned. Without negative feedback, the same circuit yielded the triangular wave shown in the
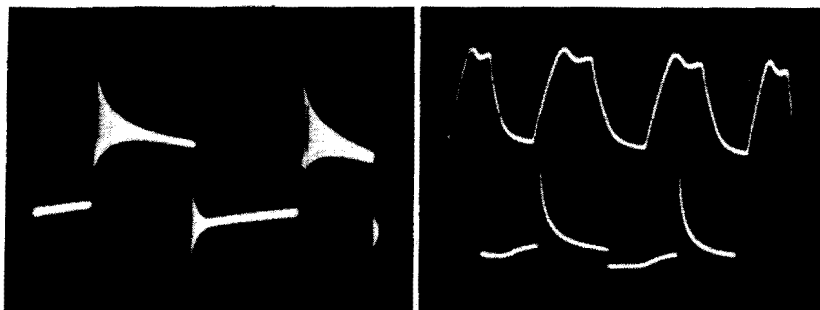
Fig. 810 (left). *Severe ringing (damped oscillations) caused by an excessive amount of negative feedback. The test frequency was a 200-cycle square wave.* Fig. 811 (right). *Distortion resulting from overload caused by too strong an input signal (no feedback used). Upper trace 1,000-cycles; lower trace 100-cycles.*

lower waveform, indicating attenuation and phase shift of high-frequency components.

As inverse feedback inevitably reduces gain, you can try to limit its action to medium and upper frequencies and thus improve low-frequency response. An 8-μf capacitor connected in series with S resulted in the waveform of Fig. 808 (frequency 180 cycles) in which the rounded tops indicate boost of some low-frequency components. This obviously implies phase shift and possible instability. Sharp pips on the leading edge, too fine to be seen in the photo, indicates a tendency toward instability, and, when a 32-μf capacitor was tried, oscillations built up.

Connecting a .01-μf capacitor across the transformer primary, following typical receiver practice, resulted in the upper oscillogram of Fig. 809 where some overshoot is noted. For this test, feedback

Fig. 812 (left). *25-cycle sine-wave test frequency. Upper trace shows clean reproduction with negative feedback. Note presence of harmonic distortion in lower trace (no feedback).* Fig. 813 (right). *Sine waves showing the presence of ringing.*
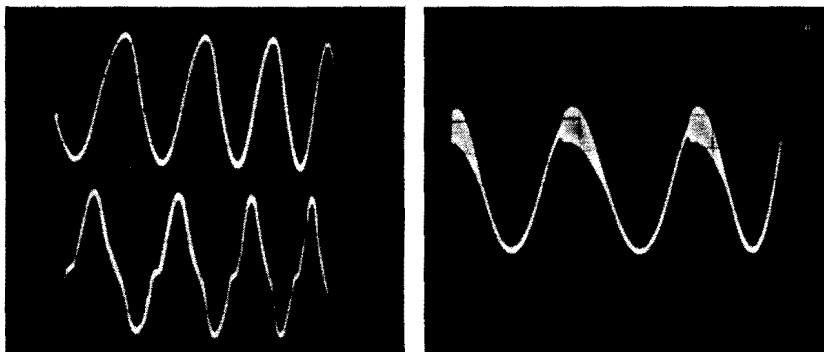
resistor R1 of Fig. 801 was made 1,000 ohms, no shunting capacitor being used. Shorting R1 resulted in the lower display where the overshoot changed over to "ringing," denoting instability. Acoustically, this means transient distortion, noticeable through the hangover effect following a percussion tone. While moderate inverse feedback actually stabilizes an amplifier, an exaggerated amount of it causes instability and eventually oscillation. Another illustration of an outbreak of damped oscillations following the leading edge of the square wave is given in Fig. 810 (the frequency was 200 cycles).

A shortcoming of square-wave tests may be the difficulty of recognizing when an amplifier is overloaded. Many misleading patterns can be obtained in this way. Two of them are shown in Fig. 811. The testing frequency was 1,000 cycles for the upper and 100 cycles for the lower display. No inverse feedback was used. As the input amplitude is gradually increased, the overload condition will be indicated by the appearance of dissymmetry between positive and negative wavetops.

Sine-wave tests

Sine waves do not simulate the actual working conditions of an audio amplifier, which is never used to reproduce single tones. A "good" sine-wave test, therefore, is insufficient to characterize the performance of the amplifier. Sine waves are, however, very useful for the rapid determination of the beginning of overload as described earlier, assuming the use of a low-distortion audio signal generator.

Injecting a 25-cycle sine wave into the input of our amplifier resulted in Fig. 812. Inverse feedback (upper waveform) removes most of the distortion of the nondegenerative amplifier (lower waveform). This type of distortion is mainly due to transformer inductance variations during the cycle, because of the nonlinear character of the magnetization curve.

The outbreak of damped oscillations, or ringing, illustrated with square waves in Fig. 810 is shown in Fig. 813 using sine waves. These oscillations start at a definite point of the cycle, depending on the bias of one or more tubes. Hum, due to poor filtering or induced hum pickup, is shown in Fig. 814. For medium and high frequencies, a smeared pattern (upper waveform) is obtained, while dancing or multiple waves are displayed at low frequencies (lower waveform).

Phase distortion

Phase distortion does not seem to be objectionable in audio amplifiers (but it definitely is in video amplifiers). While there is little or no phase distortion at medium frequencies of the audio amplifier, there generally is appreciable phase shift at the ends of the passband.

Phase ellipses are obtained by connecting the X scope input to the amplifier input, and the Y terminals to its output, as explained

Fig. 814. *Hum as seen at medium and high frequencies (upper trace) and at low frequencies (lower trace).*
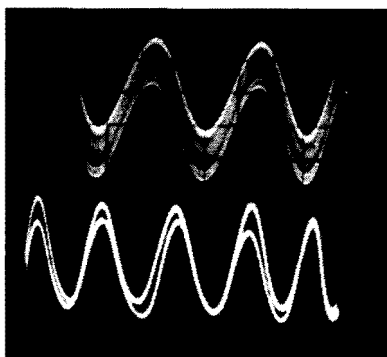
in Chapter 4. Although a straight line sloping from the lower left to the upper right was obtained at medium frequencies, the patterns of Fig. 815 were displayed at 50 cycles. No feedback was operative for loop A, indicating distortion due to the transformer and an overall phase shift of between 90° and 180°. Introducing inverse feedback not only cures the distortion, but reduces the phase shift to less than 90° (loop B). At 15,000 cycles, the phasing ellipse A (Fig. 816) shows a phase shift of about 90° for the nondegenerative

Fig. 815 (left). *Input/output phase patterns at 50-cycles: without negative feedback (A); with negative feedback (B).* Fig. 816 (right). *Phase pattern at 15,000 cycles: without negative feedback (A); with negative feedback (B).*
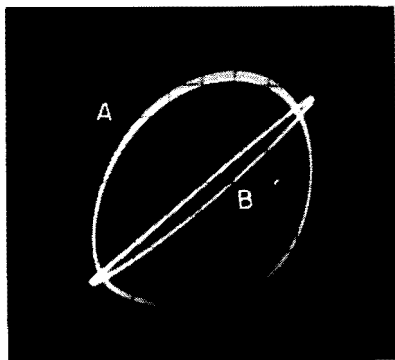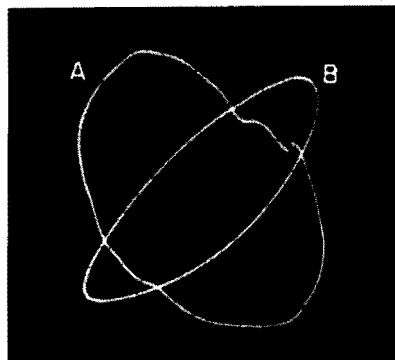
amplifier, while application of inverse feedback resulted in the flattened ellipse (B). Omission of capacitor C6 of the feedback loop (Fig. 801) reduced even this low phase shift to about zero.

Analyzing distortion

Note that no oscillograms of small-signal, medium- and high-frequency sine-wave test are given. This is because such patterns always look beautiful for any type of correctly operating amplifier, for minor amounts of distortion are not readily visible in such displays. To evaluate and analyze such distortion, waveform analyzers
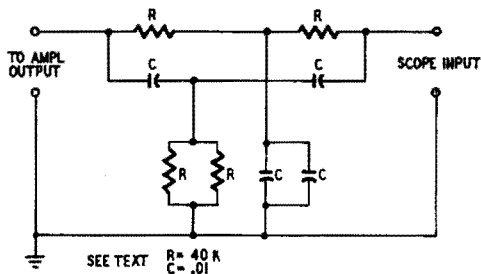
Fig. 817. *Twin-Tee filter used to cancel the fundamental frequency.*

and distortion meters can be used to filter the fundamental as well as possible and to examine the remaining components qualitatively and quantitatively.

While wave analyzers are very intricate and expensive instruments for laboratory use, fixed-frequency distortion analysis can be carried out simply and economically using a twin-Tee circuit such

Fig. 818 (left). *Amplifier output before removal of the fundamental frequency (upper trace); after removal (lower trace). No feedback was used.* Fig. 819 (right). *Same as in the photo to the left except for the use of negative feedback.*
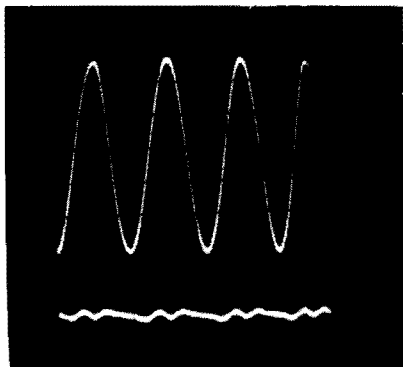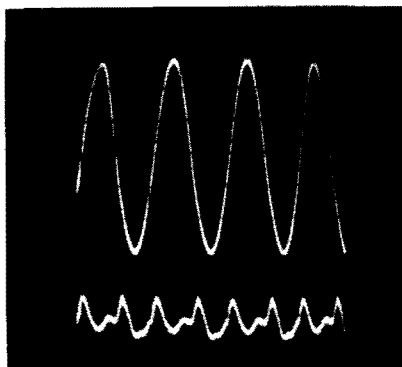
as shown in Fig. 817, operating at about 400 cycles. This twin-Tee must be carefully matched for efficient cancellation of the fundamental. High-grade components must be used for stability. As the exact absorption frequency is unimportant, it is best to select four resistors and four capacitors of about 40,000 ohms and .01 µf, respectively, on a bridge to get them matched at 1% or better. These components are then assembled on a bakelite board, and the whole

Fig. 820. *Hum component recorded above a frequency reference. Capacitor C3 was removed (see Fig. 801).*
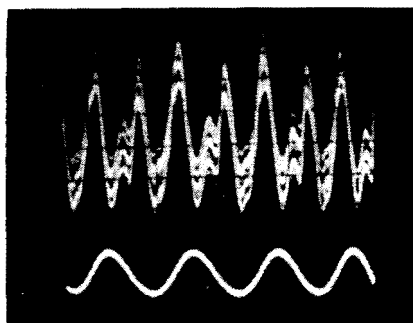
affair is inserted between the amplifier output and the scope amplifier. The scope is switched to external sync, and the sync input is connected to the signal source to secure locking-in on the fundamental after cancelling it on the scope input.

With this simple device, the oscillograms of Figs. 818 (no degeneration) and 819 (inverse feedback applied) were obtained,
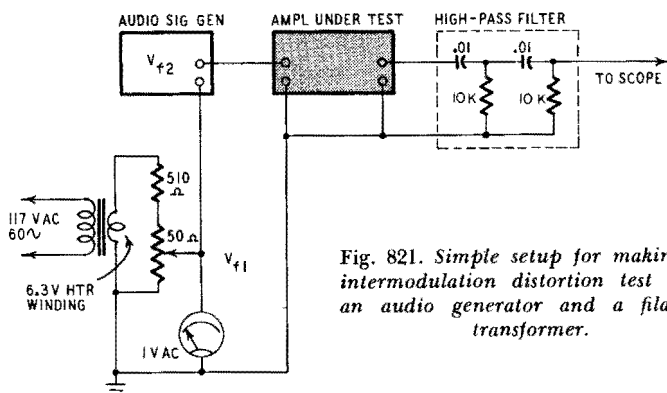
Fig. 821. *Simple setup for making an intermodulation distortion test using an audio generator and a filament transformer.*

showing (upper waveform) the sine wave at the amplifier output and (lower waveform) the remaining components after filtering the fundamental, the scope amplifier gain being increased 10 times. The input signal being set to produce equal output power in both cases, the efficiency of inverse feedback is indicated by the fact that

the ratio of the residue to the unfiltered output is about 2 to 100, or 2% in the first case and perhaps 0.5% in the second. (Because of the small amplitude, no exact evaluation could be made. Expressing distortion percentage by this ratio holds only approximately.)

A qualitative evaluation of the residue shows a predominant second harmonic (twice the fundamental frequency) and a low fourth-harmonic content for Fig. 818. No odd harmonics can be perceived. The residual components of Fig. 819 cannot be evaluated without additional amplification. Contemplating the corresponding sine waves alone, it would have been impossible to state that the distortion percentage of the first one is about four times greater than that of the second, and no one could say how much it actually is.

Eliminating filter capacitor C3 (Fig. 801) resulted in an important hum component superimposed on the residue, as shown in Fig. 820. (The signal recorded in the lower waveform is for frequency reference only.) In the unfiltered output voltage, the increased hum was scarcely noticeable.

Checking intermodulation distortion

The injection of two signals into a nonlinear device produces modulation of the higher-frequency signal. Similarly, if an amplifier is impressed with two simultaneous tones, combination tones due to intermodulation will be generated if the working characteristic is not strictly linear, and it seldom is. Intermodulation distortion (especially if high-order harmonics are present, generating combination tones of increased number and strength) is more objectionable than other types of distortion.

There are special two-signal generators for intermodulation analysis. Simple intermodulation tests can, however, be made with a power transformer heater winding as a 60-cycle source (V_{f1}) and an audio signal generator set at 2,000 cycles (V_{f2}), as shown in Fig. 821. By series-connecting the two sources, both signals are injected into the amplifier input. A simple high-pass filter inserted between its output and the scope amplifier eliminates the low-frequency component. For examination, the sweep is synchronized with the power line and run at, say, 20 cycles. V_{f2} then is displayed as a bright band whose borders may be just straight or show modulation.

Using this device with our amplifier, the intermodulation patterns of Fig. 822 were obtained with inverse feedback (upper waveform) and without degeneration (lower waveform). Signals were set for approximately the same output, leaving the scope controls untouched. The upper oscillogram, taken with $V_{f1} = 0.5$ volt and $V_{f2} = 1.5$ volts, presents practically no intermodulation. In spite
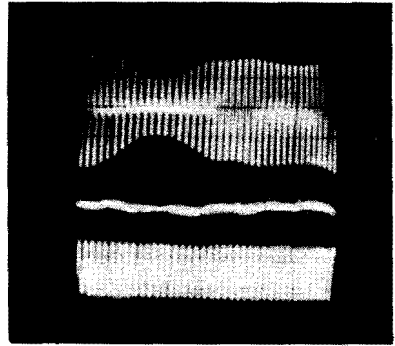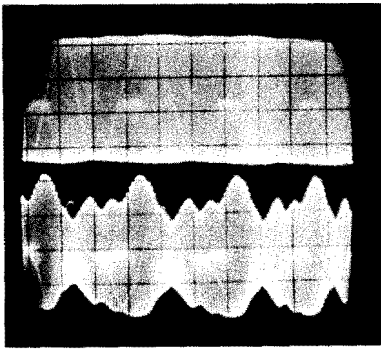
Fig. 822 (left). *Intermodulation patterns: with negative feedback (upper trace); without feedback (lower trace).* Fig. 823 (right). *Push-pull amplifier intermodulation patterns: without feedback (upper trace); with feedback (lower trace).*

of the reduced voltages ($V_{f1} = 0.2$ volt; $V_{f2} = 0.3$ volt), the lower pattern is modulated to about 40%. This again emphasizes the
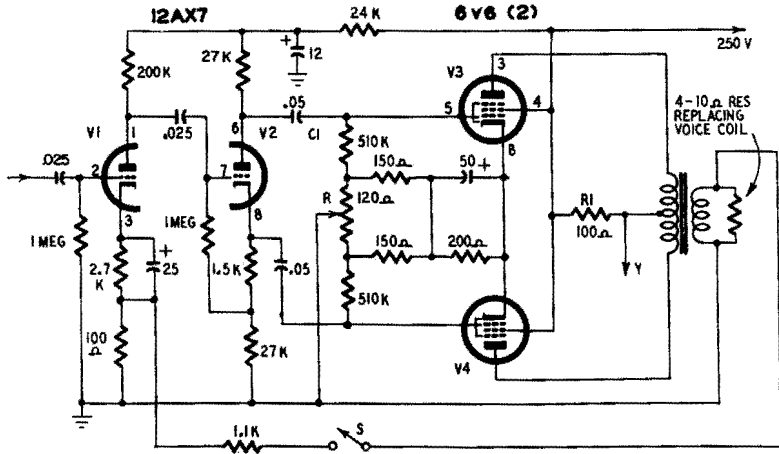
Fig. 824. *Conventional class-A push-pull audio amplifier.*

straightening effect of inverse feedback on the working characteristics. Note that the modulation envelope is not a sine wave as might be expected, but is comprised of strong harmonic components, implying the presence of unpleasant "new" tones.

Another intermodulation test carried out on a push-pull amplifier is illustrated in Fig. 823. The same signal voltages ($V_{f1} = 0.2$ volt; $V_{f2} = 0.3$ volt) were used for the tests without degeneration (upper waveform) and with inverse feedback (lower waveform). Inverse feedback practically eliminated intermodulation distor-

tion. To show the efficiency of the high-pass filter, the line between the two oscillograms represents the V_{f1} component alone, V_{f2} being reduced to zero and the scope amplifier gain being increased 10 times.

Push-pull amplifiers

Tests used on single-ended amplifiers also apply to push-pull amplifiers. To investigate possible special testing methods, the circuit of Fig. 824, a conventional class-A push-pull job, was hooked
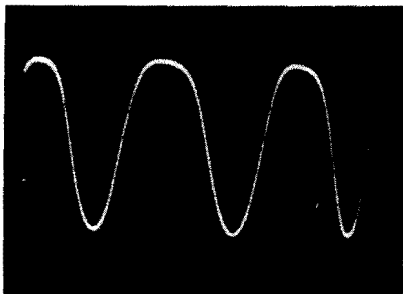
Fig. 825. *Distortion caused by open output-tube grid capacitor (C1 in Fig. 824).*

up. It features optional inverse feedback (switch S) as well as a potentiometer (R) for correct balancing of the push-pull stage.

Plate and cathode voltages of the phase-inverter tube V2 as well as the plates of V3 and V4 are out of phase. To check this, the X and Y scope inputs are connected to the corresponding points, and a straight tilted line is obtained (not shown). The phasing was correct all over the audio band. An open output tube grid capacitor (C1) introduced appreciable dissymmetry of the output waveform as shown in Fig. 825. An open or shorted grid leak produces similar distortion.

Low-frequency transformer distortion, examined with a 20-cycle sine wave, was important as shown in Fig. 826 (lower waveform). Introduction of negative feedback did not improve this situation much, as shown by the upper oscillogram. The third-harmonic component is predominant, and this is easily explained by the fact that even order harmonics are eliminated in push-pull circuits.

To yield the best possible performance, a push-pull circuit has to be carefully balanced. To carry out this balancing operation, potentiometer R permits balancing the output tube bias conditions. The scope input is connected to resistor R1 in series with the transformer tap. As the voltage developed across R1 is low, power supply hum may be disturbing. It is best to set the audio generator to an exact multiple of the power-line frequency to obtain a stable pattern. Connecting the scope ground to B-plus would be an im-
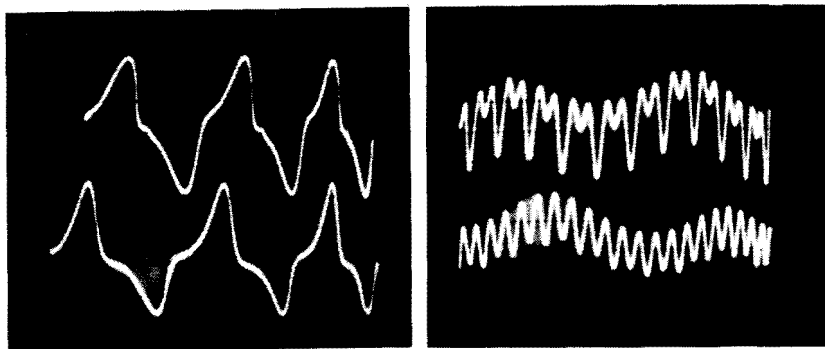
Fig. 826 (left). *Low-frequency distortion at 20 cycles is nearly the same with (above) and without (below) negative feedback.* Fig. 827 (right). *Voltage across R1 in Fig. 824 for unbalanced (above) and balanced (below) push-pull output.*

provement but is hazardous as well as leading to a possible insulation breakdown of the power transformer. It is definitely not recommended.

The action of the balancing control is illustrated by Fig. 827, the setting being correct (lower waveform) and incorrect (upper waveform). The 120-cycle ripple is clearly seen.

Tone controls

Tone controls are used to boost certain parts of the audio band and to attenuate others. This obviously introduces distortion and
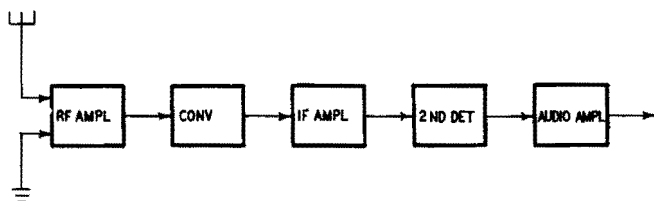
Fig. 828. *Block diagram of a radio receiver.*

makes for unintelligible and misleading test patterns. That is why no tone control circuits were used in the tested amplifiers.

This does not mean that tone controls are a nuisance; but you must be cautious when interpreting oscillograms, especially if square waves are used. Of course, frequency and phase distortion are deliberately introduced, but there should be no amplitude or intermodulation distortion.

Investigating AM and FM radios

The block diagram of a radio receiver is shown in Fig. 828. As

187

the audio amplifier section has already been studied, only the stages ahead of it will be examined now.

A radio set should supply good-quality sound reproduction, a fair sensitivity to incoming signals and a low level of interference. Audio distortion can be produced only from the if amplifier on. Because of the wide passband of the rf amplifier and converter stage, inadequate tracking of the local oscillator and signal circuits can only reduce the overall sensitivity and increase interference. Thus, qualitative tests will involve second detector operation and if trans-
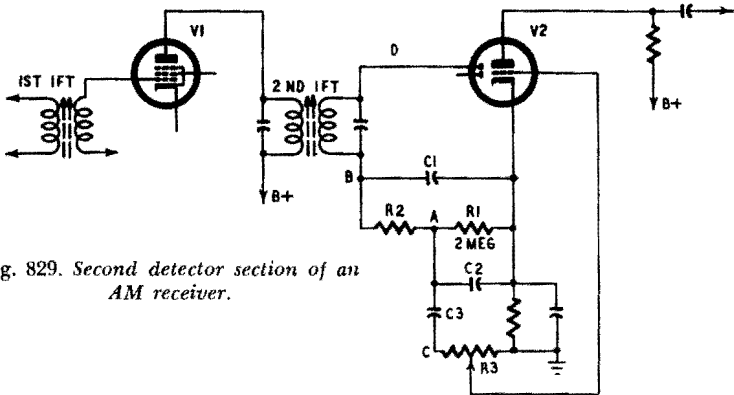
Fig. 829. *Second detector section of an AM receiver.*

former alignment only as far as one is interested in transmitted bandwidth. On the other hand, a sweep generator can be used to achieve top sensitivity and freedom from interference when performing if transformer alignment and top-end tracking.

Diode detector operation

A typical second detector section of an AM radio is represented in Fig. 829. A modulated signal generator is connected to the grid of V1, using a coupling capacitor of, say, 1,000 μμf to avoid upsetting bias conditions. Shielded cables are used for generator and scope connections to avoid stray rf coupling and hum pickup.

Connecting the scope input to the diode plate (point D) results in Fig. 830, which explains the mechanism of detection (or rectification). While the full modulated rf wave appears for half-cycles, making the diode plate negative with respect to its cathode, the positive half-cycles are short-circuited by the conductive diode–cathode space. Because of the limited resistance of the diode and the low capacitance of C1 (to avoid loss of high-frequency audio components), the clipping action is far from perfect though satisfactory. Removing the diode results in Fig. 831, which shows the
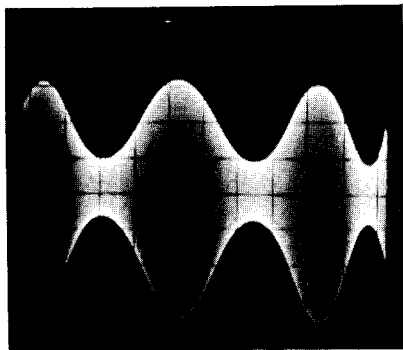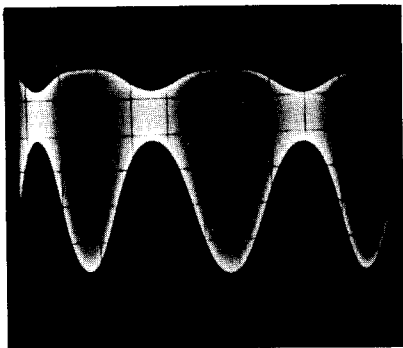
Fig. 830 (left). *Clipped modulated rf wave at point D in Fig. 829 showing detection prior to filtering.* Fig. 831 (right). *Removing the diode detector (V2 in Fig. 829) results in reproduction of the signal generator output without demodulation.*

modulated output of the signal generator, no detection taking place.

Remember that connection of a shielded cable to "hot" points such as D in Fig. 829 adds sufficient stray capacitance to detune the circuit. Always use a low input capacitance probe. (These patterns
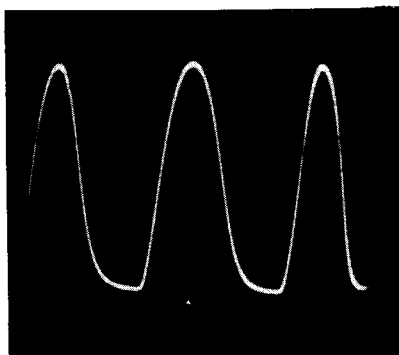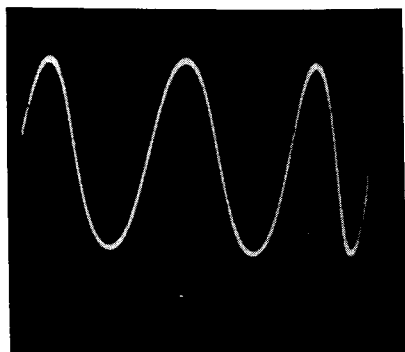
Fig. 832 (left). *Detected signal at point A (junction of R1 and R2) in Fig. 829. Note absence of rf carrier.* Fig. 833 (right). *Demodulation distortion as a result of too high a value of diode load resistance (R1 in Fig. 829).*

are presented for demonstrating checking techniques only; they are useless for performance evaluation or alignment purposes.)

By connecting the scope input to point A, a fair reproduction of the 400-cycle signal-generator modulation is obtained (Fig. 832). An excessively large diode load resistor R1 (2 megohms instead of 0.2 megohm) is responsible for the distortion shown in Fig. 833. Some residual rf is superimposed on the detected wave if the scope is connected to point B, ahead of the rf filter C1–R2 (Fig. 834).

189

Compare the modulating and demodulated waves by connecting the signal-generator audio output (if accessible) to the X deflection amplifier of the scope. A Lissajous pattern is obtained, but remember that the loop thus tested includes the modulator as well as the detector circuitry. So this method can also be used to test the performance of the signal-generator modulator stage. A distorted pattern may indicate poor generator performance.

A fair ellipse such as shown in Fig. 835 is indicative of good modulation as well as detection performance. The fact that an ellipse is obtained instead of a straight line indicates the presence of phase
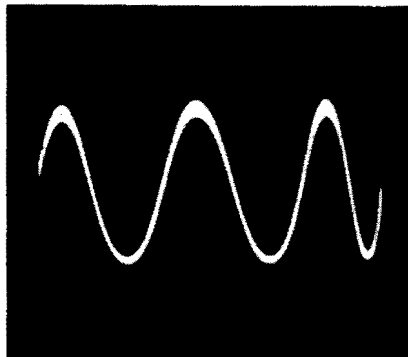
Fig. 834. *Connecting the scope to point B in Fig. 829 shows residual rf in the demodulated signal.*

shift, but this is not objectionable here. Increasing R1 to 2 megohms resulted in the distortion visible in Fig. 836 (compare with Fig. 833), while an rf component due to the scope connection to point B will be noticed in Fig. 837 (which corresponds to Fig 834).

These methods are good for qualitative evaluation of detector performance. They are useless, however, for alignment and tracking operations, which must be done with the aid of a sweep generator.

Using a sweep generator

The following patterns were obtained with the scope input connected to point A of Fig. 829, the sweep generator output being injected first into the control grid of V1 to tune the second if transformer. The generator is then shifted to the converter input to tune the first if transformer.

The double-trace method is useful for showing a lack of symmetry of the selectivity curve. Tuning the generator to make the tops of the curves coincide (Fig. 838) shows the slopes of the sides. A slight detuning to obtain base coincidence (Fig. 839) indicates the lack of symmetry even more clearly. Another case of lack of symmetry of an incorrectly tuned overcoupled transformer is shown
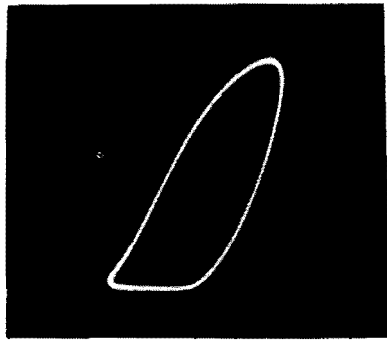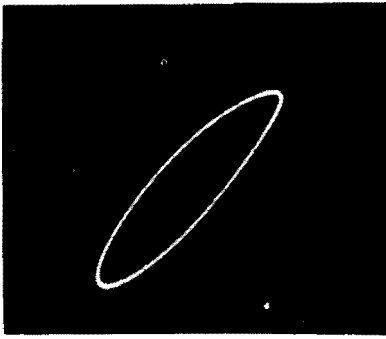
Fig. 835 (upper left). *Lissajous pattern (modulated input vs detected output) showing correct detection.* Fig. 836 (upper right). *Increasing the value of the diode load resistor R1 (in Fig. 829) results in distortion. Compare this with Fig. 833.* Fig. 837 (lower left). *Connecting the scope to point B (in Fig. 829) shows the presence of rf in the detected wave.* Fig. 838 (lower right). *Selectivity curve (double trace). Frequency correct; some skirt dissymmetry.*
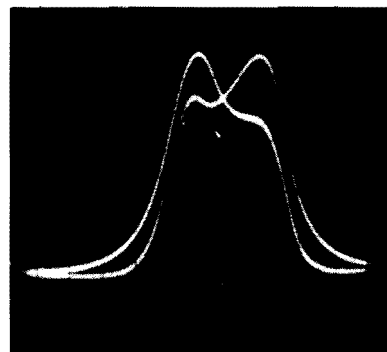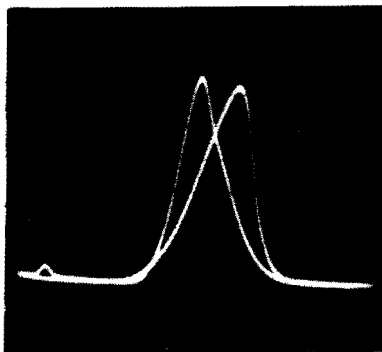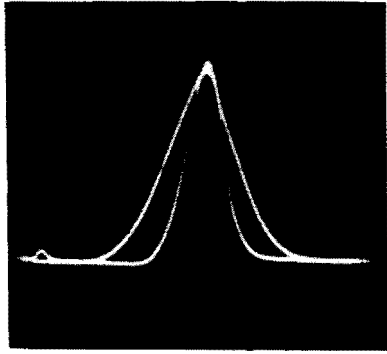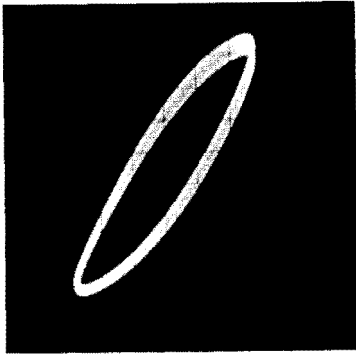
Fig. 839 (left). *Same waveform as in Fig. 838, but generator slightly detuned to separate the traces.* Fig. 840 (right). *Incorrectly tuned double-hump curve of overcoupled if transformer. (These are the illustrations at the bottom of the page.)*

in Fig. 840, the two "humps" being unequal. Note that the lower hump is different on the two traces. This obviously is not due to the circuit under test, but to a nonlinearity of the modulating triangular wave.

Incorrect setting of the time base may result in confusing patterns such as Fig. 841, where the sweep frequency was too low, or Fig. 842, combining incorrect frequency setting and exaggerated sync.

Using the single-trace method with 60-cycle sine sweep and modulation and blanking of one trace, the selectivity curve of an overcoupled if transformer is shown in Fig. 843. Though the double hump is correctly reproduced, a double trace would evidence a slight lack of skirt symmetry. The rounded top in Fig. 844, apparently due to a fair passband characteristic is misleading for it is due to amplifier overloading. To avoid this drawback, it is important always to make sure that the lowest possible signal producing a legible trace is used.
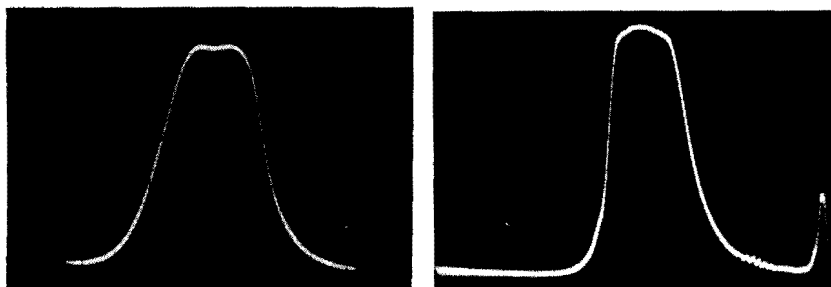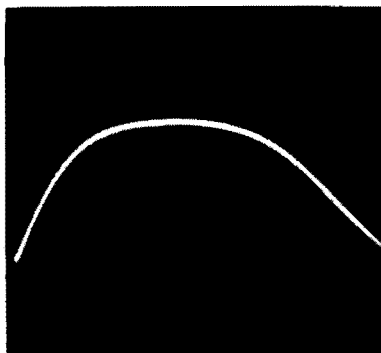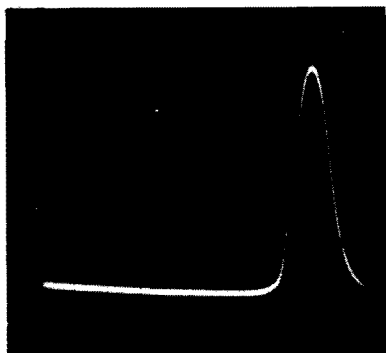
Fig. 845 (upper left).*Single trace. Incorrect sweep frequency shifts the trace.* Fig. 846 (upper right). *Sweep width too low. Only the top of the curve appears.* Fig. 847 (lower left). *Sweep width is too high. No detail is visible on the curve.* Fig. 848 (lower right). *Instability on the low-frequency side of the curve.*
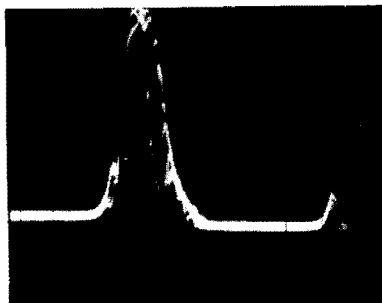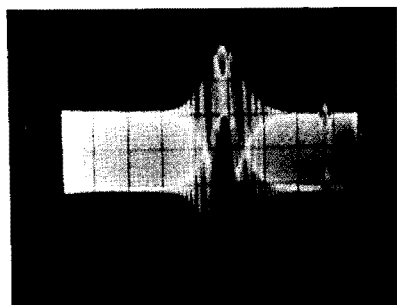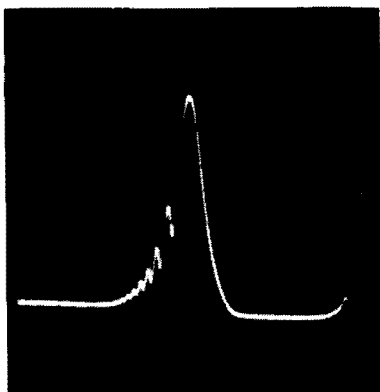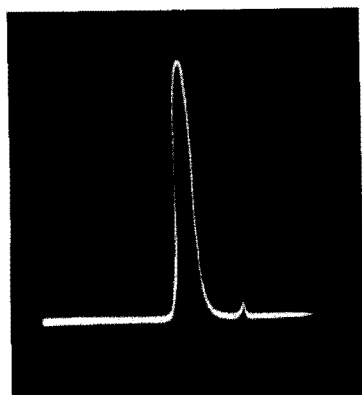
Fig. 849 (left). *The instability shown in Fig. 848 has become sustained oscillation.* Fig. 850 (right). *Interference caused by local oscillator operation. (These illustrations are at the bottom of the page.)*

A single-hump curve somewhat off resonance is shown in Fig. 845. In the single-trace method, an incorrect frequency setting produces off-centering of the pattern. If the swing is too low, only the top of the curve is displayed and the resultant pattern (Fig. 846) is useless. On the other hand, if the swing is too high, a curve of apparently exaggerated selectivity (Fig. 847) appears.

An interesting feature of visual alignment of if amplifiers is the clear indication of a tendency toward instability even before oscillation actually occurs. Thus, Fig. 848 shows instability at a frequency slightly lower than the tuning frequency. This instability has become a sustained oscillation in Fig. 849, which shows an im-

Fig. 851 (left). *Base-line distortion resulting from connecting scope input to point C of Fig. 829.* Fig. 852 (right). *Superimposed rf component appears when the scope is connected to point B.*

portant superimposed high-frequency component. On the other hand, the beats seen in Fig. 850 are due only to local oscillator operation during reception of a strong local station. To avoid this type of interference, it is common practice to ground the local oscillator grid, or even to pull out the converter tube (if this does not hinder operation of the following stages, as in ac–dc sets).

Point A is best for connecting the scope input. Because of the

Fig. 853 (left). *Diode rectifying effect. The scope is connected to point D in Fig. 829.* Fig. 854 (right). *Rf response of overcoupled transformer. Diode removed, scope connected to point D.*
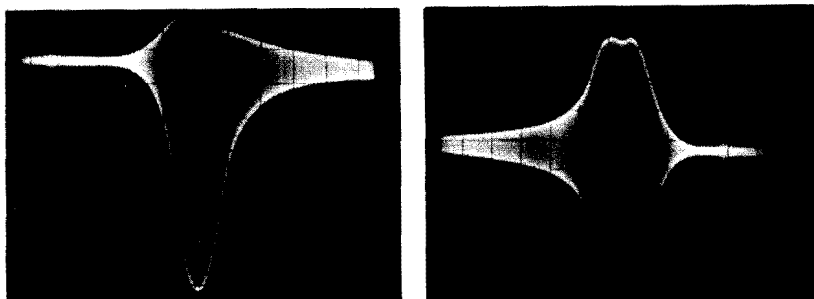
insufficient time constant of R3–C3 at 60 cycles, connection to point C results in the broken base line of Fig. 851, making skirt observation somewhat difficult. An rf residue appears if the scope is connected to point B (Fig. 852).

The rectifying operation of the diode (Fig. 853) can be shown by connecting the scope to point D. Eliminating the diode results in Fig. 854 (compare with Figs. 830 and 831). Because of the de-
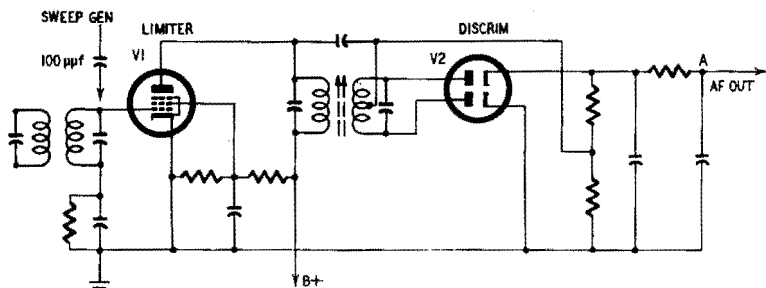
Fig. 855. *Typical FM discriminator circuit.*

tuning due to stray capacitance, this connection prevents correct alignment and is not recommended.

Aligning the rf section

Once the if amplifier is correctly aligned, the sweep generator is shifted to the antenna terminal of the set to obtain correct tracking of the local oscillator and signal circuits. As the bandpass of the rf circuits is wider than that of the if amplifier, the overall selectivity curve is practically that of the if circuits. Correct tuning of the signal circuits will only enhance the sensitivity, increasing the amplitude of the response curve. Aligning the local oscillator circuits will allow for correct location on the dial of the frequencies of incoming

Fig. 856 (left). *Assymetric S-curve. Incorrect center frequency is shown by the double-trace method.* Fig. 857 (right). *Correct frequency trace shows fair linearity and lower gain.*
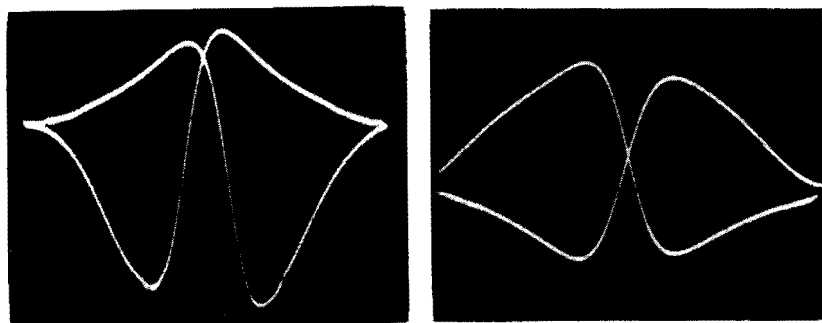
Fig. 858 (left). *Assymetric S-curve displayed by single-trace method.* Fig. 859 (right). *Approximately symmetric S-curve with acceptable linearity.*

stations, simultaneously providing best sensitivity by realizing the specified tracking conditions.

Discriminator alignment

A typical discriminator circuit is represented in Fig. 855. The sweep generator signal is injected into the grid of limiter V1 by a coupling capacitor of, say, 100 μμf. The scope input is connected to point A.

The so-called S-curve that will be obtained has to satisfy several conditions. The center frequency has to be 10.7 mc for FM sets and 4.5 mc for TV sound. The slope has to be high to yield a high gain, and linear too. It has to be symmetric regarding the baseline, and the usable bandwidth corresponding to the linear part of the characteristic has to be adequate. Because of interaction between the primary and secondary transformer adjustments, some difficulty is experienced in trying to approach the ideal S-curve. The primary adjustment determines the gain of the circuit and, to some extent, the symmetry and the center frequency. Tuning the secondary acts very effectively on the symmetry and on the center frequency too.

The double-trace method is often recommended by manufacturers for tracing S-curves because any lack of symmetry is easily shown. A somewhat asymmetric curve is shown in Fig. 856, the crossing of the traces above the baseline indicating an incorrect center frequency. The linearity is good. In Fig. 857, the center frequency is correct and the symmetry is good, but the gain is somewhat lower.

Using the single-trace method, Fig. 858 was obtained, showing lack of symmetry. The curve of Fig. 859 is fairly symmetrical, but its linearity appears less good and its gain is lower.

These tests are qualitative only; markers or other quantitative means are necessary to ascertain a correct center frequency and adequate bandwidth of the slope of the S-curve.

waveforms in black-and-white and color television

GETTING top performance out of both black-and-white and color television receivers is facilitated enormously by waveform observations. Manufacturers' manuals show correct waveforms, with peak-to-peak voltages for key check points in the receiver circuits.

The *peak-to-peak voltage* of a waveform is just as important as the *shape* of the waveform. In most cases, a tolerance of $\pm 20\%$ is permissible in the specified peak-to-peak voltage value. Likewise, reasonable tolerances in waveshapes are permissible.

Key check points occur in the rf tuner, if and video amplifiers, sync, sweep and intercarrier sound circuits in black-and-white receivers. In color receivers, additional key check points are in the bandpass amplifier, color sync, chroma demodulator and matrix circuits.

Rf tuner

Fig. 901 shows a typical rf response curve, obtained in the course of tuner alignment in both black-and-white and color receivers. The picture-carrier, color-subcarrier, and sound-carrier markers are indicated. Some sweep generators have built-in facilities for displaying them simultaneously. This is the preferred type of generator for this type of work.

This curve shows that the tuner is badly out of alignment. The bandwidth is much too great, and the curve is not reasonably flat. The bandwidth should be approximately 6 mc, with the sound and picture carriers fully up on top of the curve.

The test setup is made by connecting the vertical input leads

of the scope to the rf test point (looker point) on the tuner, as shown in Fig. 902. This is a tap on the mixer grid leak. An isolating resistor of about 51,000 ohms should be used in series with
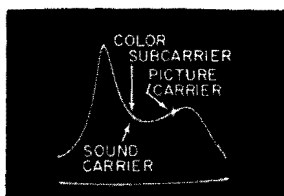
Fig. 901. *Rf tuner out of alignment. The bandwidth is much too great and the response curve is not flat. Compare the positioning of the carriers with those shown in Fig. 904.*

the scope input lead, so that the leads do not act as resonant lines and distort the response curve.

Both rf and demodulated low-frequency voltages are found at
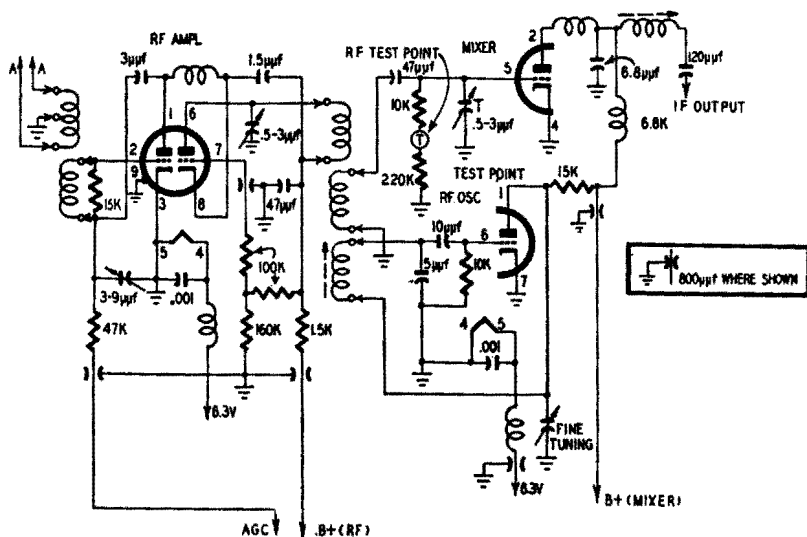
Fig. 902. *Typical television front end. The scope input can be connected to the rf test point (T) shown in the circuit diagram.*

the looker point. This is because the mixer tube is a detector (often called the first detector). Hence, we use a direct cable to the scope and obtain a demodulated display on the scope screen.

The generator output impedance is made 300 ohms, and the sweep signal is applied at points marked A in Fig. 902. The agc line should be stabilized by applying 2 or 3 volts of negative dc bias, obtained from batteries or a bias box.

If amplifier

A typical if response curve is illustrated in Fig. 903. The small

bump to the left of the curve is the after-response of the sound trap. The top of the response curve is not flat, but is considered acceptable—particularly for black-and-white reception.
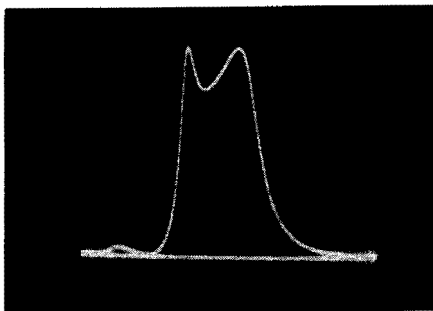
Fig. 903. *Typical if response curve for a black-and-white television receiver.*

A severe case of misalignment of an if amplifier in a color receiver is seen in Fig. 904. The bandwidth is much too great, and there are excessive peaks and dips in the response.
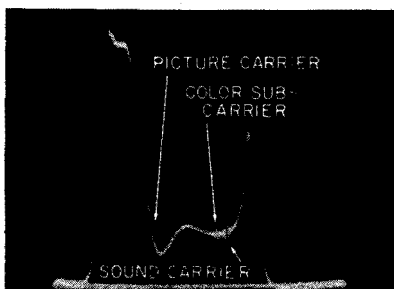
Fig. 904. *Severe misalignment of an if amplifier in a color television receiver.*

Note that the marker order is reversed, as compared with Fig. 901. This is because the local oscillator in the rf tuner operates on the high side and inverts the frequency progression in the heterodyning process.

Sometimes the sweep circuits must be disabled during alignment procedures. Otherwise, interference appears on the response curve, as illustrated in Fig. 905. The horizontal output tube is usually removed to eliminate this spike type interference.

A sharply peaked response curve, as shown in Fig. 906, which cannot be brought into standard form by alignment adjustments

is caused by if regeneration. The circuit fault must be corrected before proceeding with alignment.
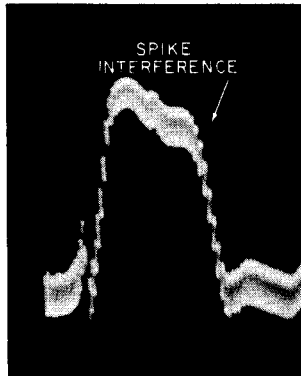
Fig. 905. *Spike interference from the horizontal sweep circuit.*

To obtain if response curves, the sweep and marker signal voltages are commonly applied at the plate of the mixer tube by a
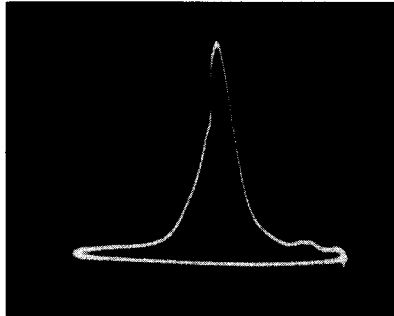
Fig. 906. *Waveform obtained when the if amplifier of the television receiver goes into regeneration.*

floating tube shield as in Fig. 907. The scope is connected at the picture detector load resistor, with a series isolating resistor of approximately 51,000 ohms. This avoids possible curve distortion due to cable resonances and also provides a low-pass action which sharpens the marker indication.

Video amplifier

The video amplifier is the signal channel from the picture detector to the picture tube. It is often neglected, but good quality pictures cannot be obtained without good video-frequency re-

sponse. Modern sweep generators provide a video-frequency sweep and marking facilities.

A typical video-frequency response curve is shown in Fig. 908. The shape of the curve and its bandwidth are determined by the
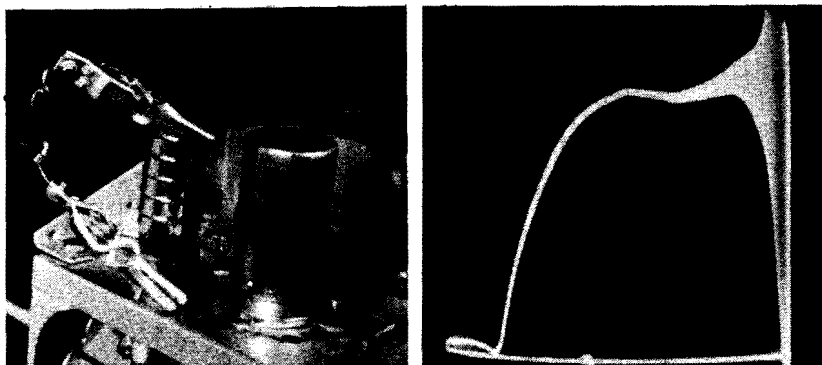
Fig. 907 (left). *The if signals are injected by using a floating shield over the mixer tube.* Fig. 908 (right). *Video amplifier response curve.*

values of peaking coils and load resistors in the video amplifier circuits.

Note that a video sweep signal can be obtained from if sweep and CW signals, as illustrated in Fig. 909. This is the preferred
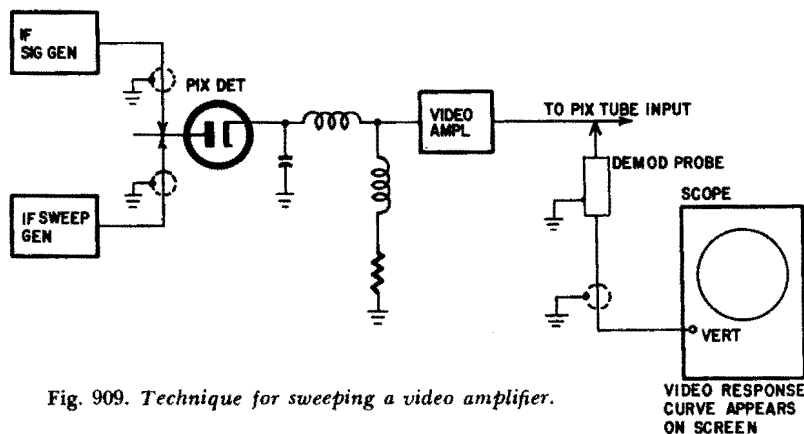
Fig. 909. *Technique for sweeping a video amplifier.*

VIDEO RESPONSE CURVE APPEARS ON SCREEN

method of sweeping a video amplifier because the response of the picture detector peaking coils is taken into account. A demodulator probe is used at the video amplifier output. This gives a standard demodulated response on the scope screen.

Often an if tube must be pulled to avoid excessive noise inter-

ference on the video response curve (Fig. 910). A video curve can be marked with either beat or absorption markers. Both are seen in Fig. 911. Absorption markers are usually preferred, since there
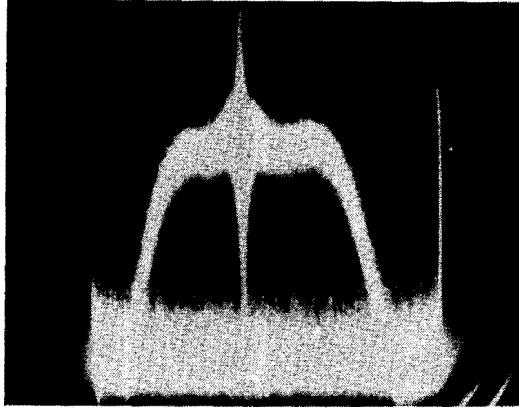
Fig. 910. *To avoid noise modulation of video curve an if amplifier tube should be pulled. Use a dummy tube (all leads clipped, except filament) in series-string receivers.*

is much less likelihood of cross-beats causing spurious marker indications.

Also seen in Fig. 911 is curve undershooting of the base line. This is caused by high-frequency fields being picked up by the
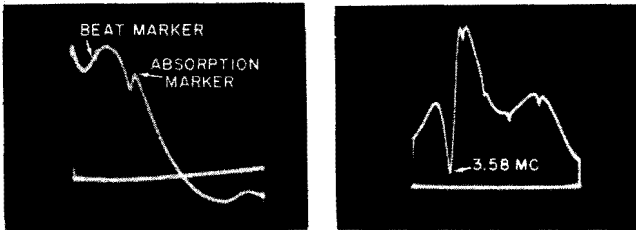
Fig. 911 (left). *Illustration of a beat and an absorption marker on a video curve.* Fig 912 (right). *Y amplifier response curve.*

demodulator probe. The probe and its cable must be kept at a distance from the generator cables to avoid this difficulty.

Y amplifiers

The Y amplifier in a color receiver is similar to the video amplifier in a black-and-white set. However, the Y amplifier response shows a deep dip at 3.58 mc, caused by the color subcarrier trap

(Fig. 912). Note the small dips at intervals on the curve—these are absorption markers.

Absorption markers are often obtained from marker boxes. The box is connected in series with the output cable from the video

Fig. 913. *Display obtained in check of generator flatness. A marker box provides absorption markers.*

sweep generator. It provides spot-check absorption markers, usually at 0.5, 1, 1.5, 2.5, 3.1, 3.58, 4.1 and 4.5 mc.

When the output from a video sweep generator is passed through a marker box and then into a demodulator probe and to the scope, these markers appear on the swept trace (Fig 913). This is a useful display because it shows whether the generator
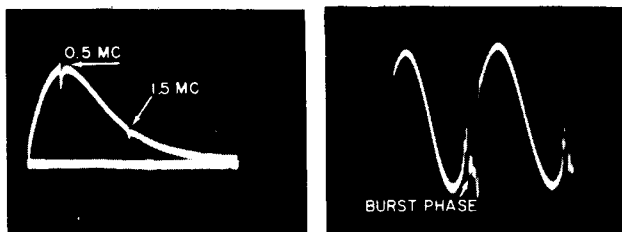
Fig. 914 (left). *Typical chroma demodulator response curve.*
Fig. 915 (right). *Sine-wave and phase pulses are obtained from the chroma demodulator when a rainbow signal is applied to the color receiver.*

sweep is "flat." A sweep signal which lacks flatness make for difficulties in alignment work.

Chroma demodulators

Sweep alignment of chroma demodulators is made in the same manner as checks of video or Y amplifier response. However, bandwidth is less. The bandwidth of a chroma demodulator should be from 0.5 to 1.5 mc, depending upon receiver design. On the other hand, a good video amplifier has a bandwidth of about

4 mc. A properly operating Y amplifier usually has less—about 3.1 mc.

A typical (R—Y) demodulator response curve is shown in Fig. 914. The first marker appears at the top of the curve, at 0.5 mc. The second absorption marker appears at 1.5 mc.

When a rainbow signal is applied to a color receiver, the scope
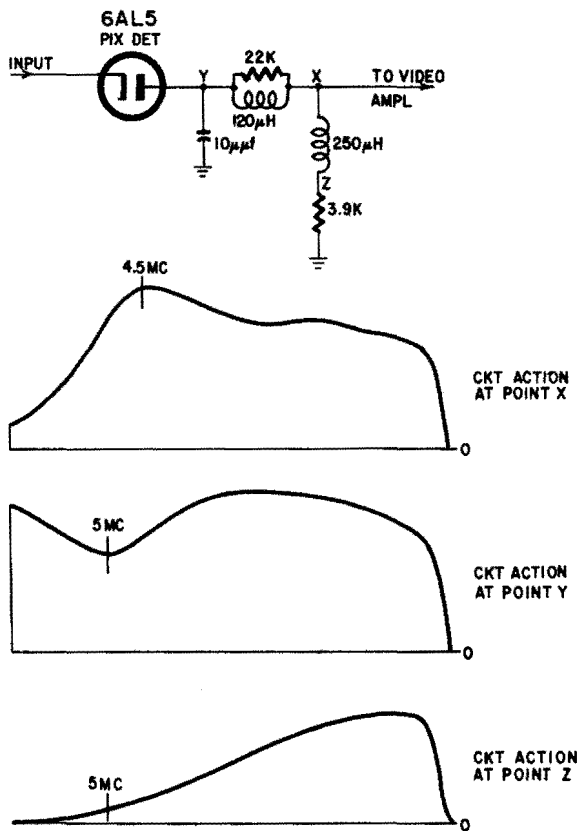
Fig. 916. *There is sufficient frequency response at points X and Y to reproduce the color burst. Very little burst is found at point Z.*

display obtained at the output of a chroma demodulator is a sine wave with a superimposed pulse (Fig. 915). The pulse corresponds to the burst. It marks the phase of chroma demodulation and is a useful indication of quadrature transformer adjustment.

Color burst

The color burst first appears in demodulated form at the output

of the picture detector. You must test at a suitable point. Fig. 916 shows that points X and Y have suitable frequency response to reproduce the color burst (3.58 mc) correctly. On the other hand, the frequency response at point Z is poor, and little or no burst
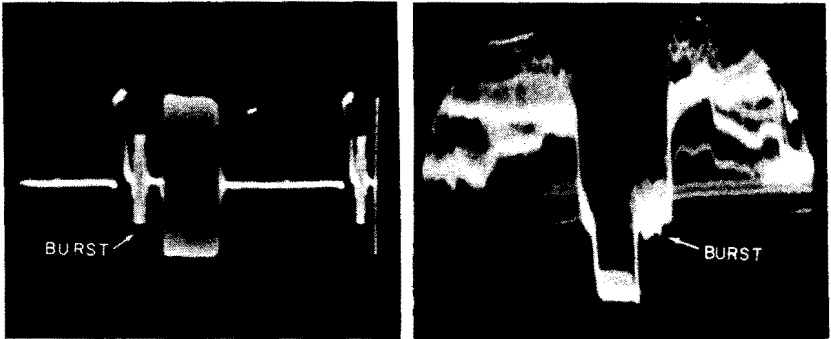
Fig. 917 (left). *Burst and chroma bar signal from a color bar generator.* Fig. 918 (right). *Burst and camera signal from a color broadcast transmission.*

is found here. Point Z is suitable only for low-frequency displays, such as frequency response curves.

The color burst is very clean and sharply defined when you
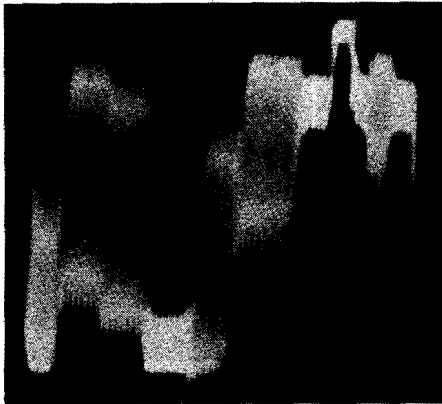
Fig. 919. *Beat between the 3.58-mc color subcarrier and the 4.5-mc sound carrier causes a 920-kc wavy edge along the top and bottom of this waveform.*

apply the output from a color bar generator directly to the vertical input terminals of a scope (Fig. 917). On the other hand, the burst obtained from a color broadcast signal is mixed with noise and cross-talk, as seen in Fig. 918. This often confuses the beginner,

205

who feels that he should see a clean-cut burst from the picture detector.

In high-signal areas, the broadcast burst is cleaner on locally originated signals but never has the sharpness of a direct output
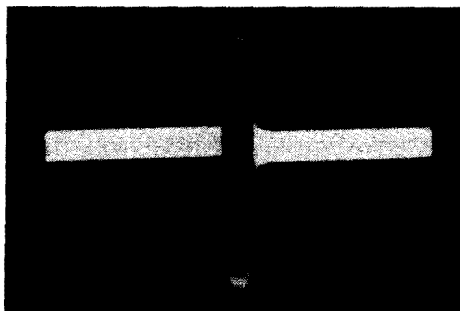
Fig. 920. *The output from the burst amplifier is the 3.58-mc color burst only.*

signal from a color bar generator. When a color receiver is driven from a color bar generator, the burst and chroma signal at the picture detector have less fuzziness than a broadcast burst, but
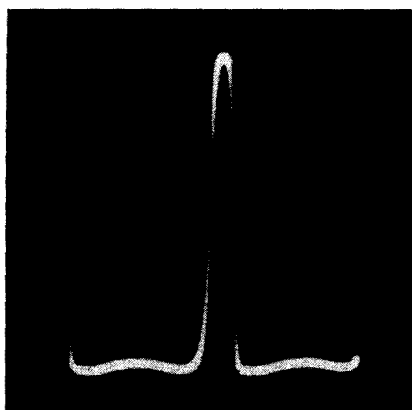
Fig. 921. *Gating pulse at the screen grid of the burst amplifier tube.*

lack the sharpness of the waveform obtained directly from the generator. This is caused by introduction of circuit noise and cross-talk from the receiver circuits.

When the 4.5 mc sound carrier mixes appreciably with the color subcarrier, a 920-kc beat appears at the edges of the chroma waveform (Fig. 919). On the picture-tube screen, this causes diagonal 920-kc beat lines.

A scope used for display of the burst and chroma waveforms must have full response at 3.58 mc. Otherwise, the chroma portion

Fig. 922. *Driving waveform at the grid of the horizontal-output tube. Note the effect of ringing on the waveform.*

of the waveform will become attenuated in the vertical amplifier of the scope.

Burst amplifier

The burst amplifier is tuned to a bandwidth of about 600 kc and is gated at burst time. Hence, the output from a normally
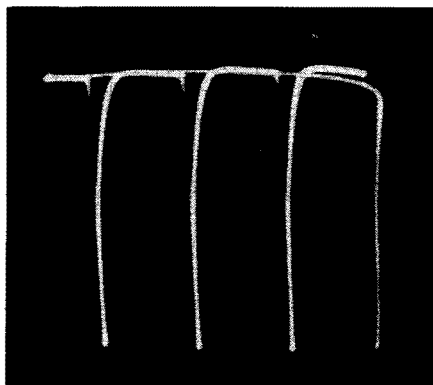
Fig. 923. *Waveform obtained across the horizontal-deflection coils in the yoke.*

operating burst amplifier is the burst waveform only, as seen in Fig. 920. The Y and camera signals do not appear at the burst amplifier output.

The gating pulse applied to the screen grid or cathode of the burst amplifier tube has a pulse waveform, as seen in Fig. 921. In checking all such waveforms, both the peak-to-peak voltage and the waveshape are observed.

Checks in most chroma circuits should be made with a low-capacitance probe. This minimizes circuit loading and avoids the possibility of distorting and attenuating the waveform under test.

Horizontal sweep system

The grid of the horizontal output tube is driven by a combination sawtooth and pulse waveform, as seen in Fig. 922. This waveform is somewhat faulty in that "ringing" or ripples appear along the sawtooth. This is an indication of trouble in the horizontal oscillator circuits.
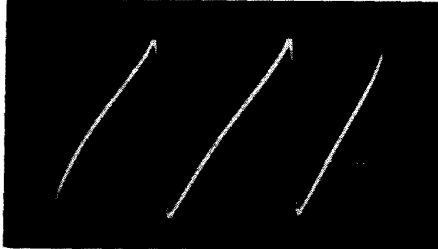
Fig. 924. *The current flowing through the horizontal-deflection coils is a sawtooth waveform.*

Across the horizontal deflection coils, we find a pulse type of voltage waveform (Fig. 923) but the current through the coils is a sawtooth (Fig. 924). The current waveform is obtained by connecting a 5-ohm resistor in series with the return lead from the yoke and applying the scope across the resistor.

oscilloscope fault patterns

JUST like any other instrument, the scope is likely to introduce distortion and deformation of its own. Such accidents can lead to misleading and even meaningless oscillograms—some patterns are difficult enough to interpret as it is. Fortunately, the scope may be used to check its own performance, the supplementary instrumentation required for servicing it being negligible.

Incorrect scope operation can result from poor design, misapplication or component failure. We will be concerned here only with specific scope troubles. Faults common to servicing practice, such as broken heaters, open resistors and shorted capacitors will not be considered.

Action of external fields on the CRT

Although the cathode-ray tube used in instruments generally is of the electrostatic type, its beam can be deflected by magnetic as well as electric fields. Actually, magnetic fields alone are troublesome, for electric fields strong enough to deflect the beam are rarely encountered in the vicinity of a C-R tube and if they were, the metallic box enclosing the instrument would provide sufficient shielding.

Static magnetic fields such as those produced by the earth or by permanent magnets are not troublesome, for they· can be counteracted by the centering controls. On the other hand, the stray magnetic field of power transformers and chokes can produce serious spot deflections. For that reason, the power supply unit of old-time laboratory scopes was placed a good yard away from

the C-R tube. This, of course, does not prevent deflection from other nearby ac fields, and thus offers no complete solution.

The only way to protect the tube from ac magnetic fields is to enclose it in a shield made of a ferromagnetic material. The higher the magnetic permeability of the shield, the more efficiently it works by collecting the force lines of the ambient magnetic fields. Mumetal is extensively used for magnetic shields and is more effective than a soft iron tube of a 10 times greater wall
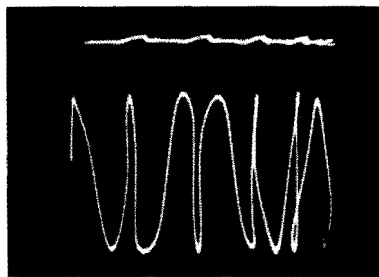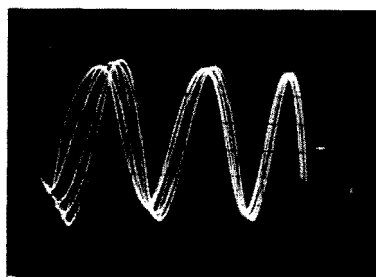
Fig. 1001 (left). *Effect of a stray magnetic field close to the screen of a shielded CRT displaying a sine wave*. Fig. 1002 (right). *Effect of a scope power supply transformer magnetic field on an unshielded CRT with and without a sine-wave signal.*

thickness. Any machining or even rough handling of a Mumetal shield deteriorates its high permeability and its initial properties can be restored only by reprocessing by the manufacturer.

To check the influence of an external field on the shielded cathode-ray tube, the primary of an output transformer was connected to the 60-cycle line, its air gap being increased to about 1/16 inch to increase its stray field. Displacing this "field generator" along the shield proved its efficiency, for no influence upon the beam could be detected. Placing this transformer near the screen at the part of the tube not protected by the shield resulted in Fig. 1001, showing a low-frequency sine wave periodically expanded and compressed. Unlike the field generated by a TV deflection unit, the stray field is far from uniform, and its effect is strongest at the left, in the vicinity of the transformer. The principal interfering field component appears to be vertical (because the beam is displaced horizontally), but the amplitude variation indicates presence of a somewhat smaller horizontal component.

Removing the shield to study the action of the scope power supply transformer on the beam resulted in Fig. 1002, showing (above) a slight vertical deflection of the baseline and (below) a rather significant "wobbulation" of a low-frequency sine wave,
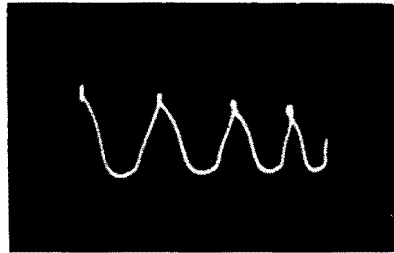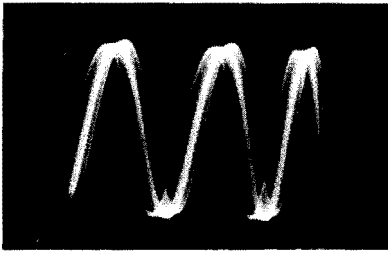
Fig. 1003 (left). *Effect of a stray magnetic field on a higher-frequency sine wave.* Fig. 1004 (right). *Deflection produced by an external magnetic field on an unshielded CRT.*

alternatively compressing and expanding the successive cycles. Presence of closed loops indicates that the trouble arises from the scope, for a spot swept by a linear time base cannot trace such figures without reversing its direction. Effect of the same stray

Fig. 1005. *Deflection due to an external magnetic field superimposed on electrostatic sinewave deflection.*

field on a 5,000-cycle sine wave is shown in Fig. 1003. The principal offending component appears to be vertical. Note that this type of interference can be minimized by positioning the power transformer as far away as possible from the screen end of the C-R tube.

To demonstrate the effect of a much stronger external magnetic field upon the unshielded tube, the field generator probe was placed beside the tube, producing the vertical deflection shown in Fig. 1004. Injecting a sine wave of about 85 cycles into the Y-amplifier resulted in the very distorted waveform of Fig. 1005. These patterns emphasize the very real need of an efficient shield for correct operation of a cathode-ray tube.

CRT power supply troubles

The high operating voltages of C-R tube power supplies using

high-value resistors and controls and high-voltage capacitors require good quality, conservatively rated components for reliability. An important change of resistance of a component may sufficiently upset the working voltages to eliminate the spot
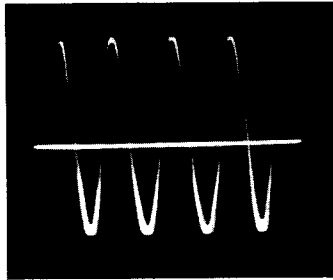
Fig. 1006. *Correctly focused base line and out-of-focus deflected beam resulting from astigmatism.*

entirely. If, however, the spot is untraceable, the trouble generally stems from incorrect dc deflection voltages or an open plate lead "freeing" the plate concerned. In this case, grounding the four plates will make the spot appear.

Of course, the tube may be defective too. The author once was faced with one that displayed no spot, broke down the power
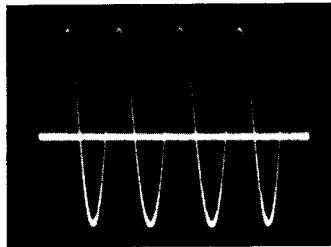
Fig. 1007. *Focusing the deflected trace results in an out-of-focus base line.*

supply voltage to only several hundred volts and showed a faint glow in the part of the bulb near the gun. The tube obviously was gassy, a somewhat rare case.

Astigmatism is a type of distortion characterized by a lack of focus along one axis, the other axis being correctly focused. Many tubes are more or less astigmatic due to internal misalignment, but this effect generally is not too pronounced. Very noticeable
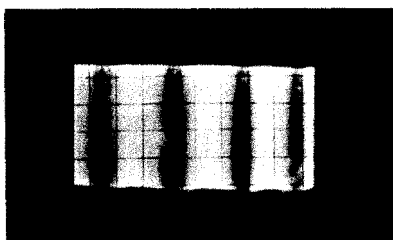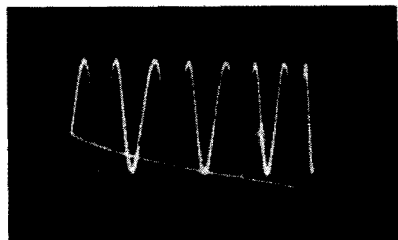
Fig. 1008 (left). *120 cps hum modulation of the CRT grid.* Fig. 1009 (right). *Hum modulation of the CRT grid showing display of a higher frequency.*

astigmatism is introduced by incorrect working conditions of the tube. The effect is minimized if the final anode potential equals the mean potential of the deflection plates. If a special control is provided for varying the final anode voltage, it will allow for correction of specific C-R tube astigmatism too.

Astigmatism is most likely to occur in scopes using dc amplifiers, especially if the deflection-plate pairs have differing mean potentials. In the author's scope, the deflection plates are directly coupled to the push-pull output amplifiers, and their mean potential is about 220 volts. Setting the astigmatism control to that voltage, no defocusing is discernible. Grounding the final anode resulted in the typical astigmatism shown in Fig. 1006. While a correctly focused baseline is obtained, application of a Y-deflection voltage produces an out-of-focus trace. If we correct the focus of this trace (Fig. 1007), the baseline is no longer in focus.

Considerable off centering of the trace (several times the screen diameter) obviously accentuates the unbalance of potentials and may necessitate a new setting of the astigmatism control.

A quite different type of interference is hum induced into the

Fig. 1010 (left). *Display of 60-cycle wave, low-capacitance pickup.* Fig. 1011 (right). *Observation of details by trace expansion and off-centering.*
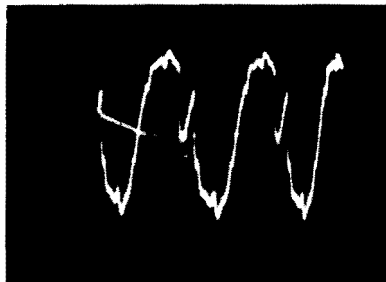
grid (or even into the cathode) of the C-R tube by pickup or by poor filtering of the power supply. This produces an intensity modulation of the trace as shown in Fig. 1008 (a 120-cycle wave is displayed). For a sine wave of higher frequency and the same time-base setting (15 cycles), an intensity-modulated rectangle (Fig. 1009) is obtained.

It takes a lot of ripple to modulate the other electrodes, and thus elaborate CRT power supply filtering is not only cumbersome, but even unnecessary. As the tolerable amount of ripple
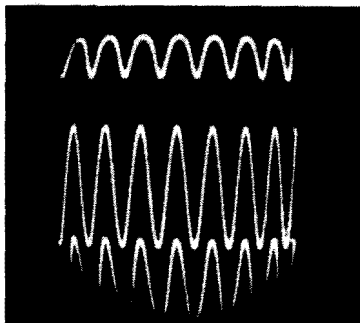
Fig. 1012. *Saturation in a dc amplifier resulting from trace shifting*

between cathode and grid is, however, much lower, a simple low-voltage R-C filter connected between cathode and grid may be used to smooth the bias voltage.

Y-amplifier defects

It is customary to test a scope by putting a finger on the Y-input terminal and observe the 60-cycle sine waves. Newcomers may be puzzled to see a wave such as Fig. 1010 (obtained by connecting an "antenna" of some yards of wire to the Y-input) instead of a more or less pure sine wave. There is nothing wrong with the scope but, as this is a very-low-capacitance coupling, the higher frequencies are favored and the display emphasizes the harmonics of the fundamental.

To observe the details of such an irregular wave, trace expansion and sometimes considerable off centering must be provided. A portion of that wave, expanded about six times and much off center, is shown in Fig. 1011. The thickening of some lines is due to rapidly fluctuating components, probably noise, not harmonically related to the fundamental.

To allow for trace expansion and off centering, an amplifier
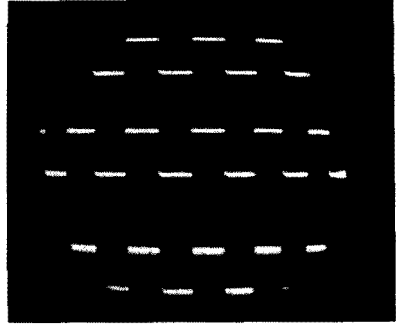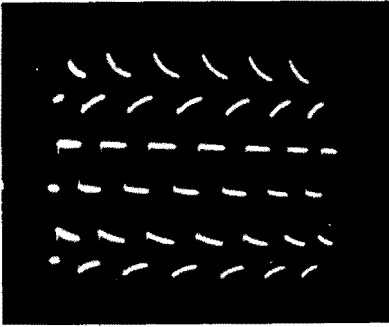
214

must provide ample output voltage. In dc amplifiers, the position-ing control may upset the operating voltages and produce satura-tion in the off-centered condition. The three sine waves shown in Fig. 1012 demonstrate this. The signal voltage was the same, but saturation occurred when the trace was shifted upward or
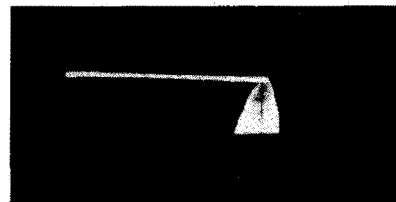
downward. This type of saturation obviously does not exist with ac amplifiers where the trace shifting is accomplished independ-ently of the amplifier.

Another case of distortion found in a dc amplifier is shown in Fig. 1013 where the same square wave appears differentiated when the trace is shifted. The trouble came from an incorrect screen supply of the push-pull output amplifier. Correct operation is shown in Fig. 1014.

Trouble arising from spurious oscillations and all types of coupling between the Y- and X-channels may be hard to eliminate. In the oscillograms of Figs. 1015 and 1016, a time-base-triggered oscillation probably built up in the Y-amplifier. Rearrangement of the wiring completely cured the trouble.

Crosstalk

Crosstalk means unwanted coupling, or transfer of a signal from one channel into the other. Let the time base be the first offender. Coupling the time-base triggering pulse into the Y-input by a
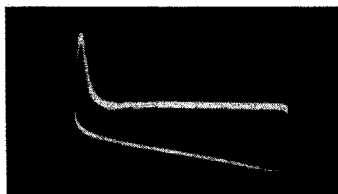
Fig. 1017. *Time-base triggering pulse penetrating into the Y amplifier by low-capacitance coupling.*

small capacitance, a spike is obtained at the beginning of the sweep (Fig. 1017) and the return trace (made visible for demonstration) is noticeably deviated. Note, however, that the short duration of the pulse leaves the major part of the baseline straight.
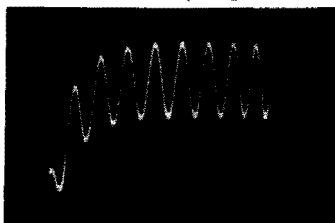
Fig. 1018. *Time-base voltage penetrating into the Y amplifier by capacitive coupling.*

The actual form of distortion introduced depends on the offending coupling element. Inducing some time-base voltage into the Y-amplifier by a definite capacitance causes lifting of the trace

Fig. 1019 (left). *Purely resistive time-base voltage coupling into the Y amplifier results in a linearly rising trace.* Fig. 1020 (right). *Effect of injecting a signal voltage into the X amplifier by resistive coupling.*
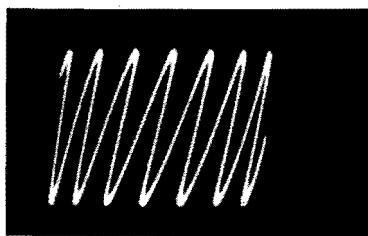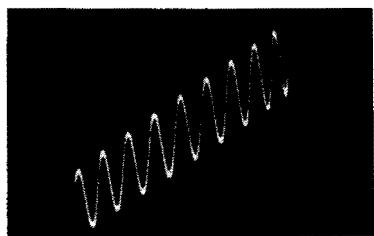
as shown in Fig. 1018, while a purely resistive coupling means a superimposition of the linear sawtooth voltage upon the displayed signal (Fig. 1019).

Just as the X-induced crosstalk in the Y-channel is discernible as a curved or sloped baseline, action of the Y-amplifier upon the X-channel is characterized by horizontally directed waveform
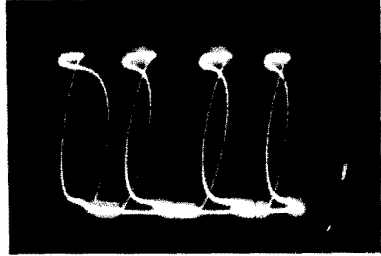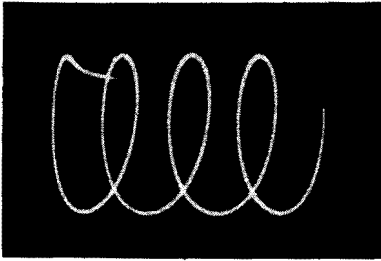
Fig. 1021 (left). *Effect of injecting signal voltage into the X amplifier by capacitive coupling.* Fig. 1022 (right). *Severe distortion of a 15-kc square wave due to signal injection into the X amplifier through a capacitance of about 5 μμf.*

distortion. By resistively coupling some signal voltage into the X-amplifier, the pattern of Fig. 1020 was obtained, showing back-and-forth motion of the sweep. Capacitive coupling gives the pattern of Fig. 1021, which shows several spot returns during each stroke.

Waveforms presenting steep variations such as square waves are likely to produce crosstalk because of very low coupling capacitances. Simply bringing a wire connected to the X-amplifier to
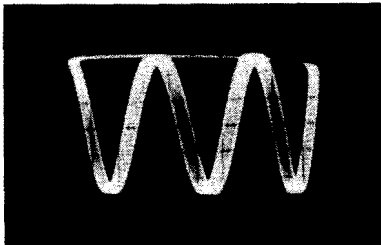
Fig. 1023 (left). *Hum in the X amplifier. The whole trace is shifted back and forth.* Fig. 1024 (right). *Time-base hum. While one end of the trace remains stationary, the other end is swept back and forth.*

the Y-input fed with a 15-kc square wave resulted in Fig. 1022, in which the original waveform is hardly discernible. Note, however, that the flat portions are comparatively well reproduced, the voltage being constant.

217

Trouble in the X-channel

When studying time-base operation, we examined the causes and effects of nonlinear sweep and faulty sync, and so they will not be considered here.

It is clear that a hum voltage in the X-channel will sweep the trace laterally. Note, however, that a ripple voltage acting upon the X-amplifier alone "vibrates" the whole trace horizontally (Fig. 1023) while time-base hum is characterized by an apparently elastic pattern that is fixed on one end and shaking on the other (Fig. 1024). This lateral discrimination is due to the fact that the hum component periodically varies the time-base triggering voltage.

This list of troubles is by no means exhaustive, but it should prove useful in servicing oscilloscopes.

index

219

220

T

U

V

W

X

Y

Z